ABN

Australian Acoustical Society

ACN 000 712 658

NOISE AND SOUND: *NUISANCE AND AMENITY*

ANNUAL CONFERENCE
CANBERRA 9 - 11 November 1994

Proceedings

PLEASE RETURN TO:
LIBRARY
NATIONAL ACOUSTIC LABORATORIES
126 GREVILLE ST
CHATSWOOD 2067

BUILDING IN QUALITY CSR Gyprock® Bradford™

Proceedings Sponsor CSR Gyprock Bradford

NOISE AND SOUND : NUISANCE & AMENITY (AUSTRALIAN ACOUSTICAL SOCIETY ANNUAL CONFERENCE : 1994 : CANBERRA)
534.83.047:711.5NOI94

DATE DUE

RAECO

ABN holdings record rid abn95- 2/97

534.83.047:711.5NO194
(noise - community reaction)

$50

NOISE AND SOUND: *NUISANCE AND AMENITY*

CONTENTS

ARCHITECTURAL ACOUSTICS

PSYCHOLOGICAL ACOUSTICS

DoBIS document No. 933266

Australian Hearing Services
6610

ACOUSTICAL PROPERTIES OF MATERIALS AND SYSTEMS

NOISE AND VIBRATION IDENTIFICATION AND CONTROL

ENVIRONMENTAL NOISE

TRANSPORTATION NOISE

NOISE AND SOUND: *NUISANCE AND AMENITY*

The 1994 Annual Conference was organised by the following Conference Committee of the Australian Acoustical Society New South Wales Division.

Marion Burgess
Stephen Samuels

Secretarial support for the Conference was provided by the Acoustics and Vibration Centre at the Australian Defence Force Academy and by the Department of Transport Engineering at the University of New South Wales.

The Conference was greatly assisted by the generous support of three sponsors:

Bruel and Kjaer Australia Pty Ltd
CSR Gyprock Bradford Pty Ltd
Qantas Airways Ltd

NOISE AND SOUND: *NUISANCE AND AMENITY*

The views expressed in this publication are those of the individual authors and not necessarily those of the Australian Acoustical Society.

Published by: Australian Acoustical Society
c/ Professional Centre
Private Bag 1
Darlinghurst, NSW 2010

November 1994

Printed by: Cronulla Printing Co Ltd Pty
16 Cronulla Plaza
Cronulla NSW 2230

ISBN 0 909882 14 2

ARCHITECTURAL ACOUSTICS

APPLICATION OF MEASUREMENT AND PREDICTIVE TECHNIQUES FOR THE ACOUSTIC EVALUATION OF LARGE MULTIFUNCTIONAL ROOMS.

Joseph Lai*, Marion Burgess*, Mark Eisner†, Eric Taylor§ and Glen Thurecht#

* Acoustics and Vibration Centre, University College, University of New South Wales, Australian Defence Force Academy, Canberra ACT 2600.
† Mark Eisner and Associates, 5 Sprent St, Narrabundah ACT 2604.
§ Eric Taylor Acoustics, Canberra ACT 2600.
\# Newton Pty Ltd, GPO Box 733, Canberra ACT 2600.

INTRODUCTION

The traditional objective methods for the assessment of the acoustic performance of a space have been based on recordings, on some form of paper chart, of the sound distribution or the sound decay in the space. The analysis of the decay curve is then used to determine the reverberation time and many other descriptors such as early decay time, clarity, definition, lateral energy efficiency, speech transmission index to name but a few. While the reverberation time can be relatively easily determined, the other descriptors require careful analysis of the detail of the decay curve and their determination can be quite time consuming. With the advent of modern computer technology, the traditional methods are being replaced with powerful software and hardware packages to assist with the determination of these descriptors and consequently the assessment of the acoustic performance of a space.

For the prediction of the acoustic performance of a space, there have basically been two types of traditional objective methods. One has involved calculations of the decay rate based on data for the sound absorption characteristics of the room surfaces. The second has used two dimensional geometrical analysis to investigate the distribution of the sound reflected from the various room surfaces and the nature of the reflection sequence at specific points. Once again, the increased capabilities of modern computer technology has enabled more extensive analysis and software packages have been developed which enable the prediction of the performance of a three dimensional space based on the determination of the various descriptors from the reflection pattern sequence at receiving positions.

The use of modern technology for such measurement and prediction techniques is of great benefit in the assessment and prediction of the acoustic performance of large spaces which may be required to function in a number of different configurations. In this paper, results from experimental measurements and predictions for some large multifunctional rooms will be compared.

MEASUREMENT TECHNIQUES

The traditional method for analysing the acoustic characteristics of a room involves producing a known sound and monitoring the sound at a number of locations in the space. The analysis of the decay curve can be used to determine the reverberation time and many other descriptors. The development of Time Delay Spectrometry (TDS) in the early 1980s allowed discrimination between the direct and reflected sound fields. The disadvantage of such a system was that only part of the frequency range could be examined at any one time, so multiple measurements were required for each measurement location. The use of the impulse response has enabled all the frequency data to be obtained with a single measurement. The disadvantage of the impulse response in practice is that the signal/noise ratio is not good [1].

The MLSSA method, described in [1] and commercially available, provides all the information which could be obtained with the impulse technique but without the signal/noise problems. A Maximum Length Sequence (MLS) is a special type of pseudo random noise that has autocorrelation properties which allow the impulse response to be recovered by efficient deconvolution. The MLS sounds like a white noise with low level cycling due to its periodic nature. The MLSSA system consists of a plug-in board for a PC and special software. Once the data has been captured, a wide range of acoustic descriptors, from reverberation time to speech transmission index, can be determined with the aid of the software package.

PREDICTION TECHNIQUES

Geometric acoustic techniques enable consideration of the direct and reflected sound within a space. At high frequencies, where the dimensions of the room are large compared with the wavelength, sound can be considered to behave as rays and the principles of reflection, ie the angle of incidence equals the angle of reflection, can be applied. While the technique can be performed manually, it can be rather tedious as the procedure must be repeated for even very small changes in the position of the source or of the reflecting surfaces. There are now over 20 commercially available software programs which can be used to undertake geometrical acoustics investigations once the model of the space has been produced. The algorithms used for such computer models are normally based on the mirror image source method, the ray tracing method or the canonical beam method (for further explanation of these methods see Lai [2]). The software RAYNOISE, version 2.0a (supplied by Numerical Integration Technologies), which makes use of the conical beam method, was used for the predictions described in this paper. The calculations were made using a SUN SPARC 10 workstation.

While there have been numerous studies on errors involved in calculations based on geometrical acoustics (for example Lehnert [3]), it has been remarked by Graham Naylor, the guest editor of the special issue (vol. 38) of Applied Acoustics devoted to computer modelling, that '.... *there is a yawning gap in the literature concerning verification of computer models against measurements*'.

COMPARATIVE INVESTIGATIONS

The opportunity to compare the analysis and predictive techniques for some large multifunctional rooms arose when modifications and a new sound reinforcement system were required.

ROOM A

Computer generated models of the room are shown in Figure 1. While the floor plan for the room is basically rectangular, approx. 14 m x 30 m with the first 20 m flat and then a tiered balcony, the ceiling is quite high and complex - height of main portion approx 9 m rising to approx 16 m at the peak of the roof light. The volume of the room is approx 3,700 m^3. This room is used in various configurations ranging from lecture style with the speakers at one end through to forum style with the speakers and listeners around a table centrally in the flat section of the room. The different configurations place great demands on the natural acoustics and the speech reinforcement system in the room.

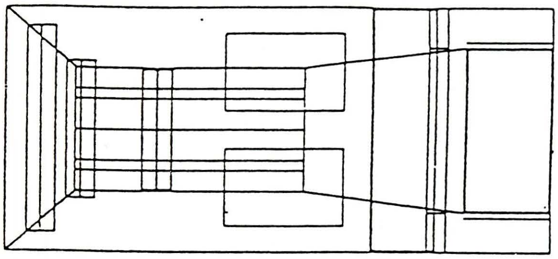

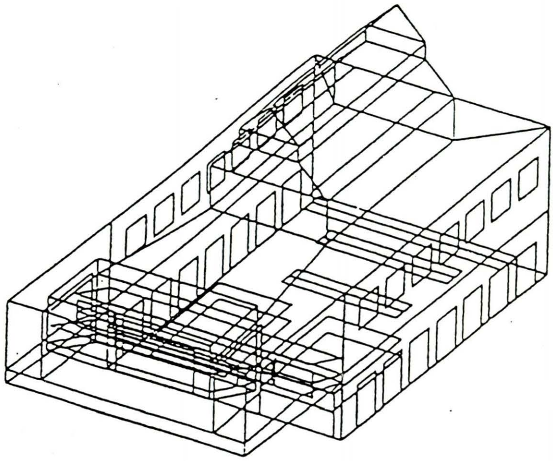

Figure 1 Plan and isometric view for room A.

Measurements of the acoustics characteristics in the existing room were made using traditional methods and MLSSA. A number of source and receiver locations were selected to be representative of the various uses for the main floor area and the gallery. Comparison between the reverberation time and the early decay time determined using the traditional method with impulsive noise as the source and using the MLSSA method showed good agreement. By way of example, comparisons for two combinations of source and receiver are shown in Table 1. The agreement was generally within 0.2 sec over the important speech frequency range with somewhat greater differences more common in the lower frequencies.

The predictive method first required a 3D model of the space to be generated. As suitable CAD plans were not available, this was quite a task for such a complicated room. Once the model was available, the absorption coefficients for the various surfaces were determined from available data bases. The RAYNOISE analysis then produced plans showing the distribution of the various descriptors for the space and the reflection pattern sequence at any one receiver position could be examined. Comparison between the early decay time, determined using the MLSSA method and the predicted values using RAYNOISE showed good agreement. Typical comparison for two combinations of source and receiver is shown in Table 1.

Table 1

Comparison of various descriptors

	Octave Band Centre Frequency, Hz						
	125	250	500	1000	2000	4000	8000
Room A - EDT, sec, for Source/Receiver Location S3R5							
Traditional	1.7	1.7	1.4	1.7	1.4	1.3	1.0
MLSSA	1.8	1.6	1.4	1.5	1.4	1.2	1.0
RAYNOISE	2.0	1.7	1.5	1.5	1.4	1.2	0.9
Room A - EDT, sec, for Source/Receiver Location S3R8							
Traditional	1.0	1.3	1.8	1.5	1.3	1.2	0.8
MLSSA	1.4	1.5	1.2	1.1	1.4	1.3	1.1
RAYNOISE	1.8	1.6	1.5	1.5	1.5	1.3	0.9
Room A - D50, %, for Source/Receiver Location S3R5							
MLSSA	49	31	44	44	60	51	69
RAYNOISE	42	43	47	50	53	62	72
Room A - D50, %, for Source/Receiver Location S3R8							
MLSSA	38	51	65	56	54	60	75
RAYNOISE	46	51	55	54	58	66	76
Room B - Spatial averaged RT, sec							
Traditional	1.3	1.1	1.1	1.3	1.3	1.3	0.8
MLSSA	1.5	1.3	1.2	1.2	1.3	1.1	0.7
RAYNOISE	1.4	1.2	1.1	1.1	1.1	1.1	1.1
Room B - Spatial averaged D50, %							
MLSSA	49	51	54	58	61	69	78
RAYNOISE	43	45	52	54	57	61	71

The advantage of the MLSSA and RAYNOISE methods is that many other indicators can be obtained with much less effort than is required for the traditional methods. In this particular room, good speech clarity was essential. One indicator of speech clarity is 'Definition', D50, which is the ratio of the sound energy received in the first 50 ms to the total sound energy [4]. A value for D50 of about 65% will give almost 95% speech intelligibility. Comparison between the D50, determined using the MLSSA method and the predicted values using RAYNOISE showed good agreement, generally within 5 to 10%, and typical comparisons for two combinations of source and receiver are shown in Table 1. Figure 2(a) shows the predicted distribution for D50 for the existing space in the lecture configuration and without any speech reinforcement. It can be seen that, in the seating areas, the values ranged from as low as 35% to around 70%. The prediction technique was used to investigate the effects of various acoustic treatments and selection of the one which would give the maximum benefit. Figure 2 (b) shows the predicted distribution for D50 for the space with the recommended acoustic treatments and the improvement can be observed by comparison with Figure 2(a).

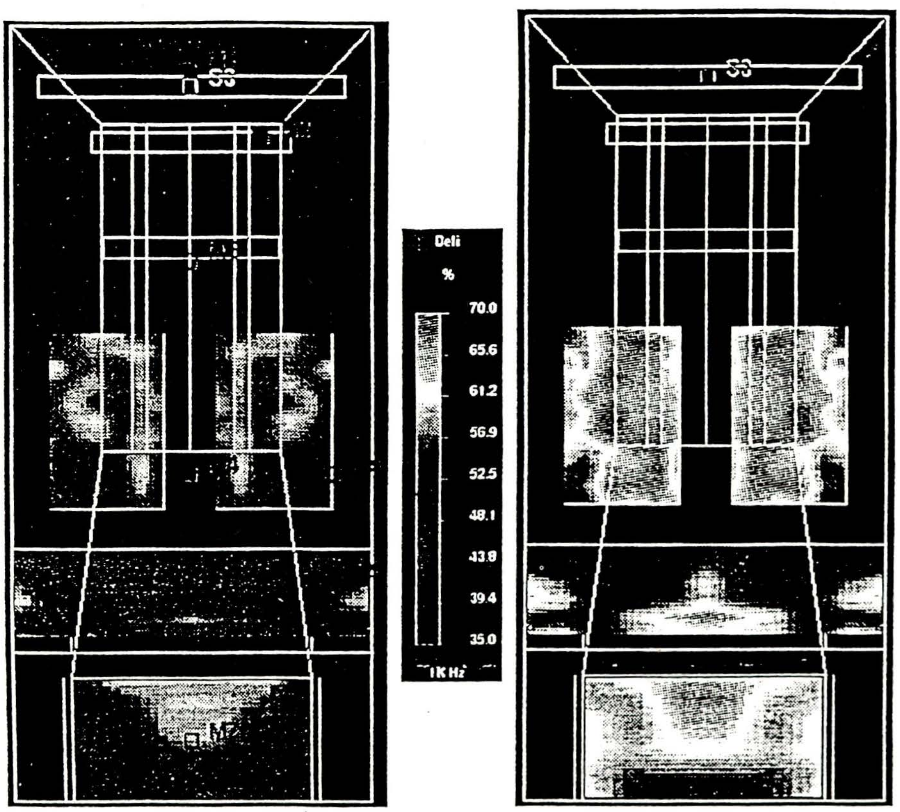

(a) (b)

Figure 2 Predicted contours for D50 at 1 KHz for: (a) the existing room; and (b) the room incorporating the recommended acoustic treatments.

ROOM B

Computer generated models of the room are shown in Figure 3. The floor plan for the room is basically rectangular, approx. 16 m x 12 m with the height to the ceiling approx 6 m. The volume of the room is approx 1,100 m^3. This room also is used in a number of configurations from lecture style through to forum style and the different configurations place great demands on the acoustics and the speech reinforcement system in the room.

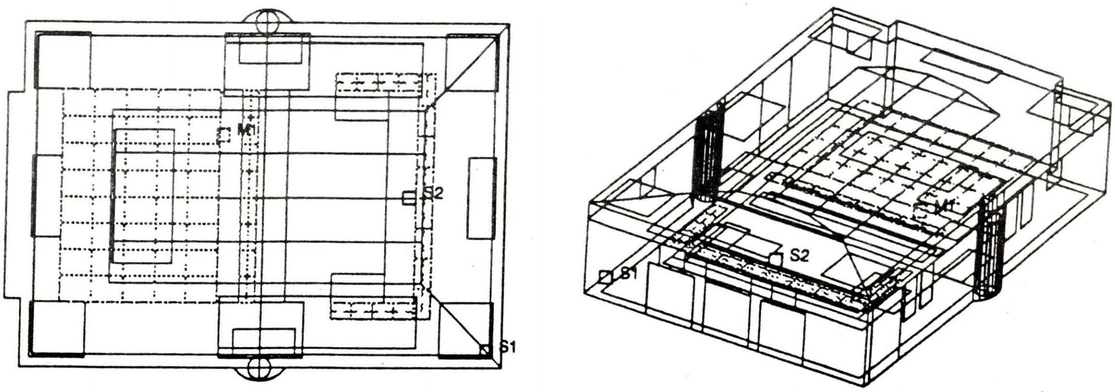

Figure 3 Plan and isometric view for room B.

Measurements and predictions of the acoustics characteristics in the existing room were made using the same technique as for Room A. The agreement was generally within 0.2 sec over the important speech frequency range with somewhat greater differences more common in the lower frequencies. Comparisons of spatial averaged values for RT and D50 are shown in the lower panel of Table 1. Figure 4(a) shows the predicted distribution for D50 for the existing space in the lecture configuration and without any speech reinforcement. It can be seen that, in the seating areas, the values ranged from as low as 40% to around 70%. Figure 4(b) shows the predicted distribution for D50 for the space with the recommended acoustic treatments and the improvement can be observed by comparison with Figure 4(a).

The prediction method can also be used to assess the various options for sound reinforcement systems in the room. The combination of the acoustic treatments and the sound reinforcement system can be investigated. The analysis is undertaken with sources, having the characteristics of the loudspeakers, at the proposed locations in the room. Figures 5(a) and (b) show a comparison for D50 for Room with the speech reinforcement system in the original room and in the room with the recommended acoustic treatments.

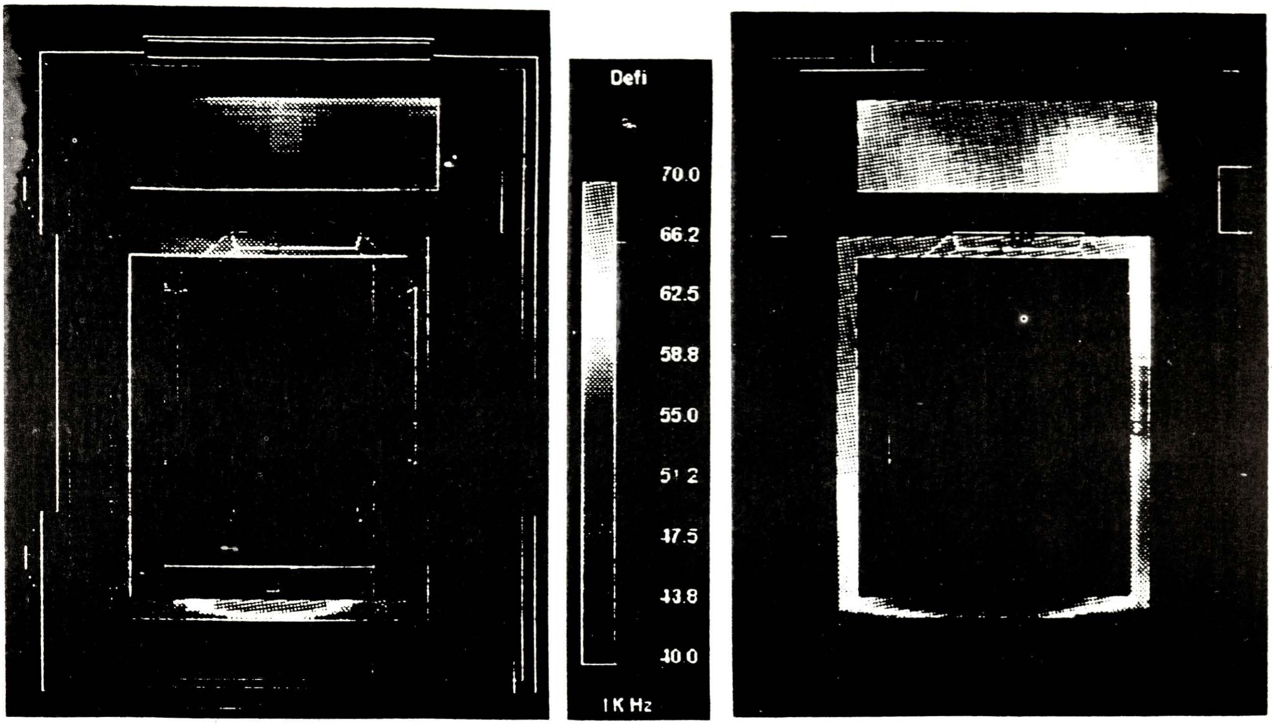

(a) (b)

Figure 4 Predicted contours for D50 at 1 KHz for: (a) the existing room; and (b) the room incorporating the recommended acoustic treatments.

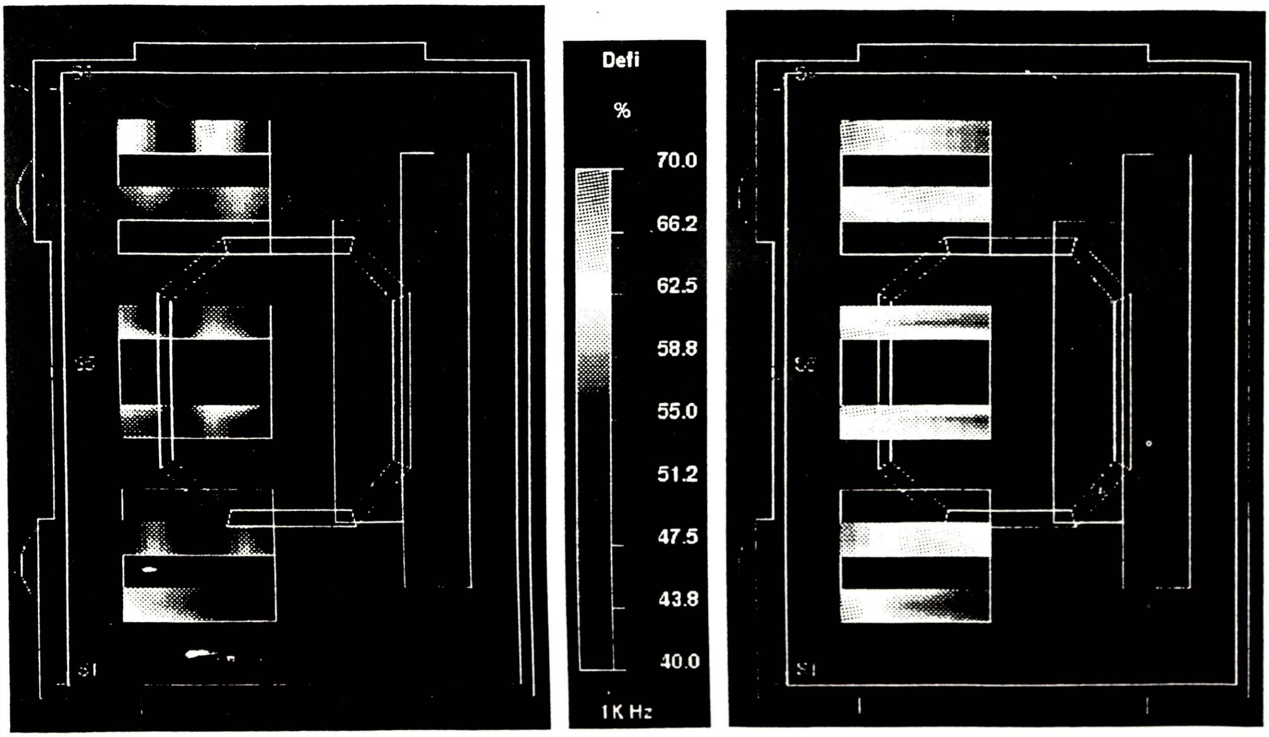

(a) (b)

Figure 5 Predicted contours for D50 at 1 KHz for the speech reinforcement system: (a) in the existing room; and (b) in the room incorporating the recommended acoustic treatments.

CONCLUSION

This paper has presented a comparison of the analysis and prediction methods which utilise modern computer software packages applied to complex rooms. Good agreement was found between the traditional method and the MLSSA method for determination of reverberation time. Reasonable agreement was also found between the MLSSA method and the predictive RAYNOISE method for more sophisticated indicators of speech clarity such as Definition (D50). Examples were given to illustrate how the prediction method could be used to investigate a range of options for acoustic treatments to the room and for the design of the speech reinforcement system.

ACKNOWLEDGEMENT

The results presented were obtained as part of a project commissioned by the Sound and Vision Office, Department of the Parliamentary Reporting Staff. Their support and approval to release the results are gratefully acknowledged.

REFERENCES

1 D D Rife "The MLSSA measurement system", *Sound and Video Contractor*, Oct, 36-56 (1989).

2 J C S Lai "Some applications of geometrical acoustics", *MECH 94 Congress,* Perth, May, 213-218 (1994)

3 H Lehnert 'Systematic errors of the ray-tracing algorithm. *Applied Acoustics* , vol. 38, 207-221 (1993).

4 H. Kuttruff *Room acoustics*, 2nd edition, Applied Science Publishers Ltd., London (1979).

AN INVESTIGATION OF A POSSIBLE MUSIC PERCEPTION TEST FOR ROOM ACOUSTICS

J. Y. Jeon and F. R. Fricke
Department of Architectural and Design Science
University of Sydney, NSW 2006

ABSTRACT

Speech intelligibility testing has been undertaken to investigate the suitability of rooms for speech. There is no musical equivalent to speech intelligibility testing. This paper describes the results of an attempt to develop such a test. Pairs of sounds having differences in duration were presented to a subject using a 2AFC experimental procedure. The stimuli were varied in their waveform through a digital signal processor which simulated different rooms and reverberation times. The subject was asked to determine differences in signals under the different room conditions.

INTRODUCTION

One of the difficulties encountered in improving the design of auditoria for music is that it is difficult to get reliable and repeatable information on whether any change to the acoustics of a space is an improvement or not. Probably as a response to this little emphasis is placed on subjective assessments of acoustics. The preference for the acoustics of spaces is very subjective. Nevertheless, the ability to hear subtle changes in musical sounds almost certainly forms part of an individual's assessment of a space. In this work the ability of a subject to hear a small change in the duration of a sound is investigated as one measure of 'music intelligibility' and hence acoustic performance.

An experiment was first carried out to find the effects of reverberation time on duration discrimination. The reverberation time varied in a room acoustic condition 'CHURCH' implemented by a digital signal processor (YAMAHA DSP-1). The subject's task was to judge duration difference in pairs of signals processed with different reverberation times. In a second series of experiments the subject was again presented with pairs of stimuli, processed with five different room conditions, which had an equal reverberation time. Pure tones were used with a standard stimulus duration of 200 msec as it was found that the difference limen (DL) was constant for durations between 100 msec and 2 sec (Jeon and Fricke 1995).

Divenyi and Hirsh (1974) pointed out that auditory discrimination performance is substantially affected by at least four factors: (1) the number of stimuli in the sequence of items to be discriminated, (2) how the sequences are presented (separate presentations or continuously), (3) the kind of task which the subject must perform, and (4) the amount of training the subject has had. Allan and Kristofferson (1974) also revealed in their investigations, that the amount of practice a subject has with a particular set of duration values is a critical variable.

Another practical application of these results concerns the use of musician subjects for studies of the auditory system. As Spiegel and Watson (1984) pointed out, use of trained musicians may eliminate a subpopulation that has not yet learned how to, or who cannot, listen carefully. The experiments reported in this paper employed a highly practiced musician for duration discrimination. The subject had thresholds within 10 dB of the ISO-1964 standard at all audiometric frequencies.

EXPERIMENT I : THE EFFECT OF REVERBERATION TIME ON DURATION DISCRIMINATION

SUBJECT

There was one female subject. She had 17 years of musical experience and had previously taken part in other experiments on auditory duration assessments.

APPARATUS

A Macintosh IIci computer controlled the experiments. The MacRecorder sound system with its application, SoundEdit™, enabled the recording, editing, playing and storing of sounds. The generated pure tone stimuli were saved in a range of file formats. Then the tones were filtered by a bandpass filter KROHN-HITE 3700 (low cut-off 800 Hz and high cut-off 1.2 kHz) and fed into YAMAHA Digital Sound Field Processor, DSP-1. Stimuli were presented by an application, MacroMind Director. MacroMind Director was originally used as computer animation and presentation package, but the control for presentation of audio only was used in this experiment.

The processed stimuli were amplified (JVC Integrated Stereo Amplifier) and presented through four speakers (two in front and two behind). The subject was asked to respond on answer sheets. The experiment was undertaken in an anechoic room.

STIMULI

In the present work, stimulus pairs had a frequency of 1 kHz. Pairs of standard (S) and comparison (C) tones (where S was 200 msec and the values of C/S were 1.03, 1.06, 1.09, 1.12, and 1.15) were generated and processed using the 'CHURCH' room condition.

PROCEDURE

The processed stimuli with 'CHURCH' condition were presented in eight different reverberation times from 0.5 sec to 4.0 sec. The subject was presented with a pair of stimuli composed of different durations and asked to select the sound she believed to be longer.

The ISI (Interstimulus interval) for each pair of sounds was 0.5-1.0 sec while the time between pairs of sounds was 2-2.5 sec. All the stimuli pairs were presented 160 times and the order of the longer and shorter duration stimuli was equally distributed. The subject served three hours a day and completed the experiment over two weeks. The data for the experiment were collected using a 2AFC procedure.

RESULTS AND DISCUSSION

The proportion of correct responses, P(C), obtained in an investigation of effects of reverberation time difference on duration judgements is shown in Fig. 1. The arithmetic means of the P(C)s in the five duration cases (C/S = 1.03-1.12) from the 160 trials were calculated for each reverberation time.

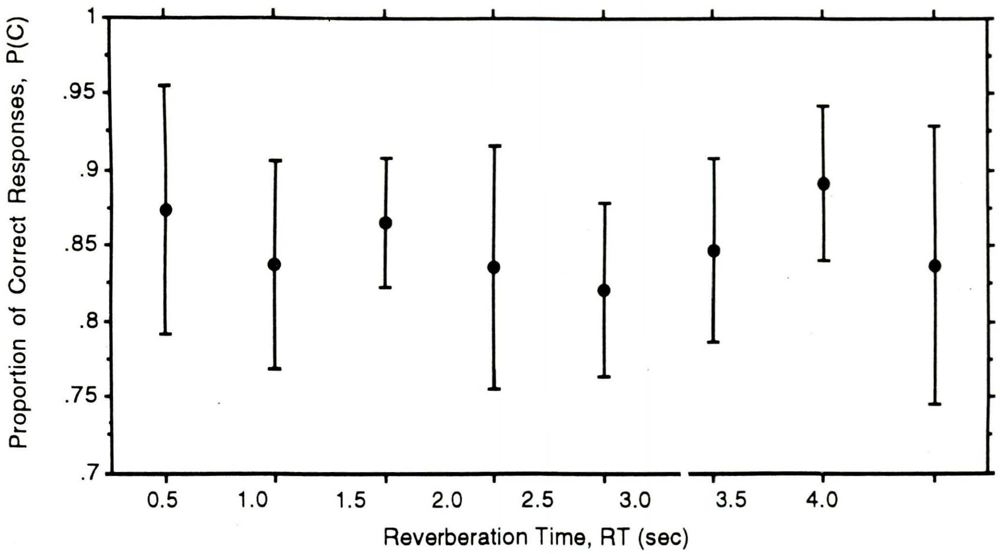

Fig. 1 - Proportion of correct responses, P(C), obtained by a subject, for different reverberation times, with C/S = 1.03-1.12. Pure tones were processed with the 'CHURCH' sound field before presented to the subject.

As shown in Fig. 1, P(C) was around 0.85 for all the reverberation times from 0.5 to 4.0 sec. When the duration was varied for the comparison tone of each sound pair, but fixed for the standard stimulus within a pair, duration discrimination performance was not affected by reverberation time for the 'CHURCH' sound field. This is possibly because the difference in duration is within main envelope, not in the decay envelope. Length differences of main envelope are shown in Fig. 2 (See the differences between (a)-(e) and (a')-(e')). Length changes in main envelope have a more discernible effect on timing discrimination than the length of decayed envelope.

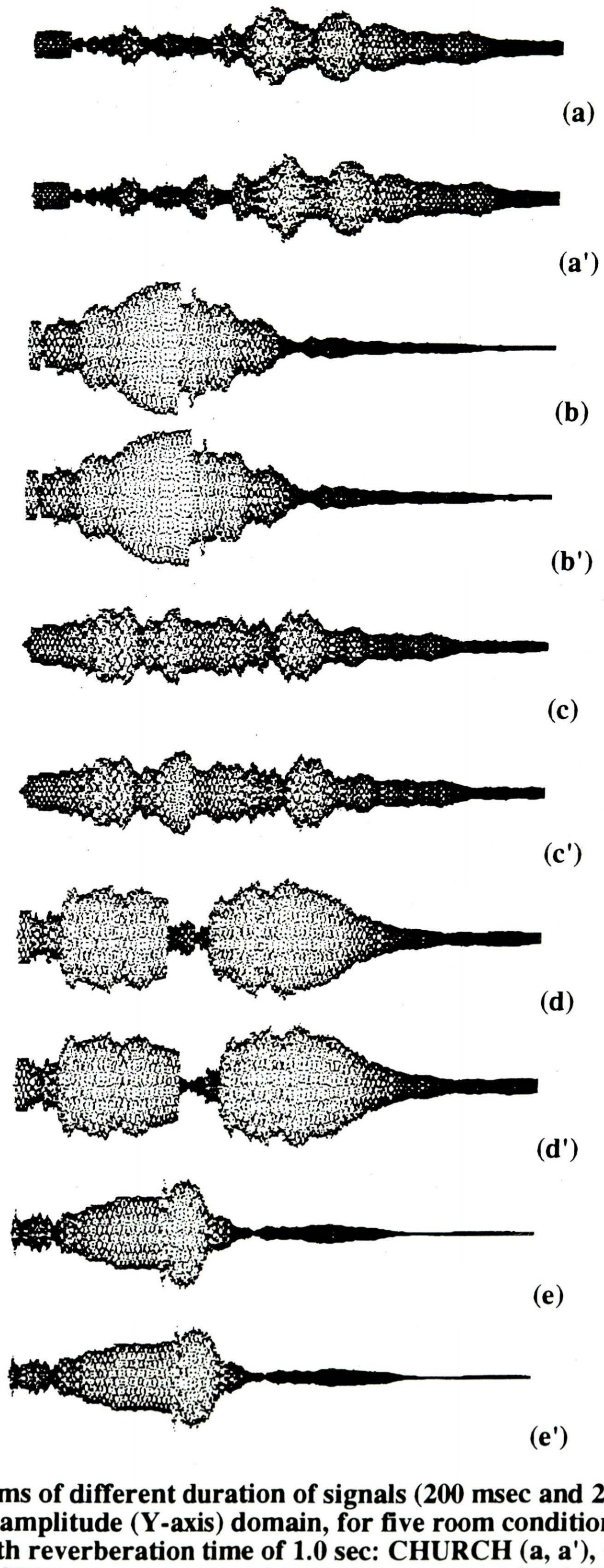

Fig. 2 - Waveforms of different duration of signals (200 msec and 220 msec) in time (X-axis) and amplitude (Y-axis) domain, for five room conditions, using a 1-kHz pure tone with reverberation time of 1.0 sec: CHURCH (a, a'), CHAMBER (b, b'), MUENSTER (c, c'), PAVILION (d, d'), and WAREHOUSE (e, e').

EXPERIMENT II : THE EFFECT OF ROOM CONDITIONS ON DURATION DISCRIMINATION

SUBJECT

The female musician subject in the previous experiment again served in the present experiment.

APPARATUS

The apparatus used for this experiment was the same as that described for the preceding experiment. The listening and answering procedure was also carried out in the same way as in the first experiment.

STIMULI

In this experiment, stimulus pairs were again used with a frequency of 1 kHz. Pairs of standard (S) and comparison (C) tones were generated and processed with five room conditions, which were 'CHURCH', 'CHAMBER', 'MUENSTER', 'PAVILION' and 'WAREHOUSE'. S was 200 msec and the values of C/S reduced to 1.02, 1.04, 1.06, 1.08, and 1.10.

PROCEDURE

The processed stimuli for five room conditions ie the simulated were presented in a reverberation time 1.0 sec. The subject was presented with a pair of stimuli composed of different durations and asked to select the sound to be believed longer.

The ISI for each pair of sounds was 0.5 sec while the time between pairs of sounds was fixed at 2 sec. All the stimuli pairs were presented 160 times and the order of the longer and shorter duration stimuli was equally distributed. The subject served three hours a day and completed the experiment over two weeks. The data for the experiment were collected using a 2AFC procedure.

RESULTS AND DISCUSSION

The proportion of correct responses, P(C), obtained in an investigation of effects of room condition on duration judgements is shown in Fig. 3. The arithmetic means of the P(C)s in the five duration cases (C/S = 1.02-1.10) from the 160 trials were calculated for each room condition.

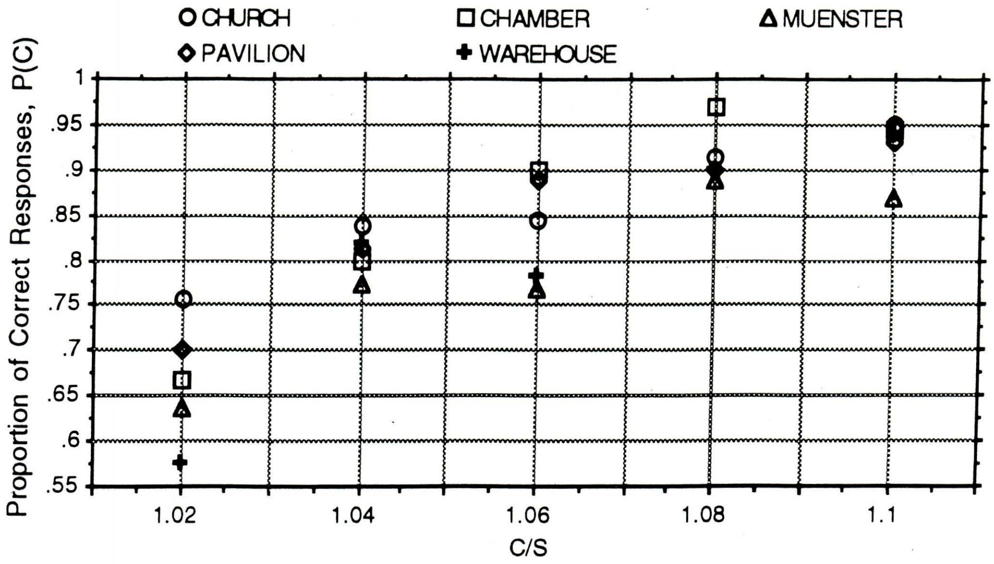

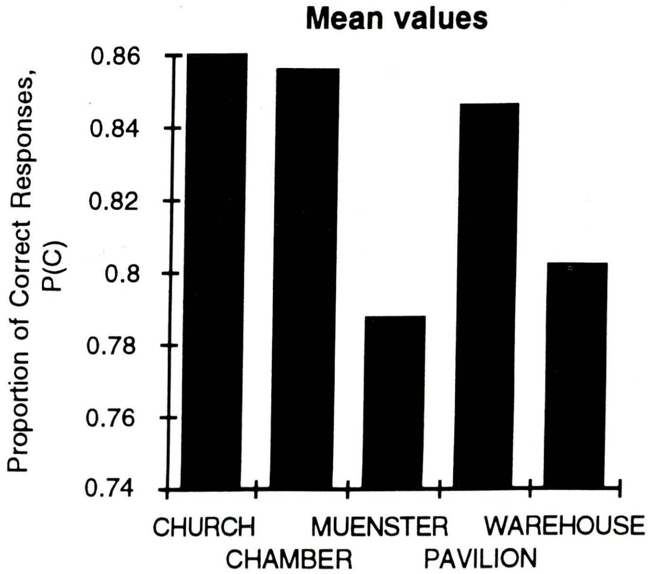

Fig. 3 - Proportion of correct responses, P(C), obtained by the subject for five different room conditions, using pure tones with a standard stimulus duration of 200 msec. and a reverberation time of 1.0 sec.

As shown in Fig. 3, P(C) varied from 0.79 ('MUENSTER') to 0.86 ('CHURCH'), ie duration discrimination performance was affected by room conditions. The reason may be because the sounds processed in different sound fields had particular waveforms, especially in relative amplitudes and envelope variations, which could be represented as 'signal voltages' (Creelman 1962).

From the envelope variations in different room conditions, shown in Fig. 2, it is likely that the signal in the 'CHAMBER' (b) sound field has higher amplitude and less variation. The signal in the 'PAVILION' (d) sound field has relatively high amplitude but has more variation than in the 'CHAMBER'. The signal in the 'WAREHOUSE' (e) sound field has less variation but has lower amplitude than in the 'PAVILION'. The processed signals in both the 'CHURCH' (a) and the 'MUENSTER' (c) sound fields have relatively lower amplitude and more variation than in any other sound field.

The signal in the 'CHURCH' sound field has even more variation but has lower amplitude than in the 'MUENSTER'. The duration discrimination performance in the 'CHURCH sound fields should have scored the lowest. However, from the previous experiment using the 'CHURCH' sounds, the subject seemed to have been familiar with the 'CHURCH' sounds and scored the highest P(C).

DISCUSSION AND CONCLUSIONS

The above experiments represent a first step towards developing a 'music perception' test for auditoria. There is obviously a long way to go and it is by no means clear whether variations in the perception of duration, pitch or intensity of sounds in anyway correlate with preferences for the acoustics of auditoria. So far the results have not been encouraging. The variation of the Proportion of Correct Responses, P(C), with reverberation time, shown in Fig. 1, is small and not monotonic, suggesting that the perception of duration differences is not a good measure of the importance of reverberation time at least. (This result may well be a function of the room simulation technique so that testing in real rooms must be undertaken.) The variation of P(C) with room type is more encouraging, at least for small values of C/S.

Future work will concentrate on looking at the effect of the sample length, undertaking preference assessments and discrimination testing in real rooms. If this is successful or encouraging, the work will be extended to include perception of pitch and intensity differences, timbre changes and changes in the rise/decay characteristics of sounds.

The perception of music and the importance of hall acoustics are obviously very complex matters. Given the range of individual responses to particular performances and concert halls (Haan and Fricke, 1994) it will not be possible to accurately predict responses to concert hall acoustics. Using information on just noticeable differences could provide a valuable tool for investigating the importance of various factors on the acoustics of rooms for music as the perception of small changes and nuances is fundamental to the interpretation of music.

REFERENCES

ALLAN, L. G., AND KRISTOFFERSON, A. B. (1974). Psychophysical theories of duration discrimination, Percept. Psychophys. 16, pp. 26-34.

CREELMAN, C. D. (1962). Human discrimination of auditory duration, J. Acoust. Soc. Am. 34, pp. 582-593.

DIVENYI, P. L., AND HIRSH, I. J. (1974). Identification of temporal order in three-tone sequences, J. Acoust. Soc. Am. 56, pp. 144-151.

HAAN, C. H., AND FRICKE, F. R. (1994). The use of neural network analysis for the prediction of acoustic quality of concert halls, Proc. WESTPRAC V, Seoul.

JEON, J. Y., AND FRICKE, F. R. (1995). The effect of frequency on duration judgements, Acustica 81, To be published.

SPIEGEL, M. F., AND WATSON, C. S. (1984). Performance on frequency-discrimination tasks by musicians and nonmusicians, J. Acoust. Soc. Am. 76, pp. 1690-1695.

OPTIMISATION OF BUILDING VENTILATION OPENING SIZE IN A NOISY ENVIRONMENT

Chris Field and Fergus Fricke
Department of Architectural and Design Science
University of Sydney

This paper addresses the problem of achieving noise reduction in buildings that are exposed to road traffic noise while satisfying ventilation requirements. A design process has been developed that optimises the size of an opening in a building for ventilation while estimating the attenuation of external traffic noise inside the building. A fan with associated duct work is fitted to an opening in the building facade to provide ventilation. Therefore the optimisation of the opening size is used to determine the necessary fan characteristics which best suits the opening. The process allows the user to specify particular environmental conditions including traffic noise spectra, required ventilation rates, ventilation fan type, ventilation duct characteristics and building facade properties. Model results are presented indicating an optimum ventilation opening size with the associated internal noise levels. The work is part of a larger study into reducing noise through ventilation openings.

INTRODUCTION

The noise from road traffic in urban areas is a well known problem throughout the world. While there is an obvious requirement to reduce the level of external noise entering the building enclosure, ventilation standards must also be adhered to. Unfortunately, the methods of obtaining satisfactory levels of noise reduction and ventilation conflict. Therefore there must be a point of compromise between these two functions.

Extensive research has been carried out into the shielding of external noise provided by buildings (Lawrence 1980,1983; Mizia 1983; Cook 1980). While the need for ventilation is acknowledged, a method of ventilation and the noise characteristics associated with it has not been included in the research. Similarly, many references concerning heating, ventilation and air-conditioning systems (including fan engineering) concentrate on the resulting sound levels in enclosures due to ventilation fans or devices performing the ventilation process, without taking into account other external noise sources (such as road traffic) affecting the enclosure being ventilated (Osborne 1977, Daly 1988, SRL 1991, SMACNA 1990, ASHRAE 1991). An important combination of these two functions involves a design process that optimises the size of an opening in a building to satisfy ventilation requirements while attenuating external noise from road traffic and noise generated by the particular ventilating device. This paper outlines the development of such a design process. Two case studies are presented to demonstrate the process.

THE DESIGN PROCESS

OPTIMISATION OF BUILDING VENTILATION OPENING SIZE EXPOSED TO EXTERNAL NOISE

A design process has been developed that optimises the size of an opening in a building for ventilation while estimating the attenuation of external traffic noise and ventilation fan noise level inside the building. To provide ventilation, a fan with associated duct work is fitted to the opening in the building facade containing a window. Therefore the optimisation of the opening size is used to determine the necessary fan characteristics which best suits the opening. A spreadsheet program was used to provide a range of opening sizes in the wall for ventilation so as to obtain an optimum hole size.

Initial Conditions

Some initial conditions had to be established to begin the design process. Although particular conditions have been chosen, these could be set at any reasonable values according to the desired environment. This allows a sensitivity analysis of the results of the design process to be carried out. The dimensions of the room to be ventilated were set to be similar in size to a normal bedroom, measuring $3\times5\times2.4$ m high. These dimensions were used by Lawrence and Burgess (1983) for a bedroom in an experimental building used to measure the reduction of traffic noise by facades containing windows. The facade exposed to traffic noise measured 5×2.4 m high. The design process was developed to allow a road traffic noise spectrum in octave bands from 63 Hz to 8 kHz to be used as the source of external noise. Typical values were taken from a relevant reference (Nelson 1987). The ventilation rate of the room was required. Appropriate ventilation requirements were taken from Australian Standard AS1668 Part 2-1980. Different ventilation rates could be chosen according to the class of occupancy involved. The option was made for an inlet duct to attenuate fan and traffic noise entering the building through the ventilation opening (assuming that the air intake was on the noisy side of the building and the exhaust on the quiet side). The length of duct, number of bends and type of duct lining could be chosen as required. Calculations could be carried out without an inlet duct attached. The duct was assumed to be on the inside the building and that no duct breakout occurred into the room. Appropriate values for the absorption coefficient of the duct lining in octave bands from 125 Hz to 4 kHz were taken from a relevant reference (Osborne 1977). The transmission loss characteristics of the walls of the building were chosen to correspond to single leaf brick masonry walls and the windows were chosen to be double glazed with an area of 10% of the total wall area (Bies et al. 1988).

Fan Selection

To select a suitable fan, the fan pressure needed to circulate the required flow Q had to be determined. The total pressure drop of the inlet duct system is estimated in a similar manner to that adopted in common fan engineering references (Daly 1988, SMACNA 1990, ASHRAE 1991, Osborne 1977) i.e. the total pressure drop is obtained by adding together the elements of total pressure drop around the system including:

- Losses at entry to the inlet duct from atmosphere
- Losses due to friction along the duct length
- Losses at bends
- Losses at discharge from the system to atmosphere

The total pressure drop due to air flowing into and out of the room is calculated using the following equation:

$$\Delta P_{TOTAL}=\left(\frac{0.02L}{D}+K_{entry}+nK_{bends}+\frac{0.02L_{wall}}{D}+K_{exit}\right)\frac{1}{2}\rho V_{air}^2 \quad \text{[Pa]} \qquad (1)$$

where:
L = length of inlet duct (m)
D = diameter of duct to fit opening (m)
K_{entry} = coefficient accounting for losses at entry of inlet duct (Daly 1988)
K_{bends} = coefficient accounting for losses at the bends of inlet duct (Daly 1988)
L_{wall} = wall thickness
n = number of bends
K_{exit} = coefficient accounting for losses at discharge to atmosphere (Daly 1988)
ρ = air density (kg/m^3)

This pressure is the fan pressure needed to circulate the required flow Q. Normally there would be further resistance due to air flow through the interior of the rest of the building (as the room would be joined to other rooms). It has been assumed, however, that the air flowing out of the room flows to the surrounding atmosphere. Since the average velocity of air through the ventilation opening is inversely proportional to the area of the opening, the total fan pressure required to circulate the flow decreased rapidly at a rate of $1/A^2$ as the area of the opening A increased.

Obviously the most reliable method of determining the sound power level of a particular fan would be to obtain sound power levels in each octave frequency band from a fan manufacturer. In this design stage of the ventilation system, however, only the required duty has been established. The type of fan to be used has not been decided upon. Therefore an empirical formula must be used to estimate the likely sound power level that will be produced. An approximate idea of the sound power level of the chosen fan was gained from the following equation (SRL 1991):

$$L_w = 10\log Q + 20\log \Delta P_{total} + 37 \qquad [dB] \qquad (2)$$

There are correction factors for different fan types in different frequency octave bands. These have been incorporated into the design process to illustrate the difference in optimum opening size according to fan type (SRL 1991). The application of these correction factors allows the sound power level of a fan for a particular ventilation opening size to be calculated in octave bands.

Attenuation of Noise Provided by Lined Inlet Duct

The level of attenuation provided by the inlet duct is a function of the absorption coefficient of the duct lining. For a straight length of duct L metres, variations of Sabine's equation have been used to provide reasonable estimates.

Estimates of the attenuation provided by lined bends were very difficult to find in relevant references. The data that were found are difficult to compare because many different measurements techniques are used and the fact that there is no consistent nomenclature for the noise reduction provided by bends. Field measurements indicate that the attenuation due to a 90° bend in the duct work would be 10 dB higher than that for the same length of lined duct (Beranek 1988). This is valid provided the lining extends at least two diameters of the duct each side of the bend. Therefore the total attenuation provided by a lined duct of diameter D metres with n 90° mitre bends can be calculated using the following equation:

$$\text{Total attenuation} = 4.2\,\alpha^{1.4}\left(\frac{L}{D}\right) + n(8.4\,\alpha^{1.4} + 10) \qquad [dB] \qquad (3)$$

where n = number of bends
α = absorption coefficient of duct lining

The absorption coefficient is a function of frequency. Typical values in octave frequency bands were taken from a relevant reference (Osborne 1977) to obtain the total attenuation provided by the inlet duct.

Equivalent Transmission Loss of Wall with Inlet Duct Attached

The transmission loss of a wall with a window and an opening for ventilation with an inlet duct attached was calculated in two stages. Firstly, the equivalent transmission loss of the building facade with a hole and window in it, calculated in octave bands, was determined as an overall area-weighted average of the wall, window and duct cross sections. For this calculation, equation (4) was used. Obviously as the percentage open area increased, the equivalent transmission loss of the wall, window and hole decreased. The area of the hole dictated the level of transmission loss provided by the composite combination. The equivalent transmission loss with the inlet duct attached was then calculated using an equation similar to equation (4). The equivalent transmission loss decreased in a similar fashion, but at a slower rate, however, than that for a wall with only a hole it since the inlet duct has the ability to attenuate noise.

$$TL_{eq} = -10\log\left(\frac{A_{wall}\,\tau_{wall} + A_{hole}\,\tau_{hole} + A_{window}\,\tau_{window}}{A_{total}}\right) \quad [\mathrm{dB}] \qquad (4)$$

where $\tau_{wall} = I_{t\ wall} / I_i$

$\tau_{hole} = I_{t\ hole} / I_i$

$\tau_{window} = I_{t\ window} / I_i$

The terms I_t and I_i are the transmitted and incident sound intensities respectively.

Noise Entering Room

The noise entering the room will be a combination of fan and traffic noise that has been attenuated by the lined inlet duct and building facade.

The sound pressure level of traffic noise entering the room is determined by subtracting the equivalent transmission loss in each octave band calculated in the equation similar to equation (4), from the traffic noise spectrum in octave bands set in the initial conditions. Since the attenuation provided by the composite building facade decreased as the area of the opening for ventilation increased, the level of traffic noise entering the room increased as the area of ventilation opening increased. The traffic noise entering the room, however, was largely low to mid-frequency noise (A-weighted). The noise levels in the 250 Hz to 1 kHz octave bands were the only significant contribution to the overall traffic noise level in the room. Hence the contribution of the traffic noise in the room to the overall sound level in the room is only significant for large ventilation openings in the building facade because of the lower equivalent transmission loss provided by the wall, window, hole and inlet duct at larger ventilation opening sizes.

In addition to the fan noise being attenuated by the lined inlet duct, end reflection occurs at the end of the duct run, unless the duct diameter is very large (compared to the wavelength of sound). The maximum end reflection occurs at low frequency as the wavelength is greatest compared with the size of the opening. Equation (5) was used to calculate the end reflection loss depending on frequency and diameter of the duct being used (SMACNA 1990):

$$\Delta L = 10\log\left[1 + \left(\frac{c_o}{\pi \times f \times D}\right)^{1.88}\right] \quad [\mathrm{dB}] \qquad (5)$$

where:

c_o is the speed of sound in air (344m/s)

f is the octave band frequency

D is the diameter of the duct

The sound power level of the fan entering the room in dB will therefore be:

$$L_{w\ room} = L_{w\ fan} - \text{attenuation by inlet duct} - \text{end reflection} \qquad (6)$$

where the attenuation by the inlet duct in each octave band is calculated from equation (3) and the end reflection loss in each octave band for a particular duct area is calculated in equation (5).

The sound power level of the fan in the centre of the room is converted to an equivalent sound pressure level using the standard equation for a point source located in the centre of the wall, assuming the fan noise radiates hemispherically on a single reflecting surface. The average absorption of the interior of the room was also taken into account:

$$L_{p\ fan} = L_{w\ room} + 10 \log\left(\frac{D}{2\pi r^2} + \frac{4(1-\bar{\alpha})}{S\bar{\alpha}}\right) \quad [dB] \qquad (7)$$

where $L_{w\ room}$ = fan L_w calculated in eqn (6)
D = directivity of fan
$\bar{\alpha}$ = average room absorption coefficient
S = surface area of room (m^2)
r = distance from duct exit to room centre (m)

The sound pressure level of the fan in the centre of the room decreased as the size of the ventilation opening increased in a similar fashion to the sound power level since all the terms in equation (7), except the fan sound power level $L_{w\ room}$, are constants.

Total Sound Pressure Level in Room

The total sound pressure level in the room could then be determined by adding the contributions made by the traffic noise entering the room and the noise from the fan entering the room. The overall sound pressure level of the traffic noise in the room was determined by adding the equivalent squared pressures of the traffic noise in the eight octave bands and then converting back to a total sound pressure level. Similarly, the squared pressures of the fan noise in the room were combined and converted to a total sound pressure level. The overall sound pressure level in the room due to the fan and traffic could then be calculated using a similar technique

The fact that the sound pressure level of traffic noise in the room increases as the size of the ventilation opening increases and the fact that the sound pressure level of the fan in the room decreases as the size of the ventilation opening increases indicates that there will be a particular ventilation opening size where the total sound level in the room due to these two external noise sources is a minimum.

CASE STUDIES

VARIATION OF FAN TYPE

The correction factors for different fan types previously mentioned indicate that the noise level in the room and hence the optimum ventilation opening size is greatly influenced by the type of fan used for ventilation. Figure 1 shows the total sound pressure level in the room as a function of percentage open area (corresponding to the size of the opening for ventilation) for different types of fans. The different fan types considered were forward curved centrifugal, backward curved centrifugal, radial, axial and propeller fans.

Forward curved and backward curved centrifugal fan types were the quietest while the radial type was the noisiest for the same volume flow and fan pressure. Correspondingly, the optimum ventilation opening size for forward curved and backward curved centrifugal fans is smaller, allowing a more compact size for a given duty than other fan types. The smaller ventilation opening size also increases the effective transmission loss of the building facade to the external traffic noise. Therefore the type of fan used will also affect the amount of traffic noise entering the room in addition to the amount of fan noise entering the room. From Figure 1, the optimum ventilation opening size for the quietest fans (forward and backward curved centrifugal) were approximately 1 % of the total facade area exposed to external noise and 1.6 % for the noisiest fan (propeller). From the nature of the curve for areas greater than the optimum percentage area, it is reasonable to expect that any opening size between 1 and 4% of the total wall area could be considered for ventilation purposes.

VARIATION OF TRAFFIC NOISE CHARACTERISTICS

The design process required that the traffic noise spectrum be set in the initial conditions. The typical spectrum chosen (Nelson 1987) characterised urban flow traffic (below 60 km/h) directly outside the building facade, which is dominated by the large amount of acoustic energy concentrated in the 63 Hz and 125 Hz octave bands (due to exhaust noise generated by heavy diesel commercial vehicles). Obviously this type of traffic noise will not always be present. For traffic flowing at steady speed (greater than 80 km/h) the spectrum contains energy concentrated at higher frequencies due mainly to tyre/road interaction noise (not present at low speeds) and mechanical noise from power train components. The nature of the noise will also vary with distance from the building facade. Hence it is necessary to investigate the effect of different traffic noise characteristics on the optimum ventilation opening size in the building facade exposed to the traffic noise.

A traffic noise spectrum with acoustic energy concentrated in the low frequency bands was used to simulate suburban traffic. Likewise, a spectrum with energy concentrated in the high frequency bands was used to simulate freely flowing traffic. To allow a comparison to be made between the two forms of traffic, the dB(A) values of the two spectra were kept equal. Figure 2 shows the total sound pressure level in the room for various ventilation opening sizes predicted using the design process. The optimum ventilation opening size for the suburban traffic noise was 1.0 % of the total wall area and was 1.5 % for the freely flowing traffic (both points are shown on Figure 2). This indicates that a larger opening size can be used for the freely flowing traffic because the building facade and attenuating duct are able to attenuate the high-frequency noise more effectively than the low-frequency dominant suburban traffic noise. The difference in attenuation of the two types of traffic flow can be seen by the distance between the two curves (the ventilation opening sizes where the two curves overlap is the region where the fan noise is dominant).

CONCLUSIONS AND DISCUSSION

From this work it is concluded that the optimum size fan for a ventilation opening, when there is a fan and a short length of lined duct, is about 1-1.5 % of the total wall area. This compares to about 5-10 % of openable area when natural ventilation is utilised. The difference in noise level inside a building, with brick veneer construction, facing a road will be approximately 17 dB(A).

If only a fan is used (without a lined duct), the optimum opening area for minimal sound level will be 0.75 % with a sound level reduction of 9.2 dB(A) over the case for 10 % of the facade open for natural ventilation. Compared to the reduction due to a barrier this is significant.

The work described forms part of a project to reduce noise entering building ventilation openings. Future work will be concerned with developing alternative methods such as 'intelligent' openings, noise cancellation and systems where there is a road barrier between the inside and outside of the building.

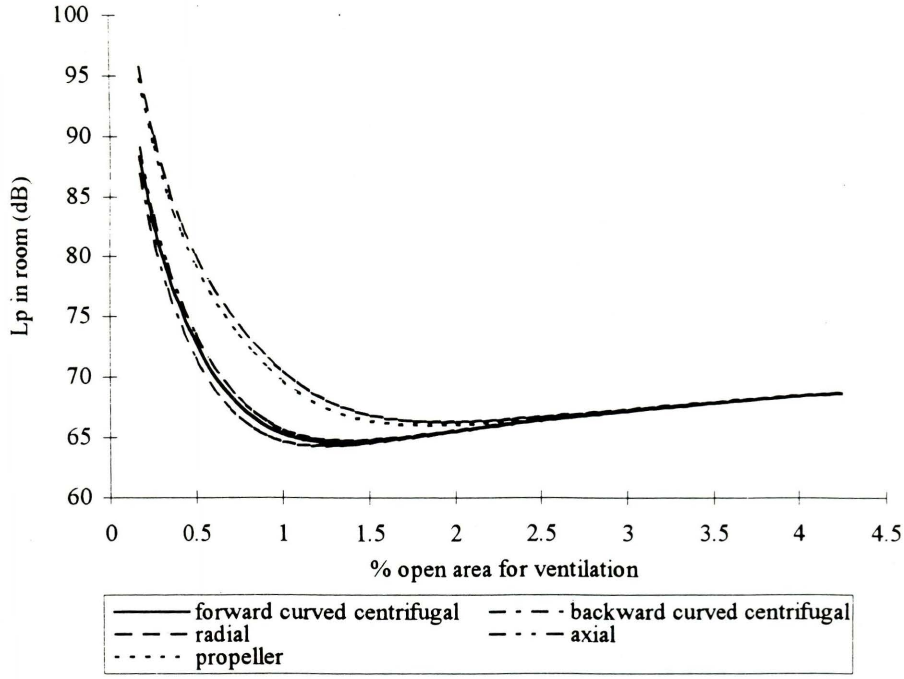

Fig. 1 - Total Sound Pressure Level in Room (different fan types) vs Percentage Open Area for Ventilation

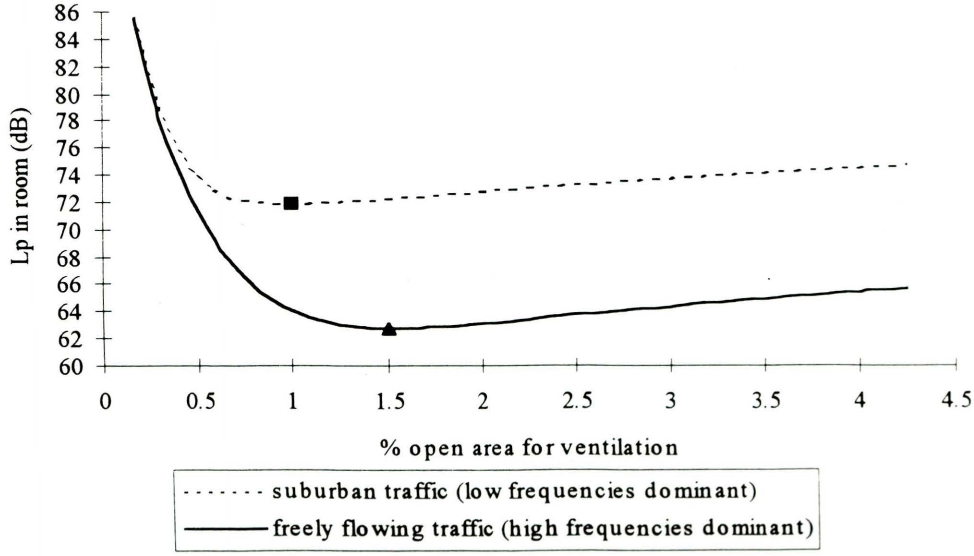

Fig. 2 - Total Sound Pressure Level in Room (different types of traffic noise) vs Percentage Open Area for Ventilation

REFERENCES

ASHRAE (1991). **ASHRAE Handbook-Applications**, American Society of Heating Refrigerating and Air Conditioning Engineers, Chapter 42 Sound and Vibration Control.

Australian Standard 1668 Part 2-1980, **Ventilation Requirements**, p9.

Beranek, L.L. ed. (1988). **Noise and Vibration Control**, Institute of Noise Control Engineering.

Bies, D.A. and Hansen, C.H. (1988). **Engineering Noise Control**, Unwin Hyman Ltd.

Cook, K.R. (1980). **Sound Insulation of Domestic Roofing Systems: Part 1**, Applied Acoustics 13, pp109-120.

Daly, B.B. (1988). **Woods Practical Guide to Fan Engineering**, Woods of Colchester.

Lawrence, A. (1980). **Measurement of Traffic Noise Shielding Provided by Buildings**, Applied Acoustics 13, p211-225.

Lawrence, A. and Burgess, M. (1983). **Reduction of Traffic Noise by Facades Containing Windows**, Proc. Aust. Acoust. Soc. Conference on the Economics of Noise Control, Tanunda, South Australia.

Mizia, U and Fricke, F. (1983). **Putting Windows Where They Ought To Be**, Bulletin Aust. Acoust. Soc. vol 11 no3, p105-109.

Nelson, P.M. (1987). **Transportation Noise Reference Book**, Butterworth and Co. Ltd.

Osborne, W.C. (1977). **Fans**, Pergamon Press Ltd.

Sheet Metal and Air Conditioning Contractors' National Association Inc. (1990). **HVAC Systems-Duct Design**, SMACNA.

Sound Research Laboratories Limited (1991). **Noise Control in Industry**, Sound Research Laboratories Limited.

ACKNOWLEDGEMENTS

This work has been supported partly by a research grant from the New South Wales Roads and Traffic Authority and partly by an Australian Postgraduate Research Award.

INTER-LABORATORY COMPARISON OF SOUND TRANSMISSION LOSS: REFERENCE SPECIMEN STUDY

P.P. Narang
CSIRO Division of Building, Construction and Engineering (DBCE)

INTRODUCTION

Measurement of airborne sound transmission loss (STL) of partitions is one of the most common types of standard measurement carried out on a commercial basis at the CSIRO DBCE acoustics laboratory at North Ryde. The results of such acoustic tests are often used by the sponsoring companies to: (a) generate product data sheets and sales brochures; (b) meet specific acoustic requirements laid down by architects or consultants for providing appropriate levels of sound insulation in building projects; and (c) provide evidence to the relevant statutory authorities regarding the ability of their product/system to fulfil the minimum sound transmission class (STC) requirements specified in the Building Code of Australia (AUBRCC 1990). The data is also used by designers and others when comparing various options and when choosing a suitable product or system with known sound insulation characteristics. In view of the importance of these results to the users, it is essential to know the accuracy of the measurements so that comparisons with results from other laboratories can be carried out and judgments about the reliability of the data made. This paper presents and discusses results of STL measurements on a reference specimen developed by the American Society for Testing and Materials (ASTM) for comparison and quality control purposes.

SOUND TRANSMISSION LOSS STANDARDS

In Australia, the Australian Standard AS 1191 (SAA 1985) describes the method of STL measurements in the laboratory. In North America and Canada, the procedure prescribed in the ASTM E90 (ASTM 1990) standard is used for such measurements on building partitions. In Europe and the UK, ISO 140–Part 3 (ISO 1990) is used for STL measurements and the quantity determined is termed as sound reduction index (SRI) rather than STL. From the STL results, the STC is derived in Australia using the criterion of Australia Standard AS 1276 (SAA 1979) which is identical to the criterion of the equivalent ASTM standard E413.

With the increasing internationalisation of Australia's economy, many products and systems are entering the Australian market that were developed and tested for acoustic performance overseas. At present, a majority of such products/systems being imported have STL results determined by laboratories in accordance with either the ASTM, the ISO or the British Standard BS 2750–Part 3 which is identical to ISO 140–Part 3. In all the above standards, the STL (or SRI) is defined in terms of the ratio of incident sound power W_i to the transmitted sound power W_t through the partition which, for measurement purposes, is redefined in terms of the average sound pressure levels on both sides of the partition assuming that the sound fields are diffuse and that the only means of sound transmission is through the partition itself. Then,

$$STL = L_{p1} - L_{p2} + 10 \log_{10} (S/A) \quad (1)$$

$$STL = NR + 10 \log_{10} (S/A) \quad (2)$$

where $L_{p1} - L_{p2}$ (= NR) is the average difference between the sound pressure levels on the two sides of the partition under test. The S and A are the partition specimen area and the equivalent absorption area (calculated from reverberation time) in the receiving room.

As the essential requirements for STL measurements can be met by several methods, the construction of the laboratory test facility for such measurements is not completely specified in any standard but guidelines for achieving ideal diffuse sound field conditions are given. As a result, many laboratories exist with different room volumes and shapes, different size of specimen frames, and have been built using different materials for room surfaces. It is not surprising, therefore, that some differences in results are observed when STL of the nominally same partition system is measured in different laboratories. The ASTM recognised this problem and has developed a standard reference specimen which may be used for comparison of STL measurements.

TEST ROOM AND MEASUREMENT PROCEDURE

The CSIRO DBCE North Ryde acoustics laboratory where the reference specimen was studied comprises a source room and a receiving room with an opening in the specimen frame for installation of test specimens. Both the source and receiving rooms are irregular in shape with approximate volumes of 170 m^3 and 193 m^3 respectively. The rooms are equipped with stationary diffusers and are acoustically isolated from each other so that the specimen serves as the only practical means of sound transmission between the rooms. The nominal opening size of the specimen frame is 3.55 m $\times$ 2.85 m which corresponds to a specimen area of just over 10 m^2 for STL measurements. The STL measurements on the standard reference specimen were made by following essentially the procedure described in AS 1191 (SAA 1985) to a precision better than that recommended in the standard. The frequency range of measurements was extended to include the 63, 80 and 6300 Hz one-third octave bands in addition to the standard 100–5000 Hz range.

REFERENCE SPECIMEN DESCRIPTION AND INSTALLATION

The ASTM reference specimen (ASTM 1991) is basically a single-leaf construction comprising framed steel panels. Attempts were made to duplicate the construction detail given in the ASTM standard in every respect so that the STL results of the ASTM standard could be directly compared with the results presented in this paper. This, however, proved impossible because of the non-availability of certain components in Australia. Some of the differences are minor but are noted in Table 1 to point out factors that could have an influence on the measured results. The ASTM standard prescribes that the mass/area and the thickness of the steel sheets shall be 5.1 $\pm$ 0.7 kg/m^2 and 0.62 mm respectively. The equivalent sheets available and used for the reference specimen construction had a nominal thickness of 0.6 mm and their average mass/area was determined as 4.45 kg/m^2 which is just above the minimum requirement.

For the reference specimen assembly and installation, the steel right angles were cut and welded to form a frame for each sheet. The 1200 mm wide galvanised steel sheets were mechanically fastened to the frames to construct the specimen panel. Three panels were required to fill the nominal 3.55 m wide by 2.85 m high opening in the specimen frame.

The 90 mm wide wood frame was bolted to the 780 mm thick specimen frame with a double bead of caulking between the frame and the perimeter of the laboratory opening. As the bolt holes are located approximately in the middle of the 780 mm thickness of the specimen frame, this resulted in an approximately 345 mm niche on the source room side and a similar niche on the receiving room side. The installation of the specimen panels was carried out by following the procedure described in ASTM E1289.

RESULTS AND DISCUSSION

Of the two quantities NR and $10\log_{10}(S/A)$ calculated for STL determination in the laboratory, the former dominates in the total and the latter acts as a small correction term. Therefore, a given percentage error in determining NR has a much greater influence on the STL than the same error in determining reverberation times for calculating equivalent absorption area. The repeatability of the NR determination was tested by making three sets of NR

TABLE 1

DIFFERENCE BETWEEN ASTM AND DBCE REFERENCE SPECIMEN

ASTM E1289 reference specimen	CSIRO DBCE reference specimen
Galvanised steel sheets of mass/area 5.1 ± 0.7 kg/m^2 and 0.62 mm thickness	Galvanised steel sheets of average mass/area 4.45 kg/m^2 and 0.6 mm thickness
Steel right angles with 25 mm flanges and 3.2 mm thickness	Steel right angles of size $25 \times 25 \times 3.0$ mm
Blind rivets, 3 mm diameter	Blind rivets, 3.2 mm diameter (aluminium rivet with steel mandrel)
Duct tape, 50 mm wide (not specified)	Stylus tapes – duct tape, 50 mm wide
Drywall screws, type W length 31.8 mm	8# × 1.1/4 pan comb S/tapper steel zinc bolts
Bolts (10–24 by inch) with appropriate nuts and washers (not specified)	3/16 by 1 inch, cheese slot steel zinc bolts, 3/16 BSW brass nut with steel washers
Fasteners to hold wood frame to perimeter of test opening	Bolted to the perimeter of test opening with M16 bolts
Caulking – non-hardening (not specified)	Dow Corning silicone and glass sealant
Wood framing (not specified)	Oregon timber
Timber attachment to laboratory opening via bolts at maximum 300 mm centres	Bolt spacing 400 mm centres
Panel sheet size 1200 mm but one sheet to be cut to suit laboratory opening	Two panels nominal 1200 mm wide; third reduced to suit laboratory opening (possible different widths for third panel)

measurements, and the results are shown in Fig. 1. The excellent repeatability observed throughout the frequency range can be taken as a measure of confidence in the results with respect to random, i.e. non-systematic, influences or errors. Similar measurements were made by reversing the source and receiving rooms, and the results shown in Fig. 2 again indicate excellent repeatability throughout the frequency range.

The STL for the reference specimen in the forward and reverse directions determined from the averaged NR values are shown in Fig. 3. The two sets of results agree well with each other but the reverse direction yields slightly lower STL at low frequencies. The agreement at higher frequencies would be expected because room eigenmodes will be more evenly distributed and the effect of changing the roles of the source and receiving room should disappear. At low frequencies when the specimen lateral dimensions are not large in comparison with the wavelength of flexual waves in the specimen, the results may be affected by impedance discontinuity and damping at specimen edges, particularly for materials with low internal damping.

The STC in the forward direction for the reference specimen was derived as 24 with a deficiency of 32 which is the maximum allowable, while it was 23 in the reverse direction. As the forward direction is used for standard STL measurements in the laboratory, these results should be compared with the values given in ASTM E1289 for the reference specimen. This comparison is shown in Table 2 and is plotted in Fig. 4. The frequency range for comparison is restricted to 100–5000 Hz because the published ASTM results are only available for this range. Although the mean STC rating is not provided in the ASTM standard for the reference specimen, substitution of individual STL values yielded a rating of 26.

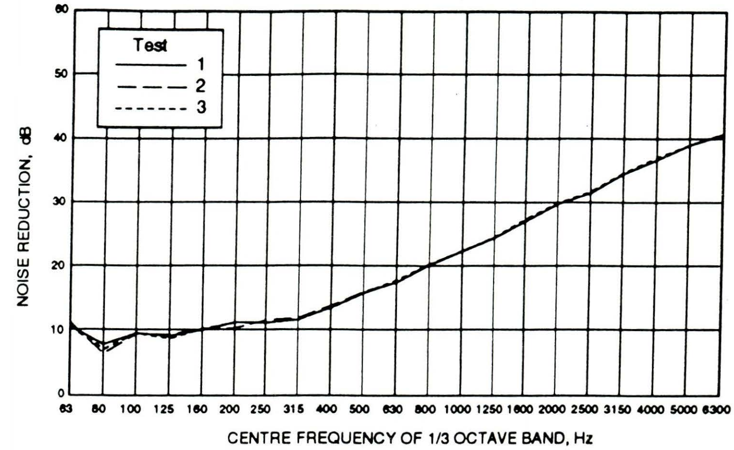

Fig. 1 – Repeatability of noise reduction measurements on the reference specimen – forward direction.

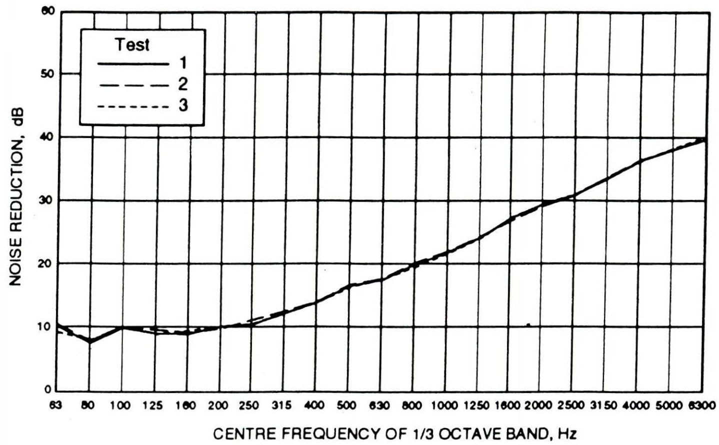

Fig. 2 – Repeatability of noise reduction measurements on the reference specimen – reverse direction.

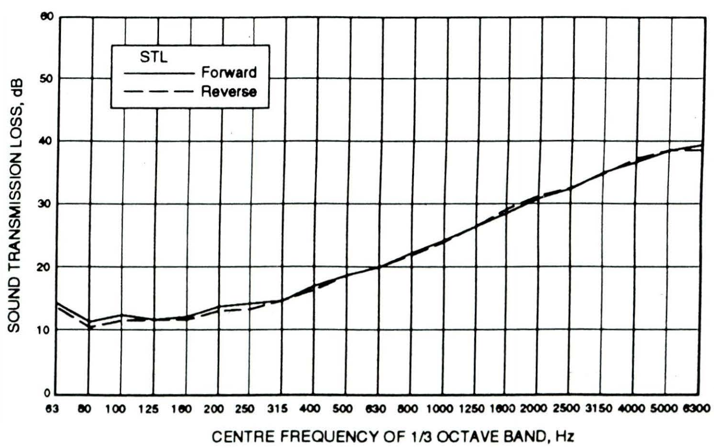

Fig. 3 – Comparison between measured STL in the forward and reverse directions for the reference specimen.

The results show that the ASTM values are higher than the measured STL at the DBCE laboratory for most of the frequency range, even after making allowance for the ASTM inter-laboratory standard deviation. The ASTM results are based on a six-laboratory round robin, and a comparison of the six individual laboratory test results (obtained from the ASTM research report E33–1007) with the DBCE results is given in Table 3. It can be seen from the table that the DBCE results are within approximately 1 dB of that reached at the laboratory code named F in the ASTM report. Before discussing possible reasons for variations in the results, it is instructive to examine the reproducibility of STL results in general. ISO 140–

Part 2 (ISO 1991) provides information on reproducibility of the sound reduction index (equivalent to STL) based on inter-laboratory tests on single glazing, double glazing, a lightweight partition and two brick walls carried out in European countries.

The reproducibility value R is defined in ISO 140–Part 2 (ISO 1991) as the value below which the absolute difference between two single test results obtained under reproducibility conditions may be expected to lie with a probability of 95%. Thus for 18 one-third octave bands, the difference between results should not exceed R more than once in the whole frequency range. The reproducibility value R is given by:

TABLE 2

COMPARISON BETWEEN DBCE STL RESULTS AND THE ASTM DATA

One-third octave band centre frequency (Hz)	Average STL of reference specimen (dB)			
	DBCE results		ASTM data	
	STL	95% confidence interval	STL	Standard deviation
100	13.1	1.6	10.4	2.6
125	12.0	1.7	11.8	1.2
160	12.5	1.3	12.8	1.2
200	14.0	1.0	14.8	1.3
250	14.5	0.9	16.1	1.2
315	14.9	0.7	17.5	1.2
400	17.1	0.5	19.2	0.9
500	19.0	0.5	20.8	1.2
630	20.0	0.5	22.7	1.1
800	22.2	0.4	24.6	1.1
1000	24.2	0.4	26.4	1.0
1250	26.3	0.3	28.3	1.1
1600	28.3	0.3	30.3	1.0
2000	30.7	0.3	32.3	1.0
2500	32.1	0.4	34.0	1.0
3150	34.8	0.4	35.8	1.4
4000	36.4	0.3	37.4	1.5
5000	38.1	0.3	39.5	2.0

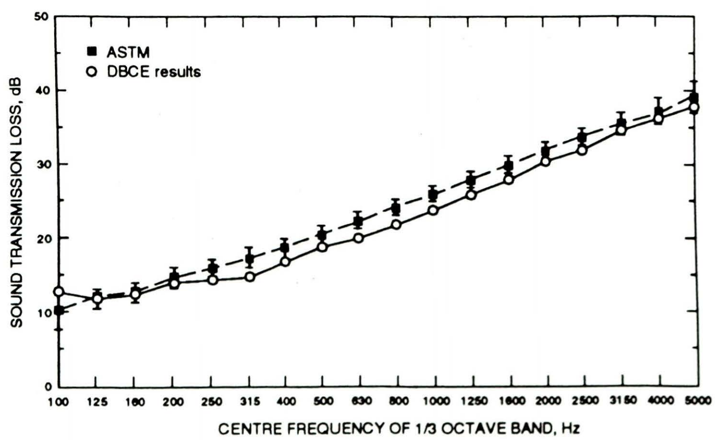

Fig. 4 – ASTM STL data and standard deviation and DBCE STL results for the reference specimen.

TABLE 3

COMPARISON OF INDIVIDUAL ASTM LABORATORY RESULTS WITH DBCE RESULTS

One-third octave band centre frequency (Hz)	Sound transmission loss (dB) ASTM laboratory code A	B	C	E	H	F	DBCE results (dB)
100	7.0	12.0	10.0	9.2	13.7	—	13.1
125	10.4	11.0	14.0	11.6	11.9	12.0	12.0
160	12.3	12.0	15.0	13.0	12.3	12.0	12.5
200	14.1	15.0	17.0	14.8	15.0	13.0	14.0
250	16.6	16.0	18.0	16.4	14.8	15.0	14.5
315	18.7	17.0	19.0	17.7	16.4	16.0	14.9
400	20.2	19.0	20.0	19.3	18.4	18.0	17.1
500	21.9	21.0	22.0	21.1	20.0	19.0	19.0
630	23.7	23.0	24.0	22.4	21.9	21.0	20.0
800	26.1	25.0	25.0	24.7	23.8	23.0	22.2
1000	28.0	26.0	27.0	26.3	25.8	25.0	24.2
1250	30.0	28.0	29.0	28.5	27.4	27.0	26.3
1600	31.2	31.0	31.0	30.6	29.0	29.0	28.3
2000	33.1	33.0	33.0	32.5	31.1	31.0	30.7
2500	35.2	34.0	35.0	34.0	32.8	33.0	32.1
3150	37.2	37.0	37.0	35.2	33.7	35.0	34.8
4000	38.9	38.0	39.0	37.3	35.3	36.0	36.4

$$R = 2.8\,(s_R{}^2)^{0.5} \tag{3}$$

where $s_R{}^2$ is the reproducibility variance and the factor 2.8 comes from the fact that the value R applies to the difference between two single results. The reproducibility data in ISO 140–Part 2 for laboratory SRI is given for frequencies up to 3150 Hz only, and these values superimposed on the ASTM data are plotted in Fig. 5. Using this criterion, the DBCE STL results fall within the reproducibility limit. In fact, if the standard deviation of the ASTM results is also multiplied by 2.8, the DBCE results will also be within the reproducibility limits of ASTM data.

The reproducibility of the ISO single number index (similar to STC) is given as 3 in ISO 140–Part 2, and on that basis too the DBCE results are within the reproducibility limits.

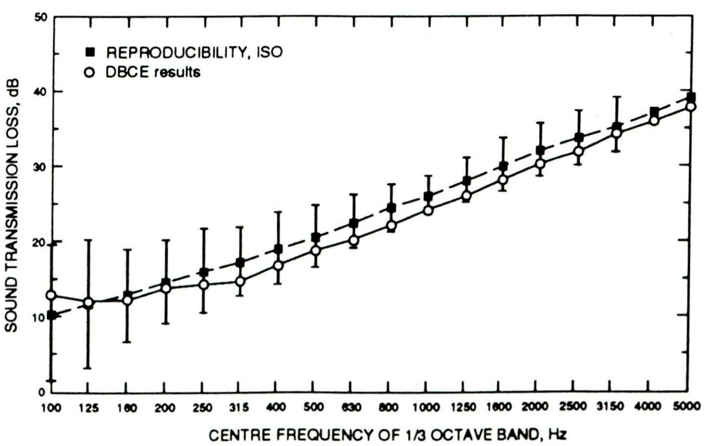

Fig. 5 – ISO reproducibility values applied to the ASTM data and DBCE STL results for the reference specimens.

POSSIBLE REASONS FOR VARIATION IN RESULTS

For steel panels with low STC ratings, the laboratory flanking transmission is unlikely to be of significance. Small differences due to variations in construction details listed in Table 1 are a possibility. A factor that could have a major influence is the tolerance allowed in the mass/area. In the frequency range well above the natural resonant frquency (f_r) for the panels and well below the critical coincidence frequency (f_c) the single-leaf steel sheets are likely to follow the mass-law behaviour. Substitution of the material parameters in the well established equations for f_r and f_c can easily show that the frequency range under consideration in this work is well within the mass-law behaviour range. Then the STL and STC of the panels can be estimated using the equations (Northwood and Warnock 1979):

$$\mathrm{STL} = 20 \log_{10}(mf) - 48 \qquad (4)$$

$$\mathrm{STC} = 20 \log_{10}(m) + 10 \qquad (5)$$

By taking m as 4.45 kg/m^2, one obtains STC as 23 which is closer to the DBCE result than the value derived from the ASTM data. It can also be shown that the DBCE measured STL for frequencies in the range 315–5000 Hz are within 1 dB of the theoretical mass-law values but differ by slightly greater amounts at low frequencies. The ASTM standard recommends mass per unit area in the range 5.1 ± 0.7 kg/m^2. As mentioned earlier, the DBCE panels were at the lower end of the range. If the laboratories that participated in the ASTM round robin used panels with mass/area towards the upper end, the difference in STL expected from variations in mass/area alone would be 2.4 dB. Because the mass/area of ASTM panels is not available from published data, this could be an important factor for possible discrepency.

Other factors which could contribute to the differences between the ASTM and DBCE results are discussed below. The room volume has a major influence on sound diffusion and should be sufficiently large to support a diffuse field at the lowest frequency of interest. The ASTM E90 requires the volume of each room to be not less than 80 m^3 and recommends a minumum volume of 125 m^3 for measurements down to 100 Hz. AS 1191 recommends a minimum volume of 100 m^3 but preferably of the order of 200 m^3. In addition, AS 1191 calls for a difference in source and receiving room volumes of 10% but no such requirement exists in the ASTM standard. The room sizes, however, are expected to affect STL at low frequencies only, but observed differences persist throughout the frequency range, suggesting other factors at work.

Other possible factors for observed variations in results are the specimen size and specimen frame effects. AS 1191 requires a minimum area of 10 m^2 with a smallest dimension (excluding thickness) of 2.4 m. ASTM E90 only requires minimum dimensions of 2.4 m, i.e. a minimum area of 2.4 × 2.4 m or 5.76 m^2. In finite sized panels with low damping, the resonant transmission component below the critical frequency will depend on the panel dimensions, and the full effect of stiffness and fundamental panel resonance will be different if different size panels were tested. In addition, if the specimen width is restricted to 2.4 m only, two panels with one centre joint are needed, whereas to meet the 10 m^2 requirement three panels were used for DBCE tests, resulting in an additional joint. The recommendation for specimen frames in test standards is that the depth from the surface in each room of the wall should be small, but it cannot generally be controlled as frames are built to accommodate all types of specimens and this can result in deep niches. For DBCE tests, the reference specimen wall was installed in the middle of the frame and had a niche on both sides. Kihlman and Nilsson (1972) have shown that the STL can be somewhat lower for frequencies below f_c if there is a niche on both sides than if the niche is only on one side. They also showed that the lowest STL would occur for the cases when the design approaches the ideal design for a sound transmission laboratory, i.e. no niches or deep niches on each side of the panel. Sewell (1970) has shown theoretically that smaller panels have greater SRI at low frequencies.

Guy and Sauer (1984) also found that the position of the panels in the aperture between the test rooms can have an effect on the STL below the critical coincidence frequency of the panels. The edge conditions of the panels, i.e. simply supported versus clamped edges, or intermediate boundary conditions can also affect the measured STL values by up to 3 dB.

CONCLUSION

From the study of STL of the ASTM reference specimen, the following conclusions can be drawn. The repeatability of noise reduction measurements in the DBCE laboratory in both the forward and reverse directions is excellent. Except for minor variations at low frequencies, no significant differences were observed in the STL by reversing the source and receiving rooms. The STL values for the ASTM reference specimen were found to be somewhat higher than those measured at the DBCE laboratory and possible reasons for the differences have been suggested. The reproducibility of the STL results and the STC rating were found to be within the ISO reproducibility limits despite possible minor variations in the specimens.

REFERENCES

AMERICAN SOCIETY FOR TESTING AND MATERIALS (1990). *Test Method E90: Method for Laboratory Measurement of Airborne Sound Transmission Loss of Building Partitions.* ASTM, Philadelphia.

———(1991). *Standard E1289: Standard Specification for Reference Specimen for Sound Transmission Loss.* ASTM, Philadelphia.

AUSTRALIAN UNIFORM BUILDING REGULATIONS CO-ORDINATING COUNCIL (1990). *Building Code of Australia.* AUBRCC, Canberra.

GUY, R.W. and SAUER, P. (1984). The influence of sills and reveals on sound transmission loss. *Applied Acoustics*, Vol. 17, pp. 453–476.

INTERNATIONAL STANDARDS ORGANISATION (1990). *ISO Standard 140–Part 3: Laboratory Measurements of Airborne Sound Insulation of Building Elements.* ISO, Geneva.

———(1991). *Standard 140–Part 2: Measurements of Sound Insulation in Buildings and of Building Elements – Determination, Checking and Application of Precision Data.* ISO, Geneva.

KIHLMAN, T. and NILSSON, A.C. (1972). The effect of some laboratory design and mounting conditions on reduction index measurements. *Journal of Sound and Vibration*, Vol. 24, pp. 349–364.

NORTHWOOD, T.D. and WARNOCK, A.C.C. (1979). Airborne sound insulation. In *Handbook of Noise Control*, 2nd edn, ed. C.M. Harris, Chapter 22, McGraw-Hill Book Company, New York.

SEWELL, E.C. (1970). Transmission of reverberent sound through a single leaf partition surrounded by an infinite panel. *Journal of Sound and Vibration*, Vol. 12, pp. 21–32.

STANDARDS ASSOCIATION OF AUSTRALIA (1985). *AS 1191: Method for Laboratory Measurement of Airborne Sound Transmission Loss of Building Partitions.* SAA, Sydney.

———(1979). *AS 1276: Methods for Determination of Sound Transmission Class and Noise Isolation Class of Building Partitions.* SAA, Sydney.

PSYCHOLOGICAL ACOUSTICS

PITCH PERCEPTION - A PSYCHOMETRIC STUDY OF PERCEPTION OF 440 Hz AND ITS HIGHER HARMONICS.

Suhashini Shankar and Suzanne Hogg
Department of Applied Physics, University of Technology, Sydney, Sydney.

ABSTRACT

A4 440 Hz was adopted as the International standard of concert pitch in 1939. The scientific importance of choosing 440 Hz as standard by the musicians has not been studied so far. In this paper preliminary study on the perception of pitch of 440 Hz and its higher harmonics is reported. Just noticeable difference (*jnd*) in perceived pitch for pure tones of frequency 440Hz, 880 Hz, 1320 Hz, 1760 Hz, 2200 Hz are measured by pitch matching tests. Final analysis of the results will include whether the subjects are musically trained/untrained, male/female, left/right handed and hearing normal/impaired listeners.

INTRODUCTION

In 1939, an international conference under the auspices of the International Standards Association, adopted a standard for musical pitch in terms of the frequency of the note A in the treble clef, as reported by Kaye (1939) . Five countries, (France, Germany, Great Britain, Holland and Italy), International Union for Broadcasting and International consultative committee on Telephony, represented by delegates, unanimously chose A440 as the standard of pitch .

HISTORICAL REVIEW

Ellis(1880) summarised the history of musical pitch for 500 years since 1361.

* From the fourteenth to seventeenth century, note A fluctuated between 374 Hz to 567 Hz without any order.
* In the eighteenth century the pitch spread was from 377 Hz to about 423 Hz.
* In the nineteenth century the range was from 424 Hz to 494 Hz.
* The highest value of 567.3 Hz was reached in 1619.
* The lowest value of 373.7 Hz was in 1648.

Figure 1 shows the overview of the fluctuations in the standard pitch in the past. The graph is plotted from Ellis 's data.

A conference of physicists in 1834 adopted 440 Hz as standard for the note A4. A conference of musicians and physicists appointed by the French Government in 1859 established 435Hz as standard. Other than that, there is no evidence of involvement of physicists/scientists in determining the standard for the concert pitch. Pitch shifts had been mainly determined by musicians and musical instrument makers.

REASONS FOR PITCH SHIFTS

Aspiration for high 'brilliance' seems to be one of the main reasons given for the rise in pitch. The introduction of new musical instruments (brass) in concerts contributed to the effect.

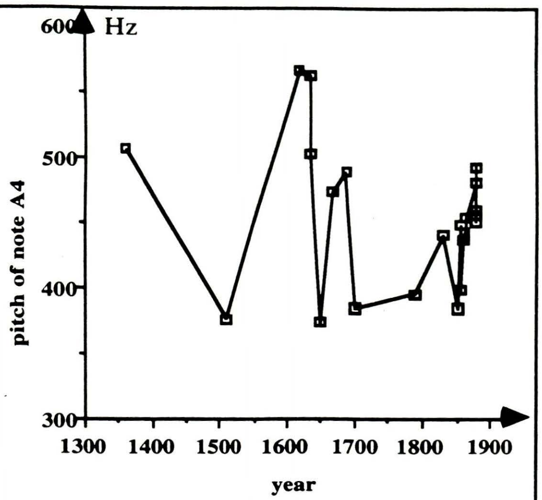

Fig 1 - History of musical pitch

NEED FOR A STANDARD

Initially, the International standard for musical pitch was of commercial importance. Instruments, especially woodwind, designed to perform well at one pitch may not do so at another. In the case of string instruments neck and bass bar needed to be strengthened to accommodate an increase in the string tension. Two performances of the same work by the same performer at two different pitches will be perceived to be different by listeners. So therefore unless the same piece of music is played at the same pitch by two different performers, listeners cannot appreciate any differences between the two performances. The increased exchange of concerts and musical programs in different countries, international broadcasting and the advent of electro-acoustic instruments emphasised the need for the international standard for the concert pitch. As a result 440 Hz was adopted as the "concert pitch". Non-adjustable tuned instruments such as xylophones, handbells, churchbells, chimes etc are made to this standard and require accompanying instruments to tune to that standard.

IS THE STANDARD UNANIMOUS?

Recently the pitch has started to rise again. Musicians differ in opinion as to the merit of the standard being set to values ranging between 440 and 446 Hz.

PERCEPTION OF PITCH

Considerable time is spent in musical ensembles obtaining a consensus that all instruments are "in tune" with each other. This is attributable to the differing harmonic qualities of the instruments and the different perception of these by the listeners. The pitch of a sinusoidal tone and of a complex tone with the same fundamental frequency are slightly different. Terhardt(1971, '72) reported that the pitch of a complex tone is perceived lower than the pitch of the same fundamental frequency. Moore et al (1984) studied the just noticeable differences in frequency and intensity of harmonics of complex sounds. Moore et al (1985) measured the thresholds for the detection of inharmonicity in complex tones. Their subjects were presented with two complex tones, in one, all the partials were at exact harmonic frequencies; and in the other, one of the partials was slightly mistuned. The percentage of mistuning that makes the two tones sound different was the threshold for the detection of inharmonicity in complex tones. They also measured the threshold for different fundamental frequencies and stimulus duration at a given sound pressure level.

Deutsch D(1983, '91, '92) reported the relation of handedness to octave illusion and the tritone paradox: an influence of language on music perception. Based on her results, she implies the possible direct influence of the two modes of communication speech and music on each other. She says

> 'Musical discourse is not precise or accurate enough for such perceptual differences to become apparent through normal communication and only in the laboratory that we can develop a clean idea of what the listener really perceives. The possibility of basic disagreement at the perceptual level therefore should be considered in evaluating the issue of communication between the composer, performer and the listener.'

While on one side musicians want to increase the concert pitch, perceptually what difference does it make? What is the significance of the frequency 440 Hz in the perception of pitch? How is the pitch of 440 Hz perceived by people with different background? Are there any factors that might influence the music perception?

The objective of this investigation is to understand the perceptual significance of the standard concert pitch 440 Hz and the influences of individual differences on the perception of the pitch of complex tone of fundamental 440 Hz and thereby the communication between the performer and the listener.

EXPERIMENTATION

Pitch is the subjective attribute of auditory sensation that ranks the order of the sound as 'high' or 'low' on a scale(musical). It is a sensation, the subjective correlate of frequency. Pitch discrimination of complex tones has been shown to depend on the effects of training and experience, length of exposure to sound, the method of presentation including monaural and binaural listening, time interval between presentations, tonal duration, frequency, sound pressure, envelope, the presence of other sounds and spectrum of the sound, Rossing (1990). In this study of perception of pure tones of 440 Hz and its harmonics, we are interested in the effects of individual differences like training and experience, handedness and frequency for monaural presentation. Our final study is aimed to investigate the other effects like methods of presentation, time interval between presentations, tonal duration and the spectrum of the sound.

Earlier studies in the perception of pitch are psycho-acoustic studies. Most of the work has been done with a small number of musically trained subjects. The subjects' ears are usually test - trained before the actual tests are done. Since music perception is also of importance to the general listening population, not just the selected sample of trained ears, it was decided to do psychometric studies on ALL listeners with a range of characteristics.

In this preliminary study pure tones of frequencies 440Hz, 880Hz, 1320Hz, 1760Hz and 2200Hz were electronically generated. Reference and test tones were presented through headphones to left and right ear separately at the same time. At first the test tone was presented to the left ear and the reference tone to the right for pitch discrimination and pitch matching test. The results were verified by swapping the tones between the ears. If any difference in pitch discrimination at any frequency between the ears was observed, pitch matching test was repeated at that frequency Subjects have manual control of frequency of the test tone. The headphone has volume control and subjects are asked to choose a level comfortable to them for all the five harmonics. They are not allowed to change the volume during the test.

The task for the subjects is to adjust the pitch of the test tone until it is just different (higher and lower) from that of the reference tone. Subjects are asked to fill in a questionnaire from which the following characteristics are recorded.

musical training and experience
male/female
prolonged exposure to sound
handedness(left and right)
native language of listeners
ability to determine pitch - absolute/relative

RESULT

At the time of this paper nineteen subjects had so far been tested. Just noticeable differences (higher and lower) in the perceived pitch for the pure tones of 440 Hz, 880 Hz, 1320 Hz, 1760 Hz and 2200 Hz are recorded. Figure 2 summarises the results. Using the lower and higher noticeable differences in frequency, the observed mid-point of the range was calculated for each frequency. This observed mid-point of the range was divided by 'n' where 'n' is the number of harmonic and plotted for all subjects.

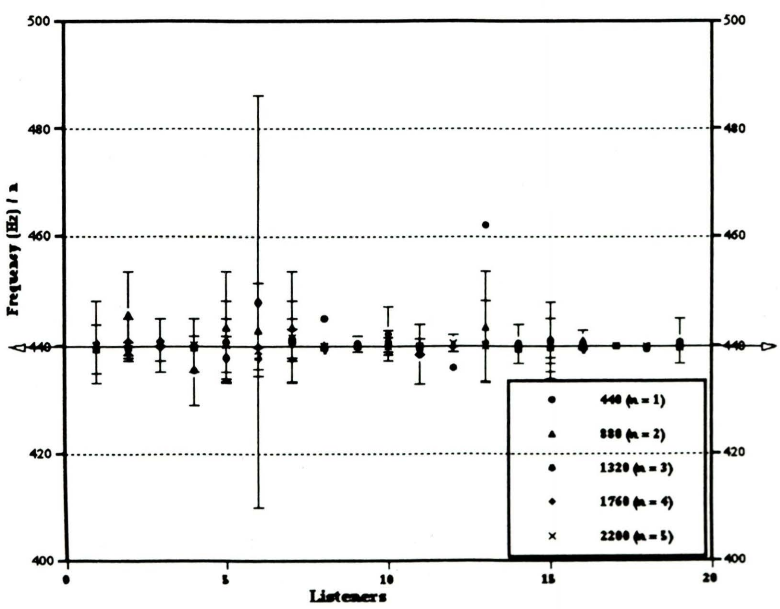

Figure 2: Initial Results of Pitch Discrimination of Harmonics of 440 Hz

The spread shows the observed lower and upper tolerances between which subjects did not perceive any difference in pitch.

DISCUSSION

OBSERVATION

The apparent ability to "fine-tune" higher frequencies was not significantly greater in actual Hz differences than at the fundamental.

This could be due to

* more acuteness in "pitch" at the higher harmonics which could be critical in the importance of the harmonics in differences perceived by individuals as to the "in-tuneness" of an ensemble of instruments.
* a bias of the listeners in the use of the experimental set-up which involves a mechanical twisting of a dial through a possible frequency range.
* an ability of the listeners to tune by beat recognition and elimination rather than by pitch recognition.

ANALYSIS

Two statistical studies were undertaken on the preliminary pure tone data - factor analysis and cluster analysis, the cluster analysis providing a clearer picture. Cluster analysis indicate four distinct clusters

* group 1 is the largest group having 'fine' pitch discrimination in the whole range of frequencies tested.
* group 2 having fine pitch discrimination at low and poor discrimination at high frequencies
* group 3 showing the behaviour opposite to that of group 2
* group 4 having no pitch discrimination in the whole range of frequencies tested.

In the subjects tested it would seem that 'music training' could be a major factor leading to the clustering above. Musical training of any vocal / instrumental nature at some stage in their lives seems to have an influence on pitch discrimination. Subjects describing themselves as "tone-deaf" did not seem to do any worse in the tests than others from the 'no musical-training' group.

Future tests will include

* binaural presentation with tones of short duration.
* studying the just noticeable differences for harmonics within the complex tone of fundamental 440 Hz.
* testing more subjects.

REFERENCES

DEUTSCH, D. (1983). The octave illusion in relation to handedness and familial handedness background. Neuropsychologia **21:** pp. 289 - 293

——— (1991) The tritone paradox: An influence of language on music perception. Music perception, 8: pp. 335-347

——— (1992) Some new pitch paradoxes and their implications. Philosophical Transactions of the Royal Society of London, Series B, Vol 336, No 1278, pp. 391-397

ELLIS J A(1880) History of musical pitch, 'On the Sensations of Tone' by Hermann Helmholtz, Translated by Alexander J. Ellis, Dover Publications, Inc, 1954

KAYE G.W.C (1939) International standard of concert pitch. Nature 143, pp. 905-906

MOORE, B. C. J., PETERS R. W. , and GLASBERG, B. R(1985). Thresholds for the detection of inharmonicity in complex tones. J. Acoust. Soc. Am. 77: pp.1861

MOORE, B. C. J., GLASBERG, B. R., and SHAILER, M. J. (1984) Frequency and intensity difference limens for harmonics within complex tones. J. Acoust. Soc. Am: 75, pp.550 - 562

ROSSING D THOMAS (1990) The Science of Sound, Second edition, Addison-Wesley publication.

TERHARDT. E. (1971). Pitch shifts of harmonics, an explanation of the octave enlargement phenomenon. Seventh International congress on acoustics, Budapest *1971*

——— (1971) The pitch of complex tones and the octave interval. Acustica 24 : pp. 126-136

EFFECTS OF NOISE EXPOSURE AT SCHOOL ON THE HEARING OF A CHILD USING HEARING AIDS

J.H. MACRAE

NATIONAL ACOUSTIC LABORATORIES

126 Greville St., CHATSWOOD NSW 2067

INTRODUCTION

This paper presents the results of personal noise dosimeter measurements of the noise exposure of a young hearing aid user and the effects of amplification of the noise by her hearing aids on her residual hearing. The child was 9 years old and had severe sensorineural hearing impairment in both ears. She attended a school for children with impaired hearing. The program of the school is aural/oral. The students are integrated into mainstream education as much as possible: they attend the school for a certain portion of the school day and spend the rest of the time at mainstream partner schools. The child therefore spent a substantial amount of time at a mainstream primary school and the noise measurements were made almost entirely at that school.

The schools are opposite one another on an arterial road of Sydney. The classrooms at the school for children with impaired hearing are well-shielded from the traffic noise by the administrative offices of the school. The rooms are carpeted and have sound-absorbing panels on the ceilings. Class sizes are small. The nominal class size is eight children but students are often away at mainstream schools and actual class sizes are often two or three children. Teachers often work on a one-to-one basis with individual children. In the mainstream primary school, the classroom that the child was in on the occasion of the measurements is adjacent to the road. The room has no carpet and no sound-absorbing panels on the ceiling. The class size was approximately thirty children. As a result of these differences, the noise levels at the mainstream school are about 15 dB higher than those at the school for children with impaired hearing. The median A-weighted noise level at the school for children with impaired hearing is about 60 dB SPL, whereas the median A-weighted noise level at the mainstream school is about 75 dB SPL.

The child's response to the higher levels at the mainstream school was to raise the volume control setting of her hearing aids, with the consequence that she would probably receive more amplification than that recommended for her hearing loss by the current National Acoustic Laboratories procedure for selecting the gain and frequency response of hearing aids. The following investigation was therefore carried out to determine the noise levels entering the child's hearing aids, the amplification characteristics of her aids, the distributions of in-ear noise levels after amplification, and the effects of the in-ear noise exposure on the child's residual hearing.

INSTRUMENTATION AND PROCEDURE

The noise exposure measurements were carried out with a Metrosonics dosimeter (Metrologger model dB-301A). The Metrologger had a dynamic range of 40 to 104 dB SPL and was calibrated at 102 dB SPL with a Metrosonics calibrator prior to use. Its frequency response was A-weighted and its detector had a slow rms response with a crest factor of 10 dB. The dosimeter sampled A-weighted sound levels in dB SPL at a rate of 4 samples/s. It accumulated each sample in a storage register corresponding to its amplitude value, quantised to the nearest integer. There were 64 individual registers, one for each dB level over the total dynamic range of 64 dB. The stored data were recovered from the Metrologger using a Metrosonics Metroreader model dB-652. The number of samples in each storage register of the Metrologger was transferred to the Metroreader, which then computed the total number of samples and the percentage of samples in each of the registers. This information was quantised in steps of 1 percent and printed out as a statistical distribution histogram.

As well as measuring the noise exposure of the child, her hearing thresholds were measured before and after the period of time in which the noise measurements were carried out. The child did not use her hearing aids until her hearing and hearing aids had been tested early in the morning before classes began. At about 8.20 a.m., her hearing was tested by means of a Demlar Bekesy audiometer and the real ear insertion gain responses and real ear input-output functions of their hearing aids for wideband noise were measured by means of a Rastronics Portarem real ear gain analyser, with the volume controls of her aids at the settings she would use at the mainstream school.

When the tests of the hearing aids were completed, the Metrologger dosimeter was attached to a belt around the child's waist and its microphone was attached to the collar of her blouse and positioned just below the left ear hearing aid (both hearing aids were worn behind the ear). The dosimeter was then turned on and the child proceeded to her classroom at the mainstream school. When the child returned at about 2.20 p.m., the dosimeter and hearing aid were removed immediately prior to placing the audiometric headphones for retesting her thresholds.

RESULTS

NOISE MEASUREMENTS

The statistical distribution histogram of the noise levels entering the child's hearing aids is presented in Figure 1. The mean of this distribution of A-weighted levels is 75 dB SPL.

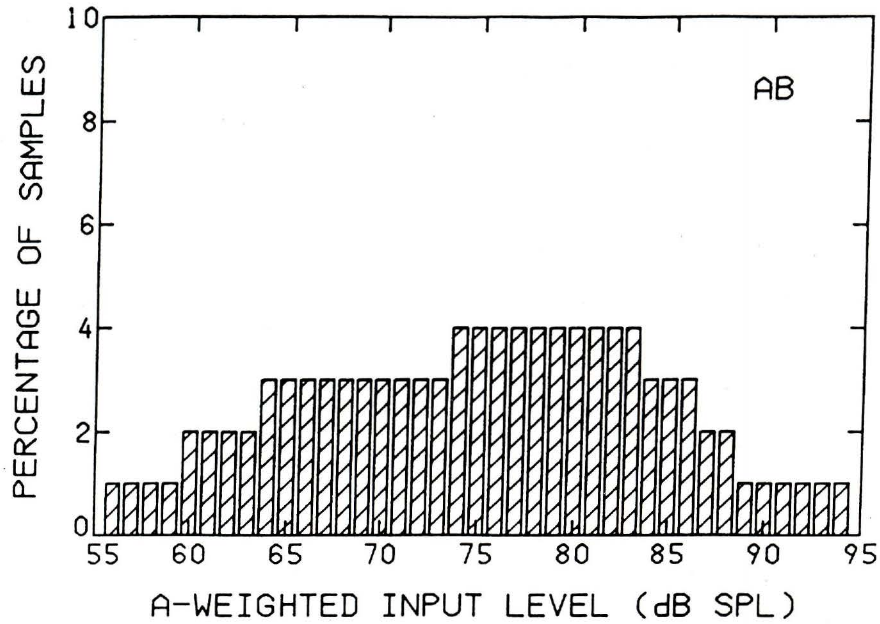

Fig. 1 - Statistical distribution histogram of the noise levels entering the child's hearing aids

HEARING AID MEASUREMENTS

Real Ear Insertion Gain Responses

The real ear insertion gain responses of the child's hearing aids are presented and compared with the recommended real ear insertion gain responses in Figure 2. The actual responses exceed the recommended responses, to a greater extent in the left ear than in the right ear.

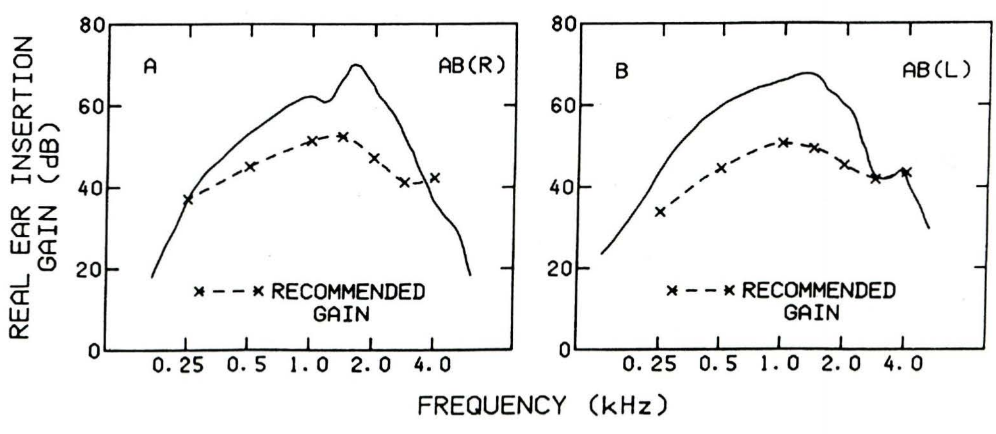

Fig. 2 - Real ear insertion gain responses of the child's hearing aids

Real Ear Input-Output Functions

The real ear input-output functions of the child's hearing aids are shown in Figure 3.

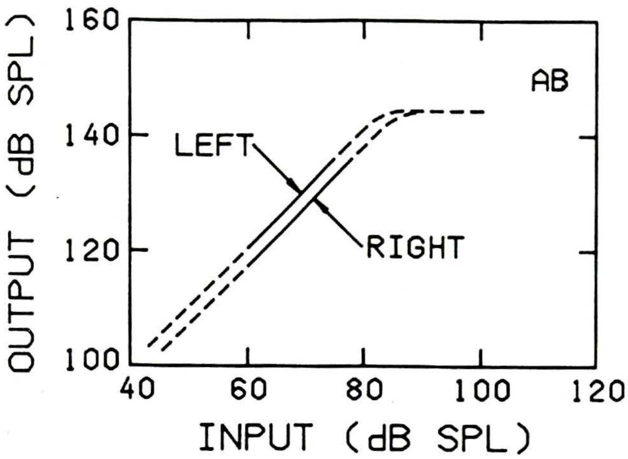

Fig. 3 - Real ear input-output functions of the child's hearing aids

Adding appropriate values from these input-output function to values of the distribution given in Figure 1, the estimated in-ear distributions of noise levels, presented in Figure 4, are obtained. The means of these distributions are 133 dB SPL in the right ear and 134 dB SPL in the left ear.

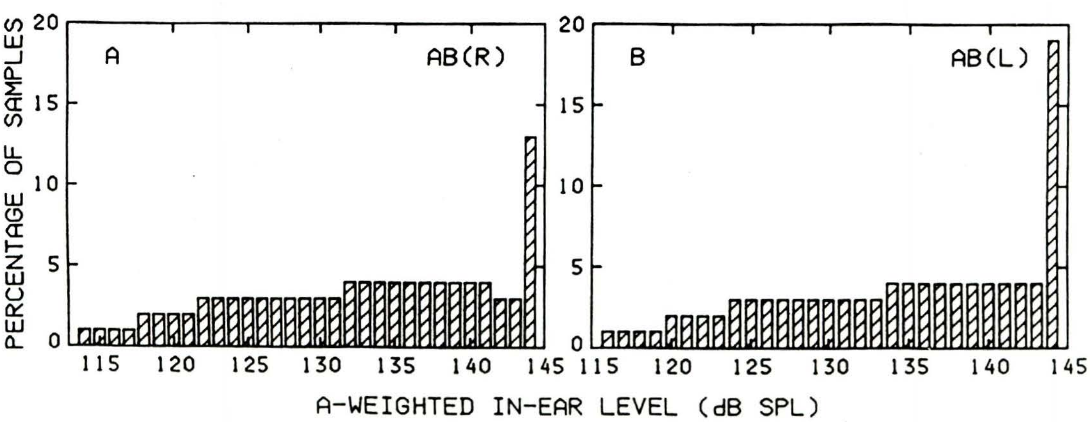

Fig. 4 - Estimated in-ear distributions of noise levels

THRESHOLD MEASUREMENTS

The child's hearing threshold levels before and after the period of noise exposure, are shown in Figure 5. The lines represent the mid-points of the excursions of the Bekesy audiograms. A substantial amount of temporary threshold shift (TTS) occurred in both ears, with more occurring in the left ear.

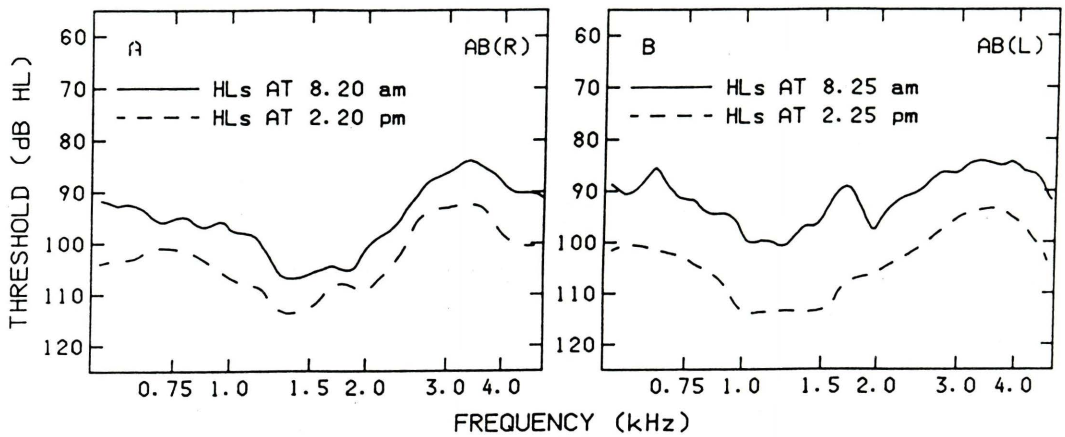

Fig. 5 - Hearing threshold levels before and after the period of noise exposure

DISCUSSION

The regular occurrence of TTS is undesirable for two reasons: first, while TTS is present, the child is functioning as if she has extra permanent threshold shift (PTS) of the same magnitude and children with severe hearing loss can ill afford to lose any of their remaining hearing; second, the regular occurrence of TTS has been shown to be associated with eventual occurrence of PTS of about the same magnitude.

The amounts of TTS observed in this child were much too high. They were caused by high in-ear levels from the hearing aid, resulting from high input levels at the mainstream school combined with the use of high amounts of amplification. They were eventually reduced, but not eliminated, by ensuring that the child used lower volume control settings at the mainstream school.

The problem of high noise levels at the mainstream school is less tractable. One solution, not likely to be adopted, would be to transfer the school to another location not on an arterial road and sell the existing set of buildings. The use of double-glazing on the windows of classrooms and of carpeting and sound-absorbing panels on the ceilings of the rooms would probably reduce the levels to some extent.

A mathematical model for prediction of TTS caused by hearing aid use has recently been developed (Macrae, 1994) and was used to predict the amount of TTS that the child's in-ear noise exposure would produce. Comparison of the observed TTS with the TTS predicted by the mathematical model is presented in Figure 6.

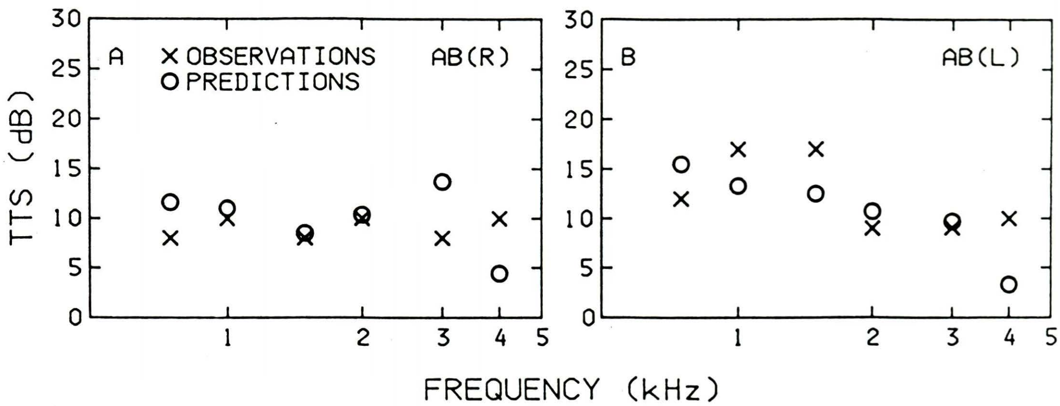

Fig. 6 - Comparison of the observed temporary threshold shift with temporary threshold shift predicted by the mathematical model

When TTS is measured as the difference between two Bekesy thresholds, as it was in this investigation, its standard error of measurement is 2.8 dB and the 95% confidence interval around its measured value is therefore ± 5.6 dB (Macrae, 1994). In view of this, the predictions agree well with the observations at all frequencies except 4 kHz.

REFERENCE

MACRAE, J.H. (1994). An investigation of temporary threshold shift caused by hearing aid use. J. Speech Hear. Res., 37, 227-237.

Siniša Djordjević, Gordon Troup, Heather Bowe*
Department of Physics
* Department of Linguistics
Monash University Clayton VIC 3168

THE EFFECT OF EMOTIONS ON THE SPECTRA OF SUSTAINED SUNG VOWELS

ABSTRACT

Three Italian songs were sung in **sad**, **happy**, and **angry** emotions by a number of choir singers. The spectra of the vowels **a**, **o**, **e**, **i**, and **u** have been analysed, and compared with the **neutral** singing of the same voices. Statistical analysis shows that the distribution of formant frequencies remains almost the same, but their intensities depend on the particular emotion.

INTRODUCTION

The spectrographic content of sounds depends on the physical shape of the vocal tract at the moment of speaking or singing. The physical shape is very often different for the same sounds, owing to a number of additional factors. One set of factors are emotions. If the same sounds are chosen and sung with different emotions, their diversity can be seen by comparing their sonagrams. The subject of the paper is to establish those differences and similarities.

METHOD

Three musical phrases from three Italian songs were chosen for the experiment. They were *'Lasciatemi morire!' (No longer let me languish!)*, *'O cessate di piagarmi' (O no longer seek to pain me)*, and *'Nel cor più non mi sento' (Why feels my heart so dormant)*. The songs were sung projecting **sad**, **happy**, and **angry** emotions. Choir singers took part in the experiment. There were nine male (bases and tenors) and six female (sopranos and altos), and they could be considered as trained but not professional singers. From the sung context only vowels **a** (ah), **o** (aw), **e** (eh), **i** (ee), and **u** (oo), ie. **a4**, **o5**, **e2**, **i4** and **u2** were taken out, as shown in Fig.1.

The same vowels were taken as control sounds, sung emotionally **neutrally** at the same pitch as in the above songs, in the following sequence: C4-E4-G4-C5-G4-E4-C4 [Eg. a(C4)-a(E4)-a(G4)-a(C5)-a(G4)-a(E4)-a(C4)] (Fig.2).

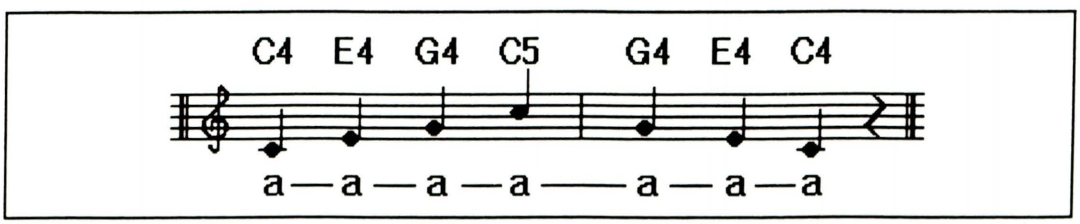

Fig. 2 - The sequence of neutral singing

The singing was performed in an anechoic chamber under the same recording conditions for all singers. Frequency and intensity (gain) of the three first formants (F1, F2, F3) were measured for each sound and singer and statistical analysis of the data performed. A spectrographic method was used for frequency measurement and linear predictive analysis (LPC) for intensity. The voices were recorded with a VII (Voice Identification, Inc.) Series 700 Sound Spectrograph, analysed with a KAY (Kay Elemetrics Corp.) CSL™ (Computerized Speech Lab) Model 4300B, and the descriptive statistics done with Microsoft Excel.

RESULTS

As a result of the analysis, four groups of diagrams were obtained: formant frequencies of emotional male vowels (Fig. 3), formant frequencies of emotional female vowels (Fig. 4), formant intensities of emotional male vowels (Fig. 5), and formant intensities of emotional female vowels (Fig. 6). Each of them compares **sad**, **happy**, and **angry** emotions with the **neutral** one and with each other, regarding corresponding frequencies and their intensities. Only for the **u** sound there were no neutral data.

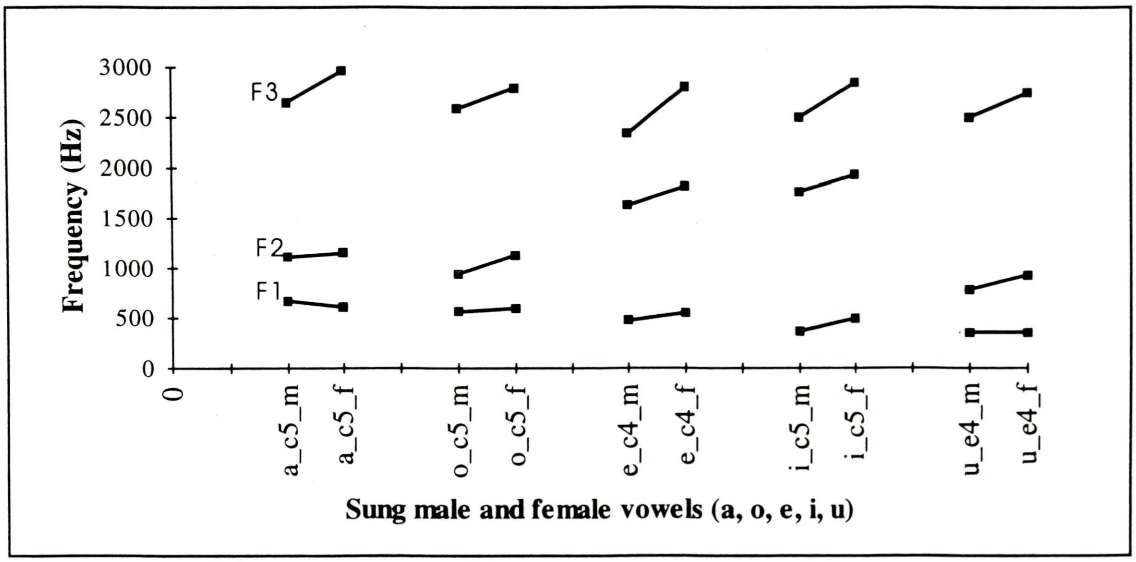

Fig. 7 - Average formants of male and female vowels

Generally, F1, F2, and F3 are relatively flat in all diagrams. Errors are inside the standard deviation, even for F2 in ***i_c5_male*** (Fig. 3), which looks like the most extreme exception, where F2 = (1951 ± 224) Hz. On that basis the frequencies of neutrally and emotionally sung vowels can be averaged together. Results are presented in Fig. 7.

This kind of averaging, however, does not make sense in the case of the corresponding intensities. Emotions show their effect right here. For example, for ***e_c4_male*** (Fig. 5) the intensity of each formant drops down most obviously for the sad emotion. There is also a slight lowering of the formant frequency in this case (Fig. 3).

At the beginning of the experiment we predicted that, if there were going to be changes at all, their increase would be in the sequence Neutral-Sad-Happy-Angry (N-S-H-A). We found that formant frequencies were not affected by emotions, and the intensity of the formants had the expected order only in some cases. Eg. (1) G1; N-S-H-A; ***a_c5_male***; (2) G1, G2, G3; S-H-A; ***e_c4_male***; (3) G1, G2, G3; S-H; ***o_c5_female***; (4) G1, G2, G3; S-H; ***u_e4_female***. The behaviour of the intensities can be directly seen from the diagrams (Fig. 3-6).

If the intensity of emotion is defined as the change in formant intensity from neutral, then it can be said that the **sad** emotion is weakest for ***e_c4_male*** (Fig. 5), but the strongest for ***i_c5_female*** (Fig. 6). Also the **happy** emotion is strongest for ***a_c5_male***, but weakest for ***o_c5_male***, etc.

CONCLUSION

The effect of emotions on the spectra of sung vowels can be detected by analysis of the formant intensity. A general rule cannot be stated for all vowels and all emotions. **Sad** is not always the weakest, nor **angry** the strongest emotion. **Happy** is often stronger than **sad**, and weaker than **angry**.

These results, obtained from a relatively small number of samples, indicate the importance of formant intensity as a relevant feature. Further research examining effects of emotions on formant intensity is clearly warranted.

REFERENCES

DENES, P., PINSON, E. (1973). The speech chain. An Anchor Press Book, New York.

FLANEGAN, J.L. (1972). Speech analysis, synthesis and perception. Springer-Verlag, Berlin.

FONAGY, I. (1981). Emotions, voice and music. Publication issued by the Royal Swedish Academy of Music, No. 33.

GABRIELSON, A. (1993). Emotional expression in music performance. Stockholm Music Acoustics Conf., July 28 - Aug. 1, 1993.

SUNDBERG, J. (1970). Formant structure and articulation of spoken and sung vowels. Folia Phoniatrica, pp. 22, 28-48.

TITZE, I., SUNDBERG, J. (1992). Vocal intensity in speakers and singers. J. Acoust.Soc. Am. 91 (5), May 1992, pp. 2936-46.

TROUP, G.F. (1981). The physics of the singing voice. Physics Reports, Vol. 74, No.5. Aug. 1981, pp. 380-401.

Fig. 1 - Musical phrases of emotional singing

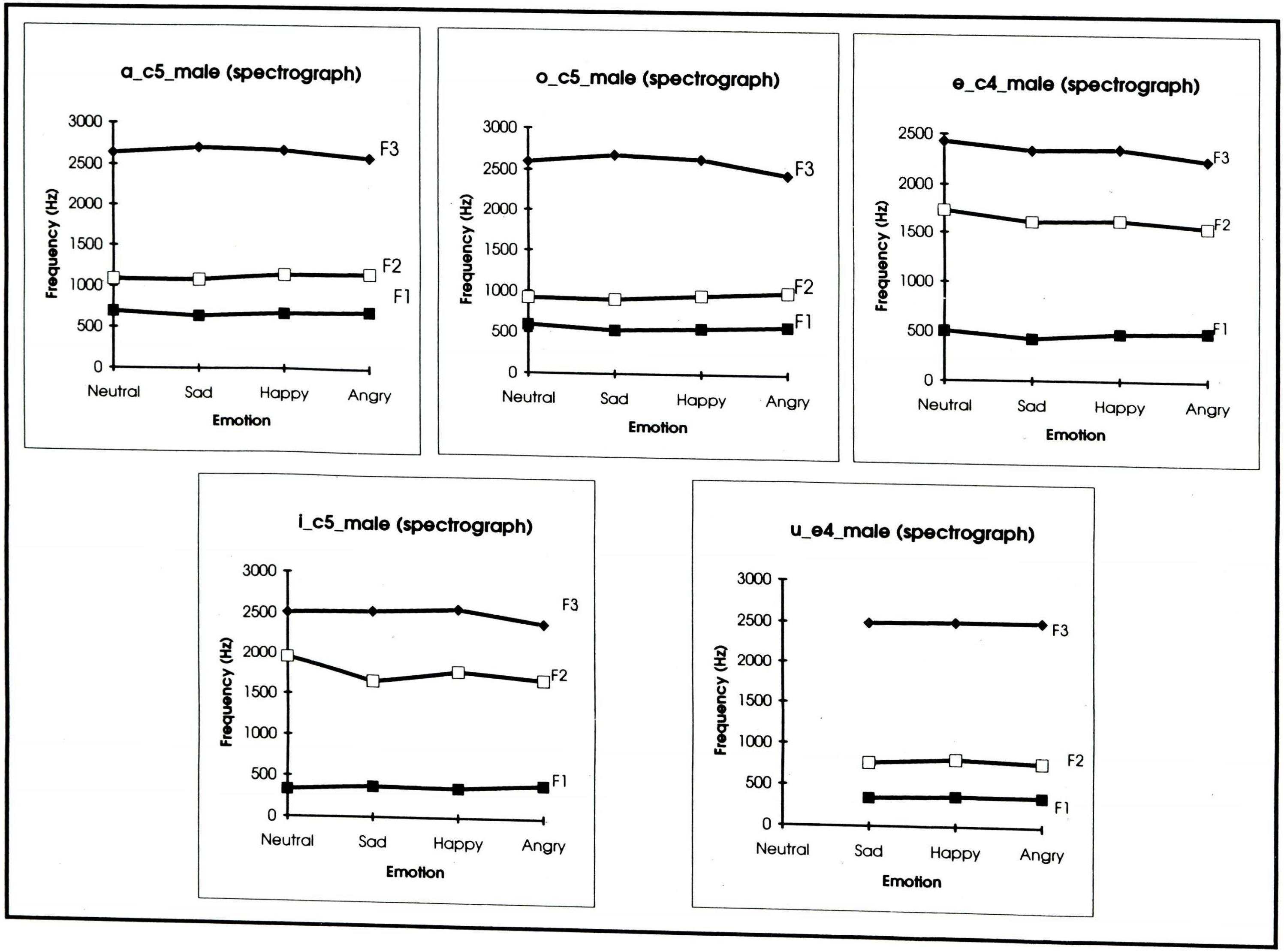

Fig. 3 - The formant frequency of emotional male vowels

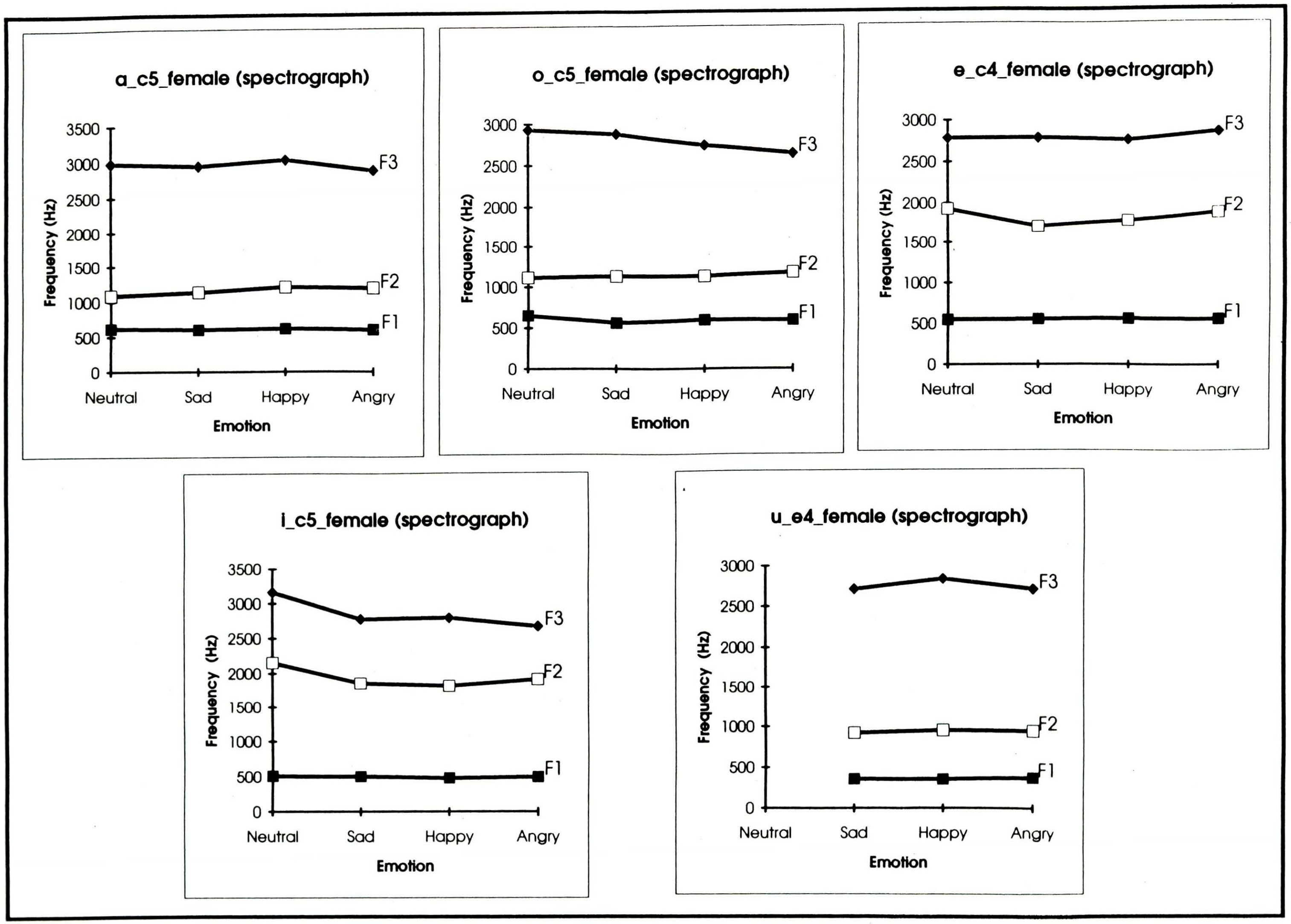

Fig. 4 - The formant frequency of emotional female vowels

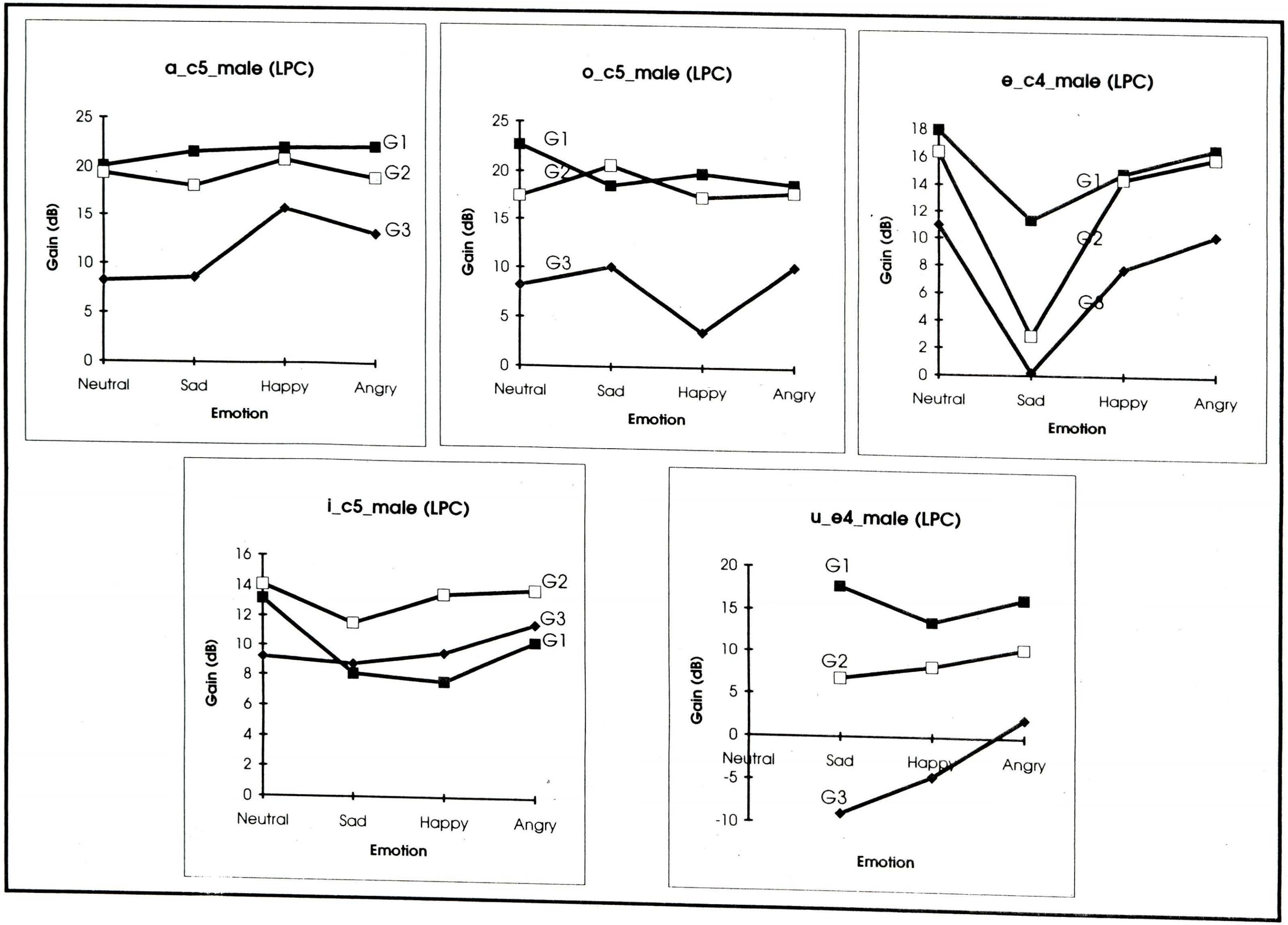

Fig. 5 - The formant intensity of emotional male vowels

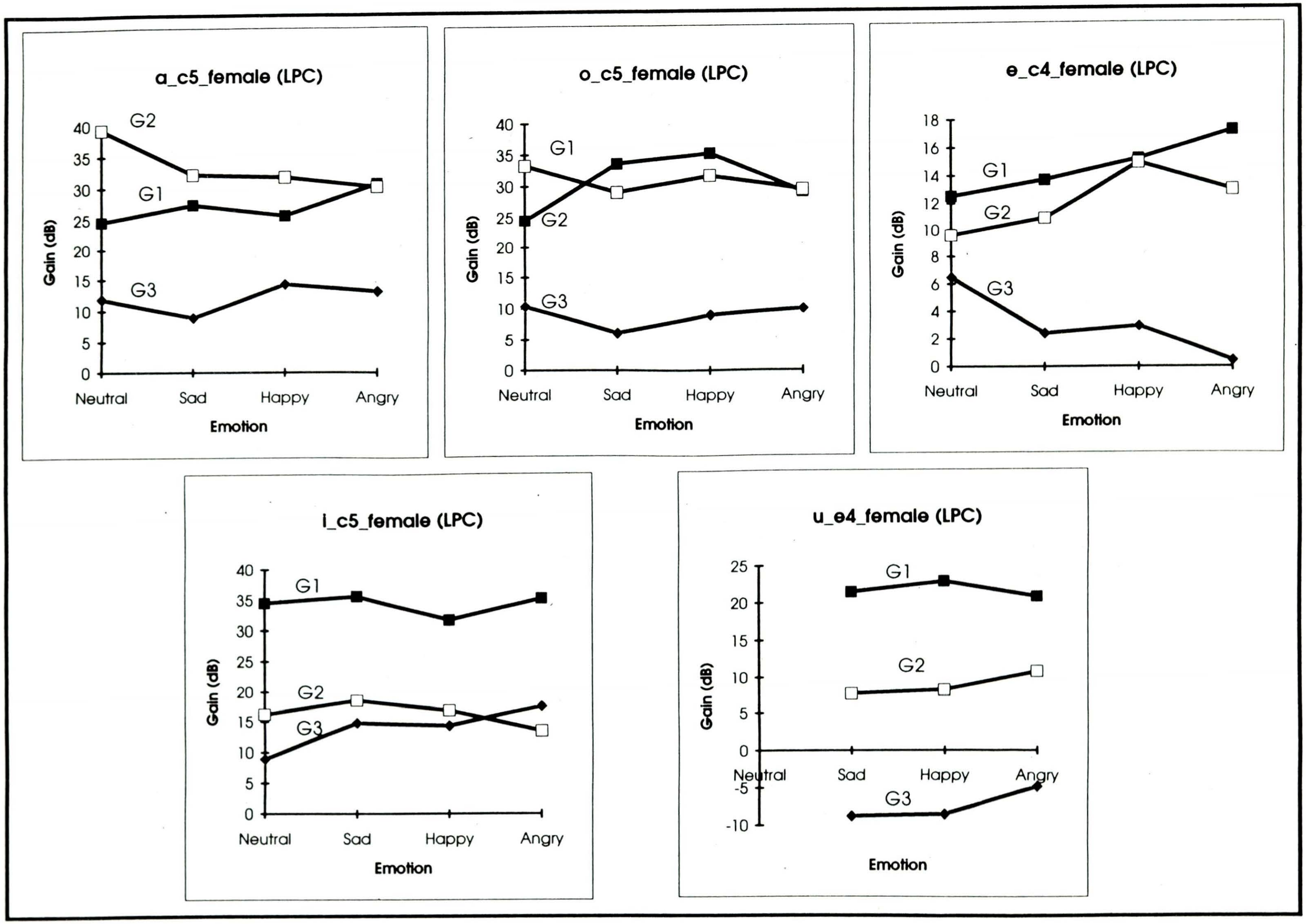

Fig. 6 - The formant intensity of emotional female vowels

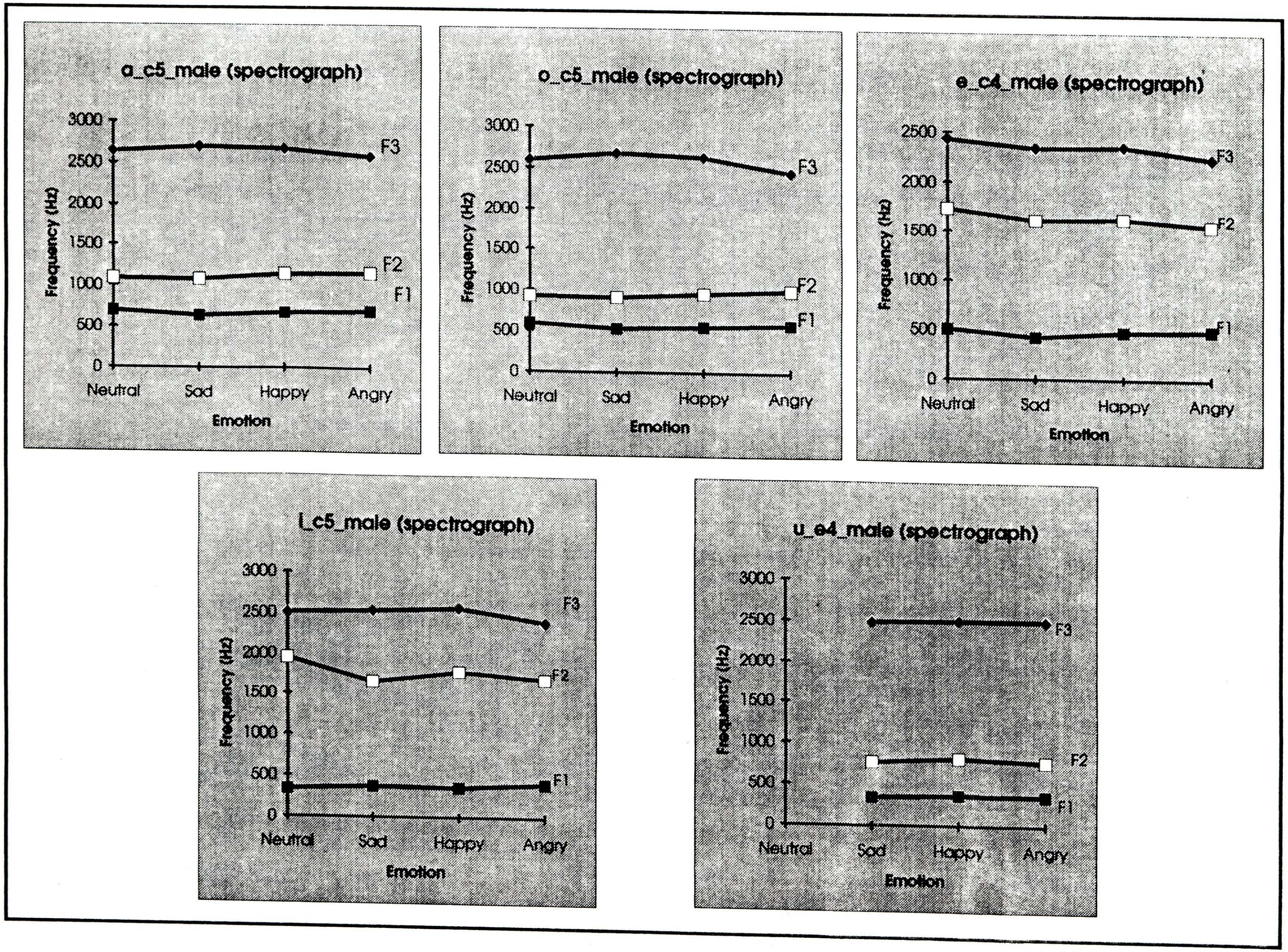

Fig. 3 - The formant frequency of emotional male vowels

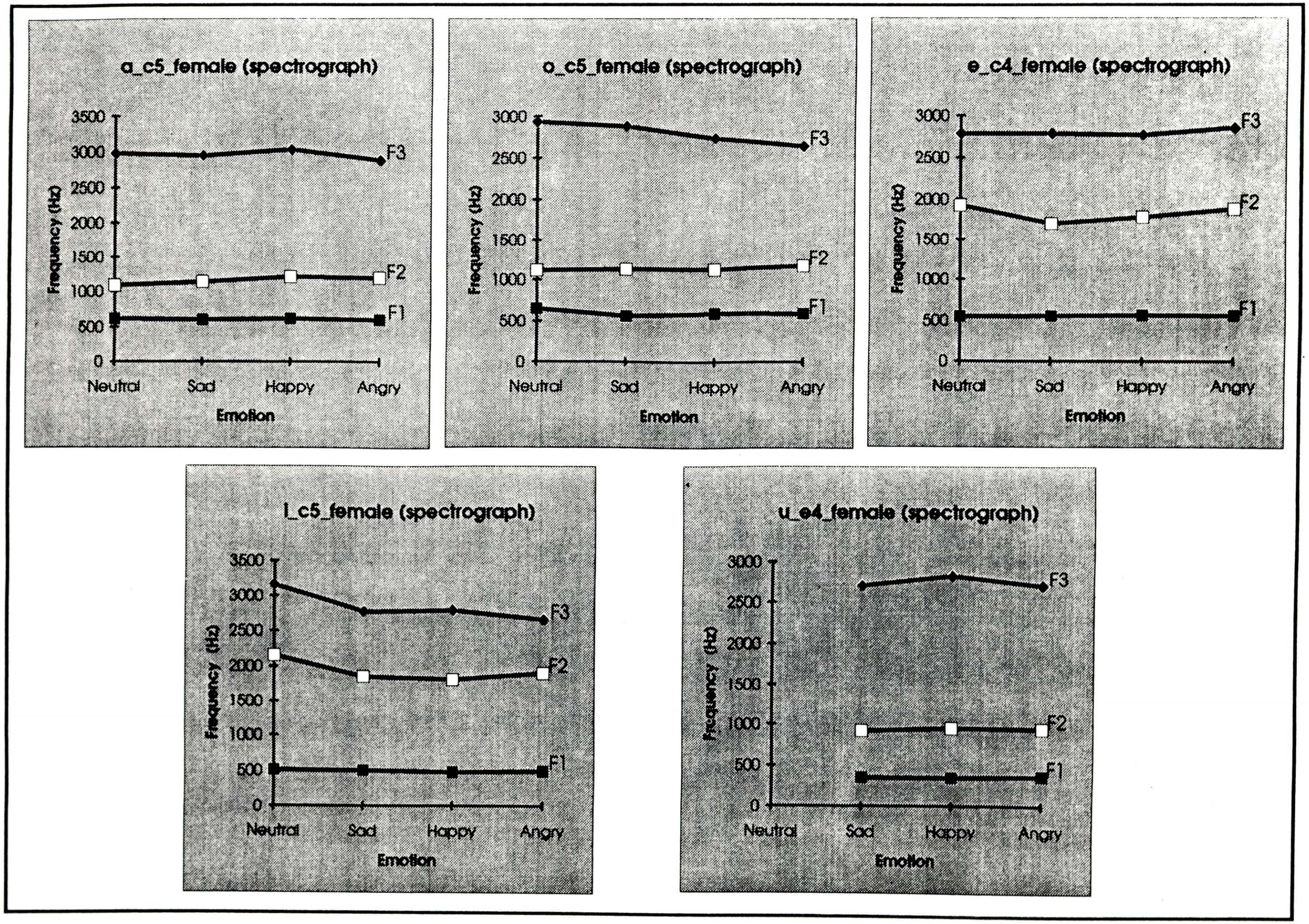

Fig. 4 - The formant frequency of emotional female vowels

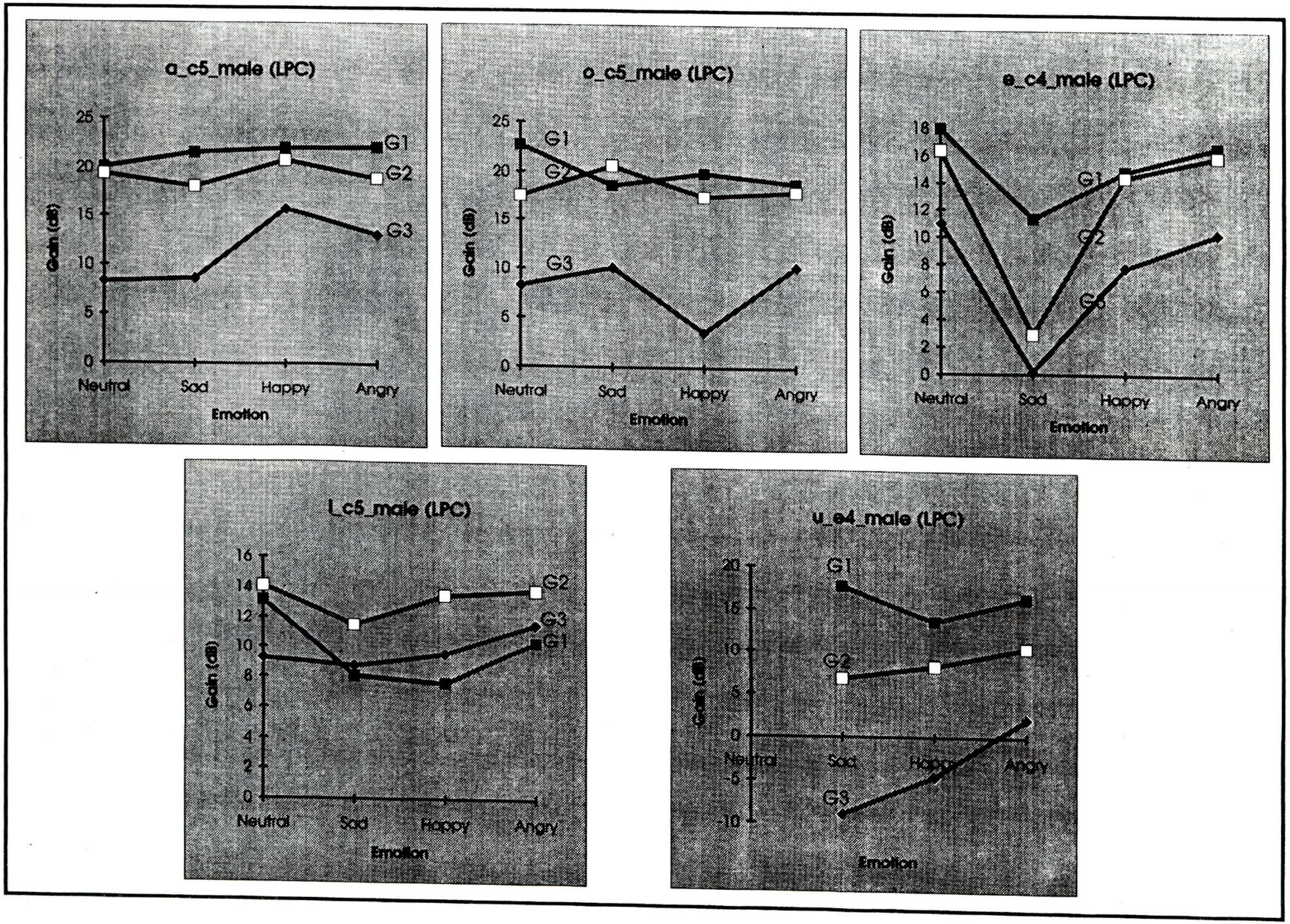

Fig. 5 - The formant intensity of emotional male vowels

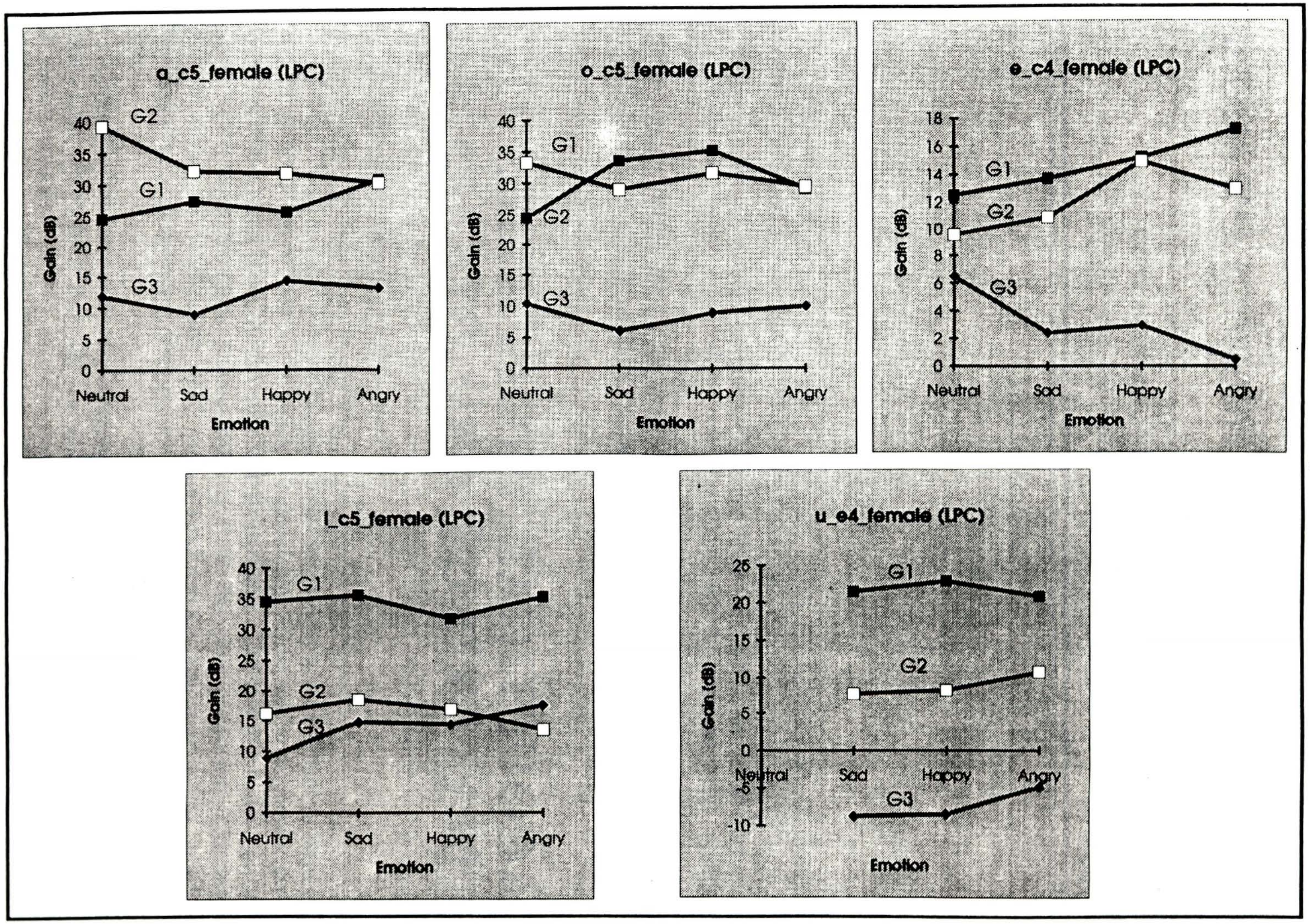

Fig. 6 - The formant intensity of emotional female vowels

ACOUSTICAL PROPERTIES OF MATERIALS AND SYSTEMS

MEASUREMENT OF FOUR-POLE PARAMETERS USING FLOATING MASSES

Dickens, J. D. and Norwood, C. J.
Defence Science and Technology Organisation
Aeronautical and Maritime Research Laboratory
Ship Structures and Materials Division
506 Lorimer Street
Fishermens Bend
Victoria 3207

ABSTRACT

Four-pole parameters are used to provide a full characterisation of isolator performance which is independent of the foundation system upon which the isolator is located. To date the standard test developed to measure the four-pole parameters of a pre-loaded isolator has involved the use of a large blocking mass in order to have "zero" velocity on the isolator output. The limitations of using this approximately blocked mass approach are analysed, and an improved technique using floating masses is proposed. Experimental results for isolator properties are presented.

FOUR-POLE PARAMETERS

Knowledge of the dynamic properties of vibration isolators, machine mounting locations and foundations are needed to be able to estimate the vibration power transmitted through the isolators and to predict the effect of mounting a vibrating source on flexible vibration isolators.

In the design and selection of vibration isolation mounts it is important to have a description of the mount behaviour which is independent of the test arrangement and the foundation system upon which they are to be installed. The dynamic behaviour of anti-vibration mounts may be characterised by their four-pole parameters, (Molloy 1957, Snowdon 1976, Snowdon 1979, Verheij 1982 and Dickens et al. 1993), which provide one such independent description.

An anti-vibration mount may be represented as a linear mechanical block system, Figure 1, for which the relationship between the inputs and outputs can be described by the matrix equation:

$$\begin{bmatrix} F_1 \\ V_1 \end{bmatrix} = \begin{bmatrix} A & B \\ C & D \end{bmatrix} \cdot \begin{bmatrix} F_2 \\ V_2 \end{bmatrix} \qquad (1)$$

where A, B, C, and D are the four pole parameters, and are complex, time invariant functions of ω.

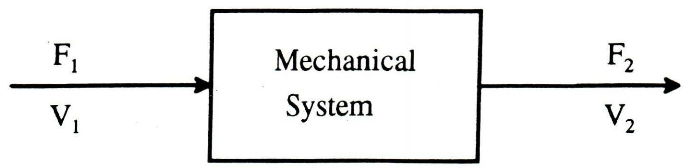

Figure 1
Block representation of an isolation mount

If the input and output ports are now swapped and the signs of F1 and F2 reversed then equation (1) gives:

$$\begin{bmatrix} F_2 \\ V_2 \end{bmatrix} = \frac{1}{A.D - B.C} \cdot \begin{bmatrix} D & B \\ C & A \end{bmatrix} \cdot \begin{bmatrix} F_1 \\ V_1 \end{bmatrix} \tag{2}$$

If Maxwell's law of reciprocal deflections is assumed to apply to the system, then it follows that the transfer impedance or mobility between any two ports is independent of which port is treated as the input or output (Snowdon 1976). Therefore the two blocked transfer mobilities given by equations (1) and(2) are equal, ie.:

$$\left.\frac{V_1}{F_2}\right|_{V_2=0} = \left.\frac{V_2}{F_1}\right|_{V_1=0} \tag{3}$$

Solving equation (3) using equations (1) and (2) gives:

$$A.D - B.C = 1 \tag{4}$$

For the case of symmetric isolators i.e. those that behave the same if the input and output ports are interchanged, then interchanging these ports gives:

$$\begin{bmatrix} F_2 \\ V_2 \end{bmatrix} = \begin{bmatrix} A & -B \\ -C & D \end{bmatrix} \cdot \begin{bmatrix} F_1 \\ V_1 \end{bmatrix} \tag{5}$$

Solving equations (1) and (5) gives:

$$A = D \tag{6}$$

Equations (4) and (6) mean that only two independent four-pole parameters need to be measured for a symmetric isolator in order to completely characterise it.

EXPERIMENTAL MEASUREMENTS USING A BLOCKING MASS

In general the dynamic properties of a vibration isolator are dependent upon its pre-load, and so measurements should be made with a pre-load similar to that experienced in service.

One possibility of determining two independent four-pole parameters is given by considering the special case in which the output side is blocked, i.e. $V_2 = 0$, which in equation (1) yields:

$$A = \left.\frac{F_1}{F_2}\right|_{V_2=0} \qquad \text{and} \qquad C = \left.\frac{V_1}{F_2}\right|_{V_2=0} \tag{7}$$

This allows a pre-load to be applied to the input side of the isolator which is reacted by the blocked output. Measurements would then need to be made of the input force and velocity and the output force required to hold the isolator blocked.

Verheij (1982) describes a method for making measurements of the blocked transfer impedance of a resilient isolator, defined as the force out divided by the input acceleration. A similar method was used at the Aeronautical and Maritime Research Laboratory (AMRL) to measure the pre-loaded, blocked four-pole parameters. A schematic of the test arrangement of the experimental set-up is shown in Figure 2. The test isolator is held between two masses M_1 and M_2, which behave as rigid bodies in the test frequency range. To simulate the static load of shipboard machinery, a pre-load is applied to the test isolator by the air bag located above the excitation mass, and can be adjusted by varying the air pressure. The dynamic input excitation to the test isolator is provided by two electro-magnetic shakers, which are decoupled from the frame and drive the upper mass via stingers. The mass M_2 is supported on very soft mounts, and may be considered as effectively blocked if its mass and rotational inertias are so large that it forms a high impedance termination for all excitation components of the test isolator. In this situation the displacement of M_2 will be much less than the displacement of M_1 and $V_2 \cong 0$, i.e. M_2 is blocked. However, the mass M_2 still has a small but measurable acceleration which can be used to determine the blocked output force on the isolator, termed the inferred force measurement.

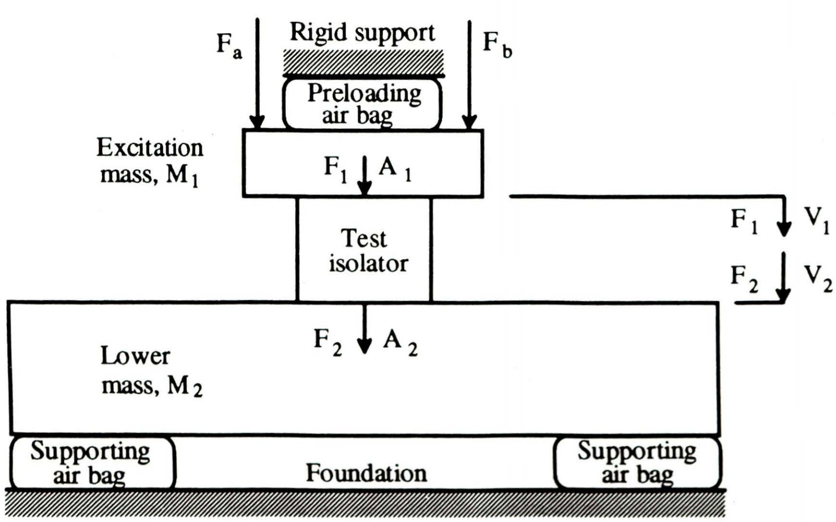

Figure 2
Schematic test arrangement for usual method

As defined above F_1 and F_2 are the forces on the input and output of the isolator respectively. Let F_a and F_b be the sinusoidal forces exerted on the excitation mass by the two vibrators at an angular frequency of ω. A_1 and V_1 are the acceleration and velocity at the excitation mass / test isolator interface, and A_2 and V_2 are the acceleration and velocity at the test isolator / blocking mass interface. We have:

$$F_1 = F_a + F_b - M_1.A_1 \qquad \text{and} \qquad F_2 = M_2.A_2 \tag{8}$$

Combining equations (4), (6), (7) and (8) gives:

$$A = D \cong \left.\frac{F_a + F_b - M_1.A_1}{M_2.A_2}\right|_{V_2 \approx 0}$$

$$C \cong \left.\frac{A_1}{j.\omega.M_2.A_2}\right|_{V_2 \approx 0} \qquad \text{and} \qquad B = \frac{A.D - 1}{C} \tag{9}$$

The upper frequency limit of the structural set-up is governed by the lowest structural resonance in the two masses. The method relies on the assumption that the mass on the output side of the isolator, which is supported on very soft mounts, may be considered as effectively blocked.

ERROR ANALYSIS OF BLOCKED MASS MEASUREMENT

In this section the errors introduced from the blocked mass assumption and the limitations in the measurement technique will be discussed. Solving equation (1) for A and C gives:

$$A = \frac{F_1}{F_2} - \frac{B.V_2}{F_2} \qquad \text{and} \qquad C = \frac{V_1}{F_2} - \frac{D.V_2}{F_2} \tag{10}$$

The application of equations (7) therefore introduces errors in the calculated magnitudes and phase angles of A and C, because the second terms in the respective equations (10) are ignored. Let the calculated values of A and C from equations (7) be denoted as A_M and C_M respectively, then equations (10) can be rewritten as:

$$A = A_M - \frac{BV_2}{F_2} \qquad \text{and} \qquad C = C_M - \frac{D.V_2}{F_2} \tag{11}$$

Also

$$\frac{F_2}{V_2} = j.\omega.M_2 \tag{12}$$

Define the relative magnitude errors E_A and E_C as:

$$E_A = \left|\frac{A_M}{A}\right| - 1 \qquad \text{and} \qquad E_C = \left|\frac{C_M}{C}\right| - 1 \tag{13}$$

Let ϕ_A and ϕ_C be the angles between the phasers A and A_M, and C and C_M respectively. Then examination of the phaser diagrams shows that the maximum magnitudes of the errors, termed $E_{A_{max}}$ and $E_{C_{max}}$, are:

$$E_{A_{max}}(\omega, M_2) = \frac{1}{\omega . M_2} . \left| \frac{B(\omega)}{A(\omega)} \right| \quad \text{and} \quad E_{C_{max}}(\omega, M_2) = \frac{1}{\omega . M_2} . \left| \frac{D(\omega)}{C(\omega)} \right| \quad (14)$$

These maximum magnitude errors occur at $\phi_A = n.\pi$ and $\phi_C = n.\pi$, where n is an integer. The maximum phase errors ϕ_{Amax} and ϕ_{Cmax} occur when the magnitude of the error is zero, and are given by:

$$\phi_{A\,max}(\omega, M_2) = 2.\mathrm{Sin}^{-1}\left[\frac{1}{2.\omega . M_2} . \left| \frac{B(\omega)}{A(\omega)} \right| \right]$$

and

$$\phi_{C\,max}(\omega, M_2) = 2.\mathrm{Sin}^{-1}\left[\frac{1}{2.\omega . M_2} . \left| \frac{D(\omega)}{C(\omega)} \right| \right] \quad (15)$$

For a given isolator under specified operating conditions, the values of A, B, C and D are fixed. Therefore over a specified operating frequency range the only way to reduce the errors E_{Amax} and E_{Cmax} is to increase the blocking mass M_2. However, for a given driving force F_1, and therefore given F_2, increasing M_2 results in A_2 decreasing and so the measured A_2 signal-to-noise ratio also decreases. This will place an upper limit on the size of the blocking mass. The force capabilities of the two exciting vibrators, the mass M_1 and the isolator's properties determine the maximum input force F_{1max}. The isolator's four-pole parameter A then determines the maximum blocked output force F_{2max} from equation (7). The sensitivity and characteristics of the blocking mass' sensing accelerometers / amplifiers, the background acceleration levels of the blocking mass and the level of accuracy required determine the lowest measurable acceleration A_{2min}. Therefore the maximum value of M_2 is given by the following equation, which will in turn place a limit on the reduction of the errors:

$$M_{2max} = \frac{F_{2max}}{A_{2min}} \quad (16)$$

The actual value of F_2 which is to be measured is quite small. Tests conducted at the AMRL on a variety of isolators and using an input force from the shakers of approximately 200 N have shown that over the frequency range of 200 to 800 Hz the magnitude of F_2 varies from units to hundredths of a Newton, for both a 576 kg and a 1076 kg blocking mass.

ALTERNATE MEASUREMENT METHODS

Two alternate measurement methods are proposed in order to overcome the deficiencies of the blocked mass method. These are the floating mass and two mass methods.

FLOATING MASS METHOD

This method does not assume that the lower mass in Figure 2 is blocked, but rather considers it to be floating and corrects for the velocity of the mass by including the second terms in the expressions for A and C in equations (10). The large blocking mass can therefore be replaced with a smaller mass, if required, to provide higher acceleration levels on the output side of the isolator. The floating mass provides a seat for the isolator and is chosen to be sufficiently small so that its acceleration levels can be measured with sufficient accuracy over the frequency range of interest. The output velocity is given by:

$$V_2 = \frac{A_2}{j.\omega} \tag{17}$$

and using equations (1), (4) and (6) the four-pole parameters are:

$$A = D = \frac{F_1.V_1 + F_2.V_2}{F_1.V_2 + F_2.V_1}$$

$$B = \frac{F_1^2 - F_2^2}{F_1.V_2 + F_2.V_1} \quad \text{and} \quad C = \frac{V_1^2 - V_2^2}{F_1.V_2 + F_2.V_1} \tag{18}$$

The output force F_2 may be determined by either direct measurement, using force transducers interposed between the isolator and the lower mass, or by an inferred measurement as with the blocked mass method. Use of the inferred measurement will impose a lower frequency limit on the measurements. If ω_n is the natural frequency of the lower mass on the supporting air bags then the error in F_2 is $A_2.M_2.(\omega_n/\omega)^2$, so that for measurements at frequencies a decade or more above the natural frequency the error will be less than 1%. In this case the size of the lower mass will limit the frequency range.

TWO MASS METHOD

Both the above methods assume that the isolator is symmetric. A refinement of the floating mass method employs two sets of measurements, each made with a different floating mass, and thus does not rely on the symmetry assumption. The two sets of data allow the determination of the four-pole parameters from equation (1), as follows. Let the masses of the two floating masses be M_{2a} and M_{2b} and the measurements corresponding denoted by subscripts a and b. The four-pole parameters A, B, C and D are the same for both sets of data. Therefore the two matrix equations are:

$$\begin{bmatrix} F_{1a} \\ V_{1a} \end{bmatrix} = \begin{bmatrix} A & B \\ C & D \end{bmatrix} \cdot \begin{bmatrix} F_{2a} \\ V_{2a} \end{bmatrix} \quad \text{and} \quad \begin{bmatrix} F_{1b} \\ V_{1b} \end{bmatrix} = \begin{bmatrix} A & B \\ C & D \end{bmatrix} \cdot \begin{bmatrix} F_{2b} \\ V_{2b} \end{bmatrix} \tag{19}$$

Combining these two matrix equations gives:

$$\begin{bmatrix} F_{1a} \\ V_{1a} \\ F_{1b} \\ V_{1b} \end{bmatrix} = \begin{bmatrix} F_{2a} & V_{2a} & 0 & 0 \\ 0 & 0 & F_{2a} & V_{2a} \\ F_{2b} & V_{2b} & 0 & 0 \\ 0 & 0 & F_{2b} & V_{2b} \end{bmatrix} \cdot \begin{bmatrix} A \\ B \\ C \\ D \end{bmatrix} \tag{20}$$

Solving for the four-pole parameters gives:

$$\begin{bmatrix} A \\ B \\ C \\ D \end{bmatrix} = \frac{1}{F_{2b}.V_{2a} - F_{2a}.V_{2b}} \cdot \begin{bmatrix} -V_{2b} & 0 & V_{2a} & 0 \\ F_{2b} & 0 & -F_{2a} & 0 \\ 0 & -V_{2b} & 0 & V_{2a} \\ 0 & F_{2b} & 0 & -F_{2a} \end{bmatrix} \cdot \begin{bmatrix} F_{1a} \\ V_{1a} \\ F_{1b} \\ V_{1b} \end{bmatrix} \tag{21}$$

EXPERIMENTAL RESULTS AND DISCUSSION

To illustrate the dependence of the error terms on both lower mass size and isolator parameters, three sets of results are presented. Two isolators, termed A and B, were tested using a 576 kg lower mass and then one of the isolators was re-tested using a 1076 kg lower mass. In each case the four-pole parameters were determined using the blocked mass and floating mass calculation methods outlined above.

The isolators were subjected to their design pre-load and measurements made for frequencies between 25 and 800 Hz. The lower limit was set because the natural frequency of the lower mass on the air bag was in the range 2 to 3 Hz. The shaker forces were measured using a pair of Bruel and Kjaer type 8200 force transducers and the accelerations of the two masses were measured using Bruel and Kjaer type 4379 accelerometers. All channels were measured simultaneously using an Hewlett-Packard type 3566A eight channel PC spectrum analyser, which also controlled the frequency sweeps. Data were then processed using the analyser / PC facilities. The results presented are the relative magnitude errors of A, B and C for each test. The relative magnitude error is the magnitude of the ratio of the blocked mass variable divided by the floating mass variable, minus one. Figures 3 and 4 are for the two different isolators on the 576 kg mass, while Figure 5 is the repeated test using the 1076 kg mass.

Comparison of the curves in Figures 3 and 4 clearly shows that the errors depend upon the properties of the isolator, and the maximum values are given by equations (14). The curves in Figure 3, isolator A, are for a stiffer isolator designed to take a higher pre-load and indicate that the ratios $|B/A|$ and $|D/C|$ are greater than those of the isolator B, Figure 4. Comparing the results in Figures 4 and 5 shows the dependence of the error terms on the blocking mass. The ratios of the errors between the two curves is approximately 1.9, compared to the mass ratio of 1.87. For all the curves the errors are greatest at the extremes of the frequency range and are relatively flat in the mid-frequency range, clearly demonstrating the measurement problems involved with such large lower masses. The increasing errors at the higher frequencies are due to the changing ratios $|B/A|$ and $|D/C|$. To extend the frequency range it is

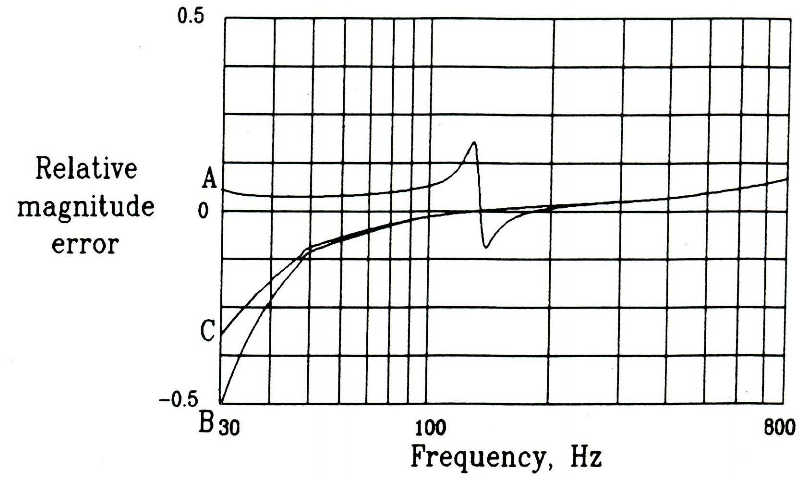

Figure 3
Isolator A on 576 Kg blocking mass.

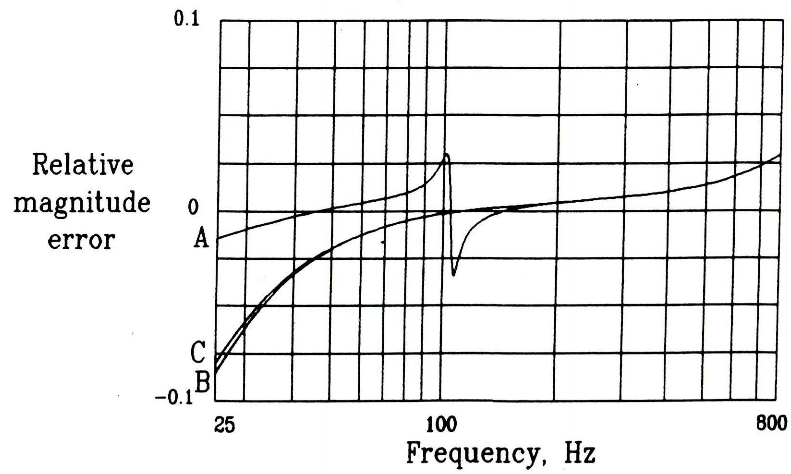

Figure 4
Isolator B on 576 Kg blocking mass.

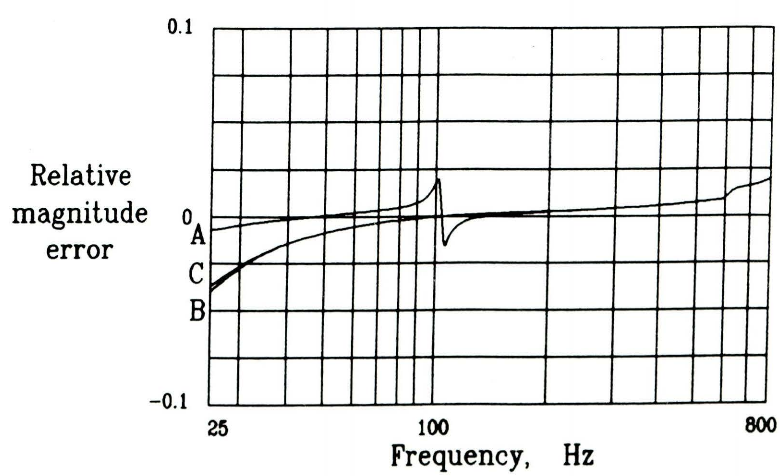

Figure 5
Isolator B on 1076 Kg blocking mass.

necessary to use a lighter lower mass, and to process the data using the floating mass measurement technique.

One aspect of all three sets of curves worth special comment is the behaviour of the error term for A in the region of 100 to 200 Hz. The pronounced deviation in the curve corresponds to a dip in the A parameter curve. The frequency of this dip is dependant upon the mass of the upper plate of the isolator and the stiffness of the elastomer. It appears to be due to a resonance of the isolator upper plate on the elastomer. This phenomena will be the subject of further study at the AMRL.

CONCLUSIONS

Methods to experimentally determine the four-pole parameters of vibration isolators have been outlined. The errors involved with the currently used blocked mass method have been investigated and the limitations of the method are discussed. An alternate measurement procedure, based on a floating mass is proposed, in order to overcome the problems associated with the blocked mass technique. Results for both blocked measurements and floating mass measurements clearly show that the blocking mass limits the upper frequency range over which measurements can be made.

REFERENCES

1. DICKENS, J.D., NORWOOD, C.J., AND JUNIPER, R.G. (1993). "Four Pole Parameter Characterisation of Isolator Acoustic Transmission Performance", Proc. 1993 Australian Acoustical Society Annual Conference, Glenelg, South Australia, pp. 110-117.

2. MOLLOY, C.T. (1957). "Use of Four-Pole Parameters in Vibration Calculations", Journal of the Acoustical Society of America, pp 842-853, vol. 29, no. 7, July 1957.

3. SNOWDON, J.C. (1976). "Mechanical Four-pole Parameters: Transmission Matrices", The Pennsylvania State University, Applied Research Laboratory report to the U.S. Naval Sea Systems Command, report no. TM 76-122, April 1976.

4. ______ (1979). "Vibration isolation: Use and characterisation", Journal of the Acoustical Society of America, pp 1245-1274, vol. 66, no. 5, November 1979.

5. VERHEIJ, J.W. (1982). "Multi-path sound transfer from resiliently mounted shipboard machinery", Ph.D. thesis, Institute of Applied Physics TNO-TH, Delft, 1982.

REAL TIME MEASUREMENT OF ACOUSTIC TRANSFER FUNCTIONS AND ACOUSTIC IMPEDANCE SPECTRA

Joe Wolfe, John Smith, Gerhard Brielbeck[1] and Fritz Stocker[1]
School of Physics, University of New South Wales, Sydney 2052 Australia

ABSTRACT

A broadband acoustic signal whose Fourier components have equal amplitude is output from a high impedance source of small physical dimensions. This is applied first to a reference system and the pressure spectrum is measured. Then it is applied to an experimental system and the pressure spectrum is measured. In the case where the reference system is purely resistive and where the impedance of the source is much higher than those measured, the measured pressure spectrum of the experimental system is proportional to its acoustic impedance. The desired broadband signal is synthesized, amplified and applied to a loudspeaker. This drives a small tube filled with fibre via an impedance matching horn. Non-uniform frequency response of this system is compensated by a digital feedback loop operating during the measurement of the reference system. We apply this technique to a flute and to a human vocal tract. This technique is the subject of a patent application.

INTRODUCTION

Impedance spectra and transfer functions contain most of the important information about the acoustic performance of linear systems (Fletcher and Rossing, 1991). In wind musical instruments, for instance, the peaks in the input impedance spectrum indicate the frequencies of resonant modes of the bore which may cooperate in the coupled oscillation of the reed-bore system. In the case of the vocal tract, the rather broader and weaker resonances or formants can be identified with features in the impedance spectrum. In compound systems, the impedance spectra of two adjacent stages determine the transmission spectrum; examples are horns or bells used to reduce impedance mismatch between successive stages. All of these examples are air-filled cavities. We shall concentrate on this class of systems in this paper, although we have made preliminary applications of the technique to other acoustic systems.

Well-developed methods for measuring acoustic impedance exist already (Benade, 1960; Backus 1976; Pratt *et al.* 1977). These methods, while capable of high precision, are slow. Although slowness is not a major problem for many aspects of acoustical research, it does make the methods unattractive for some applications, and impossible to use in others.

In this report we discuss some potential uses of very rapid measurements of the acoustic impedance (and other transfer functions) of musical instruments and the vocal tract. We then describe the apparatus which measures transfer functions in a fraction of a second. For some of the applications we consider, the transfer function is the acoustic impedance. We then report measurements made on a flute and on a human vocal tract.

MUSICAL INSTRUMENTS

The impedance spectrum is useful to instrument manufacturers because it is an important factor in an instrument's performance and because it can be objectively measured. The manufacturer Conn of Indiana has been making such measurements since 1945 (cited by Benade, 1973). The frequencies of the instrument's resonances, and the heights and widths

[1] GB and FS are undergraduate exchange students from Fachhochschule Regensburg.

of the impedance peaks corresponding to them can be correlated with the intonation of the instrument, the quality of the notes produced and with the ease of production of notes (e.g. whether they are "bright" or "dark"; whether they have or lack "centre"). The impedance spectrum is thus potentially a useful measurement for quality control in manufacture.

As a data set to characterise the instrument, the impedance spectrum is superior to the spectrum of the sound produced by a wind instrument in at least two ways. Inharmonicity in the impedance peaks is not easily deduced from the sound spectrum because the periodic vibration of the reed or air jet gives only harmonic components. Further, the sound spectrum depends strongly on how the instrument is played and is thus not necessarily reproducible: it is subject to feedback effects involving the player who will often attempt to produce the same sound, regardless of the instrument.

Although the impedance spectrum and related transfer functions in general are quantitative and precise, they have the disadvantage that, except in extreme cases, it is not simple to determine from the spectrum alone whether an instrument be good or bad. This is best judged by an expert player or a panel of such players. On the other hand, the transfer functions and impedance spectra can determine whether two instruments are acoustically similar or not. One can therefore tell whether a given instrument is similar to or different from a reference instrument of known quality. This could be a useful procedure in instrument manufacture. For mass production, such a test could be used to determine whether each instrument fell within acceptable ranges of such parameters as the frequency and height of impedance peaks. In hand-made instruments, such a test could become part of a feedback loop: the maker could make slight changes and test to see how the important parameters changed as a result.

The use of impedance spectra in this application would be much easier if they could be measured very rapidly in workshop or factory conditions. In a brass instrument, several different acoustic configurations (almost all of the permutations of valve positions or the useful slide positions) should be measured. In woodwind instruments, several dozen different fingerings are used by good players, and all or most of these should be checked.

THE VOCAL TRACT

Rapid measurements of transfer functions of the vocal tract have several uses. The most obvious is in research into acoustic phonetics, but there are other potential applications as well.

The frequencies and relative heights of the resonances or formants of the vocal tract can be determined from the impedance spectrum. These data are largely responsible for the differences among spoken vowels. There is a reasonably good mapping between vowel sounds and the frequencies (f_1,f_2) of the two formants with lowest frequencies (Rossing, 1990). Further, there is a relatively simple correlation between (f_1,f_2) and the degree of opening of the mouth and the tongue position, so it is relatively easy for someone to adjust (f_1,f_2) when the feedback is provided.

In most cases, people with normal hearing can determine the vowel sounds of their own languages by listening. There are a couple of important exceptions.

The profoundly deaf have considerable difficulty in learning to speak normally because they cannot use their ears in a feedback loop to match the sound that they produce with a target sound. While they can see the position of the lips of a speaker, this is inadequate feedback for vowel production because the internal shape of the mouth (position of tongue and palette) is also involved. The data (f_1,f_2) could close the feedback loop for such people.

Another example of inadequate auditory feedback occurs when adults learn a foreign language with different vowel sounds, particularly a language with more vowel sounds than their first language(s). In many cases, adults have difficulty distinguishing between two phonemes which are not distinguished in their own language. An example is the anglophone tourist who tells a surprised Frenchman "merci beau cul" (**mɛRsiboky**) when intending to say "merci beaucoup" (**mɛRsiboku**): many English dialects do not distinguish between the sounds of the last vowel in each phrase. A method which can provide immediate quantitative feedback may be used to teach language students to produce vowel sounds similar to target sounds provided by a teacher or native speaker.

In these cases, virtually immediate measurement is required because it is impractical to ask a speaker to hold the vocal tract in a fixed position for a substantial time while a measure is made. Further, the measurement technique should not require free field conditions.

In the examples described above, the prime requirement is for a very rapid, objective measurement of a transfer function containing the important acoustic information about the system measured. The transfer function that is the easiest to understand is the acoustic impedance, but other similar functions would serve the same purpose.

PREVIOUS WORK

Impedance spectra have been measured thus: a source with an output impedance which is high compared to that of the system measured provides a velocity source at a given single frequency. A microphone measures the acoustic pressure in the system measured and the ratio of these gives the impedance at that frequency. The frequency is varied and many measurements are made to acquire the impedance spectrum (Benade, 1960; Backus, 1976). In the method of Pratt *et al.* (1977) a hot wire anemometer is used to measure the volume velocity.

OUR METHOD

Our method is similar except that it uses a small, broadband source with known spectrum and so measures the transfer function at multiple frequencies simultaneously. Further, it relates all measurements to a reference system, and so is well suited to making comparisons and for eliminating effects due to the reverberant field.

The broadband source has a high output impedance and so is approximately a velocity source. The signal is output to a low impedance reference. For research measurements, or when the measured system has a sealed input, the reference system of choice is one whose impedance is well known and/or independent of frequency. A free field, or an effectively infinite tube (one whose length is more than half of the distance travelled by sound during a measurement) are suitable choices. Usually, however, we choose the air in the laboratory because we aim to simulate the conditions of practical applications. We record the magnitude spectrum from a small microphone close to the source. We then apply the same signal to the system to be studied and record the spectrum of the signal from the same microphone.

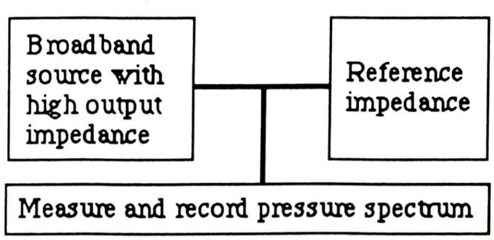

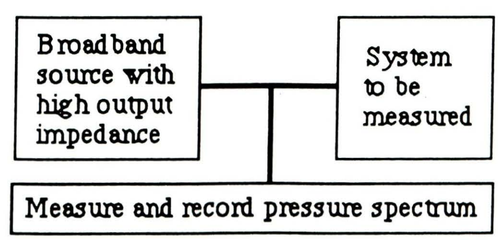

Provided that the impedance of the reference and of the system studied are both much lower than the output impedance of the source, the ratio of these two spectra is the ratio of their input impedances. In the simplest mode of operation, we arrange for the source to have component frequencies all of which have the same amplitude and we use a reference with an input impedance which is nearly independent of frequency. In this mode, and to the extent that these approximations are satisfied, the spectrum recorded from the microphone is proportional to the input impedance spectrum of the system studied.

For the vocal tract and for flue instruments such as the flute, the system studied is in parallel with the air of the laboratory in which the signal contains a substantial component from the reverberant field.

Several constraints must be met by this for this technique to work. For the applications suggested above, substantial acoustic power must be produced to achieve acceptable signal to noise ratio in a broadband signal operating over typical background noise levels in laboratories, classrooms and instrument factories. The source must have relatively small dimensions so that it can be introduced to or coupled with the acoustic systems of interest.

MATERIALS AND METHODS

A waveform with the required spectrum is calculated by a microcomputer and output via a 12 bit digital to analogue converter (NB-MIO-16) and a power amplifier to a 13 cm loudspeaker. The loudspeaker is sealed in a chamber on one side of which is the large end (60 mm diameter) of an exponential horn with a characteristic length of 300 mm. The narrow end of the horn is butted onto a cylindrical pipe with internal diameter 6.5 mm which is filled with acoustic fibre padding.

For brevity we call the whole system (computer, amplifier, loudspeaker, horn and end-tube) the source. Near the output end is located a small microphone (Tandy 33-1052). This is connected to a spectrum analyser (either a Kikusui FAE 2000 or a Spectral Innovations DSP 32). This is shown schematically in Figure 2.

First we synthesize a signal with the desired spectrum whose Fourier components with frequency f_i have amplitude a_i. In most cases this is a flat spectrum: the a_i are all equal. To minimise calculation time and computer memory, we use a periodic signal, although this is not a necessary constraint on the method. The period of this signal may be made as long as necessary to give the frequency resolution required in the spectrum. A range of frequency is selected, and some or all of those multiples of the fundamental frequency which fall within that range are included in the output signal. For example, if one uses a signal with period 5 Hz and a range 100-1000 Hz the signal could be the sum of 181 sine waves with frequencies 100, 105, 110 Hz etc.

The choice of the component frequencies in the output signal requires a compromise among frequency range, frequency resolution, sensitivity and measurement time. The signal to noise ratio is finite and so this limits the information available in a given interval. The use of a periodic signal lends itself readily to equal sampling of frequency, but this is not necessary. A strictly logarithmic spacing is impossible, but spacings which increase with increasing frequency may be achieved with a very low fundamental frequency and by omitting successively more harmonics with increasing frequency.

We input this signal to the amplifier, speaker, horn and end-tube and then to the reference system (usually the laboratory). We record the microphone signal using the ADC and the computer and compute the Fourier components (amplitudes b_i). This calculation is simplified by the fact that we know the frequencies f_i present in the signal and we use the Goertzel algorithm (Goertzel, 1958). Due to the frequency dependent gains of the amplifier, loudspeaker, horn, tube and microphone, this output spectrum is very different from that of the signal synthesized.

We then synthesize a signal with Fourier components proportional to a_i/b_i and input this to the amplifier etc. The result is an acoustic signal with a spectrum closer to that desired. We then repeat this process, usually three to six times. The result is a signal whose spectrum closely approaches that desired. (The reason for the several iterations is to compensate for non-linear effects.) Note that, because the microphone is inside the feedback loop, its response function is not relevant to the measurement.

We then replace the reference system with the system to be measured. If the spectrum input to the reference system is flat and if the response of the reference system is flat, then the spectrum recorded at the input of the measured system is proportional to the input spectrum of that system. For other cases, an arithmetic calculation is required for each spectral component.

In another related technique (covered by same patent), we replace the loudspeaker and horn with a force transducer that drives a mechano-acoustic system. We have used this technique to drive the isolated belly of a violin and the bridges of intact string instruments. The acoustic response function of this system can then be compared with a reference.

For these measurements on the flute, the instrument was clamped and the source and microphone were placed next to but not occluding the mouthpiece aperture in the position that would be occupied by the lower lip of a player. For the experiments with the vocal tract, the subject's head was firmly located and the source and microphone were positioned 15 mm outside the teeth of the subject, directly in front of the aperture. In both cases the source was thus imposed on the system under investigation in parallel with the laboratory.

RESULTS AND DISCUSSION

Figures 3 a, b and c show the spectra measured from the microphone in the reference system, in this case 500 mm outside an open second floor window. The frequency range is 200 Hz to 4 kHz and the signal contains 153 components separated by 25 Hz. Fig 3a shows the spectrum from the first iteration: it shows the frequency dependence of the total gain of the amplifier, loudspeaker, horn, end-pipe and microphone. 3b shows the output for the second and 3c the output of the sixth iteration. Note that the spectrum becomes successively flatter. The noise in this spectrum (the deviations from flatness) is dominated by the digitization of the 12 bit DAC: the r.m.s. variation is 0.5 bits. We expect to improve this aspect of the performance substantially with the use of a 16 bit DAC. More generally, the performance of this technique is limited by the available signal to noise ratio of the environment and the equipment. This requires a compromise among frequency range, frequency resolution, sensitivity and measurement time.

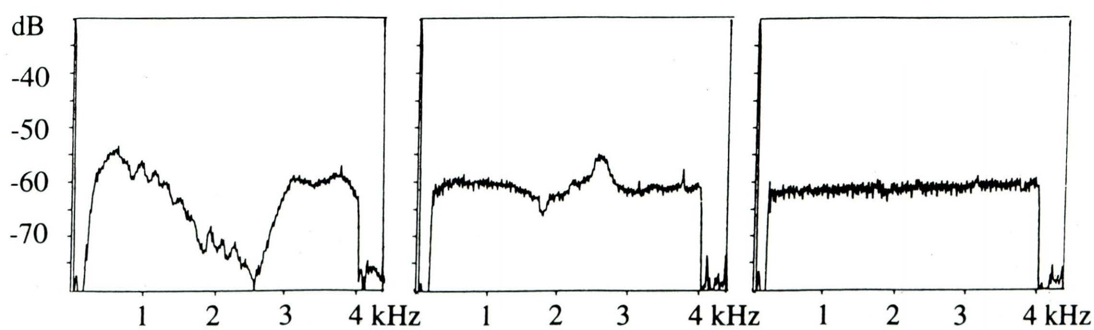

Figure 3. The pressure spectra of reference system during the first, second and sixth iterations of the loop shown in Figure 2.

Figures 4a and 4b show the spectrum, from 200 Hz to 4 kHz, measured at the mouthpiece of a Boehm flute whose keys were clamped in two different fingerings for the note F#6. The measurement time was 262 ms. The input was a signal which produced a flat spectrum as shown in Fig 1c, except that in this case the reference was the air of the laboratory in which the measurement was conducted, but with the flute removed. This is an appropriate reference because the measurement is made with the flute in parallel with the laboratory. Note that the peaks are not exactly harmonic and that the height and shape of the second and fourth major peaks are different. There are other, smaller differences. Figure 4c is the spectrum of the flute with fingering (ii), but using fingering (i) as a reference. 4c is thus similar to the difference between 4a and 4b, but obtained in a rather different way. This example is shown to illustrate the device used to compare similar systems. In a practical application of the technique, the reference system would be a specification prototype and the measured systems would be production models. In all these examples the dominant noise is the digitization error of the 12 bit D-A-D card.

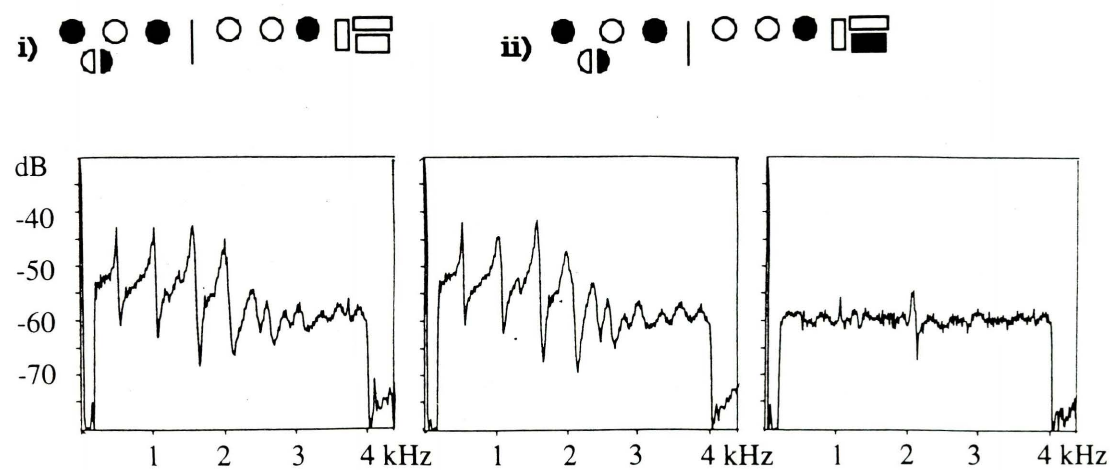

Figure 4. The first two spectra were measured for the flute, in parallel with the laboratory, using the fingerings (i) and (ii) shown above. The reference was the laboratory with the flute removed. The third spectrum is that measured for fingering (ii), but using fingering (i) as the reference.

The reason for making this comparison is because it allows a comparison between two subtly different systems by changing only one key and without repositioning the instrument. The fingering change is relatively subtle because the Boehm flute has large tone holes and this change is the closing of a hole near in the foot below three open holes. The notes produced with these fingerings are rather similar and untrained listeners may not notice the difference in timbre. The main difference is that b tends to be somewhat flatter than a, but a player usually compensates for this. Players, on the other hand, think that these notes feel quite different to play.

Figure 5 show some measurements made on a vocal tract in parallel with the air of the laboratory. The signal contained components from 200 to 4000 Hz with 25 Hz spacing. The source was in fixed position outside the mouth of the subject. For the reference, the subject's mouth was closed. Only one subject was used, so these results may be regarded as preliminary trials to show the sensitivity of the method, rather than a formal study of phonetics. Figures 5a and 5b show the spectra measured when the subject shaped his vocal tract in the form required to pronounce the French vowels **u** (as in the French word "dessous" (**d(ə)su**), meaning below) and **y** (as in "dessus" (**d(ə)sy**), meaning above). Some of the formants can be clearly seen. These spectra show that these two phonemes are

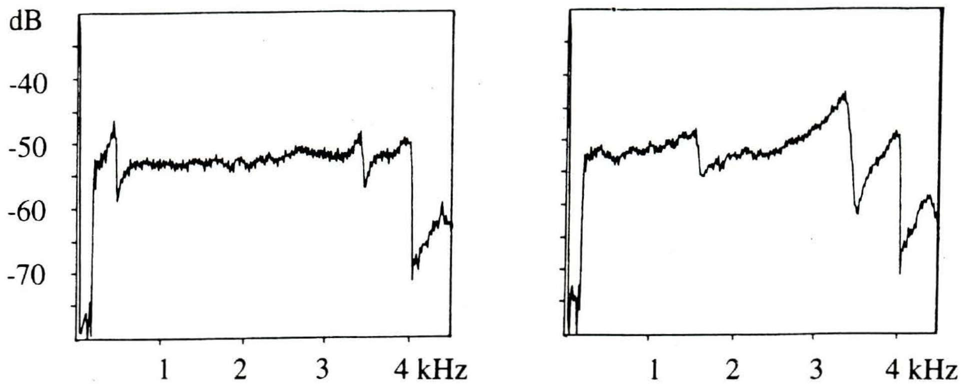

Figure 5. The first two spectra were measured for a vocal tract, in parallel with the laboratory, prepared to pronounce the French vowels "u" and "y".

not very similar at all. This is not surprising to native speakers of French who would never confuse "dessous" and "dessus". It is less clear to most adult native speakers of English, a language which does not make use of the distinction between **u** and **y**: most anglophones find the two sounds difficult to distinguish reliably. This makes an interesting example of the potential for use of formant visualisation in language laboratories or in speech pathology.

Acknowledgements. We thank John Dunlop for his comments on the draft manuscript.

REFERENCES

BACKUS, J. (1976) Input impedance curves for the brass instruments. J. Acoust. Soc. Am. 49, 470-480.

BENADE, A.H. (1960) The physics of woodwinds. Scientific American 203, 145-154.

BENADE, A.H. (1973) The physics of brasses. Scientific American 229, 24-35.

FLETCHER, N.H. and ROSSING, T.D. (1991) The Physics of Musical Instruments. Springer-Verlag, New York.

GOERTZEL, G. (1958). An algorithm for the evaluation of finite trigonometric series. Amer. Math. Monthly 65, pp 34-35.

ROSSING, T.D. (1990) The Science of Sound. Addison-Wesley, Reading, Mass.

PRATT, R.L., ELLIOTT, S.J., and BOWSHER, J.M. (1977). The measurement of the acoustic impedance of brass instruments. Acustica 38, pp. 236-246.

Numerical and Experimental Studies of Complex Sound Intensity Fields in an Absorptive Enclosure

Qinghui Zhong & Robin J. Alfredson

Department of Mechanical Engineering
Monash University, Clayton, Victoria 3168, Australia

Abstract

The Acoustic Finite Element Method was used in the prediction of the active and reactive sound intensity vectors inside an axisymmetrical enclosure partially lined with sound absorptive material. Both the local reacting model and the bulk reacting model were used in modelling the absorptive behaviour of the acoustic linings, which were made of rockwool materials. The complex speed, the characteristic impedance and the surface impedance of these linings were obtained from impedance tube measurements. An experimental rig, based on an axisymmetrical chamber, was then used to verify the numerical predictions. The active and reactive intensities were determined from the measurements using a 20 mm grid, axially and radially. The agreement between the numerical and the experimental data was good. The results gave a clear picture of the sound absorption processes for the rigid surface and the absorptive surface cases, and at the same time, verified the existence of circulatory patterns of the active sound intensity field inside the enclosure.

Introduction

In the absence of absorption and dissipation of acoustic energy, an enclosure would be purely reactive, i.e. the sound pressure and the sound particle velocity would be in quadrature with each other at any location for a pure tone sinusoidal excitation.

Such an ideal enclosure, however, is not likely to be found in real situations where sound absorption, dissipation and interference of sound sources occur. The movement of acoustic energy in real enclosures is therefore deemed to be important for acoustic design or noise control in many branches of engineering. However, for an enclosure partially lined with sound absorbing material , it is seldom feasible to derive a analytical solution for the sound pressure distribution in the enclosure. In most cases, numerical approaches are an effective alternative. Acoustic modal analysis was traditionally used to predict sound pressure fields in enclosures with rigid walls, i.e. with no energy dissipation [Morse 1944]. Although the method was sometimes used for the calculation of absorptive enclosures, it has been found to give incorrect results for sound intensity fields [Pan 1993]. The information of sound pressure distribution in a enclosure is not always adequate for design purposes. As is frequently reported in the literature, the information of sound intensity would always give additional insight into the acoustic behaviour of enclosures. It can be claimed that sound intensity studies are necessary if the details of acoustic energy movements are to be known. A clear picture of the sound intensity field in an absorptive enclosure is beneficial not only for engineering design but also for engineering acoustics. A previous effort dealt with the sound intensity evaluation in a two dimensional enclosure with two sound sources with an focus on active noise control. In the present paper, the main concern is the sound intensity field produced by the absorbing lining and radiation aperture in an axisymmetrical enclosure.

Sound intensity fields

The sound intensity is defined as the rate of the flow of acoustic energy through a unit area normal to the direction of propagation. The most fundamental quantity is probably the active sound intensity [Fahy, 1989. pp46]:

$$\vec{I_a}(r) = \overline{p(r,t) \cdot \vec{V}(r,t)} \tag{1}$$

The acoustic power flow through a certain area can then be calculated as

$$P = \int_s \vec{I_a}(r) d\vec{s} \tag{2}$$

If the surface S totally encloses a sound source (or sink), the above equation gives the sound power generated (or absorbed) by whatever is inside S. This feature of the active sound intensity is possibly the greatest attraction for noise control purposes. The physical interpretation of the reactive sound intensity, on the other hand, is less obvious. By definition, the reactive sound intensity is given by

$$\vec{I_r}(r) = \overline{\hat{p}(r,t) \cdot \vec{V}(r,t)} \tag{3}$$

where the symbol ^ denotes the Hilbert transform.

In the case of a pure-tone sinusoidal sound field, the sound pressure can be written as

$$p(r,t) = P(r) e^{j[\omega t - \Phi(r)]} \tag{4}$$

and the sound particle velocity as:

$$\vec{V}(r,t) \quad = \quad [\frac{1}{\rho\omega} P(r) \nabla \vec{\Phi}(r) + j \frac{1}{\rho\omega} \nabla P(r)] e^{j[\omega t - \Phi(r)]} \tag{5}$$

The active and reactive sound intensity fields are governed by

$$\vec{I_a}(r) = \frac{1}{2\rho\omega} P^2(r) \cdot \nabla\Phi(r) \tag{6}$$

$$\vec{I_r}(r) = -\frac{1}{2\rho\omega} P(r) \cdot \nabla P(r) \tag{7}$$

The instantaneous sound intensity for a pure-tone sinusoidal sound field is then found from

$$\vec{I}(r,t) = 2\vec{I_a}(r) cos^2[\omega t - \Phi(r)] + 2\vec{I_r}(r) sin^2[\omega t - \Phi(r)] \tag{8}$$

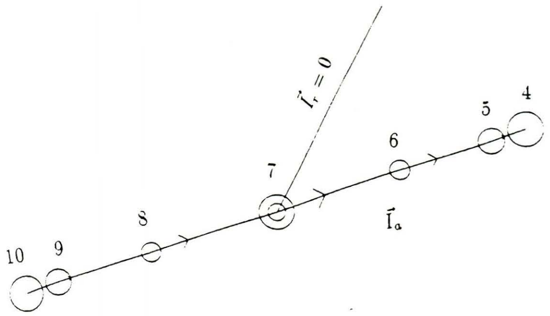

Fig.2. As in Fig. 1, but for a pure active sound field in which : $p = 1.0$; $U_x = 0.7$; $U_y = 0.25$.
Only half of the time period is shown.

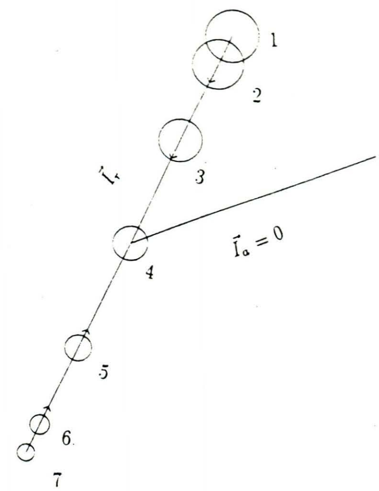

Fig.3. As in Fig. 1, but for a pure reactive sound field in which : $p = 1.0$; $U_x = j0.3$; $U_y = j0.6$.
Only half of the time period is shown.

Finite Element Calculations

The enclosure shown in Fig.4 was chosen for the finite element calculation and measurement. The loudspeaker, attached to the small cylinder on the left, provided the required sound source. On the right was a small cylinder of the same diameter with a open end which was used as a acoustic radiation load. The chamber in the middle was lined with a 50mm thick layer of sound absorbing lining. Plane wave propagation was assumed in the small cylinders.

The finite element approach previously reported [Zhong & Alfredson 1993(a,b)] was extended to study the axisymmetrical sound intensity field inside this enclosure. The Galerkin formulation was again used for the present case with only slight changes in the programming. The complex sound pressure was used as the field parameter. The sound particle velocity was derived by differentiating the interpolation function with respect to the spatial coordinates. It has been found to be convenient by the authors to subsequently decompose the sound particle velocity within a finite element into two components: the one in phase with sound pressure and the one in quadrature with sound pressure. They were found to contribute to the active and reactive sound intensities, respectively. For the results reported here, only the linear triangular ring elements were employed. The sound source, with its internal impedance, has always been a difficult issue in the modelling process. A constant sound pressure source was used, the values of which were obtained from the measurements of sound pressure variation close to the surface of the loudspeaker. Alternatively, a sound source with a particle velocity profile can be specified. It was found the choice of the sound source does not affect the calculation results. This can be explained from the fact that the load impedance from the viewpoint of the sound source remained unchanged. The radiation impedance

It can be seen that the sound particle velocity can be decomposed, as in Eq.(5), into two components — one in phase with the sound pressure and one in quadrature with the sound pressure. The decomposition can be performed everywhere in the sound field. The resulting two components contribute to the active and reactive sound intensity, respectively. The active and reactive sound intensities, in turn, contribute to the instantaneous sound intensity which gives the amplitude and direction of acoustic energy propagation at any instant in a time period. The graphical method by [Mann & Tichy 1991] is used for some of the typical sound intensities and the instantaneous sound intensities they represent. The results are given in Figs(1-3). For a pure active or reactive sound intensity vector, the sound particle moves along a straight line. The direction of the straight line depends on the coordinate components of the active (or reactive) sound intensity at the location. For the pure active sound intensity, the direction of the instantaneous sound intensity does not change within a time period — always pointing to the direction of the active sound intensity. In the case of the pure reactive sound intensity, for half of the time period the instantaneous sound intensity coincides with the direction of the reactive sound intensity. For the other half it points in the opposite direction of the reactive sound intensity. Thus, for a pure reactive sound field, no net energy transfer occurs. For a general sound field, the sound particle moves in an elliptical path, as in Fig.(1). The elliptical path shown in Fig.(1) can be considered as a combination of two movements along the straight lines, as in Fig.(2) and Fig.(3). It is thus alway possible to decompose a general sound field into a pure active field and a pure reactive field. It also appears helpful to suggest that at sufficient high frequencies, the active intensity field in an enclosure would be occupied by closely located circulatory patterns (as shown in the next section) and the reactive intensity field would be scattered closely with "sinks" and "sources" that it becomes diffuse.

It is important to note that the instantaneous sound intensity travels at the speed of sound, c, in the direction of the instantaneous sound intensity. The time-averaged sound energy, on the other hand, can travel at speed other than c, and in the direction of the active sound intensity.

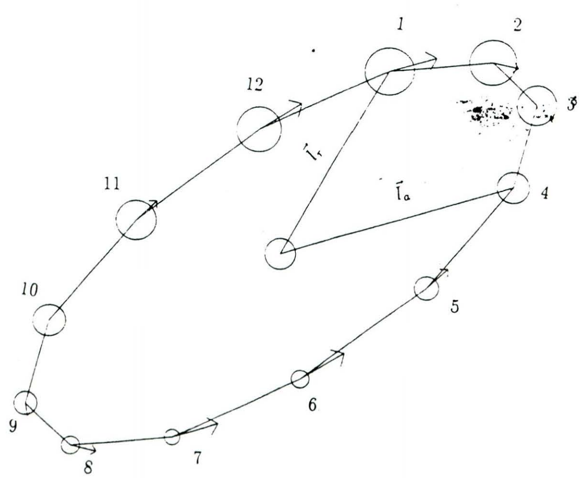

Fig.1. One time period of the instantaneous sound intensity for a sound particle. $p = 1.0$. $U_x = 0.7 + j0.3$. $U_y = 0.25 + j0.6$. The circle in the center is the initial volume of the sound particle. The arrow represents the instantaneous sound intensity, the amplitude of which is proportional to the length of the arrow. The directions of the active and reactive sound intensities are also shown.

introduced by the open end of the small cylinder was calculated from the approach by Levine & Schwinger[Levine & Schwinger 1948] for an unflanged circular tube. The absorption due to the rockwool lining was experimentally determined. Without much information of the micro-structural properties of the materials and the sound field in which they were used, it was decided to use both the locally reacting model and the bulk reacting model for the description of the sound absorbing linings. The derived quantities at 1000 Hz, which were required in the finite element calculation, were as follows: 1.The characteristic specific impedance ratio, $Z_c = 1.36 - j0.65$; 2.The complex propagation constant, $h = 32.88 - j21.54(m^{-1})$; 3.The surface impedance ratio, $Z_l = 1.1011 - j0.4906$; 4.The radiation impedance of the open end, $Z_r = 0.143 - j0.450$.

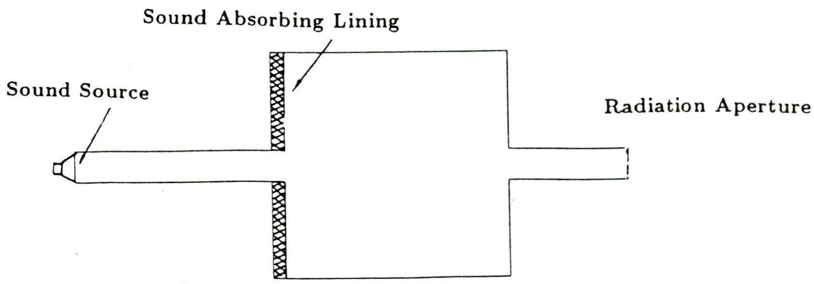

Fig.4. The partially lined axisymmetrical enclosure for sound intensity studies.

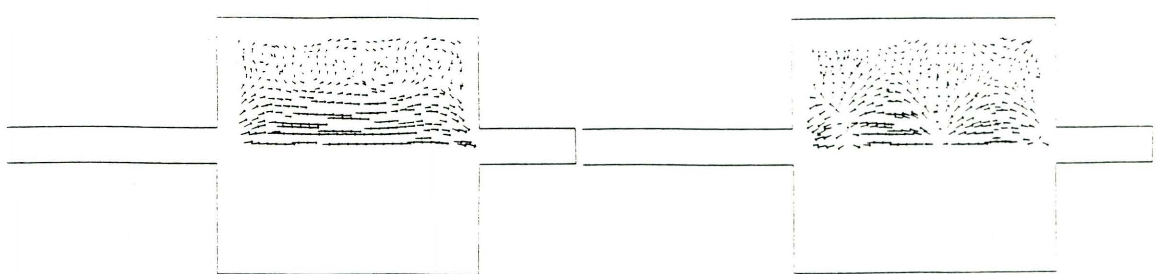

a).active sound intensity field

b).reactive sound intensity field.

Fig.5. The calculated sound intensity fields for the rigid surface case.

Fig.5 shows the calculated active and reactive sound intensities for the rigid surface case (i.e. the absorbing lining was replaced by a hard surface). The absorption of acoustic energy by the radiation aperture was evident in the active sound intensity field. As the excitation frequency (1000 Hz) was above the first transverse mode of the chamber, circulatory patterns were also present in the active sound intensity field. The finite element results for the absorbing lining case were shown in Fig.6 The absorption was partly caused by the absorbing lining and partly caused by the open end radiation, as can bé seen from the active sound intensity field. Since both the locally reacting model and the bulk reacting model gave approximately similar results for the present case, only the results for the locally reacting model are included here.

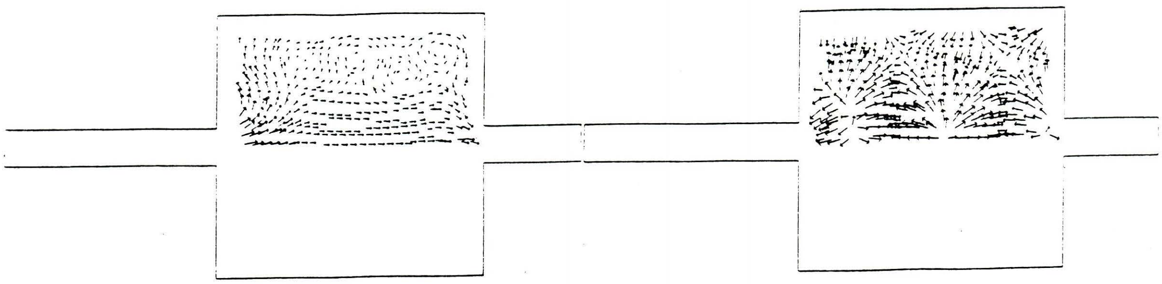

a).active sound intensity field   b).reactive sound intensity field.

Fig.6. The calculated sound intensity fields for the absorptive surface case.

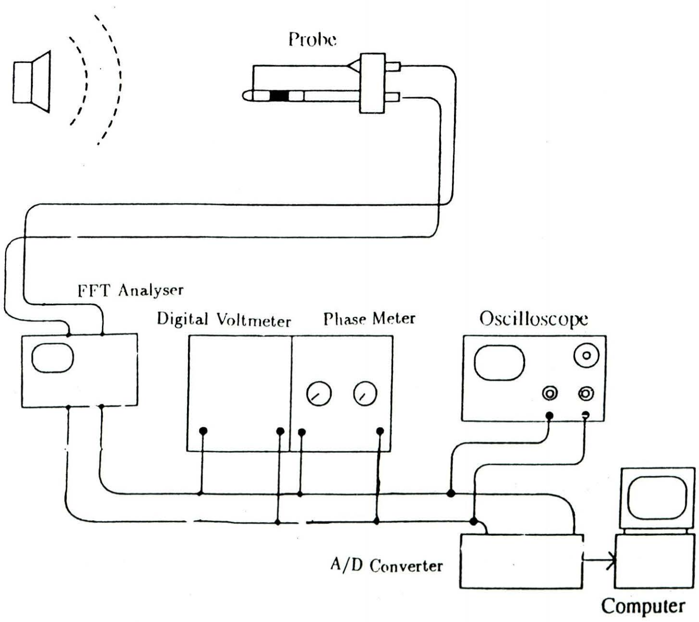

Fig.7. The experimental set-up for sound intensity measurement.

Sound Intensity Measurements

A test rig was specially designed for the verification of the numerical results. The sound intensity measurements were conducted on a precision digital lathe so as to guarantee the positioning accuracy of the intensity probe. The chamber, made of transparent perspex material in the shape as shown in Fig.4, was clamped on the lathe's carriage way, with the tailstock removed from the lathe. The sound intensity probe (B & K 3147) was attached to a hollow projection rod which held the cables from the intensity probe to the analyser. The projection rod could be moved in transverse and axial directions through a slip plate on the side wall of the chamber. With the projection rod clamped at one end to the lathe's carriage, the radial and axial movements of the sound intensity probe were thus made possible by operating the carriage handwheel and the cross feed screwhandle. Positioning accuracy in both directions were estimated to be less than 0.01 mm. A two-channel FFT analyser (B & K 2144) was used for the sound intensity measurements. The digital voltmeter and the phase meter were used to monitor the signals from the sound intensity probe. The phase mismatch of the PC based data acquisition system was calibrated prior to the measurement. The PC system was used in such regions where the field P-I index exceeded the FFT's capabilities.

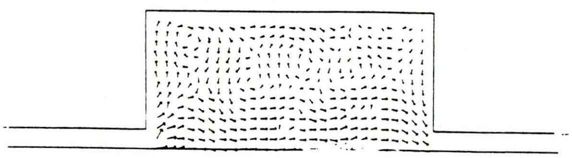

a).active sound intensity field

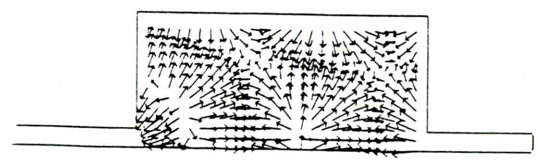

b).reactive sound intensity field.

Fig.8. The measured sound intensity fields for the rigid surface case.

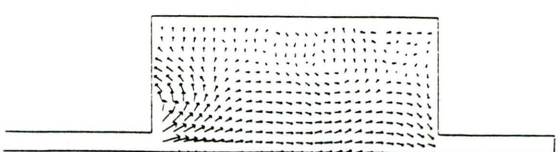

a).active sound intensity field

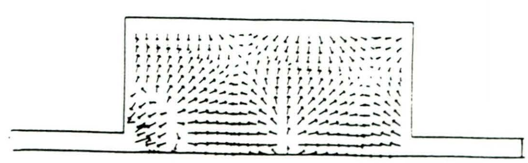

b).reactive sound intensity field.

Fig.9. The measured sound intensity fields for the absorptive surface case.

The experimental set-up is shown in Fig.7. The Pressure-Residual Intensity Index of the measurement instrumentation was around 20 dB at 1000 Hz. The measured sound intensity fields for the rigid surface are shown in Fig.8, and for the absorptive surface shown in Fig.9.

Summary

The complex sound intensity fields in an absorptive enclosure was investigated by numerical modelling and experimental verification. Good agreement was obtained for the two cases considered. The results reported would provide valuable information in the acoustic design or noise control in such an enclosure. The authors agree that sound intensity measurement is, and will continue to be a powerful tool in enginering acoustics. They also want to emphasize the importance of accurate and reliable sound intensity predictions for various situations. For instance, combined with CAD, the proposed approach would help design potentially quiet products in the concept design stage. Efforts are being made in the study of instantaneous sound intensity in absorptive enclosures by the finite element method and the relationship between the complex sound intensity and the active-reactive sound energy densities. The results will be reported in due course.

Acknowledgements

The junior author would like to thank The Department od Employment, Education and Training of Australian Government and Monash University for the financial support during the course of his postgraduate research project.

References

Levine, H. and J. Schwinger, On the radiation of sound from an unflanged circular pipe, Physical Review, 73(4), 1948, 383-406.

Mann, III, J. A. and Jiri Tichy, Acoustic intensity analysis: distinguishing energy propagation and wave-front propagation, J. Acoust. Soc. Am. 90(1), 1991, 20-25.

Morse, P. M. and R. H. Bolt, Sound waves in rooms, Review of Modern Physics, (16) 1944, 69-105.

Pan, J., A note on the prediction of sound intensity, J. Acoust. Soc. Am. 93(3), 1993, 1641-1644.

Zhong, Q. H. and R. J. Alfredson, Numerical evaluation of complex sound intensity fields for noise control, I nter-Noise'93, Aug. 24-26, 1993(a), Leven, Belgium.

Zhong, Q. H. and R. J. Alfredson, The instantaneous sound intensity in two-dimensional sound fields, Acoustics Australia, Vol. 21, No. 1, 1993(b), 22-27.

NOISE AND VIBRATION IDENTIFICATION AND CONTROL

Active Control of Extensional Vibrations in an Elastic Rod

Christopher P. Turnbull and Colin H. Hansen

In recent years active vibration control has become a viable alternative to traditional passive control for some applications. However, research has tended to concentrate on the area of flexural vibration control with very little attention being given to the study of active control of extensional vibrations. Work reported in this paper demonstrates active extensional vibration control by reducing the level of extensional vibrations travelling along an elastic rod. The demonstration is made as realistic as possible by using random primary excitation and taking into account effects such as the possibility of the vibrations travelling in both directions along a structure.

INTRODUCTION

Prior to Fuller et al (1990), all previous work on active control of vibrations in beams appears to have dealt solely with flexural motion. Redman-White et al (1987) used flexural power flow as the quadratic cost function for minimisation in their experiments to reduce the vibrations travelling along a thin beam. Gonidou and Fuller (1989) were also able to minimise flexural power flow in their experiments on a thin beam, but they were able to achieve their results with very few point forces. In these experiments involving thin beams, only one flexural wave type was able to propagate. Hansen and Pan (1990) increased the complexity of the setup by using a test beam with dimensions which simulated a more realistic practical structure. They used point control forces at various positions and angles to reduce flexural vibrations. They found that all forms of vibration (transverse, longitudinal and torsional) should be considered because an attempt to control one form had the effect of exciting another.

Fuller et al (1990) were able to use pairs of piezoceramic transducers mounted symmetrically across a thin beam to sense and control both flexural and extensional vibrations. All of these studies aimed to control only a single frequency and used anechoic terminations to ensure that waves travelled in only one direction.

However, in some practical situations, vibration is produced by a number of separate, non-periodic, mechanisms at various positions along the structure. The end result of this situation is to have random vibrations travelling in one direction along the structure that are not correlated with vibrations travelling in the opposite direction. If feedforward active control is to be considered for such an application, it must be able to attenuate the random vibration travelling in one direction without being corrupted by the vibration travelling in the opposite direction.

Therefore, this study aims to demonstrate the active control of random extensional vibrations travelling along a rod while an uncorrelated interfering vibration, of a similar bandwidth, is travelling in the opposite direction.

EXPERIMENTAL APPARATUS

A beam, which was hinged at one end and had the rod hanging from the other, was suspended by springs and connected to a vibration exciter (Fig. 1). The beam was therefore shaken by passing a signal, amplified by a power amplifier, to the vibration exciter. This shaking of the beam caused the top of the rod to be vertically displaced and hence induced an extensional vibration into the rod.

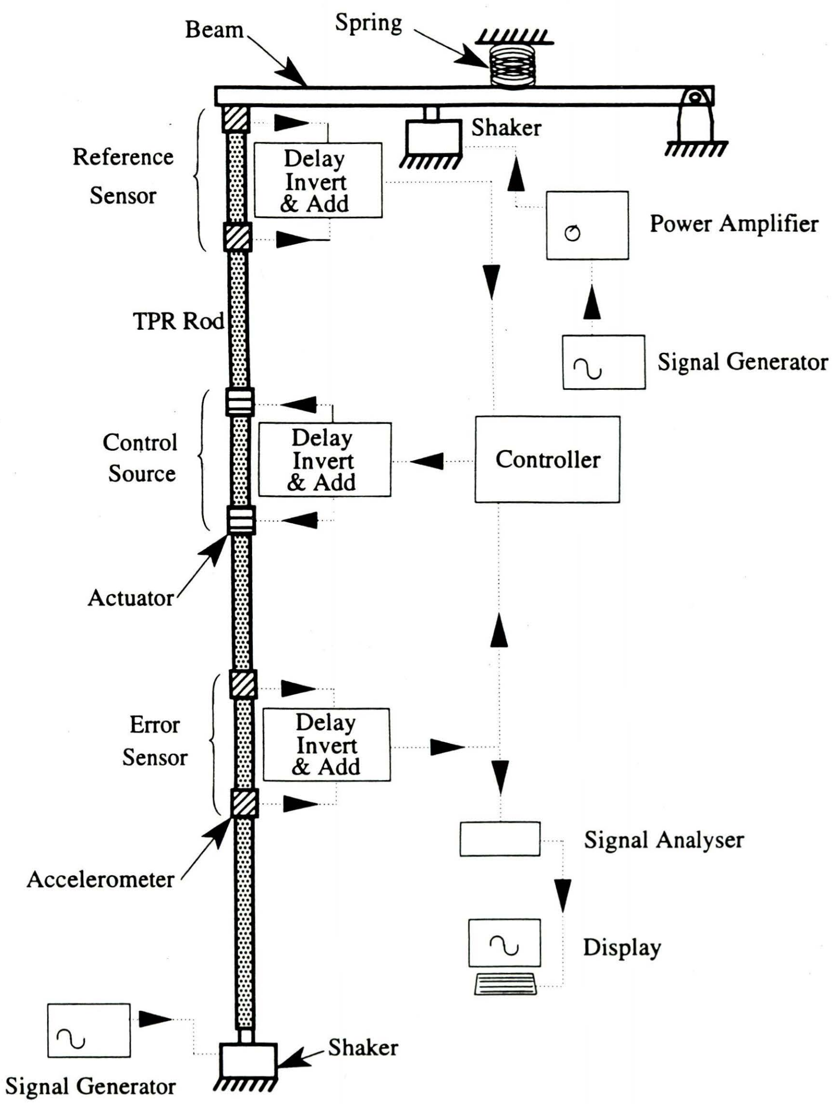

Fig. 1 - Experimental apparatus

The rod material chosen for the experiments was a thermoplastic rubber (TPR). This material was chosen mainly because of its slow wave speed (approximately 175 m/s) which enabled a relatively small sample to be used.

To induce upward moving vibration into the system a second vibration exciter was connected to the bottom of the rod. The appropriate signal was then passed from a second signal generator into this vibration exciter. The use of a separate signal generator for the primary and the interfering vibration was to ensure that the two signals were not correlated.

The reference and error sensors were required to sense the extensional vibration travelling down the rod, while an interfering vibration was travelling up the rod. This was done by using two accelerometers in each of the sensors and delaying, attenuating and inverting the signal from the bottom accelerometer before it was added to the top accelerometer of the sensor.

A wave travelling up the rod would first be sensed by the accelerometer in the sensor that was closest to the bottom. At time τ later the same vibrational wave would be sensed by the upper accelerometer in the sensor. In travelling the distance between the two accelerometers the vibration is attenuated by a factor of A. If the signal from the bottom accelerometer is delayed by time τ and attenuated by a factor of A, it should be the same as the signal from the top accelerometer. Therefore, if the delayed and attenuated signal from the bottom accelerometer is inverted and added to the signal from the top accelerometer, there should be no resultant signal. That is, an upward travelling vibration is not sensed.

On the other hand, for a wave travelling down the rod, the bottom accelerometer would not receive the vibration until after the top accelerometer and the level of vibration would have been reduced along the path. In this case, if the signal from the bottom accelerometer is delayed, attenuated, inverted and added to the signal from the top accelerometer, a resultant signal is sensed. Therefore, a wave travelling down the rod is sensed but a wave travelling up the rod is not.

The resultant waveform for a downward travelling wave is not a direct representation of the vibration travelling down the rod but it is a linear translation of it. Therefore, the controller should be able to infer the correct waveform from the unidirectional sensor because the adaptive digital filter is able to make linear translations.

The control source was composed of two piezoelectric actuators that were connected to the controller via a two channel amplifier which was designed to operate with these types of piezoelectric actuators.

A unidirectional control source was developed so that control vibration travelling down the rod could be induced without adding to the vibration travelling up the rod towards the primary source. This was achieved by splitting the signal to the control source into two and passing one of these signals to the piezoelectric actuator closest to the bottom of the rod. The second of the split signals was delayed, attenuated and inverted before being passed to the piezoelectric actuator closest to the top of the rod. The delay and attenuation were adjusted so that they were equal to the delay and attenuation experienced by the vibrational wave in travelling along the rod from one actuator to the another. This process was similar to the process used in the development of the unidirectional sensors.

A purpose built controller, designed and built at the Department of Mechanical Engineering of The University of Adelaide, was used. This active controller was capable of controlling eight error sensors with eight control actuators by the use of digital finite impulse response adaptive filters which were updated using the 'Filtered-X LMS' algorithm (Widrow and Stearns 1985).

EXPERIMENTAL PROCEDURE

A random signal with a bandwidth of 100 Hz was sent from a signal generator to the control actuators with both the primary and interfering actuators disconnected. The controller was switched on in its system identification mode and allowed to operate to identify the cancellation path transfer function (the path from the input to the control actuator amplifier to the error sensor output).

After successfully converging the cancellation path identification weights, the control system was enabled and the primary vibration was introduced. Initially the bottom shaker was disconnected from its signal generator so that the amount of vibration travelling up the rod was limited to the reflections that occurred at the bottom of the rod and at the discontinuities along the rod (at accelerometers and actuators). This was so that the unidirectional sensors and actuator could be tried and tuned before the interfering vibration was added. When the minimum power spectral density was reached over the bandwidth, its level was recorded. The control signal was then turned off so that the level at the error sensor due to the primary signal could be recorded. In this way the insertion loss due to the control signal could be found by subtracting the minimised level from the level due to the primary signal.

The bottom shaker was then reconnected and excited with random noise which had the same bandwidth as the primary vibration but was uncorrelated with it. The same procedure was then followed to calculate the insertion loss due to the controller in the presence of another uncorrelated disturbance.

RESULTS

For the case where there was a random primary vibration with a bandwidth of 100 Hz but no interfering vibration from the bottom shaker, a filter of order 16 was required to establish control. After iteration of the cancellation path identification and control parameters an overall insertion loss of 30 dB was achieved. The comparison of power spectral densities with and without control is shown in Fig. 2. This result shows the potential of active vibration control to significantly reduce random extensional vibrations in a rod.

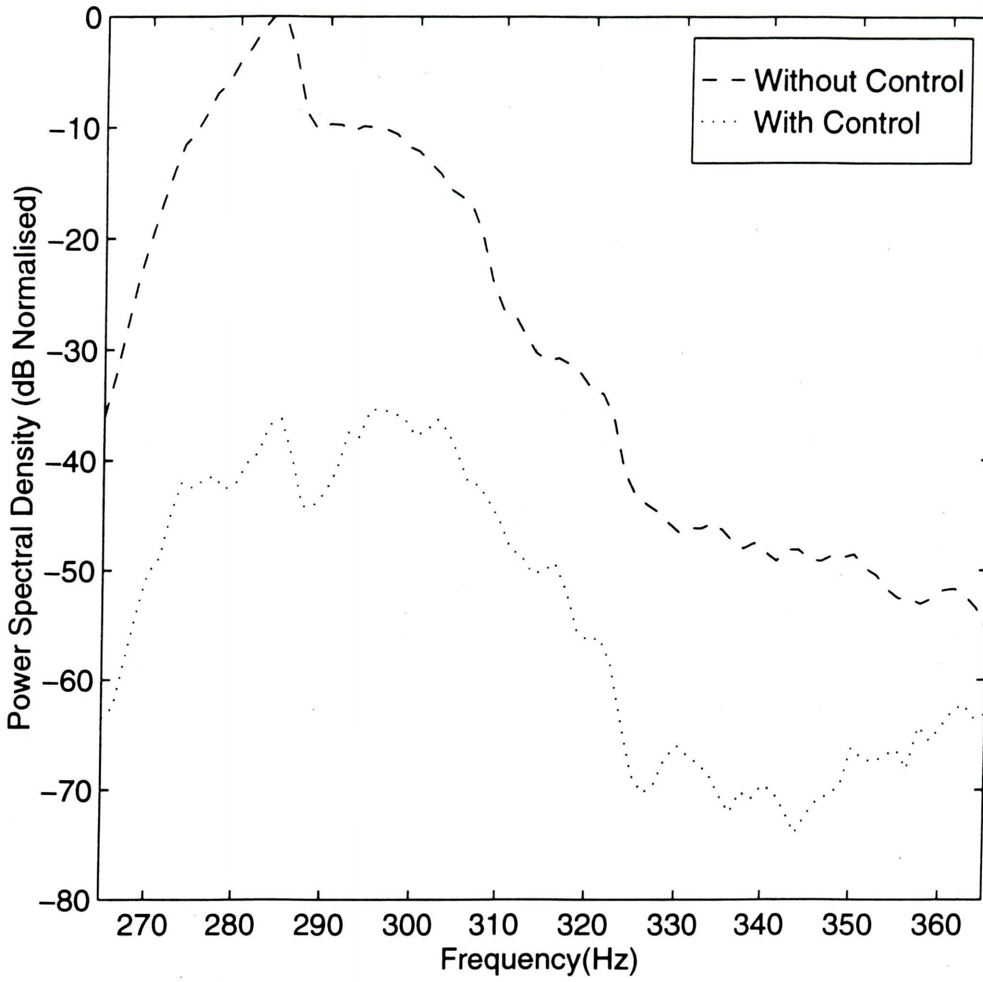

Fig. 2 Insertion loss with no interfering vibration present

After successfully demonstrating the ability of active control to significantly reduce unidirectional, random, primary vibration, the interfering vibration, travelling in the opposite direction to the direction of intended control, was introduced from the bottom actuator. The levels of the primary and interfering vibrations, measured at the bottom of the error accelerometers, are shown in Fig. 3.

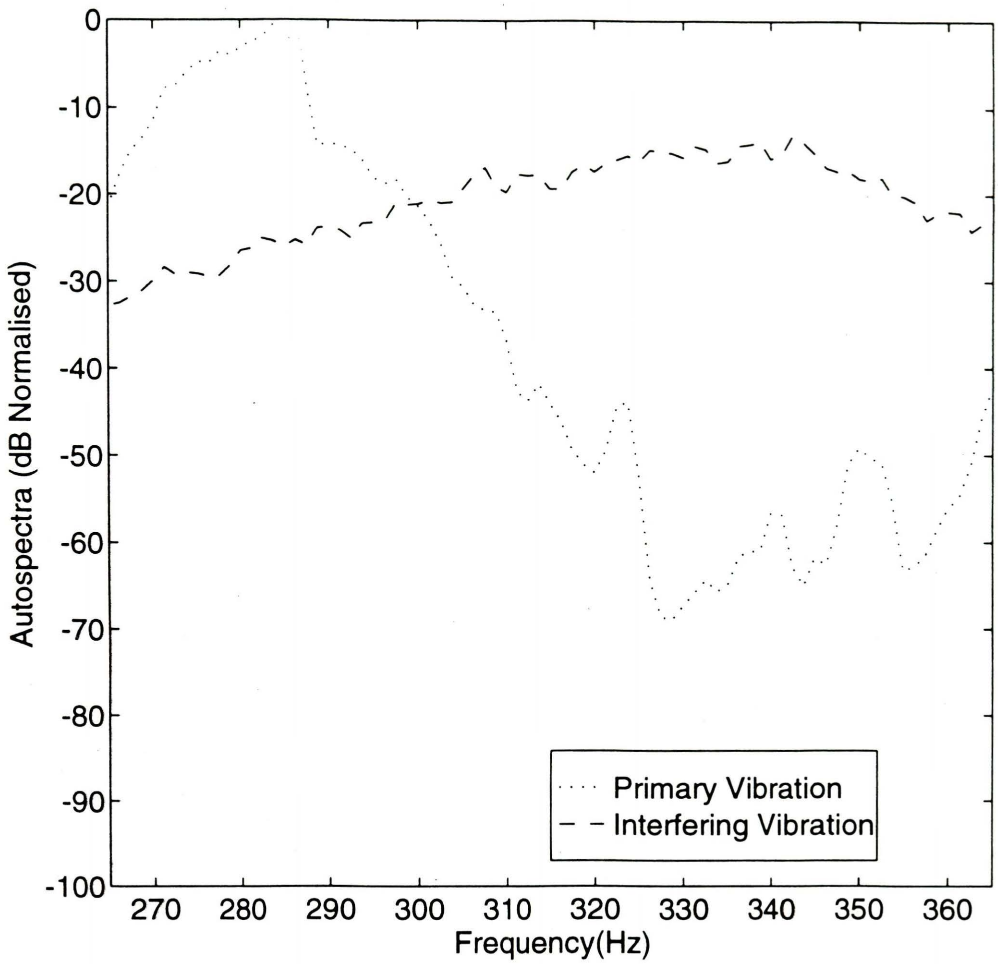

Fig. 3 - Level of the primary and interfering vibration

Once again, 16 filter weights were used to obtain the results shown in Fig. 4. The overall insertion loss over the 100 Hz bandwidth was found to be 18 dB. The figure shows that at the lower frequencies in the band the insertion loss was quite large (over 40 dB at some frequencies) but at the higher frequencies the controller actually added noise to the system.

The main reason for the high insertion loss at some frequencies and the negative insertion loss at others was the inability of the setup to produce random noise at a level that was uniform across the bandwidth of operation when sensed at the error sensor. This was due to the high damping properties of the TPR rod that gave the primary path a steeply sloping transfer function and therefore did not allow as much high frequency primary vibration to travel to the error sensor.

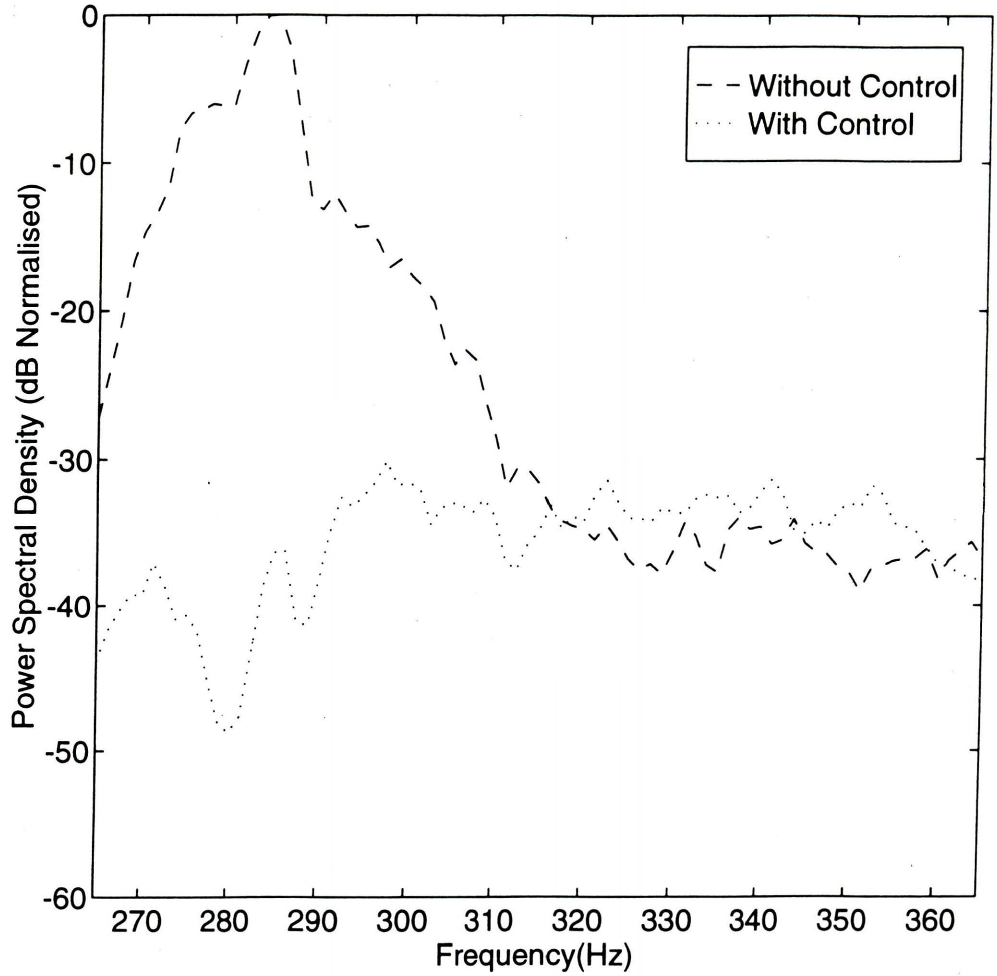

Fig. 4 - Insertion loss with interfering vibration present

Before the project began, it was expected that the unidirectional sensors would be operative for the proposed study but would need further refinement before being included in a practical system. This expectation was confirmed by the experiments performed. The unidirectional sensors were effective at increasing the insertion loss where the interfering vibration was of the same order of magnitude as the primary vibration but when an interfering vibration of greater magnitude was present it became clear that the unidirectional sensors were not fully effective.

In most practical situations it is not possible to 'turn off' the primary noise while the cancellation path transfer function is being calculated as was done in this project. Also, it would be useful to use an infinite impulse response filter to overcome any reference sensor contamination by the secondary source. Both of these problems are solvable with the use of an algorithm such as Eriksson's (1989) 'Filtered-U' algorithm with on-line system identification. However, this was not available in the controller used in this project.

CONCLUSIONS

When the system was setup to control unidirectional random primary vibration, an insertion loss of 30 dB was realised for a 100 Hz bandwidth. An interfering vibration was then added at the bottom of the rod so that it travelled up the rod in the opposite direction to the intended direction of control. The insertion loss was then measured to be 18 dB across the bandwidth with the value reaching 40 dB at some frequencies and becoming negative at others.

If this system were to be implemented to solve a practical extensional vibration problem, there would have to be further work done to adapt the systèm. The unidirectional sensors and actuators would need to become more effective over a wider frequency range, the system identification would have to be done on-line and there would need to be effort expended in the development of an actuator suitable for the environment of the particular application.

REFERENCES

Eriksson, L.J. & Allie, M.C. (1989) Development of the Filtered-U Algorithm for Active Noise Control. Journal of the Acoustical Society of America, 89(1) pp. 257-265.

Fuller, C.R., Gibbs, G.P. & Silcox, R.J. (1990) Simultaneous Active Control of Flexural and Extensional Waves in Beams. Journal of Intelligent Materials and Structures 1 pp. 235-247.

Gonidou, L.O. & Fuller, C.R. (1989). Further Research on Active Control of Flexural Power Flow in Elastic Thin Beams. 117th Meeting of the ASA Syracuse, N.Y.

Hansen, C.H. & Pan, J.(1990). Active Control of Vibration in a Beam. IEAust. Vibration and Noise Conference Melbourne pp. 334-338.

Redman-White, W., Nelson, P.A. & Curtis, A.R.D.(1987). Experiments on the Active Control of Flexural Wave Power Flow. Journal of Sound and Vibration, 112(1) pp. 187-191.

Widrow, B. & Stearns, S.D. (1985). Adaptive Signal Processing. Prentice and Hall, New Jersey.

NOISE REDUCTION OF A STEEL ROLLING MILL RUN-OUT TABLE AND SIMPLIFIED ASSESSMENT PROCEDURE OF CONTROL OPTIONS

Colin Tickell
Supervising Environmental Engineer, BHP Engineering, PO Box 1237 North Sydney, NSW, Australia

Introduction

BHP Steel - Rod and Bar Products Division (BHPS-RBP) operates a steel rolling mill at Acacia Ridge in the outer suburban area of Brisbane, Queensland. Construction of the mill commenced in 1985 and was completed in mid 1987. Production capacity is currently 225,000 tonnes per year.

Following commissioning, noise from the plant was discernible in some of the nearby residential areas, causing some complaints to be received by the mill. The particular noise discernible was a medium to high-pitched sound which occurred for a few seconds, then stopped, and then repeated in this pattern with about 8 to 10 cycles per minute. It was caused by the deformations in the steel reinforcing bar being produced striking the steel rollers of the run-out table, at the entry to the cooling bed.

The plant manager required assistance in reducing the noise emission. As project managers for the mill development and being involved in the acoustic design considerations of the building, BHP Engineering was requested to assist. This paper describes the mill in brief, the sound levels at the run-out table, alternative materials selected for source control and a simple test method to evaluate these alternatives.

The BHP Brisbane (Steel Rolling) Market Mill

Production

The BHP Steel Brisbane Market Mill produces steel merchant bar sections for the construction industry in the range 12mm to 38mm diameter. The feed stock are steel billets delivered by rail from BHP's Newcastle steel works in New South Wales.

The billets are fed into a 40 tonne per hour, gas fired walking beam furnace to raise their temperature to about 1200°C for the rolling process. On exit from the furnace the billets are rolled to the appropriate diameter and form required. Most of the product is "Tempcore®"bar, a trademarked high-strength reinforcing steel bar. Production capacity is currently 225,000 tonnes per annum.

Location

The mill is located at Acacia Ridge in the outer suburban area of Brisbane, state capitol of Queensland. It forms part of an extended heavy industrial area with other industries nearby including foundries, wire manufacture, steel sheet rollforming, vehicle assembly and a rail/road container freight and general freight transfer station/depot. The mill site is on the edge of the industrial zone, with local and interstate rail lines in a wide strip between the site and an extended residential area. A major road transport route, Beaudesert Road, is also close to the rail line.

Design Considerations

Consideration of noise emissions from the plant was a requirement of the design and layout. The Queensland Division of Noise Abatement requested at the design stage in 1985 that the environmental objective for the project should be 45 dB(A) at the nearest houses. In seeking approval to construct the Mill from the Brisbane City Council, BHP as owner and operator gave committments to include various forms of noise control in the building and plant design to achieve the objectives.

Design noise controls included plant layout, with the furnace, a major low frequency noise source, and its associated fans being placed on the distant end of the building from the nearest houses. The truck loading bay was also placed on the opposite side of the building to the houses. Design controls on the building were steel sheet cladding with no translucent fibreglass panels (as initially considered by the operators) with an internal acoustic absorptive lining of 75mm fibreglass wool face with perforated aluminium foil. With these noise controls the plant was expected (by calculation) to achieve the 45 dB(A) objective at the nearest houses 400m distant. Without these "cladding" controls the objective was predicted to be exceeded by 8 dB(A). Internal sound levels taken from a similar sized but older mill were expected to be in the range 85 to 93 dB(A), the highest continuous sound levels occurring near the finishing mill stand. The mill was constructed between 1985 and mid 1987 when commissioning and subsequent production commenced.

RUN-OUT TABLE NOISE

After the steel bar has completed the rolling to shape and metallurgical process required, it passes onto the run-out table where it is transferred to the cooling bed to allow natural air convection cooling as part of the metallurgical process.

The run-out table is some 405 metres long with the bars transported along it by motor driven steel rollers about 500mm apart. The bar enters the table at a speed of up to 12.5 m/s, depending on diameter - the narrower bars travelling faster. As the front end of the bar strikes each roller there is an impact. Also, the bars are produced with rib deformations. As each of these deformations strike the roller there is an impact. The bars pass from the run-out table to a walking beam cooling bed. The resultant sound of the bars striking the run-out table rollers is like a giant xylophone, without the change in pitch. The steel rollers, being hollow steel cylinders machined and balanced, 215mm in diameter and 325mm in length with a wall thickness of 15mm,ring like a tubular bell when struck. As there is a period between each bar passing, there is a cyclical noise where the high sound level occurs for 1 to 3 seconds with a low sound level for a period of 4 to 8 seconds, depending upon the status of production.

CONTROL ALTERNATIVES

As usual, the request for assistance came over the phone, with a solution required yesterday that the site engineering and maintenance people could install quickly and easily and at low cost (if possible). The problem was assumed to be one of damping the rollers. A further constraint to the damping treatment was the temperature of the rolls, as they pass steel bars at temperatures of several hundred degrees. The rolls had been measured at 60°C but could be expected to be up to 100°C as the steel rod is in contact during 75% of the time during rolling, but on a small contact strip. Paste damping compounds for trowelling on or resinous compounds suffer loss of performance at high temperatures, and eventual deterioration/degradation. Availability was also a potential problem, as well as application and balance effects. This approach was not followed up.

Two main alternatives were initially considered. The first was to fill the cavity of the cylinder with spray applied polyurethane foam. The second was to glue a thick rubber strip to the inside of the cylinder to act as a damping sheet. This had application problems of time, handling and balance, and was subsequently modified to a tube of high density polyurethane (HDPU) with characteristics of 80 Shore A, 10mm thick and an interference fit of 2mm to provide loading to the roller and avoid the need for any adhesive. It could be fitted rapidly with a rubber mallet and had no balance effects.

On a subjective test with a hammer the HDPU, subjectively, gave a significant reduction in sound level compared to the reduction achieved by the foam filling. On this basis 12 of the rollers were fitted with the tube during a scheduled maintenance shut-down as a test for operational effectiveness, life, and so on. This was done in June 1988. Following this a total of 70 rollers were fitted during July and August.

SIMPLE OBJECTIVE TEST METHOD AND RESULTS

Objective testing of the treatment was able to be made in mid August 1988. A comparison was sought between the original bare roller, the foam filled roller and the HDPU line unit, and whether on observation by "professional" noise control engineers, further improvements were possible.

The test method had to be objective, simple, repeatable and able to be performed in the workshop/plant environment. A roller bearing was suspended from a string to act as a pendulum to strike the surface of the roller under test. By maintaining the arc of the swing at the same length, the applied impact force remained constant. Second bounce impacts were avoided by grasping the pendulum after the first impact. The impact zone could also be controlled to that of the bars during rolling. To simulate the operational mounting of the roller, it was suspended on a shaft of 32mm(1.5"NB) water pipe in the horizontal position. This also avoided the extra damping effects of other mounting methods. Figure 1 shows the arrangement of the pendulum, roller and microphone. The heights of various parts of the system were somewhat determined by the available pallets, bricks and other improvised mounting devices in the workshop area. Initial testing confirmed repeatability within 1 to 2 dB for successive impacts.

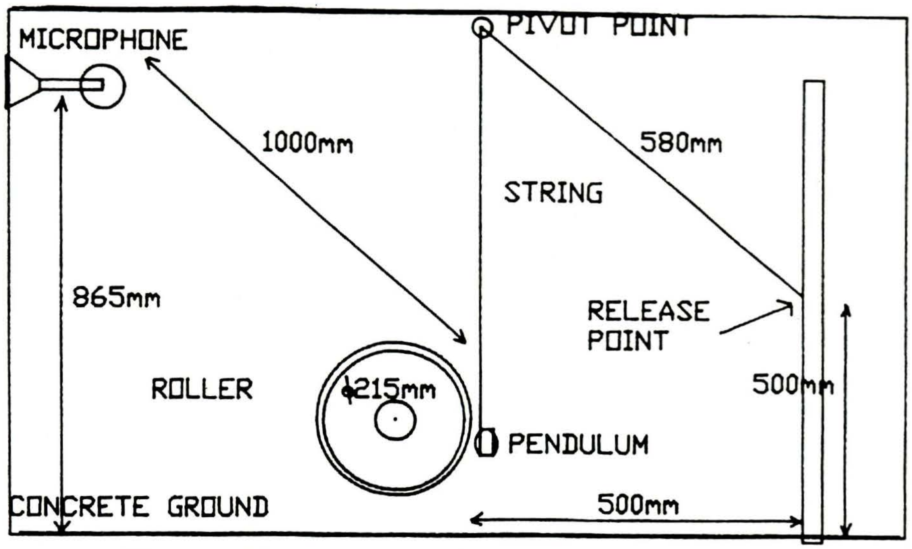

Figure 1: Elevation arrangement of roll impact test

Successive impacts of the pendulum were measured for maximum Peak and rms A-weighted, linear and octave band sound levels. This was done for the three alternatives noted, plus a fourth of fitting the HDPU liner to the inner (motor) side of the roller as well as to the outer side, as in the fitted rollers. Ambient sound levels were also measured. The results and comparison between the alternatives is given in Figure 2. The Bruel and Kjaer 2231 meter used gave both maximum Peak and rms results for the one measurement.

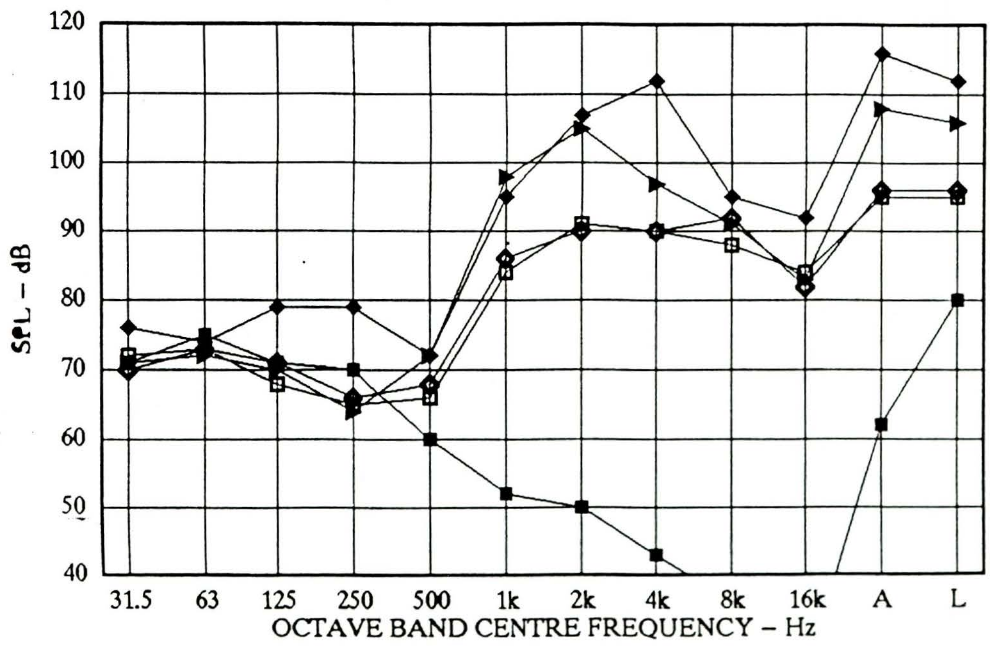

Figure 2: Mill run-out table roll impact test - maximum rms sound level comparison

The results show that the maximum sound level for the impact on the bare roller was 116 dB(A). This was reduced to 108 dB(A) for the foam filled and 95 dB(A) for the HDPU lined rollers.

The spectra show the maximum sound pressure levels occurred in the 4 kHz band for the bare roller. Maximum reduction also occurred in this band, with 22dB reduction for the HDPU and 15 dB for the foam. The treatments caused a change in spectral content by shifting the maximum to the 2kHz band for the foam filled and giving a plateau from the 1kHz to 8kHz bands for the HDPU liner. The treatments all had a similar effect in causing a significant reduction in the 125 and 250 Hz bands, where the sound level was reduced to ambient.

The comparison between a single HDPU lining on the outer impact zone and both sides being lined showed there was virtually no difference in the results. Hence the single sided application was maintained. The outer edge/impact zone damping must have provided sufficient damping so that damping on other parts of the cylinder did not affect the sound emission. It may be that the damping occurred at the 250Hz band and the mass/barrier effect of the HDPU liner and the absorption of the foam filled roller reduced noise emission from the inside of the roller cylinder at high frequencies. This was not investigated further.

Sound levels at the run-out table were not measured before the fitting of the HDPU liners was made. Measurements were obtained when 70 of the 90 rollers had been fitted with the HDPU liners. Sound levels at 2m above the inlet to the run-out table were an average of 98 to 100 dB(A) for 24mm bar. Sound levels at the adjacent wall opening (for cooling bed air inflow) were 97 dB(A) by the open section and 85 dB(A) by the sheeted part of the wall. It is expected that prior to the roller treatment, the internal sound levels at 2m would have been up to 120 dB(A), and the external sound levels similarly increased to 118 and 108 dB(A) respectively.

CONCLUSION

Following receival of complaints of noise annoyance, management of the BHP Steel Brisbane Market Mill requested assistance in reducing noise from the run-out table of the mill. Damping of the steel rollers of the run-out table was determined to be the most appropriate treatment and alternative arrangements and materials were advised to the mill for testing.

Two alternatives of lining the inside of the rollers with polyurethane foam and a high density polyurethane plastic cylinder friction fitted were applied and subjectively tested. The HDPU was assessed to be quieter and installed. Later, an objective test method was devised to provide a comparison between the two alternatives and a variation on the HDPU application. The test method, of using a roller bearing as an impact pendulum proved simple, effective and repeatable. Measurements were obtained of sound levels and spectra.

The results indicated that the HDPU liner was indeed more effective than the foam, reducing the sound level by 25 dB(A) compared to only 7 dB(A) reduction for the foam. Adding the lining to both sides of the rollers did not improve the reduction. The HDPU liners have since been fitted to all 90 of the run-out table rollers and consequently have reduced noise emissions to the benefit of both neighbouring residents and employees in the mill.

Acknowledgments

The work reported was done for BHP Steel Rod and Bar Products Division, by the author employed by BHP Engineering. The permission given by both organisations to report on the project is gratefully acknowledged.

The Identification of Noise Sources on an Expanded-Metal Press using Time-Frequency and Time Domain Techniques

D.M.Eager, W.Y.Wang and H.M.Williamson

Acoustics and Vibration Centre
Department of Aerospace and Mechanical Engineering
University College, University of New South Wales
Australian Defence Force Academy
Canberra, ACT, 2600, Australia

ABSTRACT

Expanded-metal (XPM) meshes are used in almost every branch of engineering and building. XPM is manufactured from mild steel feedstock using special power presses which simultaneously slit and expand the feedstock. The process is inherently very noisy. The impact of the cutting-blade creates large impulse forces which result in high impulse noise levels. This paper reports the results of an analysis into the effect of feedstock length on the sound pressure level (SPL) at the operators station for a 120 tonne XPM press. Several major noise sources were identified using a combination of time-frequency and time domain techniques.

INTRODUCTION

This paper reports some aspects of the continued collaborative research undertaken by the Acoustics and Vibration Centre (AVC) and BHP Building Products (formerly Lysaght Building Industries). The research aim of this particular project was to reduce noise using retrofit methods on a 120 tonne Bender press modified to manufacture expanded-metal mesh from mild steel plate feedstock. A preliminary noise survey of the area surrounding the press by Eager *et al.* [1] indicated that the noise from the inlet-side of the press was over 10 dB(A) higher than the exit-side. Further noise and vibration testing suggested that this difference was due to several factors. Firstly, the poorly constrained feedstock on the inlet-side was excited by the impact force of the cutting-blade during the cutting operation. The plate was subsequently excited in a multi-mode, resonant form with bending waves propagating throughout the plate. Secondly, the expanded-metal product on the exit-side was a less efficient radiator of sound due to pressure equalisation through the perforations in the expanded-metal mesh. Thirdly, for the majority of time, the surface area of the feedstock was greater than that of the product.

This paper presents the results of SPL measurements taken at a position equivalent to the operator's station before and after noise reduction techniques have been applied. The measurement results are presented in both the time and time-frequency domains. It was found that the various noise sources could be identified, characterised and ranked by employing a combination of time and time-frequency analyses at several operating speeds and feedstock thicknesses, before and after noise reduction was applied.

EXPERIMENTAL PROCEDURE

To minimise interruption to the normal work practices and the effects of sound reflection, the sound level meter (SLM) was positioned symmetrically opposite the machine operator as shown in Figure 1. A Brüel & Kjær type 2231 precision SLM, fitted with a BZ7110 Integrating Module, was connected simultaneously to two Toshiba T3200SXC personal computers. The Integrating Module was connected to the first computer via a RS232 interface. The details of this method were previously published by Eager *et al.* [1,2]. The AC output of the SLM was connected to the second computer via a Boston Technology PC30DX analog to digital data acquisition card. The sampling rate for the data acquisition card was set at 15 kHz. This gave an upper frequency limit of 7,500 Hz which had previously been confirmed to be adequate for this study. This sampling rate also gave good resolution when the data was exponentially time averaged. The time-frequency data was processed using Matlab ® Version 4.1 signal processing software.

All tests were conducted using 1200 mm wide mild steel feedstock sheets constrained by two hydraulic point support clamps located at the trailing edge of the feedstock, as shown in Figure 1. The following control variables were studied:

1. Feedstock thickness (mm): 1.0, 2.0, 3.0, 4.0 and 5.0;
2. Feedstock length (mm): ≈ 200 to 2400;
3. Press speed (strokes per minute): 65, 80, 100, 120 and 140; and
4. Feedstock constraint: magnets on and magnets off.

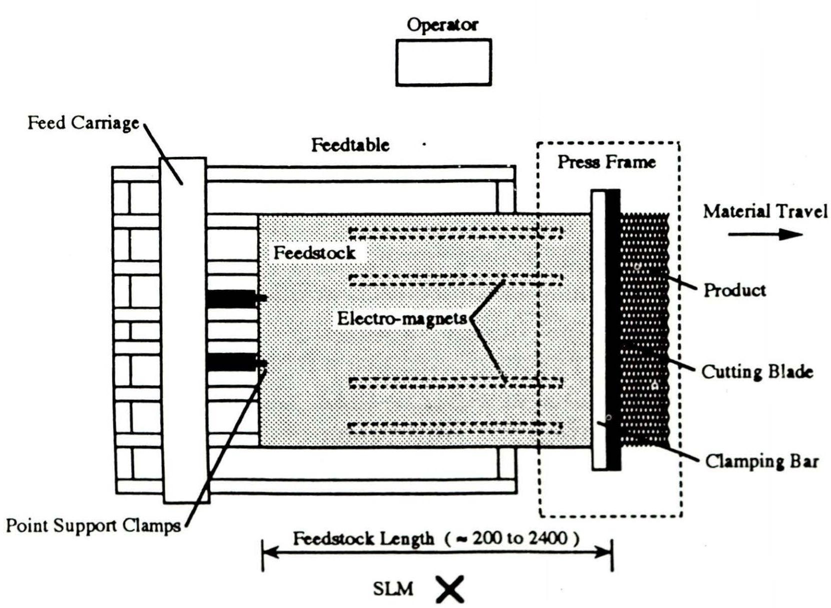

Fig. 1 - Plan view of the Expanded-metal press configuration

RESULTS AND DISCUSSION

Preliminary testing by Eager *et al.* [1] had verified that the noise from the inlet-side of the press was over 10 dB(A) higher than the exit-side. Also, it had been established that the magnitude of this noise difference was proportional to the feedstock length [2]. This testing also confirmed that the force from the cutting-blade impacting the feedstock was greater than the force constraining the feedstock. This force imbalance resulted in the feedstock being stressed, deformed and lifted above the feedtable. This deformation was visually observed as the superposition of the fundamental mode shape together with several of the lower symmetric modes of vibration for a partially constrained plate modelled with similar boundary conditions to those of the feedstock. It was also noted that the elastic and gravitational energy stored in the deformed feedstock was released as the feedstock slapped the feedtable. It was this slapping that produced the measured noise difference between the feed and exit sides of the press. Modifications were made to the original feedstock clamping mechanism located adjacent to the cutting-blade and these resulted in a noise reduction of between 3-8 dB(A) at the operator station.

Further testing by Eager *et al.* [2] confirmed that the increased clamping force adjacent to the cutting-blade had reduced the dominant feedstock-slapping noise below that of the cutting noise for the 1 and 2 mm thickness feedstocks. This was confirmed by observing that the SPL was now constant with changing feedstock length for the 1 and 2 mm thickness feedstocks. The measured SPL for the 3, 4 and 5 mm thickness feedstocks was significantly reduced, but still varied with feedstock length. A model of the major noise sources was proposed by Eager and Williamson [3] and this allowed the separation of the three dominant noise sources, namely: machine noise, cutting noise and feedstock-slapping noise. It was concluded that the feedstock still required additional constraint to remove the dominant feedstock-slapping noise for the thicker feedstocks. To achieve additional feedstock constraint the feedtable was modified by the installation of four, 1000 mm long, electro-magnets located beneath the feedstock and 180 mm upstream of the cutting-blade. The two outer magnets were located close to the edge of the feedstock. All magnets were securely fastened to the feedtable rails, being parallel to the direction of feed, as shown in Figure 1.

The effect of the electro-magnets can be clearly seen in Figures 2 and 3. Figure 2 shows a comparison of the unprocessed sound pressure traces of magnets-on and magnets-off, for four cutting cycles. This data was recorded at the beginning of a full sheet of feedstock when the press was operating at the normal operating speed of 120 strokes per minute (spm) while manufacturing a standard *GM50075 Gridmesh* product. Quantitatively, this noise reduction can be seen in Figure 3 which shows the same data presented in Figure 2 converted to SPL in dB(A) with an exponential averaging time constant of 25 ms. It should be remembered that a time constant of 25 ms is 1/5th that of the 'FAST' response as specified in 'AS1259-1982: Sound Level Meters'. A 25 ms time constant was used as it allowed the visualisation of the individual events within each cutting cycle which were clouded with the standard 125 ms time constant.

By comparing Figures 3-5 it can be seen that for magnets-on the SPL varies little with feedstock length. However, for magnets-off the SPL was proportional to feedstock length. More importantly, it was noted that as the feedstock length approached zero, the appearance and magnitude of the SPL plot for the magnets-off approached that of the magnets-on. By time aligning the magnets-off and the magnets-on data sets, as the feedstock length approached zero, it was possible to establish the peak that corresponded to the cutting noise, see Figure 5. It should be noted that this also aligned both data sets for the entire length of feedstock. Thus, by superimposing the magnets-off and magnets-on data sets, at the start of the feedstock sheet (see Figure 3), the noise removed by the magnetic clamps could be observed. From this it was possible to reason that the large peak that followed the cutting noise, within the magnets-off data set, was the feedstock-slapping noise. As expected, this peak was proportional to feedstock length and was noted to drop below the other noise sources as the feedstock length approached zero. This can be confirmed by comparing the magnets-off data in Figures 3-5.

A third and smaller peak was noted 0.1 seconds prior to the cut. This peak varied little with feedstock length. It was also noted to oscillate in magnitude from cut to cut, repeating every second cycle. The cutting-blade oscillates back and forth transversely from cut to cut to produce the expanded-metal configuration. This oscillation is produced by the cutting-blade thrower mechanism which also oscillates transversely. The length of the throw and hence the transverse displacement is controlled by removable spacer blocks.

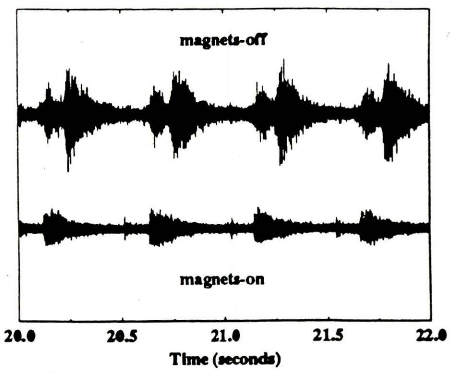

Fig. 2 - Pressure traces: 5 mm x 120 spm
Start of feedstock sheet

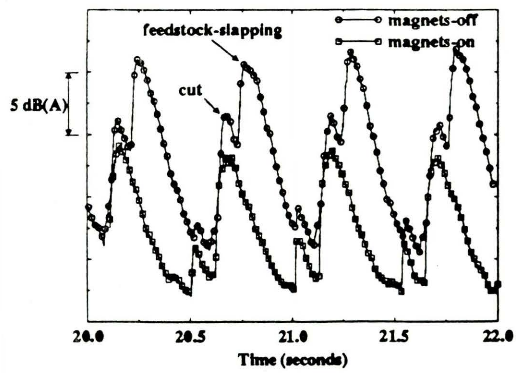

Fig. 3 - SPL: 5 mm x 120 spm
Start of feedstock sheet

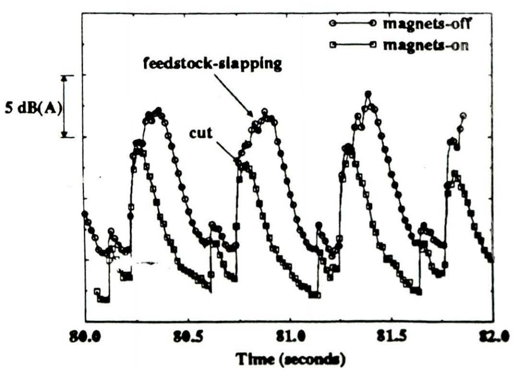

Fig. 4 - SPL: 5 mm x 120 spm
Middle of feedstock sheet

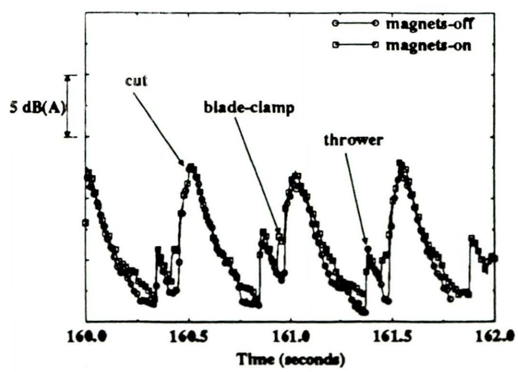

Fig. 5 - SPL: 5 mm x 120 spm
End of feedstock sheet

By taking measurements while the press was running with no feedstock at different speeds and locations it was concluded that this smaller peak was the noise from the cutting-blade thrower mechanism. This peak can be clearly noted in Figure 5 where the feedstock-slapping noise is not dominant. The characteristics of the thrower mechanism noise were noted to be directional and change with different size spacer blocks. Also, for different feedstock areas and aspect ratios the magnitude of the thrower mechanism noise remained constant for constant machine speed and feedstock thickness.

The observed difference in magnitude between magnets-on and magnets-off for the cutting noise and thrower mechanism noise in Figures 3 and 4 was checked mathematically. The combination of the SPL for the cutting noise and the feedstock-slapping noise, and summation of the SPL for the thrower mechanism noise and the feedstock-slapping noise, independently agree with the total SPL at the corresponding time. It was thus concluded that both the cutting noise and thrower mechanism noise were independent of feedstock length.

A fourth and even smaller peak was observed between the cutting noise and thrower noise peaks. This peak was caused by the blade-clamping bar striking the feedstock just prior to cutting. It was more notable for the trials conducted using thinner feedstocks and/or the when the press was operated at a slower speed. In the data presented it can only be observed in Figure 5 for the magnets-on. The reason it was only observable in this data was that the feedtable and the bolster were misaligned during this trial. With the magnets-on the feedstock was held down against the feedtable causing the leading edge to bend up at the bolster. This lifted edge was struck just prior to cutting by the blade-clamp and caused it to slap the lower bolster. This conceivably minor observation emphasises the importance of good engineering principles. Aligning the feedtable and lower bolster eliminated a potential noise source. It also highlighted the necessity for scheduling the checking of this alignment within the preventative maintenance programme.

The Spectrograms in Figures 6-9 show plots of time (seconds) versus frequency (Hz). The SPL is represented by the density of the dots per unit area. It is worth noting that each of the plots represent a complete sheet of feedstock from start to finish. Therefore one can equate time with feedstock length when reviewing the results. If Figure 6 is visualised 3-dimensionally, a broad-band hump can be observed with a centre frequency of approximately 2740 Hz. A comparison of Figures 6 and 7 shows the frequency of the noise removed by the electro-magnetic clamps for the standard product at the normal operating speed. It was noted that the magnetic clamps completely removed the board-band hump. The magnets also removed the majority of the noise above 3000 Hz. Further, it can be seen from Figure 6 that the magnitude of the broad-band hump decreased with time. This is equivalent to a decrease with feedstock length. It was concluded that the feedstock-slapping at standard operating conditions produced this broad-band hump as well as the higher frequency noise. The particular benefit of this noise reduction in the frequency range where the human ear is most sensitive was two-fold. Firstly, it reduced the potential for hearing damage within this critical range; and secondly, it made for a safer and more productive workplace as it allowed the machine operators to communicate more effectively. The tonal noise line at approximately 5000 Hz appeared to be associated with the press machinery or auxiliary equipment. It was noted that the tonal lines were not strictly proportional to the press speed. The tonal lines were also noted to

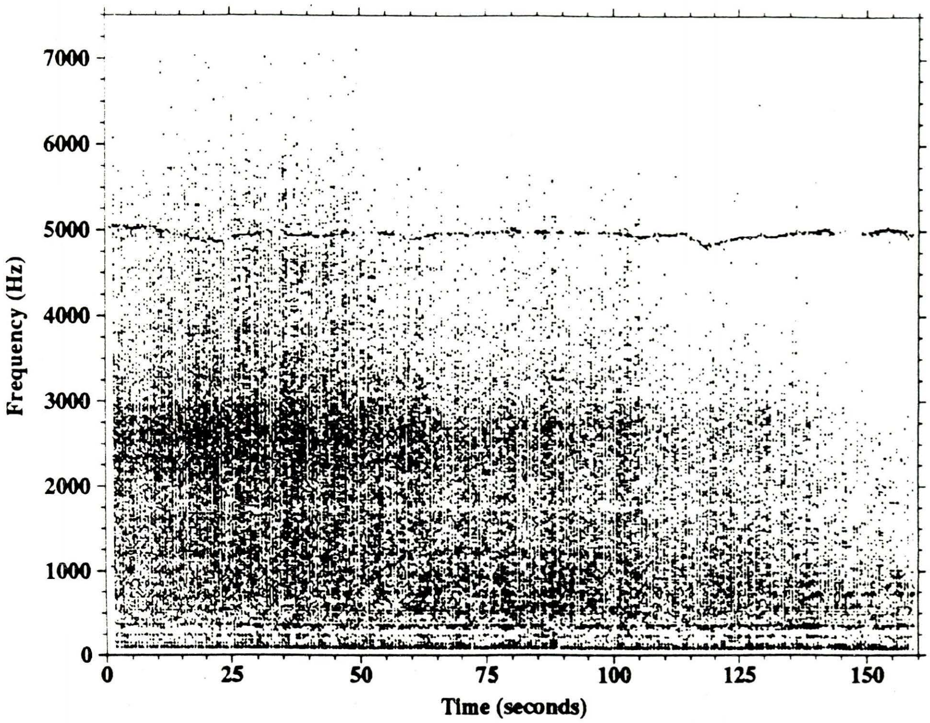

Fig. 6 - Spectrogram: 5 mm x 120 spm 'magnets-off'

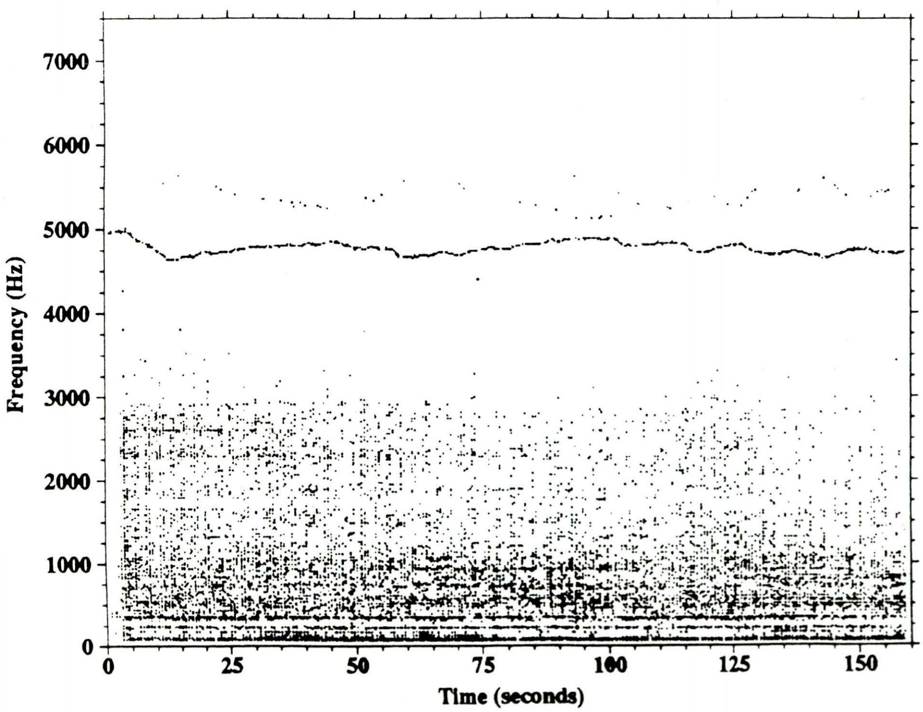

Fig. 7 - Spectrogram: 5 mm x 120 spm 'magnets-on'

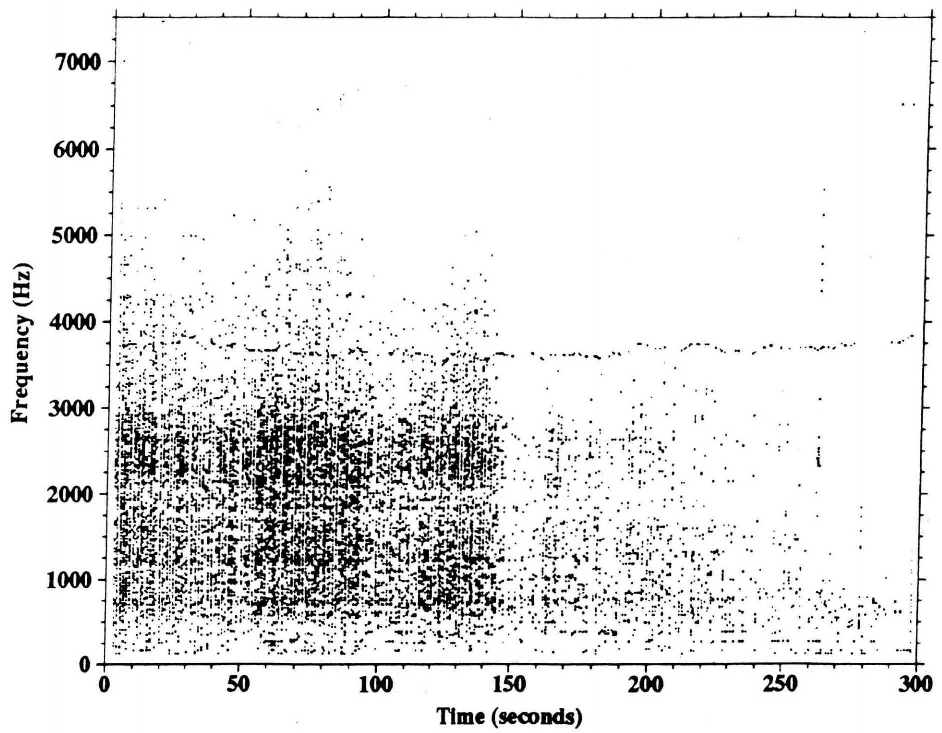

Fig. 8 - Spectrogram: 5 mm x 65 spm 'magnets-off'

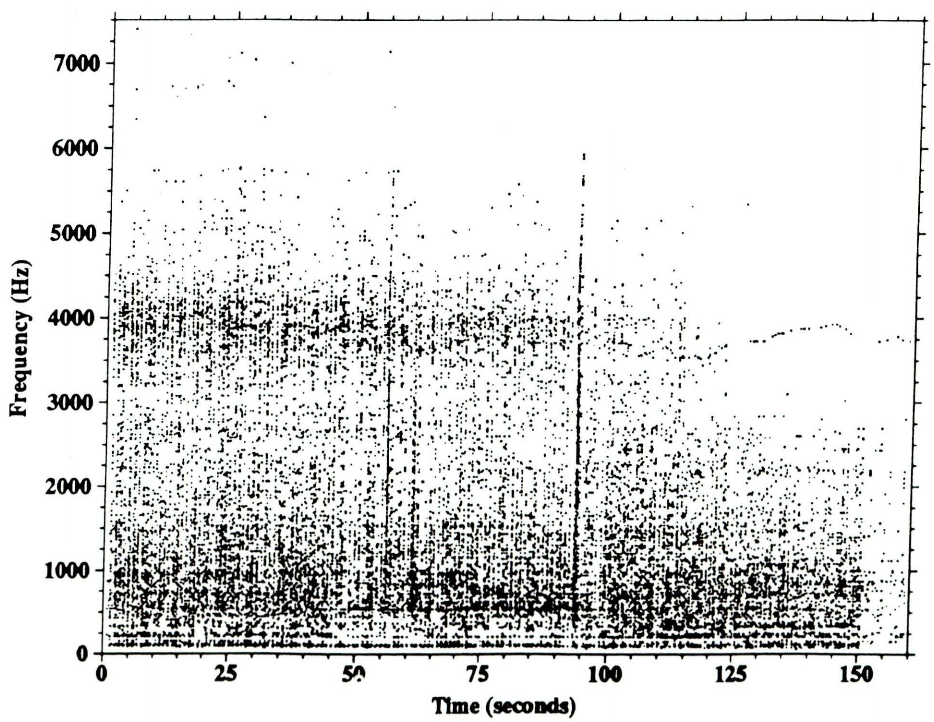

Fig. 9 - Spectrogram: 3 mm x 120 spm 'magnets-off'

be present when the press was running but not cutting. Further, they were noted to vary in frequency from test to test, even when the control variables were fixed. Future research will focus on this tonal line and it's source.

The time-frequency effects of the press operating speed can be observed by comparing Figures 6 and 8. It was noted that the frequency of feedstock-slapping noise was unaffected by changes in the cutting rate. Also, the tonal noise line was noted to drop from approximately 5000 to 3700 Hz. The effects of feedstock thickness can be observed by comparing Figures 6 and 9. It was noted that the frequency of feedstock-slapping noise was affected by feedstock thickness. For the 3 mm thick feedstock the feedstock-slapping noise was centred around 3930 Hz. This being an increase of over 1000 Hz on the 5 mm feedstock at 120 spm. It was postulated that this increase in frequency was due the flexibility of the thinner feedstock.

CONCLUSIONS

An investigation has been conducted into the noise sources associated with an expanded-metal press. Analysis of this data confirmed that radiation from the feedstock-slapping was the most dominant noise source. Modification to the blade-clamp mechanism reduced the overall noise levels by 3-8 dB(A). The installation of electro-magnets on the feedtable to constrain the feedstock reduced the maximum SPL by a further 8 dB(A). The results presented herein show details for both constrained and unconstrained feedstock in both the time and time-frequency domains. These were analysed in detail and used to characterise the various noise sources.

It was noted that the feedstock-slapping radiation frequency varied little with changing machine speed. It was also noted that the feedstock-slapping frequency was a function of the feedstock thickness and was found to increase with decreasing feedstock thickness.

ACKNOWLEDGMENTS

The authors acknowledge the financial support of Australian Postgraduate Research Award (Industry) Scheme, Worksafe Australia and BHP Building Products. The authors extend their gratitude to A/Prof Lai, Dr Harrap and Mr Speakman for their helpful and fruitful discussions throughout this research. Also, the authors thank the University College Computer Centre for the use of considerable computer resources during the time-frequency calculations.

REFERENCES

1. Eager D.M., Williamson H.M., Lai J.C.S. and Harrap M.J. A preliminary noise study of an expanded-metal press. Inter-noise 93 Proceedings, pp 1429-1432, Leuven, Belgium, August 1993.
2. Eager D.M., Williamson H.M. Noise reduction measures applied to an expanded-metal press. IEAust Mech '94 - International Mechanical Engineering Congress, Vol 3, pp 219-223, Perth, Australia, May 1994.
3. Eager D.M., Williamson H.M. Noise source parameters for an expanded-metal press. Inter-noise 94 Proceedings, Yokohama, Japan, August 1994.

PRACTICAL MEASUREMENT OF VIBRATORY POWER TRANSMISSION IN STRUCTURES

Colin H. Hansen,
Department of Mechanical Engineering,
University of Adelaide,
South Australia, 5005.

INTRODUCTION

The measurement of structural intensity is a means of studying in a quantitative way, the net vibratory power transmission through a structure. It is also a convenient means of studying intensity vortices which can be generated on structures under certain boundary and excitation source conditions. One reason for being interested in these studies is their importance in evaluating the effectiveness of active vibration control systems designed to minimise vibratory power transmission or to create intensity vortices around points on a structure to which vibration sensitive equipment is attached.

Unfortunately, structural intensity measurement is fraught with difficulty; it is an order of magnitude more complicated than the measurement of acoustic intensity and so far, reliable measurements have only been made on relatively simple structures. One of the complicating factors is the common presence of more than one wave type (bending, longitudinal, torsional or shear) or the same wave type in more than one plane. Even if only one wave type is present, near field effects arising from structural boundaries, structural discontinuities and excitation sources complicate what on the surface may seem like a relatively simple problem. For thick structures, the intensity will likely vary through the structural thickness and surface measurements may no longer be representative of the true structural intensity averaged over the structure thickness.

The ready availability and seemingly common use of dual accelerometer systems for the measurement of bending wave intensity on thin structures belies the complexity of what is actually being measured, even on relatively simple structures. In fact, in many cases, the output of such a system may not be very closely related to the structural intensity quantity which is purported to being measured.

It is the purpose of this paper to use analytical expressions for bending wave structural intensity to show under what conditions the two accelerometer techniques is valid for beams plates and cylinders. To put the analysis in context, we will begin with a general formulation of structural intensity which will tailored to the specific cases to be considered here.

GENERAL FORMULATION FOR CYLINDERS, PLATES AND BEAMS

Romano et.al. (1990) show that the structural (or vibratory power transmission in the axial x-direction per unit width) in a cylinder of radius a can be written as

$$P_x = -\left[\dot{w}Q_x + \dot{\xi}_\theta N_{x\theta} + \left(\frac{\dot{\xi}_\theta}{a} - \frac{1}{a}\frac{\partial \dot{w}}{\partial \theta}\right)M_{x\theta} + \dot{\xi}_x N_x - \frac{\partial \dot{w}}{\partial x}M_x\right] \tag{1}$$

where the dot above a variable denotes differentiation with respect to time, w, ξ_x and ξ_θ are respectively, displacements in the radial, axial and circumferential directions, Q_x is the internal shear force acting on a plane section normal to the x-axis, M_x is the bending moment about an axis normal to the x-axis, $M_{x\theta}$ is the twisting moment about the x-axis in the θ direction, N_x is the axial force in the x-direction, and $N_{x\theta}$ is the shear force acting in the $x\theta$ plane in the θ direction. In equation (1), shear waves are associated with the second term, longitudinal waves with the fourth term and flexural waves with the remaining terms.

The equation for power transmission per unit width in a plate in the x-direction can be obtained directly from equation (1) by replacing $\frac{1}{a}\frac{\partial}{\partial\theta}$ with $\frac{\partial}{\partial y}$, θ with y and ξ_θ/a with 0. Thus, we obtain

$$P_x = -\left[\dot{w}Q_x - \frac{\partial \dot{w}}{\partial y}M_{xy} - \frac{\partial \dot{w}}{\partial x}M_x + \dot{\xi}_y N_{xy} + \dot{\xi}_x N_x\right] \tag{2}$$

where the variables are defined similarly to their equivalents in the cylinder expression and are shown in figure 1. The expression for the y component of power transmission is obtained by interchanging the x and y subscripts in equation (2).

The first three terms in equation (2) correspond to power transmission associated with flexural wave propagation. The first of these is the shear force contribution, the second is the twisting contribution and the third term is the bending contribution. The fourth term corresponds to shear wave propagation while the fifth corresponds to longitudinal wave propagation.

For wave propagation in a beam, equation (2) becomes

$$P_x = -\left[-\dot{w}Q_x - \dot{\theta}_x M_{xy} - \frac{\partial \dot{w}}{\partial x}M_x + \dot{\xi}_x N_x\right] \tag{3}$$

where the first and third terms represent the flexural wave power transmission, the second term represents the torsional wave power transmission and the last term represents the longitudinal wave power transmission. The quantity θ_x is the angle of rotation about the x-axis caused by a torsional wave. It is defined as

$$\theta_x = \frac{\partial w}{\partial y} = -\frac{\partial w}{\partial z} \tag{4a,b}$$

The force and moment variables for the beam are defined in figure 2. Note the difference in sign between the beam and plate for the $\dot{w}Q_x$ term. This is because the sign convention for positive Q_x on the plate is different to that for a beam (see figures 1 and 2).

The quantities of equations (1) to (3) are functions of time as well as location on the cylinder, plate or beam. To enable us to express quantities in terms of net energy transmission or time averaged power transmission, it is useful to find expressions for time averaged intensity (Fahy, 1989). To do this we may use the same approach as that adopted for acoustic intensity. Thus, for a harmonic vibration on a beam at frequency ω we obtain

$$\langle P_x \rangle_t = -\frac{1}{2}\mathrm{Re}\left\{ \dot{w}^* Q_x + \dot{\theta}_x^* M_{xy} - \frac{\partial \dot{w}^*}{\partial x} M_x + \dot{\xi}_x^* N_x \right\} \tag{5}$$

where $\langle P_x \rangle_t$ is the time averaged power transmission and the * denotes the complex conjugate.

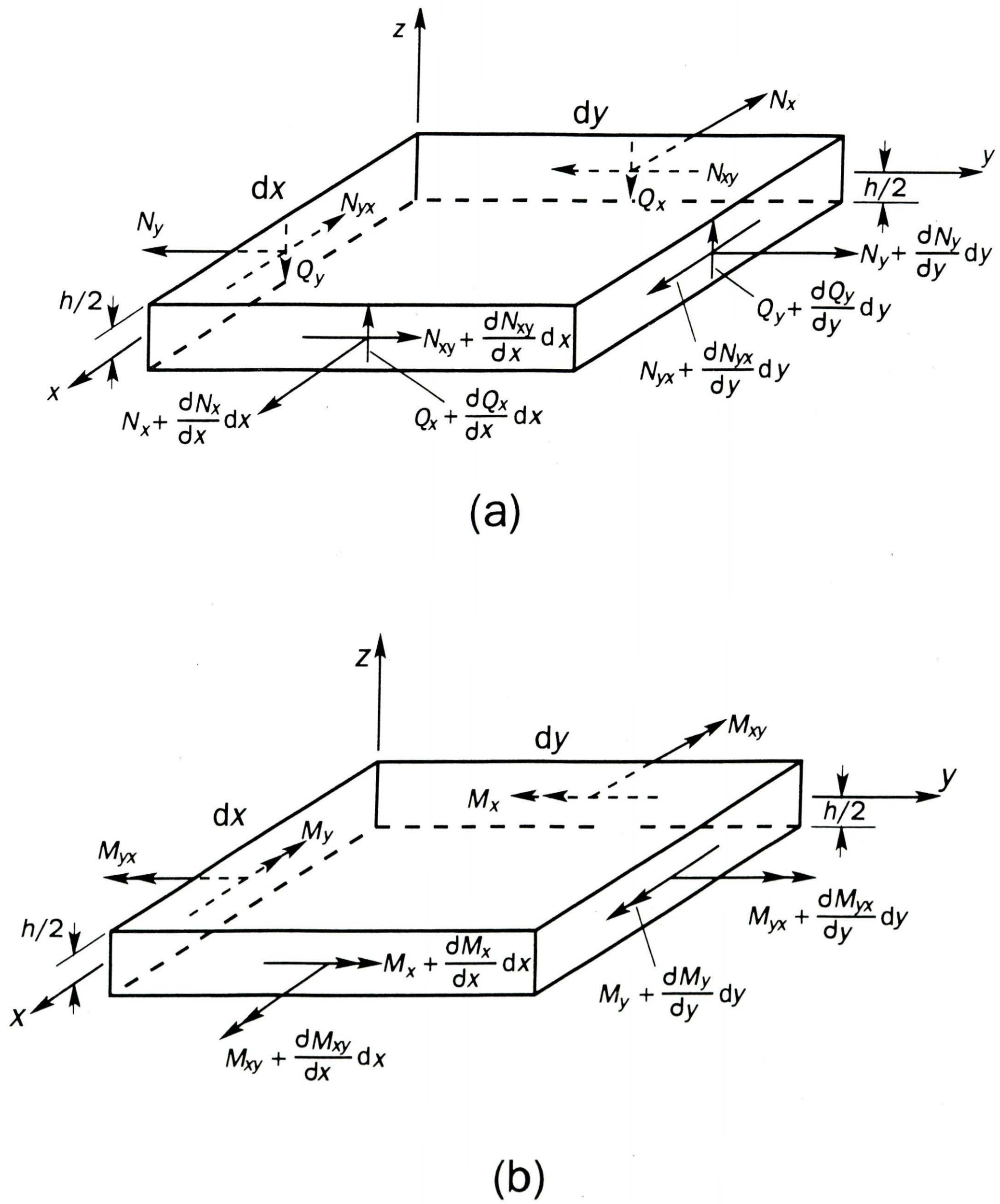

Fig.1 - Force and moment nomenclature for plate

Similar expressions can be obtained for plates and cylinders. In these latter two cases the left side of the equation will be time averaged power transmission per unit width.

In beams, plates and shells, the determination of structural intensity is possible from measurements on the surface of these elements, because relatively simple relationships have been derived between the variables which govern the energy transmission through the structure and the vibration on the surface, thus enabling the determination of the transmission of energy in a beam plate or shell by measurement of surface vibrations only. These simple relationships, however, only hold at lower frequencies where the motion of the interior of the structure is uniquely related to the motion of the surface.

Although it is clear from the preceding expressions that it is possible to derive structural intensity expressions for longitudinal and shear waves as well as for flexural waves, lack of space dictates that the treatment here be restricted to flexural waves. Here, expressions will be presented for the flexural wave intensity in beams and plates in terms of the normal and in-plane displacements and their spatial derivatives. It will be shown how, and in what special cases, it is possible to use just two accelerometers to measure single wave intensities. The measurement of flexural wave intensity on a cylinder will not be considered, because coupling between all of the different wave types means that there is never only one wave type in isolation and this precludes the use of the two accelerometer technique. In fact, a minimum of eight accelerometers would be necessary to obtain meaningful intensity measurements.

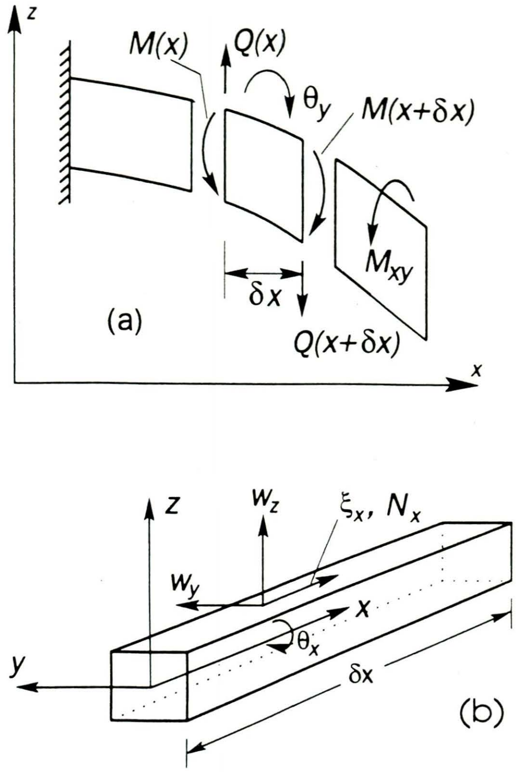

Fig. 2 - Displacement, force and moment nomenclature for beam

INTENSITY MEASUREMENT IN BEAMS

The vibratory power propagating in a beam is given by the integral of the structural intensity over the beam cross section at the point of interest. Some authors refer to this power transmission quantity as intensity, but as the units are actually power units, and to avoid confusion with the actual intensity, the quantity will be referred to here as power. In the following analysis, Classical (or Bernoulli-Euler) beam theory will be used.

Using equation (3), the power transmission expression for flexural waves characterised by deflections in the z direction is

$$P_{Bz}(t) = -\left[-\dot{w}_z Q_x - \frac{\partial \dot{w}}{\partial x} M_x\right] = EI_{yy}\left[\frac{\partial w_z}{\partial t}\frac{\partial^3 w_z}{\partial x^3} - \frac{\partial^2 w_z}{\partial t \partial x}\frac{\partial^2 w_z}{\partial x^2}\right] \qquad (6a,b)$$

where the first term represents the shear force contribution and the second term represents the bending moment contribution.

For flexural waves travelling in the x - direction and characterised by normal displacement in the y - direction, the power transmission equation is found by substituting w_y for w_z and I_{zz} for I_{yy} in equation (6). Note that I_{yy} is the second moment of area of the beam cross-section about the y-axis.

To evaluate the third order derivative in equation (6b), it is necessary to use a minimum of four accelerometers (Pavic, 1976 and Hayek et. al. 1990).

A simpler expression can be obtained if the accelerometers are located in the far field of all vibration sources and reflections. In this case, it may be shown that the shear force and bending moment contributions to the power transmission are the same (Noiseaux 1970) and the instantaneous power transmission may be written as,

$$P_{Bz}(t) = -2EI_{yy}\left[\frac{\partial^2 w_z}{\partial t\,\partial x}\frac{\partial^2 w_z}{\partial x^2}\right] \tag{7}$$

The time averaged (or active) power may be written as,

$$\langle P_{Bz}(t)\rangle = P_{Bza} = -2EI_{yy}\left\langle \int \frac{\partial a}{\partial x} \iint \frac{\partial^2 a}{\partial x^2}\right\rangle \tag{8a,b}$$

In equation (8b), the following notation has been used

$$w_z = \iint a_z \quad \text{and} \quad \frac{\partial w_z}{\partial t} = \int a_z \tag{9a,b}$$

where a_z is the acceleration measured in the z-direction.

For the frequency domain, the preceding equation becomes (Verheij, 1990)

$$P_{Bza}(\omega) = 2EI_{yy}\frac{\mathrm{Im}\left\{G\left(\dfrac{\partial^2 a}{\partial x^2}, \dfrac{\partial a}{\partial x}, \omega\right)\right\}}{\omega^3} \tag{10}$$

In the absence of near fields, the relation between the Fourier components of $\dfrac{\partial^2 a}{\partial x^2}$ and a is

$$\frac{\partial^2 a}{\partial x^2} = -k_b^2 a = a\omega(m'/B)^{1/2} \tag{11a,b}$$

where $B = EI_{yy}$ is the bending stiffness and m' is the mass per unit length of the beam.

Using the finite difference approximations:

$$a = (a_{z1} + a_{z2})/2 \quad \text{and} \quad \frac{\partial a}{\partial x} = (a_{z2} - a_{z1})/\Delta \tag{12a,b}$$

$$\frac{\partial a}{\partial x} = (a_{z2} - a_{z1})/\Delta \tag{13}$$

we obtain the following for the active power transmission

$$P_{Bza}(\omega) = \frac{2(Bm')^{1/2}}{\omega^2 \Delta} \mathrm{Im}\left\{ G_{a_{z2}, a_{z1}}(\omega) \right\} \tag{14}$$

where $G_{a_{z1}, a_{z2}}$ is the cross spectral density of the accelerometer signals z_1 and z_2.

Assuming a harmonic wave field and substituting equations (11a) and (11b) into (8), gives for the time average active power,

$$P_{Bza} = -\frac{2k_b^2 EI_{yy}}{\omega^2} \left\langle \left(\int \frac{\partial a}{\partial x} \right) a \right\rangle_t = -\frac{2(Bm')^{1/2}}{\omega} \left\langle \left(\int \frac{\partial a}{\partial x} \right) a \right\rangle_t \tag{15a,b}$$

Using equations (12a) and (12b) equation (15) may be rewritten as,

From the similarity between equation (16) and the corresponding equation for acoustic intensity (Fahy, 1989), it may be deduced that an acoustic intensity analyser may be used to determine the structural intensity for a harmonic wave field on a beam in the far field of any sources or reflections, by replacing the pressure signals with accelerometer signals and then multiplying the result by a fixed constant.

An alternative relationship for harmonic flexural wave power transmission can be derived by beginning with equation (6b) and assuming harmonic excitation immediately. Thus, from equation (6b), the time averaged active power transmission is:

$$P_{Bza} = \mathrm{Re}\left\{ \frac{EI_{yy}}{2} \left(\left(j\omega \bar{w}_z(x)\right)^* \frac{\partial^3 \bar{w}_z(x)}{\partial x^3} - \frac{\partial \left(j\omega \bar{w}_z(x)\right)^*}{\partial x} \frac{\partial^2 \bar{w}_z(x)}{\partial x^2} \right) \right\} \tag{17}$$

or

$$P_{Bza} = -\mathrm{Re}\left\{ \frac{j\omega EI_{yy}}{2} \left(\bar{w}_z^*(x) \frac{\partial^3 \bar{w}_z(x)}{\partial x^3} - \frac{\partial \bar{w}_z^*(x)}{\partial x} \frac{\partial^2 \bar{w}_z(x)}{\partial x^2} \right) \right\} \tag{18}$$

where the * denotes the complex conjugate and the bar over a variable represents the amplitude of a time varying quantity.

As for the general case, simpler expressions can be obtained for P_{Bza} if the measurements are conducted at least one half of a wavelength away from any power source or sources of reflection; that is, in a region where near field effects may be neglected. Consider the following solution for a sinusoidal flexural wave travelling in a beam,

$$w_z(x,t) = \left[A_1 e^{-jk_b x} + A_2 e^{jk_b x} + A_3 e^{-k_b x} + A_4 e^{k_b x}\right] e^{j\omega t} \tag{19}$$

The first and second terms represent the propagating vibration field in the positive and negative x directions respectively, while the second two terms represent the decaying near field. Thus if we ignore the near field, we can set $A_3 = A_4 = 0$, and if we also omit the time dependent term $e^{j\omega t}$, equation (19) becomes

$$\bar{w}_z(x) = A_1 e^{-jk_b x} + A_2 e^{jk_b x} = \bar{A}_1 e^{-j(k_b x - \theta_1)} + \bar{A}_2 e^{j(k_b x + \theta_2)} \tag{20}$$

where A_1 and A_2 are complex numbers, $\bar{A}_1$ and $\bar{A}_2$ are real, and θ_1, θ_2 are the signal phases at $x = 0$. Substituting equation (20) into (18) gives for the active power:

$$P_{Bza} = EI_{yy}\,\omega\, k_b^3 (\bar{A}_1^2 - \bar{A}_2^2) \tag{21}$$

However,

$$\mathrm{Re}\left\{ j\left(\bar{w}_z^* \frac{\partial \bar{w}_z}{\partial x} - \bar{w}_z \frac{\partial \bar{w}_z^*}{\partial x} \right) \right\} = 2\, k_b (\bar{A}_1^2 - \bar{A}_2^2) \tag{22}$$

Thus,

$$P_{Bza} = \mathrm{Re}\left\{ \left(\frac{j\omega}{2}\right) EI_{yy} k_b^2 \left(\bar{w}_z^* \frac{\partial \bar{w}_z}{\partial x} - \bar{w}_z \frac{\partial \bar{w}_z^*}{\partial x} \right) \right\} = \omega EI_{yy} k_b^2\, \mathrm{Im}\left\{ w_z \frac{\partial w_z^*}{\partial x} \right\} \tag{23a,b}$$

If accelerometers were used and mounted to measure lateral (or flexural) acceleration, then equation (23b) could be written as:

$$P_{Bza} = \mathrm{Re}\left\{ \frac{jSE}{2\omega^3}\, \bar{a}_z^* \frac{\partial \bar{a}_z}{\partial x} \right\} \tag{24}$$

where a_z is the acceleration of the centre of the beam section in the z direction.

Substituting equations (12a) and (12b) into (24) gives for the active power,

$$P_{Bza} = -\mathrm{Im}\left\{ \frac{SE}{4\omega^2 \Delta} (a_{z1} + a_{z2})^* (a_{z2} - a_{z1}) \right\} = \frac{SE}{2\omega^2 \Delta} |a_{z1}|\,|a_{z2}| \sin(\theta_1 - \theta_2) \tag{25a,b}$$

Thus the time averaged flexural wave active power transmission for harmonic waves can be measured in practice in the far field of boundaries, discontinuities and vibration sources by multiplying the amplitudes of two closely spaced accelerometers with the sine of the phase difference between the two. The direction of positive power transmission is from accelerometer 1 to 2. It can easily be shown that equation (25) is equivalent to equation (15b); however, in many experimental situations it is probably easier to measure the amplitudes of and the phase difference between two sinusoidal signals than it is to accurately perform analog integrations and multiplications.

INTENSITY MEASUREMENT IN PLATES

It can be seen from equation (2) that first, second and third order derivatives must be approximated to completely determine the sound intensity in a thin plate. However, it will be shown here that under certain conditions, the two accelerometer method (discussed for beams) may be used to determine the flexural wave component of the total power transmission.

From equation (2), the power transmission per unit plate width associated with flexural wave propagation in the x-direction is given by,

$$P_{Bx}(t) = -\dot{w}Q_x + \frac{\partial \dot{w}}{\partial y}M_{xy} + \frac{\partial \dot{w}}{\partial x}M_x \tag{26}$$

Substituting standard relations (Leissa, 1993), expressing the quantities of equation (25) in terms of the plate normal displacement and its derivatives, we obtain,

$$P_{Bx}(t) = D\left[\frac{\partial w}{\partial t}\left(\frac{\partial^3 w}{\partial x^3} + \frac{\partial^3 w}{\partial x \partial y^2}\right) - (1-\nu)\frac{\partial^2 w}{\partial t \partial y}\frac{\partial^2 w}{\partial x \partial y} - \frac{\partial^2 w}{\partial t \partial x}\left(\frac{\partial^2 w}{\partial x^2} + \nu\frac{\partial^2 w}{\partial y^2}\right)\right] \tag{27}$$

where, $D = Eh^3/12(1-\nu^2)$.

The expression for the y-component of power transmission is obtained simply by interchanging the x and y subscripts in equation (27).

Using eight accelerometers to obtain the gradients in equation (27), as demonstrated by Pavic (1976), and taking the time averaged result allows an expression to be obtained for P_{Bxa} in terms of accelerometer outputs. Because of the many accelerometers and gradient estimates required, it is very difficult to obtain accurate results. The interested reader is referred to Pavic's article (Pavic, 1976) for more details.

For the special case of harmonic wave propagation, it is possible to simplify the expression for power transmission in the x-direction. For this case, the time average of equation (27) may be written as

$$\begin{aligned} P_{Bxa} = -\frac{1}{2}\mathrm{Re}\Bigg\{ j\omega D\Bigg[w\left(\frac{\partial^3 w^*}{\partial x^3} + \frac{\partial^3 w^*}{\partial x \partial y^2}\right) \\ - (1-\nu)\frac{\partial w}{\partial y}\frac{\partial^2 w^*}{\partial x \partial y} - \frac{\partial w}{\partial x}\left(\frac{\partial^2 w^*}{\partial x^2} + \nu\frac{\partial^2 w^*}{\partial y^2}\right)\Bigg]\Bigg\} \end{aligned} \tag{28}$$

If a general solution is assumed for the plate equation of motion for any arbitrary plate edge boundary conditions, and if we further assume that the measurements will be made in the far field of any sources, the following may be written,

$$w = X(x)Y(y) = \left(A_1 e^{-jk_x x} + A_2 e^{jk_x x}\right)\left(B_1 e^{-jk_y y} + B_2 e^{jk_y y}\right) \tag{29a,b}$$

Then,

$$\frac{\partial^2 w}{\partial x^2} = -k_x^2 w \quad \text{and} \quad \frac{\partial^2 w}{\partial y^2} = -k_y^2 w \tag{30a,b}$$

and equation (28) becomes

$$P_{Bxa} = -\frac{1}{2}\mathrm{Im}\left\{\omega D\left[w\left(-k_x^2\frac{\partial w^*}{\partial x} - k_y^2\frac{\partial w^*}{\partial x}\right)\right.\right.$$
$$\left.\left. -(1-\nu)\frac{\partial w}{\partial y}\frac{\partial^2 w^*}{\partial x \partial y} - \frac{\partial w}{\partial x}\left(-k_x^2 w^* - \nu k_y^2 w^*\right)\right]\right\} \tag{31}$$

Using the relationship, $\mathrm{Im}(ab^*) = -\mathrm{Im}(a^*b)$, and assuming A_1, A_2, B_1, B_2, k_x and k_y are less than unity, then it can be shown that equation (31) can be written approximately as,

$$P_{Bxa} = \omega D k_x^2 \mathrm{Im}\left\{w\frac{\partial w^*}{\partial x}\right\} \tag{32}$$

which is similar to equation (23b) for flexural wave propagation in a beam.

A similar expression can be obtained for wave propagation in the y-direction. Thus, the intensity vector for flexural waves in a plate can be measured by measuring the x and y-components, then calculating the vector magnitude and direction in the usual way.

As equation (32) is similar to equation (23b) for beams, except for the constant multiplier, all of the techniques for power transmission measurement embodied in equations (7) to (16), (24) and (25) are also valid for any particular direction on a plate. The quantities, k_x and k_y, are dependent upon the plate boundary conditions, but in many cases may be approximated as,

$$k_x^2 = k_y^2 = \omega\sqrt{\frac{\rho h}{D}} \tag{33}$$

Indeed, this is the approximation which is implicitly assumed when the two accelerometer technique is used to determine the intensity vector in a plate. Although the approximation embodied in equations (32) and (33) gives good results in many cases, in general it is necessary to use eight accelerometers and evaluate all of the gradients in equation (28) directly (Pavic 1976). This needs to be done for each of the x and y components of intensity to obtain the overall intensity vector.

The equivalence of equations (28) and (32) can be demonstrated numerically for particular cases (Pan and Hansen 1994), where the measurements are made in the far field (0.75 of a flexural wavelength) of all sources.

SOURCES OF ERROR IN THE MEASUREMENT OF STRUCTURAL INTENSITY

Because of the increased complexity of structural wave fields compared to acoustic fields, it is much more difficult to obtain accurate structural intensity measurements than it is to obtain accurate acoustic intensity measurements. Sources of error in structural intensity measurements are associated with mass loading effects of accelerometers (which may be avoided by using very small accelerometers or by using laser doppler velocimetry), flexibility of the base to which the two accelerometers are attached, the presence of wave types other than the one which is being measured, phase matching inaccuracies between the measurement channels, inaccuracies associated with the finite difference approximation and the presence of highly reactive fields associated with sources, sinks, discontinuities and boundaries, or with the simultaneous presence of reflected and incident wave fields. Space limitations preclude detailed discussion of error quantification, but it is sufficient to point out here that a significant part of the error is dependent on the accelerometer spacing and the best compromise is to maintain this at approximately one tenth of a structural wavelength where possible (Taylor, 1990). Because of the significant measurement errors involved, it is unlikely that structural power transmission will ever be a very suitable cost function for use in active structural vibration control.

REFERENCES

Fahy, F.J. (1989). *Sound Intensity*. Elsevier Applied Science, London.

Leissa, A.W. (1969). *Vibration of plates*. NASA SP-160.

Leissa, A.W. (1973). *Vibration of shells*. NASA SP-288.

Pan, X. and Hansen, C.H. (1994). ????? Submitted for publication in *The International Journal of Active Control*.

Pavic, G. (1976). Measurement of structure borne wave intensity, Part 1: Formulation of the methods. *Journal of Sound and Vibration*, **49**, 221-230.

Pavic, G. (1990). Energy flow induced by structural vibrations of elastic bodies. In *Proceedings of the Third International Congress on Intensity Techniques*. Senlis, France. pp. 21-28.

Romano, A.J., Abraham, P.B. and Williams, E.G. (1990). A Poynting vector formulation for thin shells and plates, and its application to structural intensity analysis and source localisation. Part 1: Theory. *Journal of the Acoustical Society of America*, **87**, 1166-1175.

Taylor, P.D. (1990). Nearfield structureborne power flow measurements. In *Proceedings of the International Congress on Recent Developments in Air and Structure-borne Sound and Vibration*. Auburn University, U.S.A.

Verheij, J.W. (1990). Measurements of structure-borne wave intensity on lightly damped pipes. *Noise Control Engineering Journal*, **35**, 69-76.

POWER TRANSMISSION CHARACTERISTICS IN AN ACTIVELY CONTROLLED SEMI- INFINITE PLATE

Xia Pan and Colin H. Hansen
Department of Mechanical Engineering, University of Adelaide, Adelaide, South Australia 5005

ABSTRACT

The feedforward active control of harmonic vibratory power transmission along a semi-infinite plate excited by a pair of piezoceramic crystal actuators is investigated experimentally and theoretically. The two crystals (primary source) were attached in the same location but on opposite surfaces of the plate. A control system driving three independent actuator pairs (control sources) is designed to reduce power transmission, using a cost function consisting of the sum of the squared outputs of eight accelerometers arranged in a single row across the width of the plate in the far field of the primary and control sources. The theoretical predictions are compared to the experimental results and, in addition, power intensity distributions with and without control are investigated. These distributions are of considerable significance in the control of power transmission. Vortices which may occur under certain uncontrolled conditions are largely eliminated with the control of power transmission. Both theoretical and experimental results demonstrate that it is possible to achieve a significant reduction in power transmission in plates by the use of three independent control sources.

INTRODUCTION

Controlling the vibratory power transmission and intensity distribution in large plate-like structures is one way of minimising the transmission of vibrational energy between two items of equipment mounted on the same structure. To evaluate the effectiveness of a control system built for this purpose it is useful to measure residual power intensity distributions in the plate structure, even though it will be recognised that acceleration, rather than intensity, may be used as the cost function for the control system.

In a previous paper (Pan and Hansen 1995), the active control of vibratory power transmission in a semi-infinite plate is analysed theoretically. It is predicted that a significant reduction of power transmission can be achieved by the use of three independent control sources.

The first definitive work on structural intensity measurement in plates was by Noiseaux (1970) and this was followed in 1976 by Pavic's landmark paper on which much of the subsequent work has been based (Carniel and Pascal 1985, Rasmussen 1985, Pavic 1986 and Williams 1988). Work was carried out by Taylor (1990) to quantify the errors associated with measurements discussed in earlier studies (see for example Taylor 1990). The existence of intensity vortices on a simply supported plate structure was first reported by Tanaka et al. (1993).

Here it is demonstrated how it is possible to actively control the characteristics of these vortices with appropriately placed and driven control sources. Thus the possibility arises of controlling the vortices such that their centers lie at the mounting points of sensitive equipment.

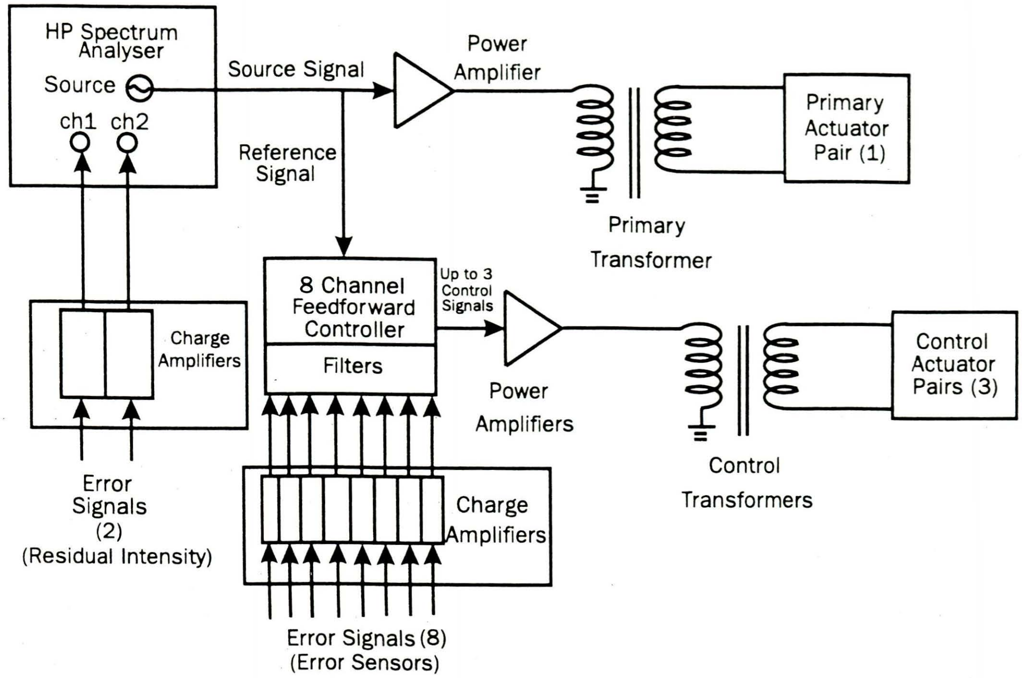

Figure 1: **Plate arrangement**

EXPERIMENTAL ARRANGEMENT

One end of a steel test plate with a working length of 1.4 m, thickness of 3 mm and width of 0.5 m was mounted in a sand filled box (1 m in length) in an attempt to provide a semi-anechoic termination. The plate was simply supported along the full length of the two edges normal to the anechoically terminated end. The remaining edge of the plate, opposite the anechoically terminated end was free.

Control of vibratory power transmission was investigated experimentally on the test plate excited near the free end using a pair of piezoceramic crystal actuators driven out of phase and with the same amplitude, with the aim of introducing pure bending excitation. Active control was implemented using a second row of three piezoceramic actuator pairs bonded on each of two opposite surfaces of the plate nearer to the anechoic end with each piezoceramic crystal pair driven independently. Eight accelerometers mounted in single row across the plate between the control actuators and the anechoic end acted as error sensors. The arrangement of sources and sensors on the plate is shown in Figure 1.

The source signal from an HP spectrum analyser was passed through a power amplifier into a primary transformer and then into the primary piezoceramic actuator pair. Error signals from the eight accelerometers and the source signal (as a reference) were passed by way of amplifiers and filters to the feedforward controller which generated the driving signal for the control actuators. Up to three control signals were used to drive up to three independent actuator pairs. Residual power intensity was measured on each of 15

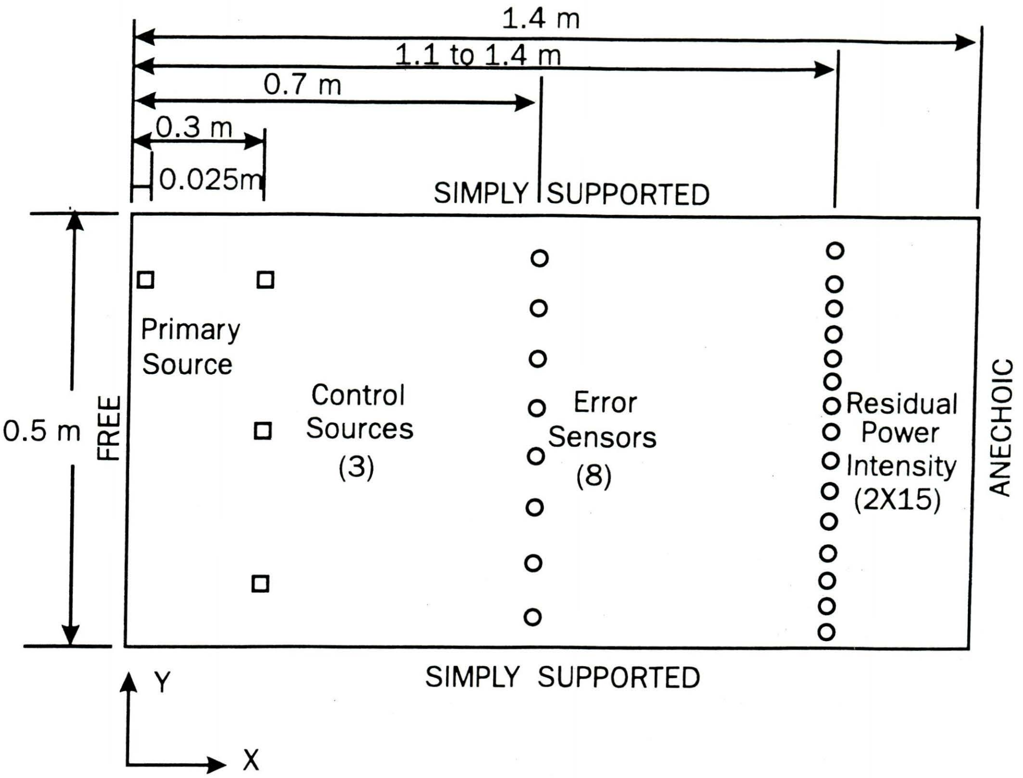

Figure 2: **Block diagram of the vibration control system**

accelerometer pairs arranged in two rows across the plate parallel to the free edge and in the far field of the control sources. A block diagram of the vibration control system for the measurement of intensity is shown in Figure 2.

NUMERICAL AND EXPERIMENTAL RESULTS

ACTIVE CONTROL OF VIBRATORY POWER TRANSMISSION

To investigate the potential for actively controlling vibratory power transmission, the plate was excited at the third modal 'cut-on.' frequency (259 Hz).

An estimate of power transmission was obtained by a method which included averaging the intensity measured by each of the 15 accelerometer pairs (Pan et al. 1994). The measured and theoretical power transmission reductions are shown in Table I, where x_e is the axial location of the row of error sensors, x_s is the axial location of the control sources, λ_b is the bending wave length, 'F_s' represents one control source and 'three F_s' represents three independent control sources. The measured power transmission reductions were determined from intensity measurements at $x = 1.20\ m$. The results presented in the table show that significant power transmission reductions for either measured or theoretical cases cannot be achieved with only one control source. However, significant power transmission reductions can be obtained (68 dB theoretical and 14 dB measured) by using three independent control sources. The difference between theoretical and measured reductions for the latter case can be attributed to the difficulty in obtaining identical output force amplitudes from each element of the control actuator pairs and the lack of precision of the controller. Table I also shows that in practice, the achievable power transmission reduction generally increases as the separation between the error sensors and control sources increases. However, the theoretical power transmission reduction is virtually independent of the error sensor location when $(x_e - x_s)/\lambda_b > 1.0$. Although the measured power transmission reduction was not as great as that predicted theoretically, a value of 14 dB does show that the approach described here could be a feasible way of controlling vibration transmission in large structures.

TABLE I
MEASURED AND THEORETICAL POWER TRANSMISSION REDUCTIONS

$(x_e - x_s)/\lambda_b$	measured P.T. redn.(dB) with one F_s	measured P.T. redn.(dB) with three F_s	theoretical P.T. redn.(dB) with one F_s	theoretical P.T. redn.(dB) with three F_s
1.36	-1	7	0	68
2.12	-2	4	0	68
2.73	2	11	0	68
3.27	0	14	0	68

STRUCTURAL INTENSITY VORTICES

An interesting aside to the results for the reduction in vibratory power transmission obtained from active control was the observation of structural intensity vortices. The presence of such vortices had been reported previously by Tanaka et al. (1993) for a harmonically excited simply supported plate. The authors demonstrated that for vortices to appear, at least two excitation sources were needed or if only a single source was used, then at least two modes had to be excited at a similar amplitude, and at a frequency close to their resonance frequencies. This meant that the resonance frequencies of the two modes had to be close together if a vortex was to be obtained with a single harmonic excitation source.

It is interesting to note that when one end of the plate is approximately anechoically terminated (as for the case considered here) such that the travelling wave field dominants the standing wave field, strictly speaking no resonant modes exist; rather, the vibration field is made up of 'cut-on' travelling modes, in much the same way as the well-known occurrence in an anechoically terminated duct. Thus at any frequency above the second modal cut-on frequency there will usually be two or more modes propagating and in most cases there will be sufficient energy in at least two modes for intensity vortices to be generated.

For the structural intensity results presented here, the primary source is at $(x, y) = (0.025, 0.417)$ m, a row of three control sources are at $x = 0.3$ m, a row of error sensors are at $x = 0.7$ m and the excitation frequency is 259 Hz. Measured and theoretical intensity vectors were determined as a function of location on the plate (see Pan et al. 1994 for plate property details). Figure 3(a) shows the distribution of the measured uncontrolled intensity and Figure 4(a) shows the corresponding theoretical result. Figures 3(a) and 4(a) essentially indicate one major vortex. This is because the path of power transmission in the plate is a combination of transmission and rotation, the latter being induced by the interference of two modes that produces a 'vortex generating block'. The theoretical and experimental results are a little different because the experimental model was characterised by some reflection from the 'infinite end' of the experimental plate (Pan et al. 1994) where

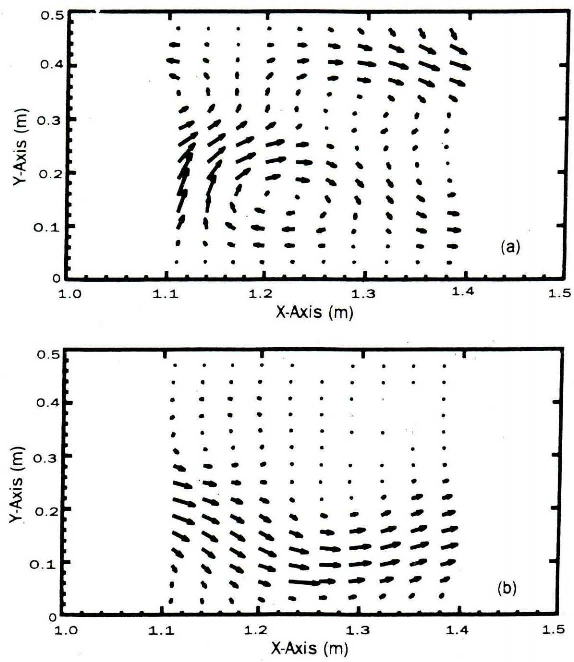

Figure 3: Measured far field intensity: (a) with one primary source; (b) with one primary source and three independent control sources.

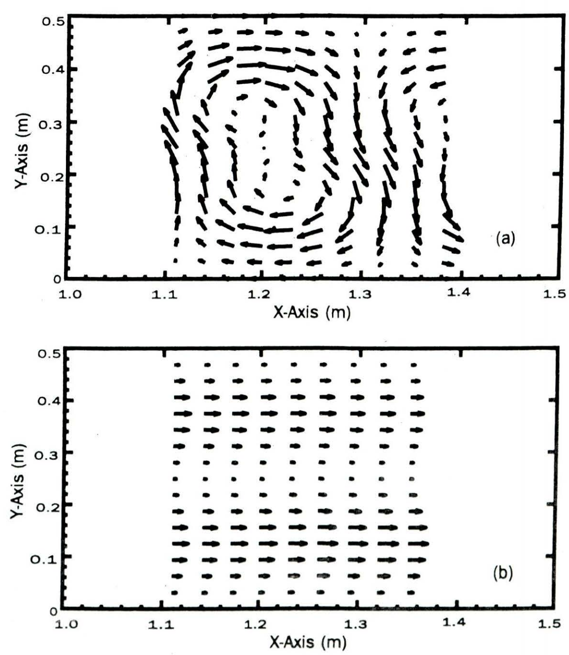

Figure 4: Theoretical far field intensity: (a) with one primary source; (b) with one primary source and three independent control sources.

the reflection coefficients were about 0.2 for the first and second modes which were cut-on at the test frequency of 259 Hz. Also the method of measuring intensity (Pan et al. 1994) assumes the absence of near field effects and thus gives only approximate results. On the other hand, the theoretical model makes no such assumption. Nevertheless, it is encouraging to see that the vortex trends are similar for the theoretical and experimental models.

Figure 3(b) shows a measured intensity distribution with one primary source and three control sources driven independently. Figure 4(b) presents corresponding theoretical results. Comparing Figures 3(b) with 4(b), it can be seen that the theoretical intensity vectors are orientated almost entirely in one direction, whereas the measured intensity vectors, there is a tendency to form a vortex. This difference is probably due to the difficulty in ensuring that in the experiment each element in each control actuator pair produces the same force. Any differences in the properties of the two piezoceramic crystals, such as differences in their sizes, their locations or their bonding layer thicknesses would cause differences in their force output. However, in both cases the control sources tend to eliminate the vortex structure from the intensity distribution.

CONCLUSIONS

In practice, harmonic vibratory power transmission in a semi-infinite plate can be significantly reduced by driving an array of independent control sources placed in a row across the plate. With three control sources it is possible to achieve maximum levels of vibratory power transmission reduction of 14 dB at the 'cut-on' frequency of the third mode. Acceleration only may be used as the error sensor cost function to be minimised, provided that the error sensors are in the far field of the control sources. For the test plate, of dimensions described and with the given arrangement of sources, a minimum of eight acceleration error sensors spaced evenly in a line across the plate are necessary; however, it is expected that results would improve further if the number of error sensors were increased.

Measurements of structural intensity on the semi-infinite plate, under primary excitation only, frequently show a vortex pattern which changes as the number and location of the primary sources changes. It is found that the addition of control sources driven to minimise power transmission, also largely eliminates the vortex pattern. In the future, it may be possible to drive the control sources to control the residual intensity vortices so that they are located at points where sensitive items of equipment are attached, thus effectively providing isolation from the plate vibration.

The theoretical results presented in this paper, generally confirm the experimental results for power transmission and intensity distribution, except that measured reductions in power transmission are less than theoretical predictions. This is due to limitations in experimentally realizing the theoretical model to a sufficient degree of accuracy.

REFERENCES

[1] Carniel, X. and Pascal, J.L. (1985), Vibrational power flow measurement: structures characterization and wave reflection coefficient measurement, *Inter-Noise* 1985, Munchen, pp.613–616.

[2] Noiseaux, D.U. (1970), Measurement of power flow in uniform beams and plates, *J. Acoust. Soc. Amer.*, **47**, pp.238–247.

[3] Pan, X. and Hansen, C.H. (1995), Active control of vibratory power transmission along a semi-infinite plate, *Journal of Sound and Vibration* (accepted to be publicated in June 1995).

[4] Pan, X., Hansen, C.H. and Snyder, S.D. (1994), Power Transmission Characteristics in an Actively Controlled Semi-infinite plate, *Journal of Active Control.*

[5] Pavic, G. (1976), Measurement of structure borne wave intensity, part I: Formulation of the methods, *Journal of Sound and Vibration* **49(2)**, pp.221–230.

[6] Pavic, G.(1986), The influence of curvature on structure-borne acoustical power propagation in a cylindrical shell, Paper D6-6, 12th ICA-Congress, 1986, Toronto.

[7] Rasmussen, G. (1985), Intensity analysis of structures, *inter-noise* 85, Munchen, pp.673–676.

[8] Tanaka, N., Kikushima, Y., Kuroda, M. and Snyder, S.D. (1993), Structure-borne intensity characteristics of an actively controlled thin plate, *Proceedings, Fourth structural intensity conference, France,* pp.273–280.

[9] Taylor, P.D. (1990), Nearfield structure borne power flow measurements, *International congress on recent developments in air and structure borne sound and vibration,* Auburn University, USA, pp.339–345.

[10] Williams, E.G. (1988), Introduction and survey of recent developments in near acoustic holography, *inter-noise* 1988, Avignon, pp.203–208.

GLOBAL ENERGY MINIMISATION USING ACTIVE CONTROL

Dan Qi

Acoustics and Vibration Centre,
Australian Defence Force Academy, ACT 2600

ABSTRACT

Active control to achieve global energy minimisation where the waves may not propagate in the same direction is complex. Current mechanism models such as primary source suppression, secondary source absorption and impedance control have been investigated in the past. In this study, a mechanism model comprises wave-wave interaction and the interaction between the active wave and the primary source has been considered. Results show the reduction of global field energy could be achieved up to 1/3 of the original progressive wave energy. Maximum energy reduction can be achieved with the anti-wave being exactly out of phase at the primary source and the amplitude ratio of the active wave to the primary wave being 0.38.

INTRODUCTION

Global control originated from the motivation to reduce the sound pressure level at all positions in an enclosed field (Nelson and Elliott 1992). It was found that there was little point in trying to achieve further reduction at points where natural destructive interference took place. Global control research then focused more on local control to achieve a "quiet zone" where the sound level was originally high and offensive. Although energy reduction at one local point may substantially increase the energy at another point where the sound level was originally low, further study (Curtis et al. 1990) on its global effect has shown that the global field acoustic energy could be reduced. This phenomena cannot be explained purely by the wave superposition theory. Numerous studies were carried out to investegate the mechanisms of reduction of global field acoustic energy, such as primary source suppression (Curtis et al. 1987), secondary source absorption (Synder and Hansen 1989), impedance control (Guicking and Karcher 1984). Current implementation of global energy minimisation control generally relies on global field real time measurements, and requires substantially complex and costly data acquisition and control systems.

The objectives of this paper were to examine theoretically global energy minimisation in one dimensional space (ie, a duct) where both the primary and secondary sources are mounted in the plane of the duct cross-section. Emphasis has been placed on considering the effect of the active wave produced by the secondary source on the radiation of the primary source. The implications of this mechanism model will be discussed.

MECHANISM FOR GLOBAL ENERGY MINIMISATION

The geometry considered here is an infinite duct shown schematically in Figure 1 where the primary source is located at x=0 and the secondary source is located at x=L. The region for global energy minimisation is the confined volume between x=0 and x=L. It is assumed that the frequency range of interest is below the duct cut-off frequencies so that only one-dimensional plane waves are considered. The mechanism model comprises consideration of both wave-wave interaction and the effect of the active wave on the radiation of the primary source.

WAVE-WAVE INTERACTION

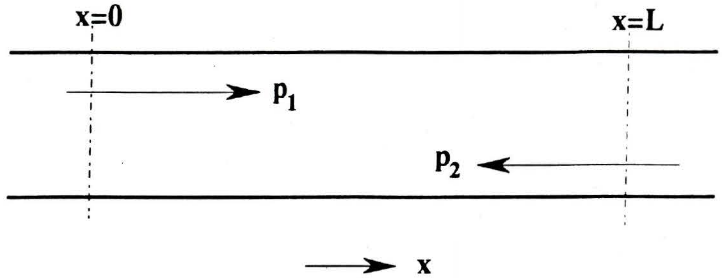

Fig.1 Model of the confined volume of a free field

Consider the sound field set up by the primary and secondary sources between x=0 and x=L. Harmonic plane waves p_1 from the primary source and p_2 from the secondary source may be expressed as

$$p_1 = A_1\, e^{j(\omega t - kx + \phi_o)}$$
$$p_2 = A_2\, e^{j[\omega t - k(L-x) + \phi_L]} \tag{1}$$

where A_1 and A_2 are the amplitudes of primary wave p_1 and the active wave p_2 respectively and ϕ_o and ϕ_L are the corresponding phases. The resulting sound field p(x,t) in $0 \geq x \geq L$ may be obtained by superposition as given in equation (2)

$$p(x,t) = A_1\, e^{j(\omega t + \phi_o)}\, [e^{-jkx} + r\, e^{j(kx - kL + \Delta\phi)}] \tag{2}$$

where $r = A_1/A_2$ and $\Delta\phi = \phi_L - \phi_o$.

In equation (2), the controllable parameters are r and $\Delta\phi$.

The distribution of total acoustic energy $E_{tot}(x)$ can be determined from the time-averaged sound pressure as follows:

$$E_{tot}(x) = \frac{1}{T}\int_o^T (1/\rho c)\,(\mathrm{Re}\; p(x,t))^2\, dt$$

$$= E_o\{1+r^2+2r\cos[2kx-(kL-\Delta\phi)]\} \qquad (3)$$

where $E_o=A_1^2/2\rho c$ is a constant energy distribution of the progressive wave p_1 alone and the terms associated with r represent the influence of the active wave on the total energy distribution.

From equation (3), the following conclusions can be drawn:

i) when r=1, the energy distribution $E_{tot}(x)= 2E_o\{1+\cos[2kx-(kL-\Delta\phi)]\}$ is that of a standing wave. The spatial-averaged energy is twice that of E_o(Fig.2).

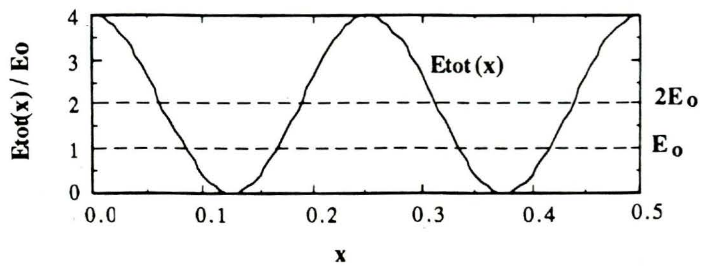

Fig.2 Normalized energy distribution for r=1

ii) let $\phi'=kL-\Delta\phi$, then ϕ' completely controls the node position. However, ϕ' has no effect on the global energy distribution (Fig.3).

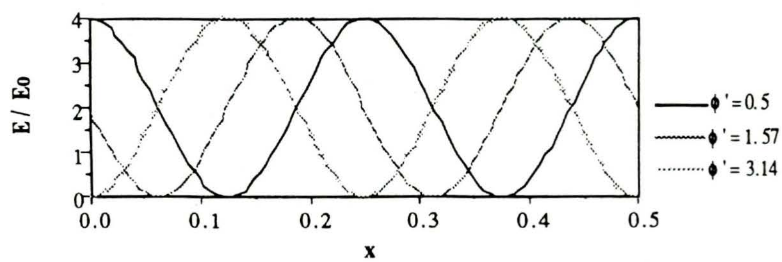

Fig.3 Normalized energy distribution for r=1 and various φ'

iii) $E_{tot}(x)$ approaches E_o as r approaches zero, as seen from equation (3).

The spatial-averaged energy $\bar{E}$ in the region $0 \le x \le L$ can be determined by integrating equation (3) as follows:

$$\bar{E} = \frac{1}{L}\int_0^L E_o\{1+r^2+2r\cos[2kx-(kL-\Delta\phi)]\}\,dx$$

$$= E_o\{1+r^2+r\,\frac{\sin(kL+\Delta\phi)+\sin(kL-\Delta\phi)}{kL}\} \qquad (4)$$

Previous studies yielded similar results to equation (4). It showed that the influence of the sine terms is significant only within the first half wavelength of the frequency of interest. If we take the integration range L being an integer number of half wavelength, i.e. $L= n\frac{\lambda}{2}$, (n =1,2,...), then, equation (4) can be reduced to the following form which is only dependent on r.

$$\bar{E} = E_0(1+r^2) \tag{5}$$

Equation (5) indicates that for the region $0 \le x \le L$, the spatial averaged energy is independent of the phase parameter $\Delta\phi$ and L. Under wave to wave interaction, it can be seen that the global energy is increased by the generation of active wave due to the secondary source and this increase only depends on the amplitude ratio r.

EFFECT OF THE ACTIVE WAVE ON THE RADIATION OF THE PRIMARY SOURCE

Results in section 2.1 indicate that global energy minimisation cannot be achieved by considering wave-wave interaction. This is because the effect of the active wave on the radiation of the primary source has not been considered (Fig.4).

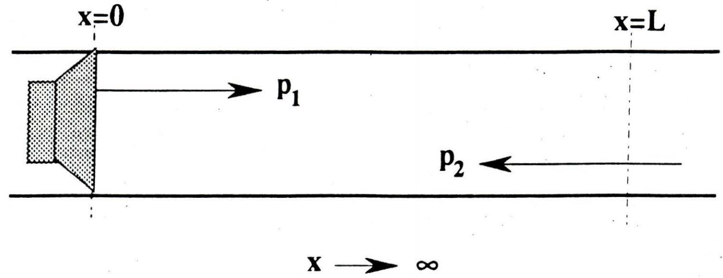

Fig.4 Model of the active wave effected on the radiation of primary source

The source radiation can be described by the mechanical surface velocity $u_{x=0}(t)$ and the pressure $p_1(x=0+,t)$ at the source. With reference to Fig4, initially, the primary source is driven by a sinusoidal force. During the time period (n=0) before the active wave p_2 arrives at the source position the initial radiation by the primary source at x=0 can be described by equation (6)

$$u\,|_{x=0,n=0} = \frac{p_1}{\rho c}\Big|_{x=0+,n=0} = \frac{A_1}{\rho c}\, e^{j(\omega t+\phi_o)} = U_o \tag{6}$$

The amplitude ratio of the active wave p_2 produced by the secondary source to p_1 is r $(=A_2/A_1)$. As soon as the active wave p_2 arrives at x=0 the radiation of the primary source can be determined from superposition of p_1 and p_2 as follows:

$$u\,|_{x=0,n=1} = \frac{p}{\rho c}\Big|_{x=0+,n=1} = \Big[\frac{A_1}{\rho c}\, e^{j(\omega t-kx+\phi_o)} + r\,\frac{A_1}{\rho c}\, e^{j(\omega t-k(L-x)+\phi_L)}\Big]\Big|_{x=0,n=1}$$

$$=U_o[1+r\, e^{j(\phi_L-\phi_o-kL)}]$$

Since the initial phase of p_2 can be fully controlled to be 180° out of phase with that of p_1 at x=0 (i.e. $\phi_L-(\phi_o+kL)=\pi$), the radiation of the primary source at x=0 is thus reduced to

$$u_{x=0,n=1} = \frac{p}{\rho c}\Big|_{x=0+,n=1} = (1-r)\, U_o \tag{7}$$

Considering the active control in the above mechanism model, once the anti-phase relationship has been dynamically established at the primary source position, a consistent suppression on source radiation p_1 can be obtained via the active wave p_2. Since the first time the active wave acts on the primary source, the effective radiation of the primary source has been changed to $(1\text{-}r)U_o$, the amplitude of the active wave for the second interaction has to be adjusted to $r(1\text{-}r)U_o$. Thus, after the second interaction, the effective radiation of the primary source is given by

$$u_{x=0,n=2} = \frac{p}{\rho c}\Big|_{x=0+,n=2} = [1-r(1-r)]U_o = (1-r+r^2)U_o\,.$$

After n times interaction by the active wave, the effective radiation of the primary source is given by

$$u_{x=0,n} = \frac{p}{\rho c}\Big|_{x=0+,n} = [1-r+r^2-r^3+r^4-r^5+\ldots+(-r)^n]\,U_o = \frac{1-(-r)^{n+1}}{1+r}\,U_o \tag{8}$$

The variation of the radiation of the primary source with n for various values of r is shown in Figure 5.

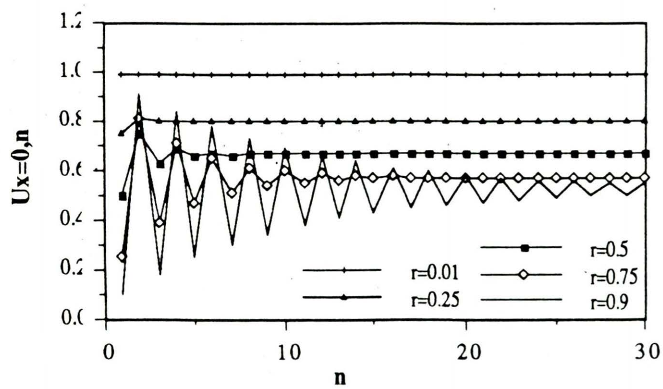

Fig.5 Variation of the primary source radiation with n for various r

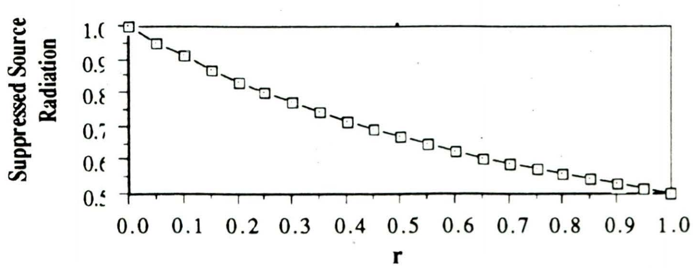

Fig.6 Variation of primary source radiation with r for n>30

Since r<1, the effective radiation of the primary source approaches a steady value $\frac{1}{1+r}U_o$ which corresponds to the maximum suppression of the primary source radiation that can be achieved. As shown in Figure 6, this value tends to a minimum value of $0.5U_o$ as r approaches 1.

The acoustic energy radiated into the field, from such a steadily suppressed primary source, can be obtained from equation (8). A harmonic wave of the primary source under steady state condition is given by

$$p_1(x,t) = \frac{A_1}{1+r} e^{j(\omega t+kx+\phi_o)} \qquad (9)$$

The averaged energy of the primary source radiation is thus given by

$$\bar{E}_1 = \frac{1}{2\rho c}\frac{A_1^2}{(1+r)^2} = \frac{E_o}{(1+r)^2} \quad . \qquad (10)$$

where E_o is the averaged energy of the progressive wave p_1 alone.

THE COMBINATION EFFECT FOR THE FIELD ENERGY MINIMISATION

For global energy minimisation, the mechanism model for active control comprises the effect of the wave-wave interaction as described by equation (5) and the suppression effect of the radiation of the primary source by the active wave as described by equation (10), which plot out in Figure 7.

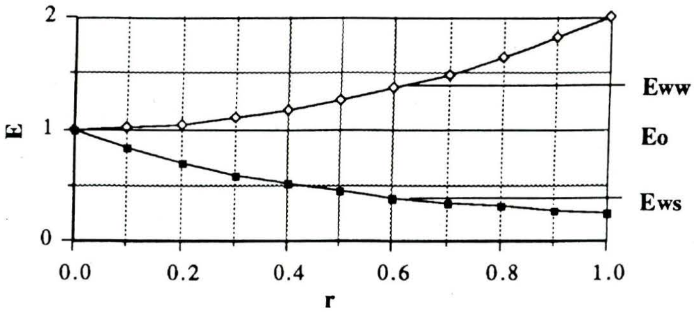

Fig.7 Energy variation with the individual interaction effects

It can be seen that for the wave-wave interaction control mechanism, the optimum value of r is zero because any opposite going wave will add its energy to the field upon the primary wave energy. However, for the primary source suppression mechanism, the best choice of r will be 1.The combined field energy reduction refer E_o is given by

$$\Delta E = (E_o - E_{ws}) - (E_{ww} - E_o) = [1 - \frac{1}{(1+r)^2} - r^2]\, E_o \qquad (11)$$

The variation of ΔE with r is shown in Figure 8. By differentiating equation (11) with respect to r, the optimum value of r to yield maximum global energy reduction has been determined to be 0.38. Under this condition, the maximum energy reduction is 1/3 of the energy of the progressive wave due to the primary source alone. This is equivalent to 1.76 dB reduction in the global energy.

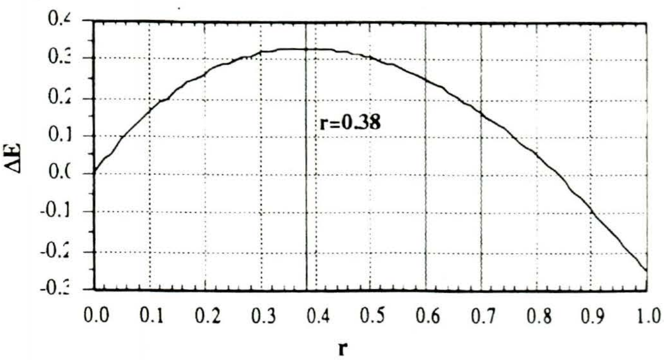

Fig.8 The global energy reduction varies with r

DISCUSSION

The 1.76 dB reduction from the original progressive wave energy is the base level for global energy control. This provides a comparable measure for our global control efforts. Although this appears to be a small value, it should be noted that control in an enclosed acoustic field is normally used to reduce the energy from its resonance. The actual level of energy reduction at resonance could be very significant depending on the individual system.

The result of this paper presented a more satisfactory explanation of global energy control than previous studies. The phenomena of global energy minimisation can be achieved by the non-equal amplitude control condition and can achieve a further reduction from the anti-resonance energy (Curtis et al. 1990). These cannot be explained by the current global control analytical model reviewed by Elliott and Nelson (1992). Which model indicated that the optimum secondary source strength should have equal amplitude to the primary one and the minimum energy - which corresponds to anti-resonance energy - should be half of the progressive wave energy. The result presented of this study is in agreement with the experiment.

The result also showed a technical advantage of active control. Using active control, the global energy in an enclosure can be reduced to below the anti-resonance energy which is the lowest energy level that passive control could achieve. This advantage will be of significance to global control under multi-frequency conditions.

CONCLUSION

In this study, combined mechanism processes are discussed which are directly linked to the global energy minimisation control. The result showed that the reduction of global field energy could be achieved up to 1/3 of the original progressive wave energy. Maximum energy reduction can be achieved with the anti-wave being exactly out of phase at the primary source and the amplitude ratio of the active wave to the primary wave being 0.38.

REFERENCES

Nelson P.A., Elliott S.J. (1992) "Active Control of Sound" Academic press.

Curtis A.R.D., Nelson P.A., and Elliott S.J. (1990) "Active reduction of a one-dimensional enclosed sound field: An experimental investigation of three control strategies" JASA 88(5), pp2265-2268.

Curtis A.R.D., Nelson P.A., Elliott S.J. and Bullmore A.J. (1987) "Active suppression of acoustic resonance" JASA 81(3), pp624-631.

Synder S.D. and Hansen C.H. (1989) "Active noise control in ducts: Some physical insights" JASA 86(1), pp184-194.

Guicking D.and Karcher K. (1984) "Active impedance control for one-dimensional sound" J. Vibration, Acoustics,,Stree, and Reliability in Design, Vol(106), July, pp393-396.

ENVIRONMENTAL NOISE

A NEW APPROACH TO ENVIRONMENTAL MEASUREMENTS

Alan D. Wallis Cirrus Research plc, Hunmanby, United Kingdom

BACKGROUND.

For many years, acousticians have had available some tools for environmental noise measurements. At the lowest level, the simple sound level meter is often used and from this simple device quite complex measurements, or rather calculations, of L10 and similar statistical indices can be made. However, for longer measurements this simple approach is at least 'difficult' and at worst 'impossible'. To solve this problem, various analyzers have been produced over the years, ranging from the old electro-mechanical high speed level recorder and its associated statistical analyzer to dedicated electronic solutions with internal print-outs, mainly from the United States and the United Kingdom. All these old technology units tended to suffer from various practical problems and these included.

The need to set the measuring parameter before starting
The paper jamming which occurred from time to time.
The weight and size of the instrument
The weight and size of the batteries, often more than the unit
Operational complexity, thus a very high skill needed for accurate results

The world was waiting for a better method, but until the advent of computers, or rather the possibility of embedding computer chips into instruments, they had to continue with the old methods. From about the late 60's, it was possible to buy micro-controllers and rudimentary processors, but they had very poor instruction sets, consumed very high current and were not very suitable for instrument usage; for this reason early electronic units used logic chips or modules rather than a micro-controller. Among the very first 'all electronic' analyzers was the CRL 2, development of which started in 1969 and which used TTL logic chips to create a computing system. It could generate all the statistical indices from L1 to L99, although not all at once, but was mainly famous as a heating system, as it consumed about 180 watts when operating and got very hot indeed. At Cirrus, we realised very early that such high power consuming instruments were fairly useless and so a new version was developed using the then new CMOS logic chips and this allowed the power to be reduced to about 20 watts, almost a scale order improvement. However, as is well known, the power consumed by CMOS logic increases with the operating speed and so the new instrument CRL6 was slowed down to a crawl in order to allow battery operation. Introduced commercially at the 1974 ICA in London, the CRL6 was clearly the way the technology was going, but had significant shortcomings.

Firstly, it was a dedicated statistical analyzer which printed the results on paper, as well as storing a few values. This therefore did not solve the mechanical problems of previous generations at all. Secondly, because of advice from the United Kingdom Government, it did not have Leq. At the time, all UK regulations were being written in terms of L10, L50 and L90 and from these, various 'single number units' could be generated. One of the first and most used was the traffic noise index (TNI) and this was generated automatically by the Cirrus unit. Like most things done on the advise of governments, it was a commercial flop. As the world now knows, Leq became the favoured method and Computer Engineering Limited, now CEL took a device designed by a United Kingdom Government laboratory and produced first a dosimeter and followed this by a series of Leq meters, or as they are correctly called by pedants 'Integrating Averaging Sound level Meters', today described by IEC 804. In Germany, the State organisation RFT in Dresden also produced an Leq measuring instrument and share with CEL, the prize of being first in the field. The CRL 6 and everything like it was consigned to history, although many of the older units took some time to die.

DATA LOGGING

The first data logging instruments were produced in the early 1980's and were very poor devices. Many were made by computer based companies, who while having a deep knowledge of the computer art had little or no acoustic skills. The result were instruments which simply failed to meet the most simple tests specified in IEC 651. One particular example featured a mean value rectifier instead of an rms circuit. The manufacturer then argued that the sound level meter standard was wrong, a little like some companies today? Others misunderstood the dynamic range requirements making units which spent most of their time at one of the dynamic limits, either at the noise floor or in overload. Indeed, one of the worst offenders had no overload indicator and thus the user had no means of knowing that the stored data was false. The result of the low performance of these devices left professional acousticians very thankful they still had their trusty old B & K level recorders. Even though the data they gave was very limited, at least it was to some defined standard.

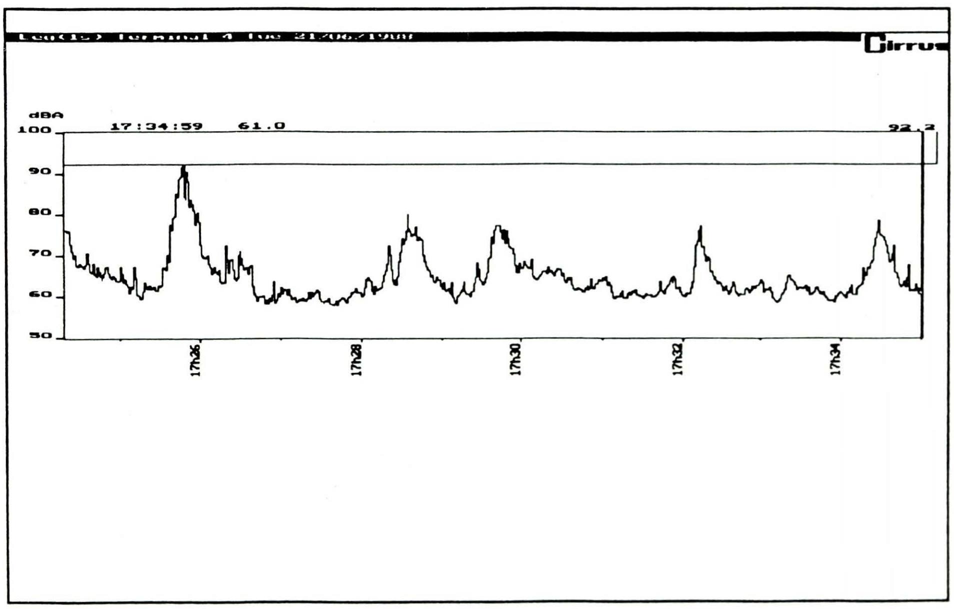

Fig. 1 - Heathrow airport in 1986

The next event in the development of today's instruments was Short Leq. This technique, well described in earlier papers, (ref 1) at last allowed data loggers to be built which could statistically reproduce the noise levels as needed. The first devices were totally 'outbox' processors where the data was acquired, stored and re-played on a host computer. Figure 1 shows such data, taken in 1986 at Heathrow airport. Instruments such as the CRL 236, even though designed as 'outbox' processors, could display some overall data, but this was simply to reassure the user rather than the main feature. Even as these units were designed, it became clear that while they would always have their place in longer term measurements and measurements made for enforcement purposes, most environmental users needed something more adapted to their needs for everyday use. In the event, the 'Pure' data logger evolved into a new generation of Airport noise monitors and smaller versions were built as hand held instruments which could be field configured. However, none of these totally solved the problems of the long periods of environmental measurements needed for many noise control tasks.

THE NEXT STAGE

By about 1992, several users, were buying dedicated data logging instruments like the CRL 236A other data logging sound level meters and putting them into waterproof cases, adding some form of weather protection to the microphone and leaving them out for long periods. To power them, car batteries were used and these typically were as large as, and much heavier than the instrument. In line with this trend, a few manufacturers made simple outdoor microphone sets, such as the MK425. The traditional outdoor microphones being too heavy, too expensive and too power hungry for long term battery use. Obviously, with the coming of the electret microphone there was not the same need to have heaters and complex enclosures if the target was simply to meet Type 1. If however a company was offering its product as 'the best in the world' it was difficult to make this claim and at the same time add simple weather protection which usually spoils the microphone response. At Cirrus however, we take a much simpler view. We claim IEC type 1 for the whole system and if an independent laboratory approves it, that is more than adequate. The abstruse minor points loved by some pedants seem to have no place in outdoor practical systems. For this reason, we added a special thick quartz coating to our capsules and used a grade of metal with wider tolerances on the coefficient of expansion, but with better weather protection. This then allowed the construction of a very simple outdoor system at a fraction of the cost of a full 'installed' system.

TODAY.

After the development by several companies of a simple weatherproof housing, it became obvious that the microphone could be attached to the housing to make a dedicated instrument. At least two companies simultaneously came up with similar concepts, Acoustic Research Labs in Australia and Cirrus Research from the UK. Both had similar problems to solve. Any method of fixing the microphone mast to the case must avoid reflections that would but the resulting instrument out of the tolerances of the relevant standard. The Cirrus solution was to fix the microphone boom on the smallest edge of the case and make the mast adequately long to ensure that the reflections were at low frequency. Even so, the initial prototypes had slight 'bumps' in the response which needed improvements to the acoustic shape and made type 1 compliance an 'only just'. situation. The disadvantage of the concept is that the mast has to be very long and this caused some problems with portability. The alternative Acoustic Research approach of making a telescopic mast initially led to the same problems, but cooperation between the companies led to a situation where the UK instrument met Type 1, albeit at a higher cost than initially hoped, while the Australian unit could meet the requirements of type 2, at a very moderate price. The Australian instrument used the largest side for the mast to allow the unit to be placed on the ground, an important practical feature; whereas the Cirrus design mandated a tripod as part of the unit. This again added to the cost and complexity, but gave better acoustic performance.

The method of meeting Type 1 for the Cirrus CR:245 is to specify the microphone reference angle at 20 degrees to the vertical. This is accepted in many countries, but where it is not or the absolute best accuracy is needed, the mast can be unplugged and mounted on a separate tripod and connected by a cable and for its PTB certification, this is the specified method of use. In this way, even the most pedantic user can be satisfied that every dot and comma of the IEC specification has been complied with. The alternative approach of a huge 'cone' over the top of the case was considered not the most sensible method, although obviously, it would work. The reality for most users is that the noise being measured is sufficiently random in frequency content for the slight 'bumps' in the pure tone response not to cause significant additional errors. In the same way, if the Acoustic Research unit was to be used where very significant high frequency pure tones were present, special care would be needed to remove the standing wave caused by the top of the case. In environmental noise use, such tones are rarely a problem. To keep the unit inside type 2, a 'skirt' was devised to keep the hardware in its acoustic shadow. This while still leaving problems of refraction round the edges of the skirt, gave the required improvement.

Power for such units can obviously come from many sources, but in general a source of ac power is not available for environmental measurements and battery power is needed. The CR:245 will operate for about 10 days on its internal battery, but as well has a solar option which will give continuous running, even in the UK low light levels. Now, we have a method of acquiring data over long periods in any type of climate.

THE UNIT LOGIC.

The basis of the new instruments is a computer controlled data logger with a very large memory. The 'standard' CR:245 has 2 megabytes of memory, but simple options of 4 and 8 megabytes give an unusual storage capability. For those companies who rely on commercial spreadsheets to analyze the data from the sound level meter, this memory size would be far too big, but with Acoustic Editor, a dedicated acoustic software package there are no such limitations of file size. There are 2,628,000 seconds per month, thus a 4 megabyte memory is needed if any sensible acoustic resolution is desired. Data resolutions of less than 1 second are not really useful for analysis, even over such long periods. A 1 minute short Leq time history is fine if only Leq is needed at the end of the measurement, but is any re-processing is to take place, a 1 second basic period is the longest which can be contemplated. This allows at least 'S' response data to be generated and statistical data over any short period as well as to investigate very impulsive events. Both the Cirrus and Acoustic Research units can generate Acoustic Editor files, thus a system can be built up of a mix of type 1 and type 2 units.

However, the new units are not just short Leq storage devices. Conceptually, their fairly powerful internal computer can be configured in many ways. The ROM chip in the unit, the core program can be changed by the user to produce different functions. For example, one ROM can simply mimic the original data logger and simply store huge quantities of data. Another can mimic the dedicated airport monitor with full recognition of noise events by template comparison. However, the main ROM for the new instrument takes a slightly different approach.

The main function of a dedicated environmental analyzer is that it should take enough data to allow the noise climate to be described in the most suitable manner. The 'most suitable manner' will depend on the noise itself and often, until this is measured, the user will not know the ideal index to use. However, one thing which is common to most situations is that it is noises rising out of the background which are of special interest. If over a long period, the L10 - L90 difference stays constant within a few decibels and neither changes by a significant amount, low data rates will suffice and a simple summary report can be generated. If however a single impulsive event takes place more data, usually at higher resolution is needed. This approach over the years has led to several instruments which could switch on a tape recorder when certain criteria were exceeded. However, this simple solution is not always good enough. Any tape system takes time to come to speed and thus the initial onset of the noise is lost. This may not matter if the tape is being used simply to identify the noise source, but if it is to be used as part of the measurement, difficulties can arise.

While the CR:245 can support the use of Digital Tape recorders by providing a 'start' signal when a threshold is exceeded, it also has parallel mode of operation. Normally, the unit is configured to have three separate computations operating at the same time. Each of these produces the basic statistical data over different periods. Typically, a unit can be set to give an Ln series Leq, SEL, LAmax etc, every hour and the same set simultaneously every nighttime period as well as for the full 24 hours. Up to a year of such data can be taken. At the same time, a threshold is set and each time this is exceeded, raw data in the form of 1 second short Leq is stored in a different area of memory. At first this does not appear to resolve the lost data problem as even an Leq meter must have time to start. What is done in the CR: 245 is to send raw data all the time to a pre-trigger register and this is only used if the threshold is exceeded, otherwise it simply runs out of the end of the register. Typically 30 seconds of pre-trigger is used, but this can be any time up to several hours if needed. With this pre-trigger, the use of a DAT becomes more practical. The short Leq trace will show how and when the level has risen and the audio record from the DAT will usually identify it. For very short events, that is those completed before the DAT has time to start, the short Leq record will still be there and give an exact timing of the event. If very impulsive events are expected such as would arise if blasting was a possible noise source, the rate of short Leq acquisition can be speeded up to give Leq periods as low as

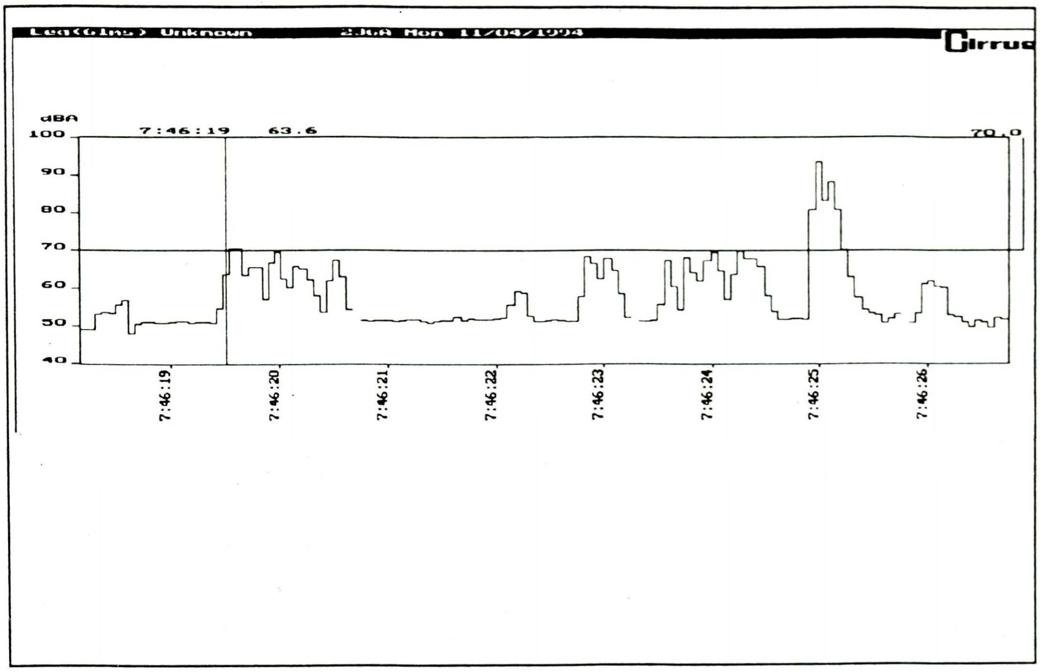

Fig.2 - A highly impulsive event, highly expanded.

5 milliseconds, or if even this is not adequate, a second channel can be added, which stores the the peak value. Figure 2 shows a very short portion of a trace with a very explosive event. A threshold set at 70dB would trigger the DAT at 07:46:19 seconds but even 6 seconds later when the real impulse occurs, the DAT may not have reached full speed. If the threshold were set to 71dB, the initial short event, would not have started the DAT and as the whole impulse is less than half a second, it would have been lost.

SUMMARY

New electronic, or rather computer technology can change the way we take environmental measurements and allows us to have access to devices which can be configured to do just the measurements required. The type and mode of measurement can be set by the user on site and , as well, raw data can be used to identify and locate separate noise sources.

REFERENCE

Wallis A.D. & Holding J.M. "A method of generating Short Leq"
Proc Internoise pp 1039- 1041 Hawaii USA Dec. 1984

CHICKENS VS HOUSING - URBAN ENCROACHMENT ON SEMI-RURAL COMMERCIAL ACTIVITIES AND THE POTENTIAL FOR NOISE ANNOYANCE

By Colin Tickell
Supervising Environmental Engineer, BHP Engineering, PO Box 1237 North Sydney, NSW 2059

ABSTRACT

As urban development in Australia expands its fringes into rural areas, there is the increasing potential for land-use conflicts with existing rural or industrial activities. These conflicts require town-planners to adequately address the impacts of and on urban development, which often include noise and other environmental emissions. As well as the impacts related to farming, there will be those of industries which have re-established in semi-rural, outer urban areas after having moved from inner urban areas to escape the complaints and constraints of the surrounding high density residential areas. This paper describes a case where a residential estate developer was seeking to locate houses immediately adjacent to poultry sheds in the outer fringes of Sydney. In these sheds up to 100,000 birds, including roosters, are woken from 3.00am to 4.00am and have the potential to cause significant noise annoyance. Measured and predicted sound levels are presented, and noise annoyance potential is discussed.

Keywords: Noise, chickens, poultry, roosters, town-planning, residential development

INTRODUCTION

An integrated poultry supplier operates two multiplication farms at a site (the study site) in the south western suburban fringe of Sydney. The farms each have six large sheds in which hens are raised for laying fertile eggs. Each shed contains approximately 8,000 birds, including roosters. The study site adjoins a proposed residential development. Also on the study site and adjoining the proposed development are a group of effluent treatment lagoons, operated for the treatment of liquid emissions from the processing plant on the same site.

The author was requested to assess the potential environmental noise issues of emissions from the farms and effluent treatment ponds on the proposed residential development. As the birds at the study site were immature and not yet making noise, measurements of mature birds were made at a similar farm in a rural area. The work requested was as follows:

1. Measure sound levels over an extended period at the rural farm site at a distance representative of the likely receiver boundary distances at the study site. Measurements to be of A-weighted statistical sound levels LA01, LA10 and LA90 for 15 minute sample periods over at least a 24 hour period. Include measurements before and after 4.00am to assess audible annoyance potential of the noise emission.

2. Measure the sound levels at the boundary of the study site to determine current daytime noise environment.

Measurements of sound level were taken in April, 1994 at both the study site and the rural farm site, where a similar set of farms operate.

CRITERIA

The criteria for assessment of environmental noise received at residential sites is given in the NSW Environmental Protection Authority's "Environmental Noise Control Manual". Chapters 20 and 21 of this document gives guidelines for acceptable outdoor sound levels at residential receiver properties in different land-use areas. Chapter 20 notes the following:

PLANNING FOR NOISE CONTROL

Planning Objectives

Residential areas adjacent to industrial areas may be subject to high background noise levels. Many people are resigned to suffer such high noise levels in order to obtain cheaper accommodation, to lessen travelling time to and from work or merely to avoid moving from familiar surroundings. Residential area noise imposes a stress on individuals and a cost on society, so existing problems should be progressively ameliorated and the creation of new high-noise problem areas should be avoided. The goals of the town planner in regard to noise should include:

(i) To control the establishment or growth of new residential areas in the vicinity of existing or planned industrial or commercial complexes, taking account of present or future background noise levels in relation to environmental noise policies. ...

The objectives give the recommended outdoor background noise levels as:

Daytime	7.00am to 10.00pm	$L_{A90.15Min}$	45 dB(A)
Night-time	10.00pm to 7.00am	$L_{A90.15Min}$	35 dB(A)

These levels are for continuous noise which does not have any annoying characteristics, such as tonality or impulsiveness. If such characteristics are present, then the objectives are effectively reduced by 5 dB(A) for each characteristic.

MEASUREMENT METHOD & RESULTS

Sound levels were measured at the rural farm site adjacent to farm sheds where the birds are currently mature. The two farms measured have sheds in a similar configuration to those at the study site.

Sound levels measured were statistical A-weighted sound levels measured over periods from 5 minutes to 15 minutes at the sides and end of the sheds at distances of 15 metres. Measurements were taken:

- during daytime,
- in the morning at 3.45am before artificial lighting commenced,
- after artificial lighting was switched on at 4.00am
- after artificial lighting commenced at 4.00am, and,
- before and after 7.00am when the birds are fed.

Measurements were also taken at the study site, adjacent to the farms where the birds are currently yet to reach maturity and their maximum noise emission level, and also adjacent to the effluent treatment dam, which has aerator units and is adjacent to the fence adjoining the proposed residential development site. The results of the 24 hour sampling are graphed in Figure 1.

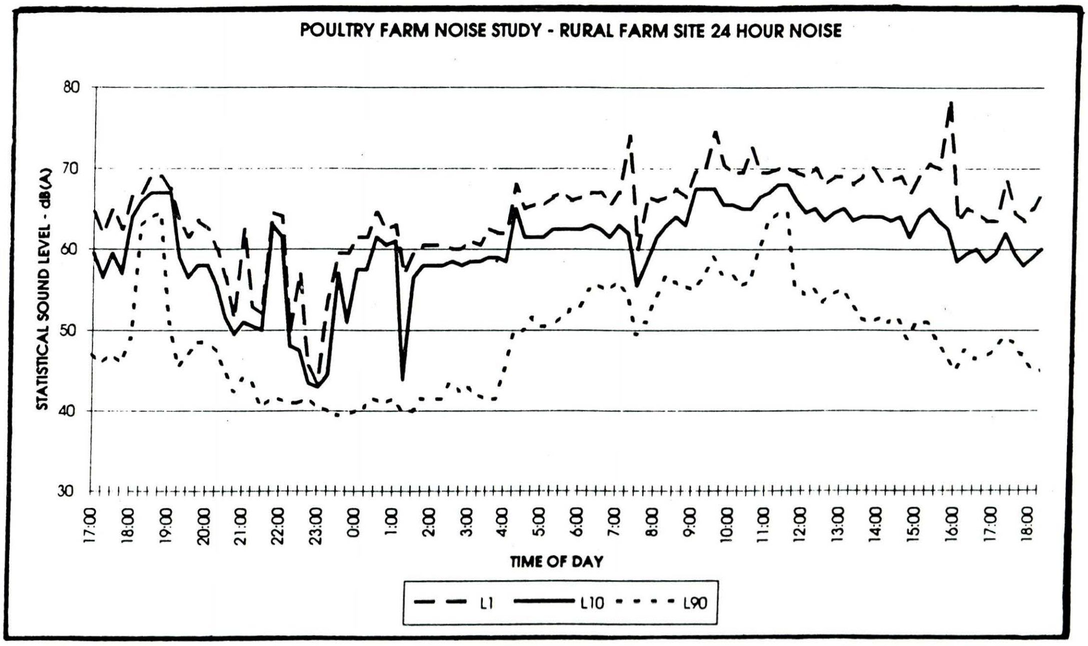

Figure 1: Results of the 24 hour statistical sound level measurements at the rural farm site

The results indicated that the sound levels at distances of 15 m from the sheds with mature birds, have LA90 sound levels of 50 to 59 dB(A) , and LA10's of 55 to 68 dB(A) whilst the birds are active. In the morning when the lights are switched on, the sound levels increase by 12 dB(A) initially, but this reduces to about 9 dB(A) increase above the "dark" sound levels within about 15 minutes. The characteristics of the noise include regular and frequent rooster crowing as the maximum and LA01 sound levels occurring, hen cackling and typical poultry laying noises. It could be considered to have potentially annoying characteristics.

The sound levels at the property boundary at the study site, adjacent to the effluent pond aerators is 60 dB(A). The characteristics of the noise are constant, broad-band water splashing noise.

The results of the 24 hour sampling show the variation of the sound levels over the day and night. It can be seen in Figure 1 that the night sound levels were about 40dB(A) at their lowest from about 11.00pm to 2.00am in the morning. After this, they increased to around 55 dB(A) over the middle of the day. The brief periods of high sound levels around 6.30pm and 11.30am may be associated with feed truck deliveries or passing vehicles from the farms at these times.

DISCUSSION

The noise sources associated with the operation of the multiplication farms are principally those associated with the activities of the birds:

- rooster crowing;
- hen cackling and laying noise; and,
- general poultry bird noises.

Other noise sources include the feed distribution system, which are auger driven and relatively low level in comparison to the birds, equipment operation around the sites, such as tractors, mowers and vehicles, and feed trucks. The feed trucks have an air compressor aboard to pneumatically convey the feed to the storage silos. The vehicle measured was typical of others used, and had a sound level of 93 dB(A) at 7m.

The location of the proposed residential development at the study site would have potentially placed the boundary of residential properties within 8 metres of the sheds of the farms. From the measurements taken, the sound levels in the proposed residential properties could have the same sound levels as those given in Figure 1. That is, background sound levels of 50 to 60 dB(A) from the time the shed lights are switched on, which can be from 3.00am in the summer months. Such levels are 15 to 25 dB(A) above the recommended EPA objective sound levels for residential areas, not considering the characteristics of the noise. As the bird noise is considered to be potentially annoying, the exceedance of the objectives is 20 to 30 dB(A). This exceedance is very significant from a **potential for noise annoyance** viewpoint.

The noise levels from the aerators on the effluent treatment pond would be 60 dB(A), again 15 to 25 dB(A) above the EPA objectives.

For a new industrial or commercial receiver, the EPA recommend (and generally require) that the new development should not cause an increase in the sound level of more than 5 dB(A) above the recommended level. In this case the guidelines noted earlier would indicate that a residential development in an area where the existing sound levels is up to 30 dB(A) above acceptable levels should not be considered by town planners in their assessment of land suitable for residential development.

The measurements taken at increasing distances from the rural farm sheds indicate that the reduction in sound level with increasing distance is similar to that of a “line source” of noise. This is because the sheds have a long side from which noise is emitted along the full length.

This information can be used to assess the distance at which the sound levels from the sheds would have been reduced to the acceptable range. Assuming a source sound level of 55 dB(A) at 15m as the centre of the range, the distance required to achieve a sound level of 35 dB(A) would be about 500 metres.

In April 1994, the NSW Department of Agriculture released the draft "New South Wales Poultry Farming Guidelines". This document was developed to assist the poultry industry and the many other bodies and individuals which relate to it to better understand the factors which, if effectively applied and managed will decrease the risk of conflict between the industry and urban dwellers and minimise environmental pollution. This document recommends separation distances between poultry sheds and an urban residential zone of 500 metres. This is in agreement with the distance calculated above for the study site.

For the aerators, which can be considered as a point source, the distance required to achieve 35 dB(A) is also about 500 metres.

The nature of the noise history of a multiplication poultry shed also needs to be considered. At the completion of the normal 60 week life of a group of hens, the sheds are emptied and cleaned out over a 10 to 12 week period. The young and immature birds are then placed in the sheds. They do not make much noise at all until they reach an age of about 20 weeks. This gives a 26 to 30 week period when there is effectively no noise emission from the site. After this the sound level increases to the levels measured and reported in this document. Such a change in sound levels involves a significant increase in annoyance potential for any residential receivers and would add further to the noise annoyance which would occur in the proposed residential subdivision at the study site.

Such characteristics of the time history, nature of the noise and the exceedance of the accepted EPA objectives would guarantee that noise annoyance would occur in residential receivers exposed to the sound levels of 50 to 60 dB(A) noted above.

Similar considerations could apply to industries which have relocated to outer urban fringe areas from inner urban areas. The relocations were often to obtain a larger area with a reduced potential for noise annoyance. Indeed, industrial zoned land and estates were established in many outer urban municipalities for this purpose over 20 years ago. Yet in some of these areas, urban development has approached the boundaries and is again imposing residential area noise objectives on industrial, commercial and rural activities.

In considering the amenity value or potential of land, it is just as important for town-planners and Councils to consider the potential effects of new residential development on existing industries, as it is to consider the effects of new industrial development on existing or proposed residential areas. Competent planning can allow acceptable co-existence of residential areas with industrial/commercial/rural activities by the appropriate location of the various land-uses.

CONCLUSION

Sound levels were measured at poultry multiplication sheds to determine the noise emission and potential sound levels at a proposed residential development adjoining the property.

The EPA recommend an objective outdoor sound level at residential receivers of 35 dB(A) at night-time. The EPA also recommend that the goals of the town planner in regard to noise should be to control the establishment of new residential areas in the vicinity of existing or planned industrial or commercial complexes, taking account of present or future background noise levels in relation to environmental noise policies.

The measurements indicate that the sound levels could be up to 30 dB(A) above the recommended EPA objectives for outdoor noise in residential receiver areas. This is a very significant exceedance of the objectives and noise annoyance in residential receivers could be guaranteed to occur at these levels.

The distances required to achieve acceptable sound levels from the site has been calculated to be approximately 500 metres. This is in agreement with recommended distances of the NSW Department of Agriculture.

Given the associated environmental issues of odour from the sheds and effluent treatment ponds, it was recommended that local Council consider the proposed residential development site incorporate a buffer zone of approximately 500m between the residential boundaries and the boundary of the site.

Similar considerations should occur with all proposed residential land developments, as occurs with industrial and commercial developments, to maintain amenity for all land users.

Acknowledgments:

The author wishes to thank BHP for permission to use the information contained within the report. The opinions expressed within the report are those of the author and do not necessarily represent those of BHP.

COPING WITH DIFFICULT ACOUSTICAL INVESTIGATIONS

CALEB SMITH MAAS MASA
Principal Consultant
Caleb Smith Consulting Pty Ltd
Acoustical Engineers
Toronto NSW

ABSTRACT

Acoustical investigations are usually given to consultants for one of two reasons. The client does not have the expertise nor the time to undertake the task, OR, the Authorities require a recognised, independent, acoustical consultant to carry out the task and report the results.

Many recognised Acoustical Consultants are Mechanical Engineers with work experience in industry, where their practical skills and ingenuity have enabled problems to be solved on the run. In the same context, experienced Acoustical Engineers can quickly see, hear, feel and assess noise and vibration problems through their eyes, ears and the tips of their fingers, and direct the necessary resources towards correction of the problem.

It may be necessary to quantify the situation with sophisticated instrumentation, however, many noise and vibration problems encountered in industry require more, or is it less, than the sophisticated analysis programmes presently available for many thousands of dollars. Common sense and background knowledge are equally as important.

I propose to describe several situations where the experienced Acoustical Engineer can save his client time and money by knowing how to get on with the job from a standing start.

INTRODUCTION

The subject of my paper today was prompted by an unusual project given to us earlier this year. This was a project where the cause and effect were not expected. A house was vibrating due to the passage of trains nearby. Earlier investigations had shown there were no significant ground-borne vibrations under or near the dwelling during the passage of trains on nearby tracks and therefore the dwelling should not be vibrating on these occasions.

Nevertheless, persistent and vigorous complaints by the resident to the SRA (State Rail Authority) indicated the presence of a problem that required further investigation.

Our investigation required the measurement of vibration of the dwelling, its magnitude in terms of possible damage and proof that such possible damage was caused by the passage of trains on the nearby tracks.

SITUATION

The residence under investigation is situated at 29 Wentworth Street, Telerah, a satellite suburb west of Maitland, NSW. The dwelling is located about 130 metres from and in clear view of the Great Northern Railway, a dual track system serving the north western country and coal mining areas of the State. Other residential dwellings located in the area are similarly exposed to the passage of trains, some with facades in the order of 85 metres from the tracks.

The subject residence is approximately 80 years old and, like most others in the locality, is of timber frame construction on piers increasing in height up to one metre towards the front. The piers of this dwelling are of brick and of recent construction provided by the SRA to overcome settlement problems and, hopefully, the vibration problem. It didn't.

The dwelling has a set of steps of monolithic construction for access to a front verandah. The dwelling and the steps have no direct connection. The verandah has a door and open framing in lieu of windows. The remainder of the framing is clad with fibre cement sheets. The dwelling itself has a front facade with central door access to the hallway. A sash window for the front rooms of the dwelling is located in the front facade each side of the door.

METHOD OF INVESTIGATION

A preliminary investigation of the vibration problem was undertaken during December 1993 when acoustical and vibration instruments were set up within the particular residence to record sound and vibration levels during night time hours when other causes are unlikely to occur. The timing of the sound and vibration measurements recorded during the night were found to correlate with the trains scheduled to run at those times.

From these results, a detailed investigation was planned to quantify the sound and vibration levels in relation to specific trains, loco types, wagon types, speeds, direction and other related matters, with the object of clearly establishing the cause of the vibration. Further, the quantified levels of vibration and noise were to be rated against established damage criteria.

The following programme of monitoring was prepared and carried out over 24 hours from 5:00pm Monday 28th March. The SRA would provide a complete schedule of trains for the period and from 7:30am Tuesday a Supervisor would advise a description of the train, its direction, speed, load and wagon type while sound and vibration recordings were undertaken.

Instrumentation

To capture as much information as possible for subsequent analysis, vibration and sound monitors were set up in the dwelling and on the street away from the dwelling. Vibration monitors were also used on a random basis to record the vibration in the ground around the dwelling, on the street in front of the house and on the ground 30 metres from the tracks during the passage of trains. A schematic arrangement of the instrument train is shown in Figure 1.

Instruments included an Etna 8 Vibration Monitor with its geophone wedged between the window and the sill in the front wall of the dwelling to measure the level and frequency of the vibration. A second geophone was placed in a similar position and coupled to a B&K Level Recorder Type 2306 via a B&K Sound Level Meter Type 2209, to provide amplification of the geophone signal. Two data loggers were set to operate on the verandah of the dwelling, one set to the Linear mode and the other to the 'A' Scale weighting. The difference in the two readings would indicate the extent of low frequency sound pressure and a possible reason for vibration of the dwelling.

On the street front, being serviced from a caravan, we set up a professional video recorder and two B&K Sound Level Microphones with extension cables connected to B&K Sound Level Meters Type 2209. One Meter was set to the 'A' Scale weighting network and the other to the 'C' Scale weighting. Each Sound Level Meter was coupled to a Sony Cassette Recorder Type WMD6C. All instruments were operated from 240 volt mains power with reducing transformers.

Two additional battery powered data loggers were set up on the street frontage set to the 'A' Scale and Linear networks. The two sets of monitors would show any significant difference in the readings between those in the dwelling and those on the street front.

Further sound level measurements were recorded from a railway overbridge in proximity to site. These measurements provided the sound emission from the locomotive exhaust, radiator fans and the wagons of the passing trains.

RESULTS

The results of our sound and vibration level measurements are shown in the following Tables which display the lead loco number, direction, wagon type, and load. Vibration measurements are given in mm/second velocity with peak and average readings taken from the level recording chart together with the vibration duration in seconds. In order to give a meaningful quantity to the level and duration of the vibration being recorded and experienced in the window wall of the dwelling, we multiplied the average vibration velocity by its duration time to give a 'Vibration Rating'. This value is also displayed in the Table followed by the vibrating frequency as registered by the Etna 8 vibration monitor.

Table 1 has been rearranged from the original, which gave the results in chronological order, to display the results in Rank Order of Vibration Rating, commencing with the highest value.

TABLE 1

RESULTS OF RAILWAY INDUCED VIBRATION

Lead Loco Nº	Dir'n	Wagons		Speed km/hr	Wall Vibration Velocity mm/sec				
		Type	Load		Peaks	Avg.	Dur'n	Rating	Hz
8129	Dn	New	MT	35	1.1	0.9	110	99	24
8131	Dn	New	MT	40	1.7	1.1	77	97.4	25
8105	Dn	Old	MT	40	1.2	0.8	115	92	26
8141	Dn	New	MT	30	1.0	0.65	130	84.5	23
8101	Dn	Old	MT	36	1.25	0.6	120	72	25
8119#	Dn	Old	MT	40	2.3	0.6	100	60	25
8111	Up	Old	C	31	0.75	0.45	90	40	20
48158	Up	Old	Wt	20	1.1	0.5	60	34	29
8158	Dn	Old	MT	--	1.0	0.65	50	35	25
4868	Dn	New	MT	40	1.45	0.9	35	31.5	25
8117	Dn	Old	MT	25	0.6	0.3	90	27	27
8133	Dn	Old	MT	40	0.6	0.4	65	26	27
4401*	Dn	Old	MT	35	0.55	0.4	60	24	23
8148	Up	New	C	45	0.5	0.15	100	15	17
8119	Up	Old	Wt	55	1.7	1.7	2.5	4.25	10
8105*	Up	Old	C	45	0.8	0.3	6	3.6	25
44219	Up	Old	Wt	35	0.8	0.7	5	3.5	8
48152*	Up	Old	Wt	30	0.5	0.2	4	1.6	11
8136*	Up	Old	C	25	0.3	0.2	4	1.6	50
8136	Dn	Old	MT	30	0.6	0.6	2.5	1.5	25
8131	Up	New	C	54	0.85	0.15	5	0.75	23
8137*	Up	Old	C	45	0.3	0.3	2	0.6	19
8103	Dn	LOCO	ONLY	40	0.1	0.2	2.5	0.5	27
8103	Up	Old	C	36	0.5	0.2	2	0.4	26
XPT	Dn	--	--	80	0.3	0.05	4	0.2	4
XPT	Up	--	--	81	0.3	0.2	--	0.2	11
48111	Up	Old	C	60	0.25	0.1	1	0.1	-

Legend:

* = Wheel Defects
# = Shunt / Stop
MT = Empty
Wt = Wheat
C = Coal

Table ll has similar information to that displayed in Table l with the inclusion of ground vibration levels taken at various positions in relation to the dwelling and the railway tracks.

TABLE II

RESULTS OF RAILWAY INDUCED GROUND VIBRATION

Lead Loco Nº	Dir'n	Wagons		Speed km/hr	Wall Vibn Velocity mm/s			Ground Vibration	Notes
		Type	Load		Peaks	Avg.	Dur'n		
8129	Dn	New	MT	35	1.1	0.9	110	0.019	6
8131	Dn	New	MT	40	1.7	1.1	77	0.038	1
8105	Dn	Old	MT	40	1.2	0.8	115	--	--
8141	Dn	New	MT	30	1.0	0.65	130	0.125	4
8101	Dn	Old	MT	36	1.25	0.6	120	0.128	3
8119#	Dn	Old	MT	40	2.3	0.6	100	0.159	4
8111	Up	Old	C	31	0.75	0.45	90	0.6	3
48158	Up	Old	Wt	20	1.1	0.5	60	0.141	4
8158	Dn	Old	MT	--	1.0	0.65	50	0.152	4
4868	Dn	New	MT	40	1.45	0.9	35	0.072	5
8117	Dn	Old	MT	25	0.6	0.3	90	0.00	6
8133	Dn	Old	MT	40	0.6	0.4	65	0.023	5
4401*	Dn	Old	MT	35	0.55	0.4	60	0.218	4
8148	Up	New	C	45	0.5	0.15	100	0.206	4
8119	Up	Old	Wt	55	1.7	1.7	2.5	--	--
8105*	Up	Old	C	45	0.8	0.3	6	0.151	4
44219	Up	Old	Wt	35	0.8	0.7	5	0.083	2
48152*	Up	Old	Wt	30	0.5	0.2	4	0.8	4
8136*	Up	Old	C	25	0.3	0.2	4	0.136	4
8136	Dn	Old	MT	30	0.6	0.6	2.5	0.187	2
8131	Up	New	C	54	0.85	0.15	5	0.031	6
8137*	Up	Old	C	45	0.3	0.3	2	0.265	4
8103	Dn	LOCO	ONLY	40	0.1	0.2	2.5	0.040	3
8103	Up	Old	C	36	0.5	0.2	2	0.155	7
XPT	Dn	--	--	80	0.3	0.05	4	0.237	4
XPT	Up	--	--	81	0.3	0.2	--	--	--
48111	Up	Old	C	60	0.25	0.1	1	0.199	4

Legend:

1. Bottom step to verandah
2. Verandah, house doorway
3. Verandah, top step
4. Railway Street 30m to tracks
5. Roadside Kerb at 29 Wentworth Street
6. Roadside Kerb opposite 29 Wentworth Street.
7. Top Step to verandah (Ground Based)

* Wheel Defects

\# Shunt / Stop

Table lll displays the vibration levels and frequency readings with the Damage Scale taken from the vibrar unit of intensity as displayed in the chart Figure 2.

TABLE lll

RESULTS OF RAILWAY INDUCED VIBRATION AND DAMAGE CRITERIA

Train Set Lead Loco	Peak Vibn Vel mm/sec	Average Vibn Vel	Frequency (Hz)	Amplitude Microns Peak	Amplitude Microns Avg	Vibrar Damage
8129	1.1	0.9	24	6.5	6	17
8131	1.7	1.1	25	10	6.5	22
8105	1.2	0.8	26	6.6	5.5	18
8141	1.0	0.65	23	7	4.5	29
8101	1.25	0.6	25	7	4	20
8119	2.3	0.6	25	15	4	27
8111	0.75	0.45	20	6	4	15
48158	1.1	0.5	29	5	< 4	20
8158	1.0	0.65	25	6.5	4	18
4868	1.45	0.9	25	8.5	6	20
8117	0.6	0.3	27	4	2	16
8133	0.6	0.4	27	4	2.5	16
4401	0.55	0.4	23	4	3	15
8148	0.5	0.15	17	5	2	12
8119	1.7	1.7	10	10	10	12
8105	0.8	0.3	25	5	2.5	17
44219	0.8	0.7	8	11	9	10
48152	0.5	0.2	11	8	4	10
8136	0.3	0.2	50	1	< 1	12
8136	0.6	0.6	25	4	4	10
8131	0.85	0.15	23	5	1	11
8137	0.3	0.3	19	3	3	10
8103	0.1	0.2	27	1	1.1	5
8103	0.5	0.2	26	3	1.2	12
XFT	0.3	0.05	4	10	1	3
XPT	0.3	0.2	11	5	3	5
48111	0.25	0.1	(25)	1.5	7	7

* See Appendix D
(25) Typical

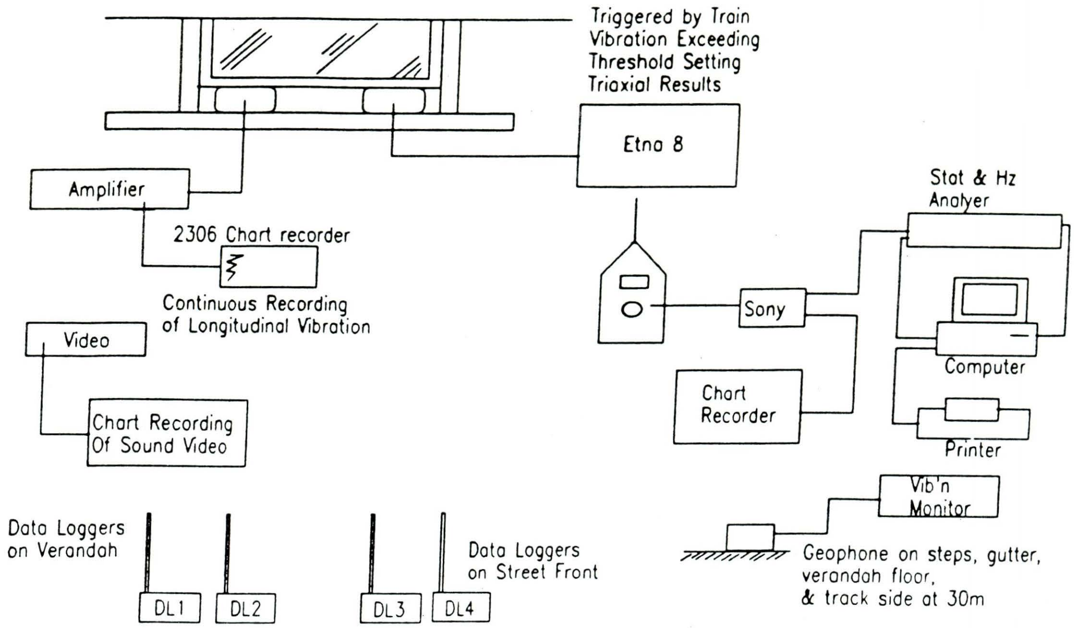

Fig. 1 - SCHEMATIC ARRANGEMENT OF INSTRUMENTS

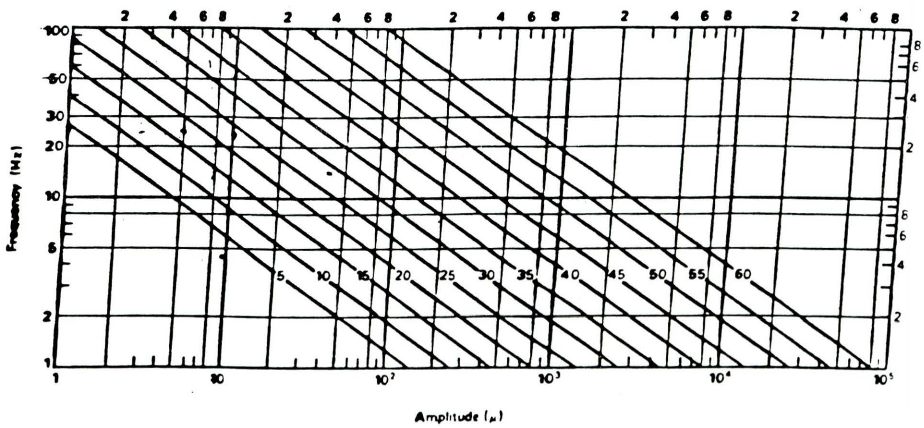

Strength (vibar)	Possible Damage
Below 30	No structural Damage
30–40	Light damage (For example cracking in rendering or plaster)
40–50	Severe damage (For example cracks in load bearing walls)
50–60	Destruction of building

Fig. 2 - THE VIBRAR UNIT OF VIBRATION INTENSITY AND ASSESSMENT OF POSSIBLE DAMAGE.

FINDINGS

The vibration levels measured in the front wall of the dwelling as generated by the passage of trains through the area and displayed in Tables l, ll and lll above, are clear but are not of a magnitude likely to cause any possibility of damage.

Of clear significance however, is that empty, down running, coal trains with 81 Class locomotives and either old or new wagons are the primary cause of the vibration at the dwelling, a vibration which is not ground borne. Conversely, the least troublesome vibration is due to up running, loaded freight and passenger trains.

On the basis of our findings, the most obvious conclusion is that vibration of the dwelling is air borne. In fact, the trouble–some vibration must occur more often than the frequency of empty, down running coal trains, due to wind velocity from a particular direction swirling around the building. Subsequent enquiries of the resident in this regard have revealed the vibration problem is exacerbated in windy weather, and is amplified by the frequent passing of down running, empty coal trains.

There appears to be only one basic cause of this vibration problem. Pulses of exhaust gas from the locomotive trigger the vibration which is then maintained by pulses of energy emanating from the open empty coal wagon's drummed by minute imperfections during the rolling interaction between wheel and rail.

While further investigations will be required to decide what action is to be taken to overcome this particular vibration problem, sufficient proof of these basic causes is found in the measured sound level results taken at both the railway overbridge and at the dwelling.

In studying these results we find the Inverse Square Law (ISL) propagation loss of 6dB per doubling of distance from locomotive 8101, having a linear sound pressure level (L1) of 150 dB at 0.5 metres, Fig 3, page 9, agrees with the measured result of 102 dB linear (Lmax) at the dwelling at 130 metres, as shown in Fig 4, page 9 .

Similarly, the propagation loss of 3 dB per doubling of distance from the line of wagons drawn by locomotive 8101 having a linear sound pressure level of 121 dB (L90) at 0.5 metres, as shown in Fig 5, page 9 , agrees with the measured result of 96 dB (L10) at the residence as shown in Fig 4.

Taking these sound levels further in relation to the possibility of damage to the dwelling, we find a dynamic pressure of 2.5 pa for the 102 dB linear measurement at the dwelling. This pressure would result from a breeze of 7 km per hour, whereas our complainant is claiming damage to his property due to the passing of trains. Even if the linear sound pressure level reached 120 dB with a dynamic pressure of 20 pascals, the equivalent wind velocity would be 21 km per hour and a more likely cause of damage to the dwelling rather than the trains.

Freq (Hz)	Leq	Lmax	L1	L10	L90
63	135.2	144.4	143.6	138.8	126.4
125	131.9	143.5	141.9	135.9	117.5
250	128.4	139.2	138	133.2	112
500	125.4	139	135.4	129.4	107.4
1000	122.2	134.6	134.6	126.6	103.8
2000	127.4	142.6	140.2	131.8	104.2
4000	128	140.8	139.2	133.2	107.6
8000	121.1	133.9	133.5	124.3	109.5
dB(Lin)	**139**	**150**	**149**	**143**	**127**

Fig.3 Locomotive at Overbridge

Freq (Hz)	Leq	Lmax	L1	L10	L90
63	89.8	101.4	99.8	96.2	67.4
125	72.2	83.4	80.6	78.2	57.8
250	58.4	70.4	66	62.8	51.6
500	51.2	66.8	58.4	53.6	46.8
1000	45.4	59.8	51.8	46.6	43.8
2000	43.2	62	47.6	44.4	40.4
4000	39.6	53.6	44.4	40.8	38.4
8000	42.8	50	44.8	43.2	42.4
dB(Lin)	**90**	**102**	**100**	**96**	**68**

Fig.4 Locomotive at Residence

Freq (Hz)	Leq	Lmax	L1	L10	L90
63	121.2	133.6	127.6	123.6	117.6
125	119.1	130.3	125.5	121.9	115.1
250	114.4	123.6	120.8	117.2	110.8
500	109.8	119	115.8	112.2	106.2
1000	105.8	117.4	112.2	108.6	101.8
2000	107.8	123.4	115.4	110.6	103
4000	106	120.4	114.4	109.2	100.8
8000	96.7	107.1	105.1	99.5	91.9
dB(Lin)	**124**	**136**	**131**	**127**	**121**

Fig.5 Wagons at Overbridge

NOISE AND VIBRATION RESULTS - LOCOMOTIVE - WAGON SET 8101

CONCLUSION

The purpose of this paper is to present the results of an investigation into the cause of vibration in a residential dwelling situated 130 metres from a railway line on which passed loaded and empty coal wagons hauled by 81 Class locomotives.

The investigation quickly revealed insignificant ground borne vibration levels between the track and the dwelling, which left an intriguing quandary as to the cause of the vibration. Continued investigations revealed the most probable cause to be the exhaust of the locomotive followed by driving pulsations from the open, empty coal wagons running past the dwelling on the down line.

The investigation found no cause against the SRA for the damage claimed by the resident.

TRANSPORTATION NOISE

ROAD TRAFFIC NOISE: THE EXTENT OF THE NATIONAL PROBLEM

A L BROWN

Australian School of Environmental Studies
Griffith University, Nathan 4111, Australia

SUMMARY

The results in this paper provide, for the first time, a definitive estimate of the state of the environment in Australia with respect to road traffic noise. Brown and Cliff (1988) reviewed previous attempts at exposure estimates in Australia, and their conclusion was that there was a need for caution as none of the studies provided information on the likely errors associated with the estimates. The present study shows that nearly one in ten dwellings in Australian urban centres is exposed to an $L_{A10,18h}$ level of 68 dB or greater. These traffic noise "black spots" tend to be located at close distances to roadways, and the inter-quartile range of traffic volumes on these roadways is 11 000 to 25 000 vehicles per day. This component of the road traffic noise problem in Australia, high exposure of existing dwellings located on arterial, subarterials and even lesser roadways, is not being actively addressed by current policy instruments.

THE STUDY

Full details of the methodology used in this study are reported in Brown (1993). In brief, it included drawing a random sample of dwellings from Australian urban centres and subsequent estimation of road traffic noise exposure at each element of this sample. Specific steps of the study were:

- rigorous selection of a sample drawn randomly from the population of Australian dwellings
- site visits to each element of the sample to determine source roadways(s) and measurement of appropriate geometric parameters
- collection of traffic data for all source roadways
- prediction of noise levels at each site.

The study has similarities to the UK and French studies of national traffic noise exposure (Harland and Abbott 1977; Maurin 1984), but used traffic noise *prediction* at individual dwellings, rather than traffic noise *measurement*. There are two sources of error in estimating traffic noise exposure of a population: sampling error and error in noise level estimate. Considerable tolerance is acceptable in the latter because noise level estimate error tends to be random, not systematic, and this has little effect on the estimate of exposure of the *population* (of course, it does affect the estimate of exposure at any *individual* site but knowledge of the noise exposure at any individual site was not of concern in this study). Limited study resources are better expended in reducing sampling error by increased sample size and by reduction in bias through rigid enforcement of a random sampling regime, than they are in attempting to obtain a non-essential reduction in the magnitude of noise level estimate error by substituting measurement for prediction. By appropriate allocation of resources in this way, reliable Australian noise exposure estimates have been obtained for a sum of money probably no more than one twentieth, or less, of the cost of obtaining equivalent results in the European studies.

SAMPLE SELECTION

The study was limited to centres with populations greater than 100 000. This included the eleven largest Australian cities, covering 62% of the Australian population and 79% of the Australian urban population. The Kolmogorov test statistic can be used to determine confidence limits to sample estimates of a population distribution (Conover 1980), and it was estimated that a sample size of about 500 would be required to ensure that an acceptable confidence band would apply over *the complete range* of noise level exposures. However in practice it is estimates of the percentage of dwellings exposed to levels *above particular critical values* of noise exposure that are of interest, rather than estimates over the *complete range* of noise level exposures, and a smaller sample size is adequate for this purpose. The sample size used was 264 dwellings, drawn randomly from the population of dwellings in Australia. This can be compared with the sample sizes of 271 used in the UK survey of national noise exposure, and 314 used in the French survey.

The sample was stratified across the eleven urban centres in the study population (3 565 097 dwellings) as shown in Table I. The sample size was selected to determine the road traffic noise exposure of the *national population*, not the exposure of the *population in individual urban centres*.

TABLE I

SAMPLING ACROSS AUSTRALIAN URBAN CENTRES

CITY	URBAN CENTRE POPULATION	NUMBER OF DWELLINGS	% OF TOTAL DWELLINGS	SUB SAMPLE
Sydney	2,989,070	1,083,775	30	80
Melbourne	2,645,484	982,248	28	72
Brisbane	1,037,815	377,885	11	28
Adelaide	917,000	350,339	10	26
Perth	864,223	333,507	9	25
Newcastle	255,787	97,092	3	7
Canberra	238,138	84,144	2	7
Wollongong	206,803	73,969	2	6
Gold Coast	185,612	87,191	2	6
Hobart	127,105	48,628	1	4
Geelong	125,883	46,319	1	3
TOTAL	9,592,921	3,565,097	100	264

The acquisition of a truly random sample of dwellings (street addresses) within each subsample was a difficult task and required a large part of the resources of this study. The practical difficulty was to obtain a sampling frame from which a random sample of street addresses could be drawn. Various candidate data bases were considered (for example, electricity connections) but had to be rejected, usually because they were not accessible because of confidentiality requirements. The eventual solution was found through linking two data sets, each of which provided part of the required information. These were the Australian Bureau of Statistics (ABS) population and dwelling census information, and the Australian Electoral Office (AEO) lists of Australian street addresses called Habitation Walks (HWs). Full details of the construction of the sampling frame, sampling from it, and field procedures at each element of the sample, are described in Brown (1993).

The sampling scheme ensured that every Australian dwelling in a Major Urban Centre, irrespective of whether it was a detached dwelling, a duplex, terrace house, unit, flat or apartment, had an equal chance of inclusion.

NOISE LEVEL ESTIMATES

Each of the 264 sites in the eleven urban centres was visited by a member of the study team. Geometric data was obtained by field inspection and traffic data was obtained from available records or by field measurement. A total of 375 traffic records were required for the 264 sites. The Great Britain Department of Transport (1988) procedure was used to predict the $L_{A10,18h\,(0600\text{-}2400)}$ at one metre from the facade of the most exposed window of the dwelling, and at window height.

There was no prior assumption, as has been made in previous studies of traffic noise exposure, that the road traffic noise level at the sampled dwelling would be generated solely by traffic on the roadway abutting the property. Field inspection determined whether the dominant source of traffic noise was the abutting roadway, or some more distant roadway, or some combination of both. The survey found that the source of traffic noise was the fronting roadway for 33% of dwellings, a "distant" roadway other than the roadway abutting the property for 26% of dwellings, and a combination of both distant and abutting roadways for 8% of dwellings. Noise levels were too low to predict at 33% of dwellings and these are reported in the group of dwellings whose noise exposure is "40 dB or less".

RESULTS

SAMPLING ESTIMATES

How well do the sample measurements reported here represent the exposure of the Australian population? Confidence intervals for population proportions in this study have been calculated (Zar, 1984) and are shown in Table II. The confidence limits depend on the magnitude of the sample proportion, but all are regarded as acceptable for the purposes of this study. For example, the next section shows that near 10% of dwellings *in the sample* were exposed to an $L_{A10,18h}$ level of greater than 67 dB. We can assume that the same proportion applies in the Australian *population* of dwellings, but Table II shows that the confidence interval for this estimate is 6.5% to 14.4% ($p < .05$). Estimates of population proportions are possible because of the use of the rigorous random sampling protocol in the selection of the Australia-wide sample.

TABLE II

CONFIDENCE ESTIMATES ($p < .05$) OF THE POPULATION PROPORTION FOR A RANGE OF MEASURED SAMPLE PROPORTIONS

Measured Sample Proportion	Estimated Population Proportion	
	Confidence Limits	Confidence Interval
1%	-0.8/+2.1	0.3% to 3.1%
5%	-2.3/+3.4	2.7% to 8.4%
10%	-3.5/+4.4	6.5% to 14.4%
25%	-5.7/+6.0	19.3% to 31.0%
50%	-6.3/+6.3	43.7% to 56.3%
75%	-6.0/+5.7	69.0% to 80.7%
90%	-4.4/+3.5	85.6% to 93.5%

EXPOSURE OF THE POPULATION OF AUSTRALIAN DWELLINGS

The specific objective of this study was to determine the road traffic noise exposure of the *national population*, and this result is shown in Figure 1(a). Over 9% of the Australian population are exposed to $L_{A10,18h}$ of 68 dB or above and 19% of the population are exposed to $L_{A10,18h}$ of 63 dB or above. Some half of the population is exposed to levels greater than 52 dB, and one third to levels of 40 dB or less. The results show that while a majority of the population live in quiet conditions, unacceptably high proportions of the Australian population are exposed to levels which are universally regarded as inappropriate for residential use.

What are the traffic conditions and locational factors for those dwellings which have high traffic noise exposure? Borrowing from an OECD (1991) classification, we can categorise dwelling exposure into four noise bands - "black spots", "grey areas" and two low exposure categories. Table III shows the differences between categories and these are also shown in Figure 2. Some 88% of black spot dwellings are subject to noise from the roadway abutting the dwelling, though 12% of them are subject to noise from a more distant roadway. The common factor for all these dwellings is their close proximity to the roadway source (median distance 14 metres). Traffic volumes on the source roadways in these black spots are not exceptionally high (median 16 395 vehicles per day) and it is a reasonable assumption that they are not dwellings located beside freeways, but instead are located near arterial roadways or even, given the relatively low traffic volumes, what might better be called subarterial roadways. While 60% of dwellings in black spots are subject to noise from roadways of four or more lanes, 40% of them are beside 2 lane roadways. By far the greatest expenditure of money and effort on road traffic noise in Australia has gone into the control of noise from urban freeways and similar, with few policies or action programmes in place for these dwellings in Australia's traffic noise black spots.

Dwellings located in grey areas are generally different to those in black spots only in terms of being near roadways of considerably lower traffic volumes (median 3831 vehicles per day), and more of them (25%) are subject to noise from a more distant roadway rather than the one abutting the property. Source roadways in grey areas are predominantly two lane roadways.

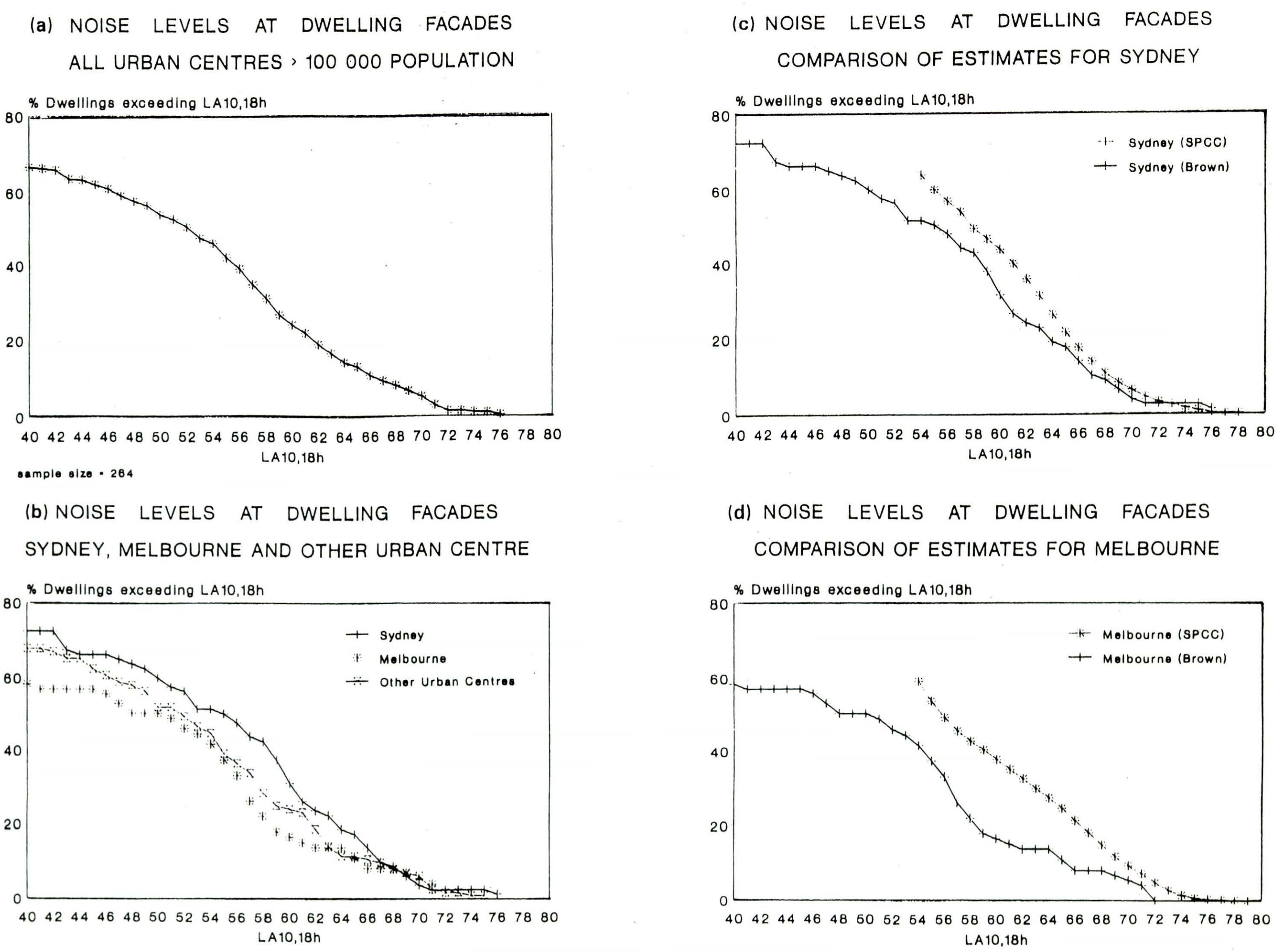
(a) NOISE LEVELS AT DWELLING FACADES
ALL URBAN CENTRES › 100 000 POPULATION
% Dwellings exceeding LA10,18h
80
60
40
20
0
40 42 44 46 48 50 52 54 56 58 60 62 64 66 68 70 72 74 76 78 80
LA10,18h
sample size - 264
(b) NOISE LEVELS AT DWELLING FACADES
SYDNEY, MELBOURNE AND OTHER URBAN CENTRE
% Dwellings exceeding LA10,18h
Sydney
Melbourne
Other Urban Centres
LA10,18h
(c) NOISE LEVELS AT DWELLING FACADES
COMPARISON OF ESTIMATES FOR SYDNEY
% Dwellings exceeding LA10,18h
Sydney (SPCC)
Sydney (Brown)
LA10,18h
(d) NOISE LEVELS AT DWELLING FACADES
COMPARISON OF ESTIMATES FOR MELBOURNE
% Dwellings exceeding LA10,18h
Melbourne (SPCC)
Melbourne (Brown)
LA10,18h

Figure 1

TABLE III
PROFILES OF DWELLING OF DIFFERENT NOISE EXPOSURE CATEGORY

	LA10,18h	<40	40-57	58-67 Grey Areas	≥68 Black Spots
Sample Proportion:					
	%	33.0	34.8	22.7	9.5
Noise Source:					
Fronting Roadway	%	0.0	35.9	75.0	88.0
Distant Roadway	%	3.4	64.1	25.0	12.0
Out of range of prediction model	%	96.6	0.0	0.0	0.0
Noise Source Roadway Type:					
Cul-de-sac	%	24.1	0.0	1.7	0.0
1 or 2-Lanes	%	75.9	83.7	80.0	40.0
4-Lanes +	%	0.0	16.3	18.3	60.0
Distance to Noise Source Roadway:					
Median	m	13.2	58.5	15.3	14.0
First Quartile	m	11.7	22.7	11.5	11.2
Third Quartile	m	19.5	109.5	38.5	16.6
Traffic Volume on Noise Source Roadway:					
Median	veh/d	200	4795	3831	16395
First Quartile	veh/d	100	1336	1927	11326
Third Quartile	veh/d	350	11647	16171	25291
Minimum	veh/d	10	700	920	6992
Maximum	veh/d	5051	80000	70597	39000

Dwellings in the 40-57 dB category tend to be located considerably greater distances from the roadways and these roadways tend to carry traffic flows somewhat higher than those affecting dwellings located in grey areas.

In Figure 2 it can be seen that black spot dwellings are fairly tightly grouped by moderate to high traffic volume and close distance to the roadway, but dwellings in grey areas are characterised by a varied combination of these factors, either very high traffic volume at large distances, or quite low traffic volumes at very close distances. Of course factors other than traffic volume and distance affect traffic noise exposure (angle of view of the roadway in particular) and this accounts for overlap in the categories shown in Figure 2.

Brown and Lam (1994) have noted that the proportion of Australian multiple dwelling units located in black spots and grey areas is much higher that of separate houses.

EXPOSURE IN INDIVIDUAL CITIES

This study was not designed to compare exposures in different cities because the sample size was determined on the basis of estimating national exposure. However, limited comparisons are possible though confidence limits of the estimates are wide. Figure 1(b) compares the cumulative exposures for three subsamples. At the higher noise levels, above $L_{A10,18h}$ of about 65 dB, the exposures in Sydney, Melbourne and All Other Urban Centres are indistinguishable. Below this level, Sydney tends to have slightly more dwellings exposed to any level than do Melbourne and the other Urban Centres. While this tendency can be noted, the confidence limits for the exposures in Sydney, Melbourne and Other Urban Centres are +10.8/-8.6%, +9.0/-5.2% and +7.9/-5.9% respectively at $L_{A10,18h}$ of 63 dB ($p < .05$) and the overlapping confidence intervals confirm that the differences are not statistically significant. In any case, the percentages of dwellings in black spots is indistinguishable between the different subsamples, suggesting that the road traffic noise problem is a national issue - and not concentrated in any one city. The exposures for the subsamples in the smaller cities (Brisbane, Adelaide etc) have not been reported separately because of the smaller subsample sizes there.

Figures 1(c) and 1(d) compare the exposure of dwellings in Sydney and Melbourne with previous estimates by the SPCC (Stewart *et al*, 1986). For Sydney there is excellent agreement above an $L_{A10,18h}$ of 65 dB, and reasonable agreement below this level. For Melbourne, the results from this study are considerably below the previous estimates. The source of this difference probably relates to the large dependence of the SPCC model on available traffic counts and an under-representation of low to middle traffic volume roadways in that data. See Brown and Cliff (1988) for a further discussion on other possible sources of error in the model.

CONCLUSIONS

Considerable effort and funds are expended annually on road traffic noise control and avoidance Australia, but reliable data on the extent and intensity of exposure is essential before proper consideration can be given to policy matters such as the level of resources to be devoted to the management of road traffic noise, and the appropriate role for different remedial initiatives (Australian Environment Council, 1988).

This study has provided a definitive estimate of the exposure of the population of dwellings in Australian Urban Centres to road traffic noise. Confidence limits to the estimates have been provided, and this fact distinguishes the current from previous studies. Over 9% of the Australian population are exposed to $L_{A10,18h}$ of 68 dB or above and 19% of the population are exposed to $L_{A10,18h}$ of 63 dB or above. The figures confirm that road traffic noise is a national problem in Australia, and the extent of the problem - at between one in ten dwellings and one in five dwellings subject to unacceptable noise depending on what criterion level is used - indicates the need for national initiatives and national solutions. There appears to be little evidence of different exposure patterns between Sydney, Melbourne and other Major Urban Centres in Australia.

REFERENCES

Australian Environment Council (1988) Strategies for the Control of Road Traffic Noise Using Non-Vehicle Based Methods. 108pp + Appendices.

Brown A L (1989) Some simple transformations for road traffic noise scales. *Australian Road Research* 19(4) 309-312.

Brown A L (1993) Exposure of the population to road traffic noise. Research Report to the ANZECC, Australian School of Environmental Studies, Griffith University, 1993.

Brown A L and Cliff D A (1988) National exposure to road traffic noise. *Acoustics Australia 17*(1) 7-10.

Brown A L and Lam K C (1994) Can I play on the road, Mum? - traffic and homes in urban Australia. *Road and Transport Research* 3(1) 12-23.

Conover W J (1980) *Practical Nonparametric Statistics.* Wiley: New York. p353.

Great Britain Department of Transport (1988) *Calculation of Road Traffic Noise.* HMSO Welsh Office.

Harland D G and Abbott P G (1977) *Noise and Road Traffic Outside Homes in England.* Transport and Road Research Laboratory. TRRL Laboratory Report 770.

Maurin, M (1984) Enquete nationale sur les nuisances dues aux transports en France. *Revue d'Acoustique n° 70* 141-149.

OECD (1991) *Fighting Noise in the 1990s.* OECD: Paris.

Stewart A C, Reardon-Small M and Scott W (1986) Computer prediction of Sydney residents affected by traffic noise with changing motor vehicle emission standards. Australian Acoustical Society Conference, Toowoomba.

Zar J H (1984) *Biostatistical Analysis.* Prentice-Hall: Englewood Cliffs. p 379.

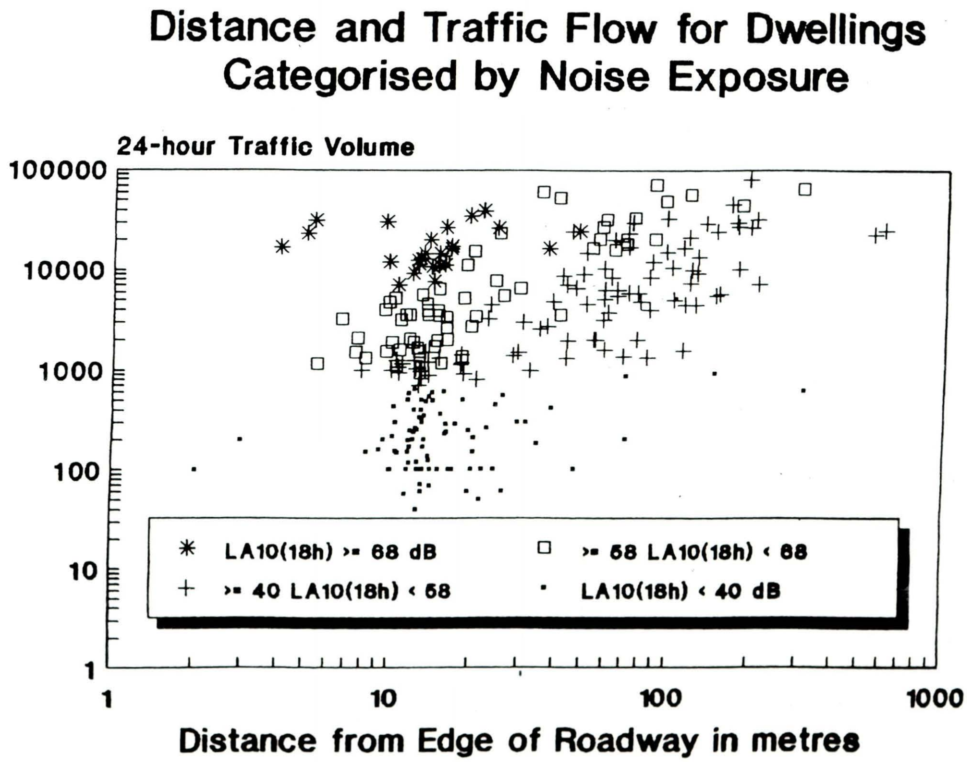

Figure 2

A Road Traffic Network Noise Evaluation Model

Jeremy E. Woolley
Transport Systems Centre
University of South Australia
The Levels SA 5095

At present, there are many PC based traffic noise prediction models in existence. Most of these are site specific and do not cater well for a network environment. At the Transport Systems Centre a four stage Environmental Impact Assessment System is being created for road traffic networks. This paper describes the noise prediction component of this system (NetNoise) and its interaction with the other components, namely: a traffic network model, an air emissions and energy use model, a land use impact model and a Traffic Network Relational Database (TNRDB) and Geographical Information Systems. NetNoise is intended for use as a planning and analysis tool in the investigation of alternative traffic schemes and land use scenarios.

INTRODUCTION

The road traffic network noise model, NetNoise, is currently under development as part of an integrated suite of PC based computer models for use as traffic planning and environmental evaluation tools. The research involving the development of these models is part of a collaborative project between the Transport Systems Centre at the University of South Australia (UniSA), Associate Professor Lex Brown and his team at Griffith University, and the Commonwealth Scientific and Industrial Research Organisation (CSIRO). Financial support is being provided by the State Energy Research Advisory Committee, the Australian Road Research Board (ARRB), the Australian Research Council and a UniSA/CSIRO collaborative research fund. The author assumes that the reader has some familiarity with the UK Department of Transport's Calculation of Road Traffic Noise (CoRTN) procedure (UK DoT 1988).

BACKGROUND

Many transport-based studies of traffic emissions and energy use have traditionally been based on micro-level studies and site specific or single vehicle modelling. Environmental models tend to look at single pollutant types rather than the combined effect of all pollutants for a given traffic scheme. The application of such models has generally fallen short of considering where the pollution is going and who it is affecting.

The work done by Taylor and Anderson during the eighties went some way to addressing these problems (Taylor and Anderson 1982 and 1984). Their work culminated in the POLDIF and MULATM models which have proven to be very useful and versatile planning tools (Taylor and Anderson 1988). Current research work concentrates on expanding the capabilities of the POLDIF model and incorporating a land use impact model and possibly an expert system into the suite of PC models. Figure 1 provides a schematic representation of the Impact Model for Predicting and Assessing the Environmental Consequences of Traffic (IMPAECT). The four-stage environmental impact assessment model consists of a road traffic network model, a vehicle energy and emissions model, a pollution dispersion model and a land use impact model. These models are capable of operating independently but may be combined through a common data structure such as a Geographic Information System (GIS) or the Traffic Network Relational Database (TNRDB).

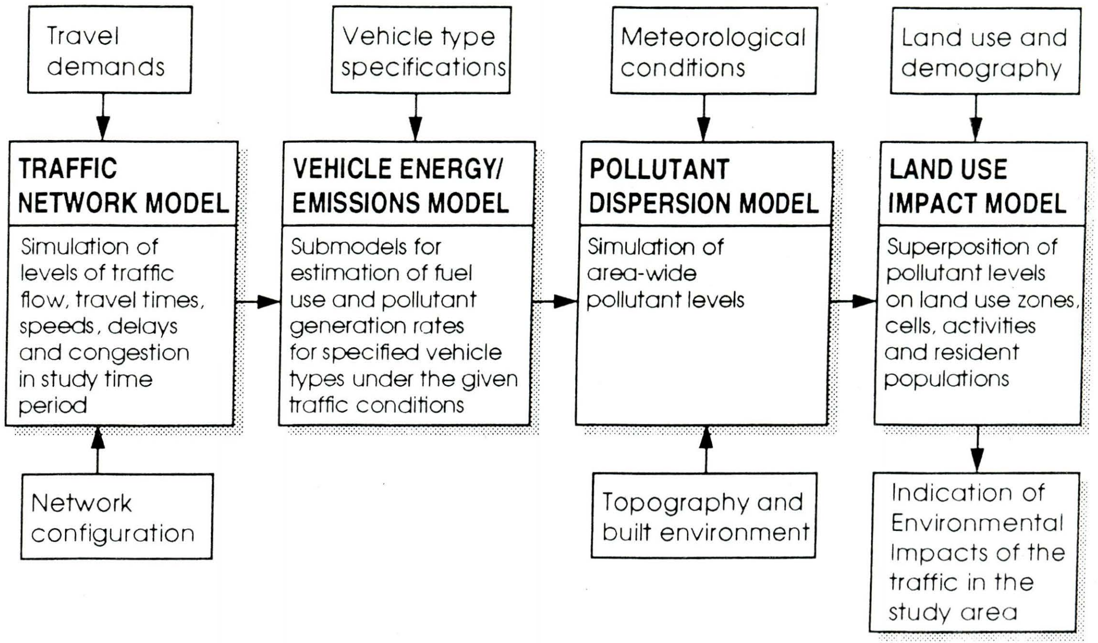

Fig. 1 - Schematic diagram of the impact model for the prediction and assessment of the environmental consequences of traffic (IMPAECT)

The traffic network model produces levels of flow and travel conditions (delay, queuing, congestion and travel times) for a given network. The model currently in use is TrafikPlan (formerly MULATM), developed by Professor Michael Taylor at UniSA. The vehicle energy and emissions model consists of two components: NetNoise and a vehicle energy use and air emissions model. The latter is being developed by Troy Young towards a PhD at UniSA. Pollution dispersion modelling is handled by POLDIF (for air emissions) and NetNoise (for noise). The land use impact model is being developed by Associate Professor Lex Brown at Griffith University. It is likely that information used by this model such as population demographics and land use characteristics will be presented on a GIS.

It cannot be expected that the IMPAECT model will provide absolute levels of pollution for a given area. Instead the model is applied on the assertion that although the actual absolute levels of pollution may be affected by many other factors besides those included in the component models, relative differences in levels of pollution can be reasonably detected by the model for alternative sets of traffic load distributions. Hence the main use of the model will be in the comparison of alternative traffic schemes where a number of pollutants and their impacts can be included together under the same set of conditions.

THE NETNOISE MODEL

The NetNoise model was developed to provide traffic engineers and planners a means of determining the noise distribution over a network area under specific sets of traffic conditions. The program is being developed by the author towards a research Masters degree at UniSA and is tailored for specific types of traffic engineering data. NetNoise operates in the windows environment and was developed using the Visual Basic application development environment. The model extends the well known and applied CoRTN procedure for use at a traffic network scale. This model was chosen for its robust characteristics and performs well within Australia (Saunders et al 1983). Whilst interrupted flow models were investigated they were considered too complex to implement at a network scale on a PC based model. There is scope for combining characteristics of interrupted flow and meteorological conditions with descriptors used in air emissions generation and dispersion modelling.

MODEL INPUT DATA

Input will be provided through text files, a TNRDB (created in MS Access), TrafikPlan, MapInfo or ARC/INFO GIS. The model uses the following information as input data:

- node coordinates
- link geometry
- traffic volume
- traffic composition
- traffic speed
- average link gradient
- road surface type
- texture depth
- barrier attributes

Links are defined by the CoRTN 2 dB(A) variation specification with emphasis placed on changes in traffic parameters. This means that nodes are not just restricted to intersections as is commonly found in network modelling packages. Links may represent aggregated two way traffic or one way traffic as deemed appropriate by the user. Where there is two way traffic, only positive gradients are recorded. At present, *noise barriers* can only be the length of an entire link. Barriers can be placed on both sides of a link and all barrier types covered in CoRTN are included.

Traffic volume can be entered as vehicles per hourly time unit; NetNoise will convert either user defined units or common units to those appropriate for the noise index being calculated. The common volume units include (peak) 1 hour counts, 11 and 12 hour turning counts, 18 hour noise counts and 24 hour or Annual Average Daily Traffic (AADT) data. The conversions are based on commonly used relationships determined by road authorities relative to the AADT or may be altered according to the user's own information.

Traffic composition data may be obtained from three sources:

1) manual commercial vehicle counts,
2) NAASRA (now AUSTROADS) classification counts, and
3) Australian Bureau of Statistics (ABS) data.

The first source provides the proportion of vehicles with three or more axles (including cars towing trailers) or two axles with double tyres on the rear axle. This figure can vary widely as it includes cars towing trailers. The second source is based on number of axles and axle spacing providing a much more detailed breakdown of the traffic biased towards heavy vehicles. Such data is often used for pavement design purposes and its collection is restricted to special studies on major roadways. The ABS data may be used only as an approximation and in the absence of any more detailed information. It details proportions of vehicles based on motor vehicle census data and can be broken down from national and state wide coverage to postal code area coverage.

CoRTN requires the proportion of heavy vehicles (vehicles with an unladen weight exceeding 1525 kg) travelling in the traffic stream. In NetNoise, the user has the option of identifying for the second and third sources which classes of vehicles should be considered as heavy vehicles. This allows some flexibility given the numerous definitions of commercial vehicles which exist within the industry. The relationship between heavy vehicles (CoRTN definition) and the above three sources will be researched by the author at a later date.

Traffic speed incorporates either the measured link speed or the speed zone classification for the link. The program first looks for the measured speed and if this is absent uses the speed zone speed for the link. If this is the case the appropriate CoRTN correction (ΔV) is applied where there is a positive gradient.

NetNoise requires one of four *road surface* types to be specified for a link. These are based on the work carried out by Samuels (pers. comm. 1993) and include the following surfaces: Portland Cement Concrete (PCC), Open Graded Asphaltic Concrete (OGAC), Densely Graded Asphaltic Concrete (DAGC), and Chip Seal (CS). Texture depth is only used if the CoRTN road surface corrections are applied but these are not recommended for use within Australia.

CALCULATION OF NOISE LEVELS

The CoRTN procedure is followed as closely as is practical at the network scale. Noise levels can be presented as either L_{10} 1 or 18 hour noise indices. An option is also provided to present levels as the L_{eq} index which involves the trivial operation of adding 3 dB(A) to the L_{10} final noise level. Source and receiver heights can also be defined by the user. The following sections outline the stages necessary for the calculation of the final noise level at each receptor.

Radius of influence and fringe effects

NetNoise uses the concept of radius of influence to determine the distances over which sources contribute to a noise level at any one receptor. CoRTN states that distances of more than 300 m are appropriate for environmental appraisal purposes (UK DoT 1988) but its attenuation charts and earlier work by Delany et al (1976) seem to suggest that 300 m is a maximum. Hood (1987) found that the probability of obtaining good agreement between measured and calculated noise levels is very remote for distances greater than

500 m. The maximum distance for predicting road traffic noise has therefore been set at 400 m by the author with a recommended distance set at 300 m.

Another concept currently under investigation is the effect of fringe areas on the network. This concept considers the amount of area surrounding a study network necessary to avoid investigating the study area in isolation from its surrounding environment. This would avoid the situation where noise levels at the edge of the network may drop off to 0 dB(A) because no noise sources were within the radius of influence. Solutions to this include applying a default background level where receptor final noise levels are 0 dB(A) or using a compulsory buffer zone around the study area in question.

Link based noise levels

The basic noise level is determined for each link in the network based on the flow along the link (converted to be appropriate for the noise index being calculated). Corrections are also determined for speed and percentage heavy vehicles, gradients and road surface. Other corrections apply for low flows if the distance between the receiver and the source line is less than 30 m.

Propagation

Distance correction is carried out for every link-receptor combination. If a noise barrier is present, the potential barrier correction is determined. An approximate form of correction for absorbent ground is applied by using an average absorbency value for the entire network. This is used because the level of detail necessary to store information for each link-receptor combination would be too much for a PC. Sensitivity tests are continuing but initial indications suggest that the use of an average absorbency value provides unnecessarily high correction values where distances between the source line and the receiver are large.

Site layout

A correction for angle of view is calculated for every link-receptor combination. Due to the level of detail required (as with absorbent ground corrections), no correction is applied for opposite facade reflections. The user does however have the option of applying the 2.5 dB(A) facade correction.

Other corrections

If the propagation distance is less than 4 m, the noise level is calculated at the distance of 4 m from the source. This also covers situations where receptors coincide with nodes which define the ends of a link and where receptors lie on the link's source line (extended or otherwise). This avoids the added complexity of implementing the calculation as described in Annex 5 of CoRTN.

Other optional corrections provided by NetNoise include the adjustment for Australian Conditions as suggested by Saunders et al (1983) and a user specified correction which is applied globally over the network, not individual links. The user does have the option of applying corrections to individual links but this information has to be included as part of an input file. The application and type of road surface corrections, facade effect, gradients, the inclusion of noise barriers and the above mentioned corrections can all be toggled on and off by the user.

Final noise levels

NetNoise calculates noise levels for receptor points laid over the network as a user specified grid. The noise levels from links which fall within the radius of influence around the receptor are aggregated after the appropriate corrections have been applied. It must be remembered that the final noise levels are approximations only (as is the CoRTN procedure) and are at best only as reliable as the information provided regarding traffic parameters and network geometry.

OUTPUT

Output from the NetNoise model may be viewed in several formats. From within the program, noise levels for each link and receptor may be viewed in the form of bar graphs and tables. Cross sections along receptor grid lines and comma delimited text files may be produced for importing into spreadsheets. Other output formats include MapInfo, ARC/INFO, TNRDB and contouring files.

Contouring output

The contouring files produced by NetNoise can make use of the SURVU and CONTOR programs from POLDIF and the surface plotting capabilities of the MS Excel spreadsheet package. At present a link between NetNoise and Excel is being established through Object Linking and Embedding technology. This will allow the user of NetNoise to view two dimensional contour plots or three dimensional surface plots as shown in Figure 2. In the Excel environment, chart views and perspectives can be manipulated allowing the user to gain a feel for the noise distribution across the study network.

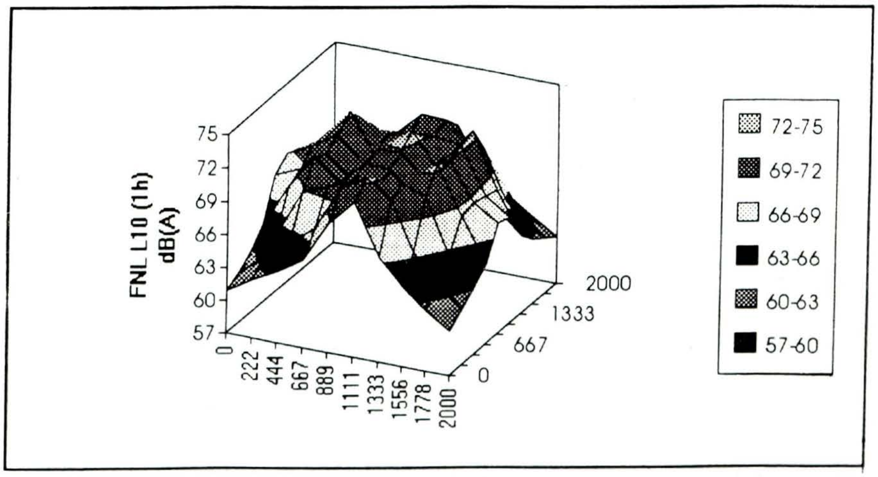

Fig. 2 - Noise distribution over a NetNoise trial network plotted in MS Excel

Graphs and tables

NetNoise allows the user to view link and receptor noise levels through tables or bar graphs. Tables allow information regarding corrections and component noise levels to be viewed on a link by link basis. Cross section tables and graphs may also be produced along receptor grid lines. These sections represent the noise level for the receiver height specified by the user.

Geographic information systems

Figure 3 shows output for a sample network in the MapInfo environment. A *shade by value* colour map of receptor noise levels has also been created and the attributes of the highlighted link are shown to the left of the screen. GIS have enormous potential for displaying environmental impact and traffic data. Information can be stored in layers and accessed through queries and graphical *point and click* techniques. Typical layers would include pollutant layers for each noise index (and air emissions), land use layers, network attribute layers (such as node and link data, speeds etc) and population demographics layers (such as age of residents, socio-economic background, etc).

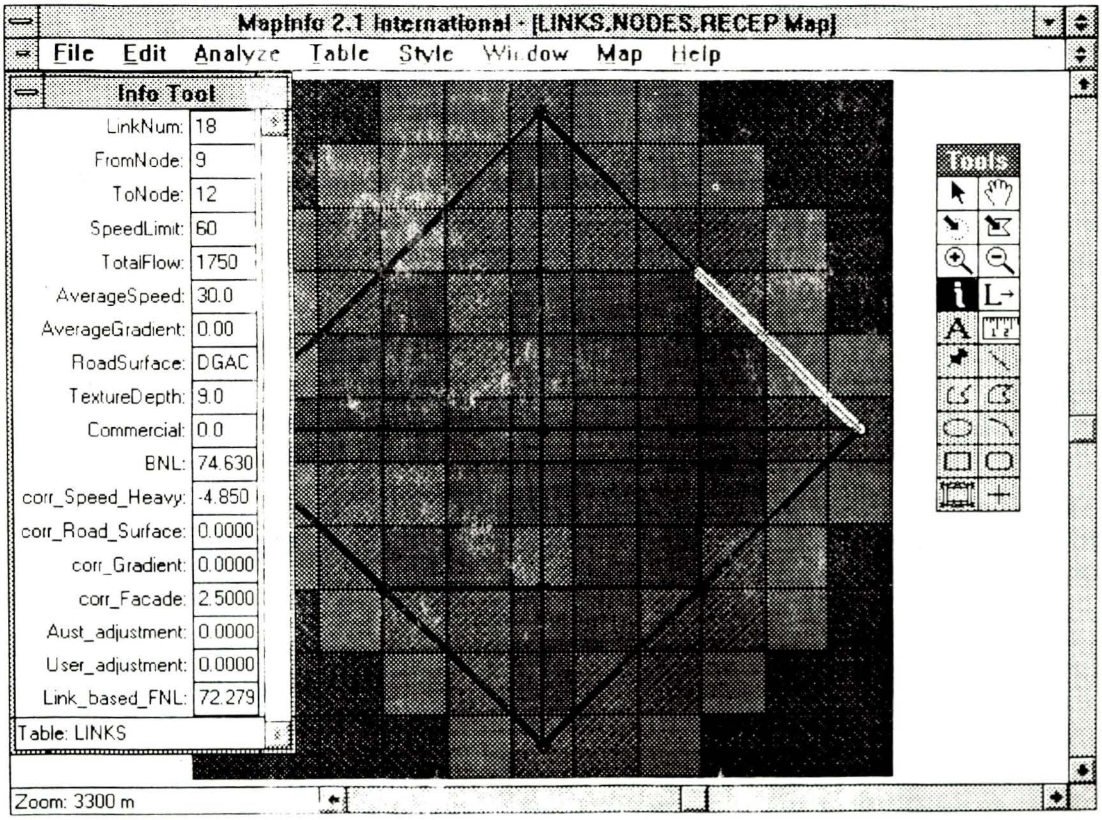

Fig. 3 - Sample NetNoise output in the MapInfo GIS environment

CONCLUSIONS

The IMPAECT model framework consists of a suite of PC models which allow traffic engineers and planners to investigate the impact of pollutants (both air and noise) on specific land uses for various traffic scenarios. NetNoise allows the user to obtain a feel for the noise environment across a road network through graphical output and interactive design scenarios whilst maintaining the ability to link the model with traffic network modelling and land use information. This will allow the user to investigate changes in noise distribution over a study area brought about by changes in traffic characteristics such as the closing of roads, the building of freeways and the application of Local Area Traffic Management schemes.

REFERENCES

Delany, M.E., Harland, D.G. Hood, R.A. and Scholes, W.E. (1976). The Prediction of Noise Levels L_{10} Due to Road Traffic. *Journal of Sound and Vibration*, London, pp. 305-325, 48(3).

Hood, R.A. (1987). Accuracy of Calculation of Road Traffic Noise, *Applied Acoustics*, London, pp. 139-146, 21(2).

Saunders, R.E., Samuels, S.E., Leach, R. and Hall, A. (1983). An Evaluation of the UK DoE Traffic Noise Prediction Method. Australian Road Research Board Research Report, ARR 122, ARRB, Melbourne.

Taylor, M.A.P. and Anderson, M. (1982). Modelling Pollution and Energy Use in Urban Road Networks. Proc. 11th Australian Road Research Board Conference, Melbourne, pp. 1-16, 11(6).

Taylor, M.A.P. and Anderson, M. (1984). Energy and Emissions in a Metropolitan Road Transport System. Proc. 12th Australian Road Research Board Conference, Hobart, pp. 63-78, 12(6).

Taylor, M.A.P. and Anderson, M. (1988). Modelling the Environmental Impacts of Urban Road Traffic with MULATM-POLDIF: a PC-based System with Interactive Graphics. Environment and Planning B, Vol 15, pp. 413-431.

UK DoT (1988). Calculation of Road Traffic Noise. HMSO, London.

AN EVALUATION OF ACTUAL AND PREDICTED ROAD TRAFFIC NOISE LEVELS

Russell Brown
Ron Rumble Pty Ltd, 17 Station Rd, Indooroopilly, Qld

INTRODUCTION

The UK Department of Transport 'Calculation of Road Traffic Noise' (CRTN 88) is the calculation procedure currently endorsed by Queensland Department of Transport for the prediction of road traffic noise levels from roads in the state of Queensland. It is similarly endorsed by road traffic authorities in other States. Since 1978, various studies have been conducted to assess the applicability of the CRTN algorithms to Australian conditions. This paper compares the results of measurements of noise levels from traffic on the South East Freeway, Brisbane with the results of predictions of noise levels from three different calculation methods. It also proposes reasons to explain why there are differences in the values of road traffic noise level calculated by two of these methods.

CRTN 88

The 'Calculation of Road Traffic Noise' procedure was developed initially by United Kingdom Department of Environment in 1975. The latest version CRTN 88 was prepared by UK Transport and Road Research Laboratory and UK Department of Transport in 1988. This revision retains a significant proportion of the original method including the philosophy of approach and much of the formulation, but includes research results which extend the method to cover a wider range of applications.

The CRTN 88 method consists of a set of calculation algorithms which have been developed to quantify the significance of a range of variables which influence the level of road traffic noise. These variables can be grouped into three categories as follows -

Vehicle-related	:	Traffic volume, speed, % heavy vehicles
Road-related	:	Gradient, road surface, split carriageways
Propagation-related	:	Distance from road, local topography, ground type, receiver height, angle of view, barrier shielding, reflections from facade and barriers

Various methods of applying the CRTN 88 algorithms have been developed since 1975. Broadly these may be categorised as follows -

. Graphical/Calculator
. Specific-user Computer File
. Proprietary Computer Program

The graphical/calculator method is outlined in the CRTN 88 document. Briefly, it requires that the road system be divided into segments so that each can be treated as a uniform section of road for which the values of the variables are constant throughout.

Each of the algorithms is then applied in turn to one segment. The result is a $L_{10(18\text{ hour})}$ noise level contribution from that segment. The set of algorithms is then applied to each of the other segments. In each case the algorithms are applied by inserting the values of the variables into the applicable equation/s or by interpolation from the relevant curve/s in the charts contained in the CRTN 88 document.

The resultant $L_{10(18\text{ hour})}$ noise level contributions are summed logarithmically to determine the net overall $L_{10(18\text{ hour})}$ road traffic noise level at that location.

Generally, evaluation of the $L_{10(18\text{ hour})}$ noise level by the specific-user computer file method differs from the graphical/calculator method only in that all calculations are conducted automatically once the values of the variables have been determined from site measurements and/or from drawings. When set up properly this method results in minimum operator error and enhanced speed of calculation. It also lends itself to plotting of noise contours and optimisation of noise control treatments. This method is suited to calculations at a small number of receiver locations.

Proprietary computer programs have been developed in recent years to allow road traffic noise level contours to be calculated over entire community areas. In general, these programs determine the $L_{10(18\text{ hour})}$ noise level by dividing the road system at any particular receiver into a large number of very small segments and applying the calculation algorithms to each of these segments in turn. Curve fitting routines can then be applied to the resultant net overall $L_{10(18\text{ hour})}$ values at the receiver locations to develop road traffic noise level contours throughout the community. 'RoadNoise' and 'SoundPLAN' are two proprietary computer programs currently in use in Australia.

SOUTH EAST FREEWAY

The South East Freeway in Brisbane consists of two three-lane carriageways separated by a median plantation of varying width. It extends from the Brisbane CBD to Springwood where it joins with the Pacific Highway which in turns runs south to the Gold Coast.

The freeway was constructed in stages. The first stages passed through the inner suburban areas of Woolloongabba and Buranda. Large-scale property resumptions were required in these areas because no road corridor provision, other than that along already existing major roads, had been made at the time of initial sub-division. Generally, the houses located in close proximity to the freeway in these areas are of the Queenslander type, ie high set timber houses with habitable spaces above and timber slated storage areas below, usually constructed on sloping ground.

In suburban areas located further from the CBD, however, corridor provision had been made in advance of construction of the South East Freeway. In the southern (newer) areas, the residences are usually of brick veneer construction. Consequently, residences in these areas are generally located at greater distances from the freeway and are of more substantial construction compared to those in areas closer to the CBD.

Eighteen-hour road traffic volumes on the South East Freeway generally lie in the range 50000 - 60000 vehicles per day on each of the inbound and outbound carriageways (ie. 100000 - 120000 vehicles per day total). Heavy vehicle percentages are typically 5% outbound and 4% inbound.

Road traffic noise levels were both measured and predicted along two sections of the South East Freeway, viz-

Section 1 - Stanley Street, Woolloongabba to Willis Street, Ekibin
Total distance: 3000 m (approx)

Section 2 - Birdwood Road, Holland Park West/ Tarragindi to Shire Road, Holland Park West
Total distance: 1700 m (approx)

(Refer Figure 1)

The legal speed on the inbound lanes of Section 1 is 100 km/h over the southern half of the section and 80 km/h over the northern half. On the outbound lanes of Section 1 the legal speed is 100 km/h for all but 1000 m (approx) south from Stanley Street. The legal speed over both the inbound and outbound lanes of Section 2 is 100 km/h throughout.

Residences are located at distances as close as 22 metres from the edge of the freeway along Section 1. The local topography in the area around Section 1 is quite undulating. In addition, the freeway passes over several major roads and a railway. As a result, the freeway is situated in cut or on fill for most of its path through the suburbs of Section 1.

Along Section 2, the closest residence is some 40 metres from the edge of the freeway. The local topography close to the freeway is generally less undulating, than that along Section 1. In addition, because the freeway does not need to negotiate as many major roads, the extent of cut and fill along Section 2 is not as great as that along Section 1.

At present there are no roadside barriers between any residences adjacent to the freeway along either of the two sections.

MEASURED NOISE LEVELS

Measurements of road traffic noise levels were conducted at twenty-three residential locations adjacent to the freeway - sixteen along Section 1 and seven along Section 2. (Refer Figure 1.) These locations were chosen to be representative of the most adversely affected residences in close proximity to the freeway.

Care was also taken to choose residences for which the dominant source of traffic noise was the South East Freeway. That is, those for which noise level contributions from traffic on Stanley Street, Ipswich Road, O'Keefe Street, Juliette Street, Cornwall Street, Bapaume Road and other suburban roads and service roads nearby could be ignored.

Figure 1 - Measurement Locations

All noise level measurements were conducted in general accordance with the requirements of AS 2702 - 1984 'Acoustics - Methods for the Measurement of the Road Traffic Noise'. For all measurements the measurement position was located 1.5 metres above ground level at the subject residence at a point one metre from the facade which was most exposed to road traffic noise.

Measurements were conducted at each of the eighteen hourly intervals from 06:00 to 24:00 midnight on a typical week day. Weather conditions were fine and calm on each occasion. At the time of measurements the road surface of section was impervious. (Open graded asphaltic concrete - a pervious surface - was applied to the road surface of Section 2 soon afterwards.)

PREDICTED NOISE LEVELS

Road traffic noise levels for each section were calculated by three methods, viz-

. User-specific computer file
. SoundPLAN computer model - single point method
. SoundPLAN computer model - grid point method

The user-specific computer file was developed on Microsoft Excel 5.0. The input data file of vehicle-related data was prepared from information supplied by Queensland Transport. The data file of road-related and propagation-related data was compiled from information derived from orthophotos and site inspections.

The SoundPLAN models were prepared from data supplied by Queensland Transport and information derived from drawings, aerial photos, orthophotos and site inspections. Separate models were prepared for each section.

Both single point calculations and grid point calculations were conducted using the SoundPLAN models. The receiver locations for the single point calculations were the same as the twenty-three measurement locations. The results of these two sets of calculations were used for direct comparison against the results of the measurements. The results of the grid point calculations were used to prepare noise level contours throughout the community areas adjacent to the freeway as well as for comparison, by interpolation, against the measured noise levels. The grid size for the contours was 5m x 5m. For selected residential locations, this was reduced to 1.5m x 1.5m.

For the grid point calculations using the SoundPLAN program, all residences along the freeway in Section 1 and the northern half of Section 2 were assumed to be typical Queenslander, ie facades half absorptive/half reflective, unless identified otherwise to be all reflective (ie brick). Conversely, all residences along the southern half of Section 2 were assumed to be all reflective, unless identified to be half absorptive/half reflective. The derived reflection loss values were 1 dBA for reflective facades and 4 dBA for half absorptive/half reflective facades.

For both methods, it was assumed that there were no significant noise level contributions from the passage of vehicles on any other nearby roads.

RESULTS

The results of the measurements and predictions are summarised in Table 1.

Residential Location	Measured $L_{10(18\ hour)}$ dBA	Calculated $L_{10(18\ hour)}$ User-specific, dBA	Calculated $L_{10(18\ hour)}$ SoundPLAN Single Point, dBA	Calculated $L_{10(18\ hour)}$ SoundPLAN Grid Point, dBA	Difference - Calculated User-specific over/(under) Measured	Difference - Calculated SoundPLAN Single Point over/(under) Measured	Difference - Calculated SoundPLAN Grid Point over/(under) Measured
1	73.0	75.6	71.3	74.0	2.6	(1.7)	1.0
2	69.8	72.3	70.4	72.0	2.5	0.6	2.2
3	66.6	70.1	66.5	70.0	3.5	(0.1)	3.4
4	66.4	67.9	68.6	70.0	1.5	2.2	3.6
5	62.4	66.0	65.3	69.5	3.6	2.9	7.1
6	66.9	65.7	70.1	69.5	(1.2)	3.2	2.6
7	67.2	70.9	71.0	68.5	3.7	3.8	1.3
8	65.2	69.4	69.1	69.5	4.2	3.9	4.3
9	70.4	71.9	70.0	68.0	1.5	(0.4)	(2.4)
10	68.9	68.1	71.2	71.0	(0.8)	2.3	2.1
11	70.4	70.8	71.2	71.0	0.4	0.8	0.6
12	67.1	68.5	70.4	72.0	1.4	3.3	4.9
13	73.9	74.5	71.0	73.0	0.6	(2.9)	(0.9)
14	61.4	63.4	63.9	67.0	2.0	2.5	5.6
15	66.9	70.7	68.9	69.0	3.8	2.0	2.1
16	66.1	66.5	68.2	68.0	0.4	2.1	1.9
17	67.6	70.0	67.7	68.0	2.4	0.1	0.4
18	65.4	68.4	66.7	68.0	3.0	1.3	2.6
19	64.3	67.4	67.1	68.0	3.1	2.8	3.7
20	60.0	63.8	66.1	67.0	3.8	6.1	7.0
21	62.3	62.9	66.4	68.0	0.6	4.1	5.7
22	63.4	66.0	64.9	68.0	2.6	1.5	4.6
23	61.9	64.5	64.7	67.0	2.6	2.8	5.1

TABLE 1 - COMPARISON OF MEASURED AND CALCULATED $L_{10(18\ hour)}$ ROAD TRAFFIC NOISE LEVELS

RELATIVE PERFORMANCE OF PREDICTION METHODS

Previous studies by others have drawn conclusions regarding the degree of variation between measured and calculated $L_{10(18\ hour)}$ road traffic noise levels. Brown and Hollingsworth (1978) determined that the 90% confidence limits for calculated over measured noise levels at locations adjacent to urban freeways to be -

-0.3 dBA and +2.5 dBA

Saunders et al. (1983) concluded that the 95% confidence limits were -

. Free-field (Qld, Vic, WA) : -2.9 dBA and +4.3 dBA
. At facade (Vic only) : -3.3 dBA and +6.7 dBA

From the set of data summarised above in Table 1, confidence limits for calculated over measured $L_{10(18\ hour)}$ have been determined to be -

User-specific -	90% :	-0.4 dBA and +4.6 dBA
	95% :	-0.9 dBA and +5.1 dBA
SoundPLAN Single Point -	90% :	-1.4 dBA and +5.2 dBA
	95% :	-2.1 dBA and +5.8 dBA
SoundPLAN Grid Point -	90% :	-1.0 dBA and +6.9 dBA
	95% :	-1.7 dBA and +7.7 dBA

DISCUSSION

Each of the calculation methods tends to over-predict the level of road traffic noise that would be expected to result. This trend was evident also in the earlier studies. The average degree of over-prediction was 2.1 dBA for the user-specific method. For the SoundPLAN methods it was 1.9 dBA and 3.0 dBA for the single point and grid point methods, respectively. Each of these values, however, is greater than those derived in the earlier studies, ie. Brown and Hollingsworth (1978) : 1.1 dBA; Saunders et al (1983) : 0.7 dBA (free field), 1.7 dBA (facade).

When the confidence intervals are compared, each of the calculation methods above produces a wider spread of results than those reported by Brown and Hollingsworth. The confidence intervals for each of these methods, however, are very similar to those derived by Saunders et al.

Both of the SoundPLAN models were prepared using common data. While the grid point results were derived by interpolation from noise contours, however, the single point results were calculated at the specific locations at which the noise level measurements were conducted. This difference in the method of deriving the results is the major the reason for the differences in the results from these two methods.

For example, close to residences the level of noise which would be measured will vary with proximity to the facade of the subject residence. This is because the intensity of the reflected sound energy, the attenuation due to shielding provided by adjoining residences and the attenuation provided by other parts of the subject residence are each quite sensitive to relatively small changes in distance from the facade. Grid point spacing was usually chosen to be 5 metres. For contour plotting this is a practical compromise between accuracy and speed of calculation. At this spacing, however, the grid point locations will seldom coincide with the single point locations. Significant differences in road traffic noise levels would be expected as a result.

Furthermore, because the local topography is naturally quite undulating and the freeway is frequently in either cut or fill, there will be a significant difference in the values of $L_{10(18\ hour)}$ that are calculated at adjacent and nearby grid point locations, especially where residences are situated close to the toe or crest of an embankment.

Taken together, these two effects may produce quite coarse changes in the values of $L_{10(18\ hour)}$ at adjacent locations. If the interval between noise level contours is relatively small (ie. up to 2 dBA), the SoundPLAN curve fitting may attempt to fit several contours between adjacent grid points. Interpolation between these contours would be expected to produce results which differ from those derived by calculation at the single point locations.

This difference may be further exacerbated by the fact that the details of the physical environment at the single point locations can be defined to a greater degree than can usually be achieved at all grid point locations. For the single point calculations, greater precision can be attained if the significance of various atypical features accounted for. Such features may include low height fences along boundaries to the freeway, garden sheds and other structures in yards facing the freeway, footbridges over the freeway, etc. These features can be identified on-site, but not be evident or present on orthophotos or aerial photos.

In addition at several single point locations, the line of the traffic is totally obscured by the combined effect of the guard rail and the embankment edge. In a practical sense, determining whether these two features align to produce this effect requires detailed inspection of the site. While it is feasible and appropriate to conduct inspections for each of the single point locations and this was done, it was not practical to do the same for all of the residences fronting each side of the of the freeway. Consequently, differences between the single point and the grid point values would be expected, esp. where the freeway was on fill.

CONCLUSIONS

The three methods for calculating $L_{10(18\ hour)}$ have each produced results which confirm the trend of over-prediction of the level of road traffic noise that has been identified previously by others. The spread of results is comparable with that identified by Saunders et al. Not surprisingly, the over-prediction and the spread of results is greatest for the method based on interpolation from the noise level contours. It is considered that the principal reasons for this are i) the relatively coarse differences in noise level values that must result as a matter of course at adjacent grid point locations close to residential facades and areas where the local topography is undulating and ii) the practical limitations of the grid point method in taking account of the effect of atypical features of the physical environment.

REFERENCES

BROWN, A.L. and HOLLINGSWORTH, G.H. (1978) Prediction of Freeway Noise Levels (L_{10}) : An Evaluation of the U.K. Department of the Environment Procedure. Proc. Ninth ARRB Conference 9 (6) pp. 248-262.

SAUNDERS, R.E. et al (1983) An Evaluation of the U.K. DoE Traffic Noise Prediction Method. ARRB Report No. 122.

Acknowledgment: Part of the data presented in this paper was developed as result of work conducted under Queensland Transport Invitation No. DSB023. The assistance of Queensland Transport and Vipac (for SoundPLAN data) in permitting this data to be reproduced here is gratefully acknowledged.

SOME ACOUSTICAL ATTRIBUTES OF CEMENT CONCRETE ROAD PAVEMENTS

Stephen Samuels
Transport Engineering Department,
University of NSW

ABSTRACT

Development of quieter road pavements is a continuing process which has been under way for a number of years. Some recent attention has been focused on cement concrete pavements and this is the concern of the present paper. It deals with one part of an ongoing research and development program aimed at producing quieter concrete pavements without compromising other important properties such as skid resistance. The acoustical attributes of a range of cement concrete pavements have been determined via full scale field trials. This paper describes the trials along with the data obtained and then presents the empirically determined acoustical attributes. In further considering the outcomes of this work, the paper places the findings in context of an ongoing program of low noise concrete pavement development.

INTRODUCTION

Road traffic represents a major source of urban noise pollution. Technically it may be regarded as the aggregation of the noise generated by individual vehicles operating in the traffic . Therefore in attempting to control noise, an important and effective strategy is to reduce the noise produced by individual vehicles (AEC 1988). With the exception of motorcycles, for all vehicles in a reasonable state of maintenance, tyre/road interaction is the major noise source under constant speed conditions exceeding around 40 km/h (Samuels 1982). It is now well known that useful and achievable traffic noise reductions may be obtained by appropriate application and design of road surface texture (Samuels and Glazier 1990).

The Roads and Traffic Authority of NSW (RTA) has been adopting this technique for traffic noise control. Several previous studies initiated and sponsored by RTA have already quantified the effects of various road surface treatments on roadside noise levels (Samuels and Glazier 1990, Samuels and Roper 1991, Mitchell McCotter and Associates 1992). Road surface treatments investigated to date have included various types of portland cement concrete (PCC), open graded asphaltic concretes, dense graded asphaltic concrete, cold overlay slurry seals and a chip seal.

More recently these studies have been extended to include a further variety of PCC surface textures. Pavement surface texture may be modified by altering the form of the pattern which is impregnated into the mortar of the plastic concrete. A number of pavement sections of varying surface texture have been constructed on freeways in the Sydney and Newcastle environs. The acoustic attributes of these pavements have been determined and compared to those of the previous studies.

FULL SCALE TRIALS

EXPERIMENTAL PROGRAM

Roadside noise data were collected on a total of 13 pavement sections. Of these, 10 were located on recently constructed yet unopened freeway sections. These conditions precluded traffic noise measurements as were done previously by, for example, Samuels and Glazier (1990). Consequently the data collection procedure at these sites involved measurement of the passby noise levels of individual test vehicles as they repeatedly traversed each test section. This was the (successful) technique adopted in the latest of the previous studies (Mitchell McCotter and Associates 1992).

Each of the remaining three sites was operational, subjected to normal traffic conditions. Logistic and financial constraints prevented collection of overall traffic noise data at these sites. Consequently the passby noise levels produced by individual vehicles in the traffic stream were monitored at these sites. One of three sites had been included in two of the previous studies (Samuels and Glazier 1990, MMA 1992). Analyses and subsequent application of all data were based on the Samuels and Glazier (1990) findings that road surface treatment had similar effects on both individual vehicle noise and overall traffic noise levels.

PAVEMENT AND VEHICLE TYPES

Details of the 13 sites are presented in Table I. Note that for the PCC pavements tested, the primary variables were tyne spacing (13 and 26 mm) and surface finish (Hessian or Astroturf Drag). Sites 10 and 11 had been used previously and were included to provide data which would facilitate results of the present investigation being related to those of the earlier studies. The rain damaged Site 13 was a late inclusion in the experimental program. At this site heavy rain fell just after the pavement surface had been finished. The resulting surface texture could best be described as having an Exposed Aggregate PCC type of finish.

Reiterating what was explained previously herein, at those sites where normal traffic conditions existed (designated as "Yes" in the "Under Traffic" Column of Table I) noise levels from individual vehicles in the traffic stream were measured. At all other sites, not yet open to traffic, noise levels from two test vehicles were measured. These two vehicles were selected to be typical of a passenger car and a moderate sized heavy vehicle (Samuels 1993). While vehicle type is an important factor in the generation of individual vehicle noise, outcomes from the previous studies, in particular Samuels and Glazier (1990), clearly indicated that noise data monitored from two carefully selected test vehicles would comfortably satisfy the objectives of the present study. The two test vehicles employed were as similar as possible to those of the most recent previous study (MMA 1992).

DATA COLLECTION

At those 10 sites where the two test vehicles were employed, passby noise data were collected in accord with the provisions of the relevant Australian Standard (SAA 1979). Both vehicles drove past the measurement station at each site nominally at 50, 60, and 70 km/h, with 5 replicate runs being undertaken at each speed. Precision instrumentation systems were employed to measure vehicle noise levels and speeds (Samuels 1993). At the remaining 3 sites (#9, #10 and #12) which were under traffic, similar measurement procedures were adopted. Here the maximum passby noise levels of individual vehicles in the traffic stream driving past in the nearside lanes were measured. Again the noise data were collected using the same precision instrumentation systems.

TABLE I

SITE SPECIFICATIONS

SITE	UNDER TRAFFIC	ROAD SURFACE SPECIFICATION
1	No	PCC - 3/13/LH
2	No	PCC - 3/26/LH
3	No	PCC - 3/13/A19
4	No	PCC - 3/26/A19
5	No	PCC - 3/13/LH
6	No	PCC - 3/26/LH
7	No	PCC - 3/13/A10
8	No	PCC - 3/26/A10
9	Yes	DGAC
10	Yes	OGAC
11	No	PCC - 3/13/LH
12	Yes	PCC - 3/13/LH
13	No	PCC - RD

Legend
PCC - Portland Cement Concrete
LH - Light Hessian Drag
A19 - 19 mm fibre Astroturf Drag
A10 - 10 mm fibre Astroturf Drag
3/13 - 3 mm tyne depth at 13 mm spacing
3/26 - 3 mm tyne depth at 26 mm spacing
DGAC - Dense Graded Asphaltic Concrete
OGAC - Open Graded Asphaltic Concrete
RD - Rain damaged during construction

ACOUSTICAL ATTRIBUTES

SURFACE TEXTURE EFFECTS

All data were collated and analysed in accord with the procedures documented in Samuels and Glazier (1990) and as described in Samuels (1993). Resulting average noise levels for the test car and the test truck at the 10 untrafficked sites have been graphed in Figure 1, along with the well known (Samuels 1982) 40 log (speed) relationships. It is apparent that both the car and the truck data conform with a 40 log (speed) relationship, as expected. What is also clear in Figure 1 is that the truck data span a range of 4dB(A) while the car data span some 5dB(A). For both car and truck Site 11 consistently produced the lowest noise levels. Note that Site 11 has also been tested previously (MMA 1992), meaning that all of the trial surfaces laid for the present study produced somewhat higher noise levels than Site 11. Both car and truck data are consistent with and overlap the comparable data of the previous study (MMA 1992).

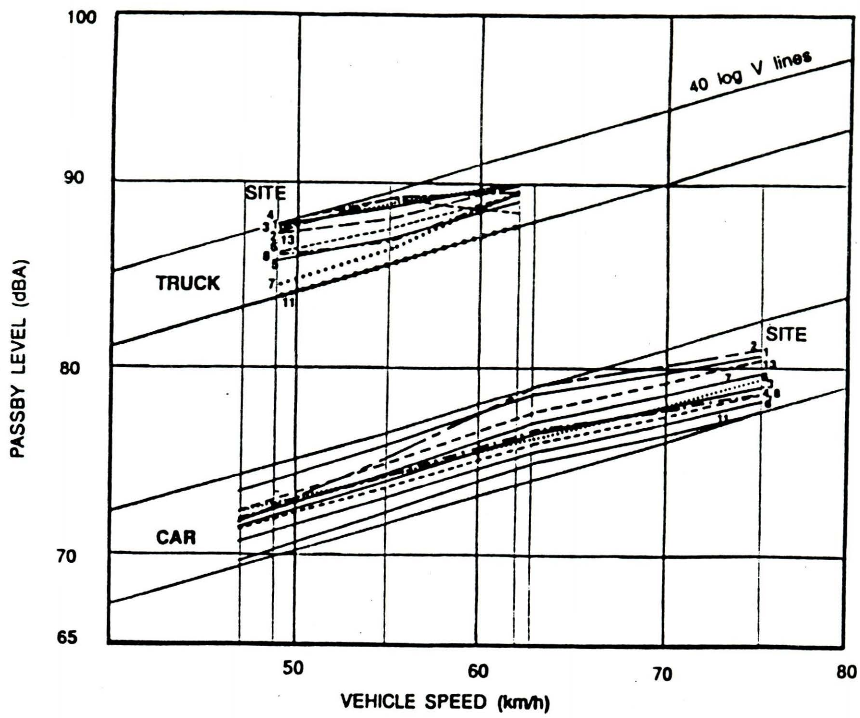

Figure 1. Vehicle Noise Data

TABLE II

RANKING OF SURFACES IN ORDER OF DECREASING NOISE, BASED ON FIGURE 1.

CAR DATA		TRUCK DATA	
SITE	SURFACE	SITE	SURFACE
2	3/26/LH	4	3/26/A19
1	3/13/LH	1	3/13/LH
13	RD	3	3/13/A19
7	3/13/A10	2	3/26/LH
6	3/26/LH	13	RD
3	3/13/A19	6	3/26/LH
4	3/26/A19	8	3/26/A10
8	3/26/A10	5	3/13/LH
5	3/13/LH	7	3/13/A10
11	3/13/LH	11	3/13/LH

Inspecting the Figure 1 data more closely indicates that there are no particularly clear trends as to which surface type produces the lowest noise levels. However, based on what appears in Figure 1, an attempt was made in Table II to rank the surfaces in order of decreasing noise output. This process merely confirmed the above observation. The data of Figure 1 and Table II are consistent with those of MMA (1992) where it was concluded that PCC pavements of the 3/13/LH type produced the lowest noise levels and was therefore the recommended choice for future applications.

As mentioned previously, noise data were also collected at three sites under traffic. These "statistical passby" data were analysed according to the Samuels and Glazier (1990) procedures and the results appear in Table III. Clear road surface effects are obvious here. For both vehicle types the noise produced on the PCC pavements is louder that on the DGAC which is in turn louder than that on the OGAC pavement. The total range of noise levels is on average 5.1dB(A) for cars and 3.7dB(A) for trucks. These are readily discernible and useful differences. Note also that the levels of Table III are consistent with those appearing in Figure 1. This expected observation supports the assertion that measurement technique did not affect the data. It also adds to the confidence with which both sets of data presented herein may be applied for the purposes of the investigation.

TABLE III

STATISTICAL PASSBY NOISE LEVELS AT 80 km/h

VEHICLE TYPE	PARAMETER	SITE 9	SITE 10	SITE 12
	Number of Samples	50	47	50
CAR	Mean Noise Level (dB(A))	81.6	79.0	84.1
	Standard Deviation of Noise Level (dB(A))	1.7	1.8	2.0
	Number of Samples	30	33	30
TRUCK	Mean Noise Level (dB(A))	90.0	89.3	93.0
	Standard Deviation of Noise Level (dB(A))	4.3	2.9	2.7
BOTH	Road surface type	DGAC	OGAC	PCC 3/13/LH

COMPARISON WITH PREVIOUS DATA

One important out come of the previous studies (Samuels and Glazier 1990, Samuels and Roper 1991, Mitchell McCotter & Associates 1992) has been the establishment of a ranking of pavement types in respect of noise output. This ranking has been carefully evolved and is finding wide application. Incorporating the pavements of the present study into that ranking was achieved once the present data were adjusted to allow for possible variations between the present and previous data sets due to test vehicle type and other relevant factors such as ambient conditions and instrumentation (Samuels 1993).

When the data from the present study were so adjusted and compared with those of the previous studies it was observed that the range of levels associated with the PCC pavements of the present study encapsulated that range established from the previous studies. The observation could reasonably be expected since the pavements of the present study are essentially of the same type as those tested previously. The overall range of noise from currently used PCC pavements has been slightly extended, particularly at the upper end of the range. This would suggest the need for some care in the selection of PCC surface texture type. Reiterating, the results of the present study are consistent with the MAA (1992) conclusion that a 3/13/LH surface texture generally produced the lowest noise levels.

The pavement noise ranking referred to above which is applied in practice is provided in Appendix B of RTA (1992). In Table IV that ranking is presented and incorporates the results of the present study. What appears in Table IV reflects the following three primary outcomes of the present study.

- There is a 4 to 5 dB(A) range of noise levels produced by PCC pavements.
- Precise specification of the PCC pavement textures associated with the "loudest", "average" and quietest" surfaces requires further investigation and analyses.
- Noise produced by the DGAC and OGAC pavements of the present study are essentially the same as those produced by these type of pavements studied previously.

TABLE IV

PAVEMENT NOISE RANKINGS

SURFACE TYPE	INCREASE (+) OR DECREASE (-) IN TRAFFIC NOISE L_{eq} OR L_{10} (dB(A))	
	CARS	HEAVY VEHICLES
14 mm Chip seal	+3.6	+1.0
Loudest PCC	+3.2	+0.9
Cold Overlay	+2.4	+0.4
Average PCC	+1.2	-1.1
DGAC	0	0
Novachip OGAC	-1.6	-1.2
Quietest PCC	-1.8	-3.1
Old OGAC	-3.6	-2.6
New OGAC	-7-7	-6.0

A WORD ABOUT SKID RESISTANCE

In a parallel with the present and previous noise studies, RTA have collected companion data on pavement surface texture depth and skid resistance properties. Some of these data have been presented and reviewed by Nichols and Dash (1992). It would appear that PCC pavements of 13 and 26 mm tyne spacing both provide similar, acceptable levels of skid resistance. Similar data have been collected for all surfaces of the present study and the indications to date are that the same satisfactory skid resistance properties have been achieved.

CONCLUSIONS

On the basis of the study documented herein, the following conclusions may be drawn.

- Noise levels produced by a range of PCC pavements varied with pavement surface type over a range of 5dB(A) for car noise and 4dB(A) for heavy vehicle noise. The noise levels associated with these pavements varied as expected with speed according to the well known 40 log (Speed) relationship.

- The measured noise levels compared directly with those of previous studies, encapsulating the range of noise levels measured previously. The quietest PCC pavement was essentially equivalent to the quietest of the PCC pavements measured previously while the loudest represented a slight increase overall on that already measured.

- The present study also included measurements on a relatively new DGAC pavement. This produced noise levels that were essentially equivalent to those of an older DGAC pavement tested previously.

- There was no particularly clear trend observed as to the detailed effects of PCC surface texture or surface finish on noise. (Determination of such a trend is the focus of current, ongoing research.) The results were, however, consistent with the previous conclusion that a 3/13/LH texture is the quietest overall.

REFERENCES

AUSTRALIAN ENVIRONMENT COUNCIL (1988). Strategies for the control of road traffic noise using non-vehicle based methods. Report of Transportation Noise Sub Committee of AEC Environmental Noise Control Committee. AEC, Canberra, ACT.

MITCHELL McCOTTER & ASSOCIATES (1992). The noise effects of cement concrete pavement surface texture. MMA Report 91112RP1, MMA, Crows Nest, NSW.

NICHOLS, J. and DASH, D. (1992). Developments in concrete road surface technology for the reduction of road traffic noise. Proc. 16th ARRB Conf., Vol. 16, Pt. 6, pp 55-69.

ROADS AND TRAFFIC AUTHORITY (1992). Environmental Manual, Volume II. RTA, Sydney, NSW.

SAMUELS, S.E. (1982). The generation of tyre/road noise. Australian Road Research Board Report ARR121. ARRB, Vermont South, Victoria.

______________ (1993). A further study of the effects of cement concrete road pavement texture on noise. Report prepared with RTA Environmental Planning Section for RTA Northern Region. S.E. Samuels, Cronulla, NSW.

SAMUELS, S.E. and GLAZIER, G.S.J. (1990). The effects of road surface texture on traffic and vehicle noise. Australian Road Research Board Research Report ARR177. ARRB, Vermont South, Victoria.

SAMUELS, S.E. and ROPER, R.L. (1991). The effects of cold overlay surface treatments on traffic and vehicle noise. Australian Road Research Board Research Report ARR208. ARRB, Vermont South, Victoria.

STANDARDS ASSOCIATION OF AUSTRALIA (1979). Methods of measurement of the sounds emitted by motor vehicles - AS2240. SAA, Homebush, NSW.

ACKNOWLEDGMENTS

This paper is based on work undertaken as part of a joint research program conducted by the Roads and Traffic Authority of NSW and the Cement and Concrete Association of Australia (CCAA). The investigation was undertaken under contract to RTA NSW as a collaborative venture with RTA's Environmental Planning Section. Mr F. Weatherall and Mr P VanderReest of the Section assisted with data collection. The work was conducted for RTA's Northern Region and was partly sponsored by CCAA.

EXPOSURE OF THE AUSTRALIAN POPULATION TO AIRCRAFT NOISE

Dr. Peter N. Georgiou[1]

INTRODUCTION

Vipac Engineers & Scientists Ltd has recently worked with Maunsell Pty Ltd to complete the 1994 OECD State of the Environment Questionnaire Forms, in the area of **Noise**, on behalf of the Commonwealth Environmental Protection Agency.

The general purpose of the Questionnaire is to collect the best available data on the environment in OECD Member countries and to promote international harmonisation of these data. The 1994 Questionnaire is the seventh sent to Member countries since 1981 and will contribute to the OECD's 1995 Compendium of Environmental Data. The Questionnaire covers the areas of Air, Inland Waters, Marine Environment, Land, Forest, Wild Life, Waste, Noise and Expenditure.

The Noise Questionnaire is concerned primarily with an assessment of noise exposure **heard at home** (residential noise) in the following categories:

- **Road Traffic**
- **Railroad Traffic**
- **Aircraft**
- **Industry**
- **Other (includes Construction Noise, Discos etc.)**

Reasonable progress was made in evaluating the national exposure and the exposure of several major individual cities with respect to Road Traffic and Aircraft. Only qualitative indications were supplied with respect to Railroad and Industry Noise and the final category of interest, "Other" (construction noise, discos etc.).

The OECD Noise Questionnaire recognises but does not address the issue of noise in the **Workplace**, although potentially useful statistics are available regarding the effects of workplace noise from such State authorities as NSW WorkCover etc.

AIRCRAFT NOISE - THE ANEF SYSTEM

The OECD Noise Questionnaire allows for the reporting of aircraft noise exposure either as 24-hour L_{EQ}'s or NNI, NEF indices. In Australia, aircraft noise is measured using the "**ANEF**" or Australian Noise Exposure Forecast system. This system takes into account the total number of flights affecting any particular location, the flight paths, the noise levels of each flight overpass, and the relevant time of day.

---

[1] VIPAC Engineers & Scientists Ltd
Unit E1-B, Centrecourt, 25 Paul Street North, North Ryde N.S.W. 2113
(Tel.) 02 - 805 6000 (FAX.) 02 - 878 1112

Figure 1 indicates the relationship between an ANEF level and the population percentage affected by the associated noise levels. For example, at ANEF = 25, 18% of the population is "seriously affected", while a further 39% of the population is "moderately affected".

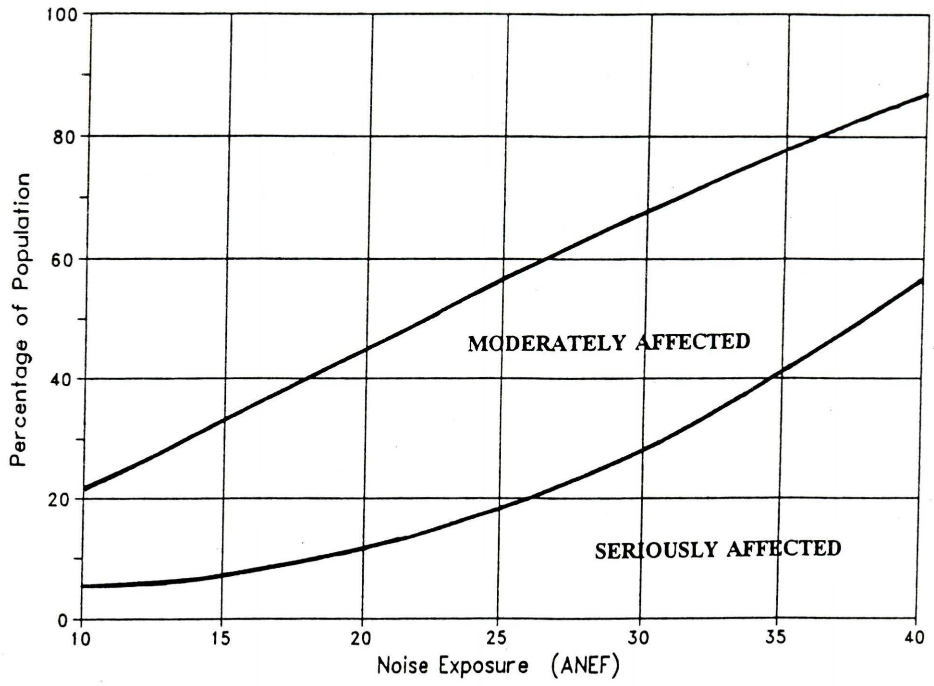

Fig.1 Percentage of Population Affected by Aircraft Noise

EXPOSURE OF MAJOR CITIES TO AIRCRAFT NOISE

Data Sources

To assess the exposure of principal Australian population centres to aircraft noise, the following ANEF/ANEI/ANEC data were obtained from CAA/FAC Offices for major Australian Airports:

Sydney - 1988 BASE CASE ANEF's determined at the time of the E.I.S. Reports for the 3rd Runway at Sydney's Mascot Airport (released 1990).

Sydney - 2010 Forecast ANEF's recently been determined as part of the Sydney (Kingsford Smith) Airport Draft Noise Management Plan (released 1994). They include the effect of the 3rd Runway.

Adelaide - 1990	The CAA's ANEI (Noise Exposure "Index") for 1990 (released 1991).
Adelaide - 2020	The Noise Exposure "Concept" computed for Year 2020, known as Option 3C ANEC 2020 (released 1991). It includes a new proposed east-west runway.
Perth - 1988 ANEI	The ANEI for aircraft noise exposure around Perth for 1988 (released 1990).
Perth - 2000 ANEF	The ANEF computed for Year 2000 (released 1990). It includes a new proposed north-south runway as well as an extension to the current SW-NE runway.
Melbourne - E.I.S. ANEF	The ANEF, released in August 1993, and based on four ANEC's (four possible future runways). The 1990 ANEI was used for the source noise input.

Calculation Procedure

To determine the noise exposure **by population** for the above ANEF's, ANEC's etc., the following procedure was used:

1. All ANEF/ANEI/ANEC Contours were copied to a uniform scale of 1:125,000.

2. The Official Australian POST CODE MAP (AUSLIG,1993) was used to generate an appropriate area encompassing the ANEF area of interest by magnifying (twice) to a similar scale of 1:125,000.

3. Tracings were then made of the above two maps including:

   ► the ANEF/ANEI/ANEC contours
   ► Post Code boundaries
   ► key geographical features (as overlay reference points)

4. The tracings were transposed onto a single graph paper sheet, examples of which are shown on the following pages.

5. From the combined graph paper diagram, the relative areas of each ANEF/ANEI/ANEC contour band, i.e. ANEF 20-25, 25-30 etc., within each respective Post Code area were determined.

The 1986 Census Data - C86.105 Number of Persons and Dwellings - was used to determine the number of persons in each Post Code and hence the percentage of people affected in each ANEF etc. zone. The individual post code population numbers were then summed to give the total number of people affected in each city.

In carrying out the previous steps, additional maps and aerial photos were used to ascertain whether the population in each Post Code was distributed evenly within the total area of the Post Code. In certain cases, adjustments to the contour area/total area ratios were made to reflect evident unevenness in the distribution of dwellings, location of extensive parklands etc.

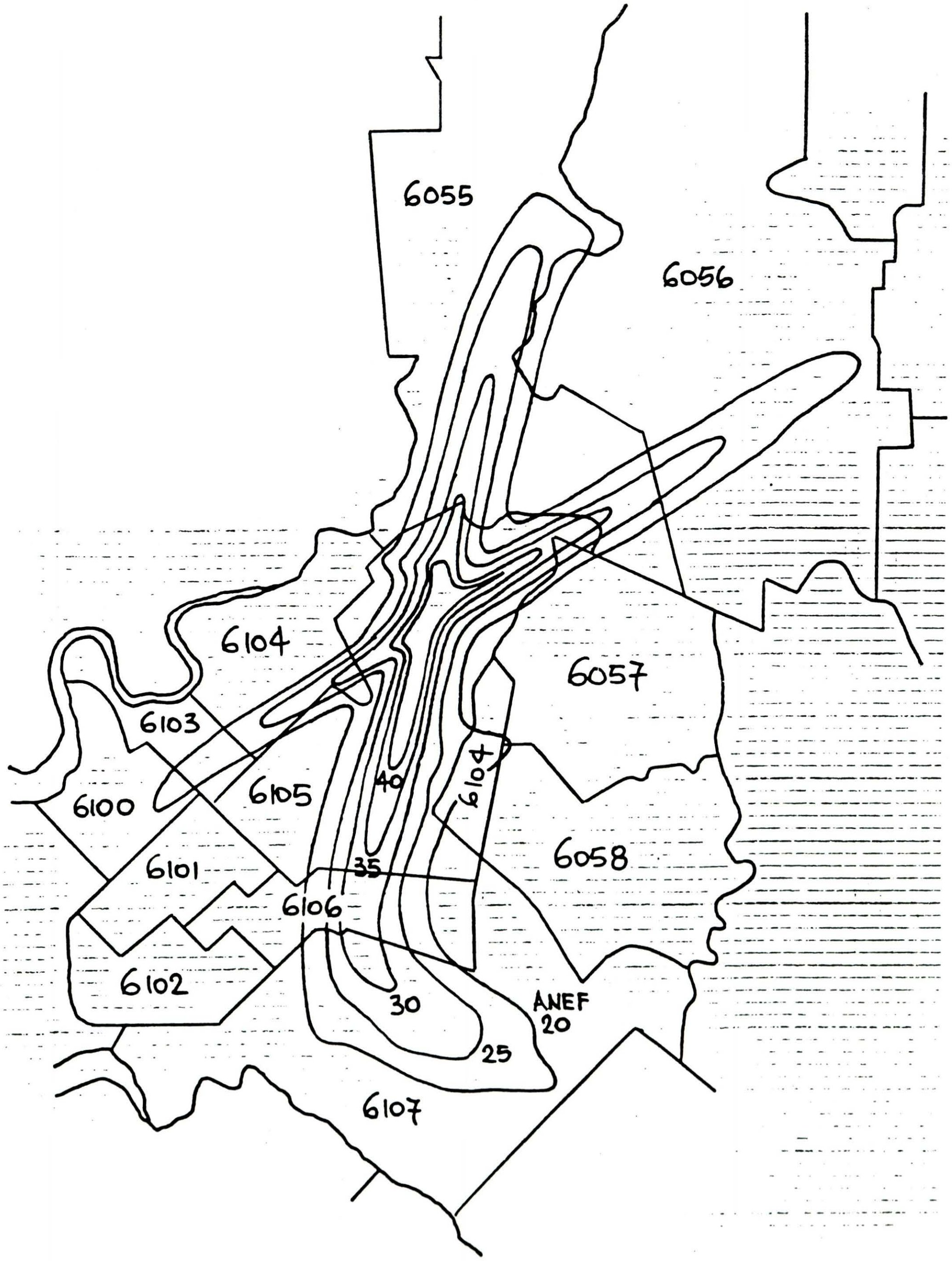

Fig. 2a Example ANEF Contour Computation Sheet - Perth 1988 ANEI

The figure below shows the change to the Perth noise exposures generated by the new N–S runway as well as the extension of the existing SW–NE runway.

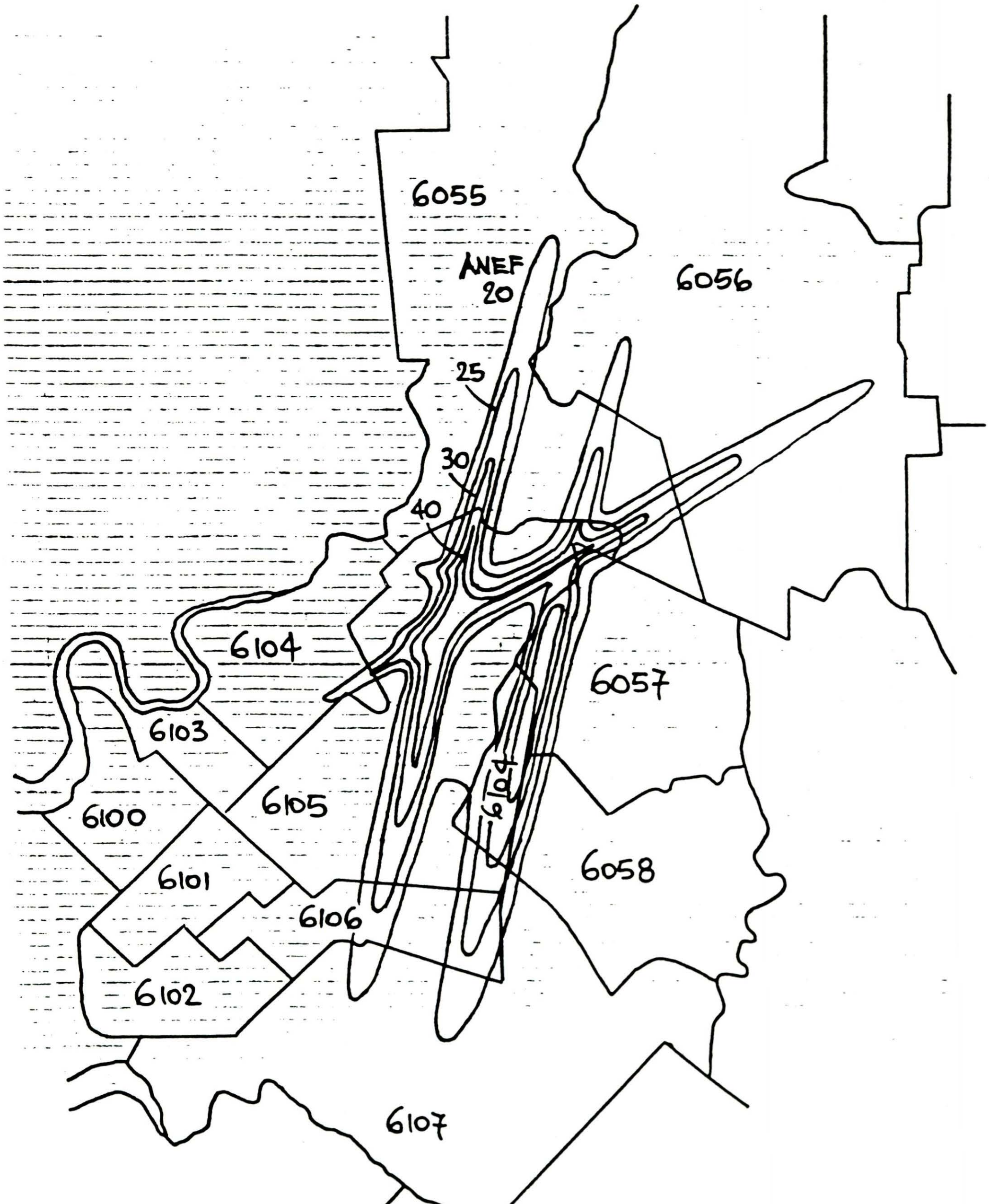

Fig. 2b Example ANEF Contour Computation Sheet – Perth 2000 ANEF

Individual Airport Noise Exposure

The results of the above computations are summarised below:

Table I
Summary of ANEF/ANEI/ANEC Exposure Counts
for Major Australian Airports
(Population Counts Based on 1986 Census Data)

Airport ANEF Year	Number of People (expressed in 1,000's) Exposed to ANEF levels of ... (Percentage of the Population Exposed)				
	< 20	> 20	> 25	> 30	> 35
Sydney - 1988 ANEF	2,843 (95.1	146 (4.9)	71 (2.4)	25.5 (0.9)	4.5 (0.2)
Sydney - 2010 ANEF	2,902 (97.1)	87 (2.9)	36.5 (1.2)	13 (0.4)	3 (0.1)
Adelaide - 1990 ANEI	899 (98.1)	18 (2.0)	6.5 (0.7)	1.5 (0.2)	-
Adelaide - 2020 ANEC	903 (98.5)	14 (1.5)	4.5 (0.5)	1 (0.1)	-
Perth - 1988 ANEI	837 (96.9)	27 (3.1)	11.5 (1.3)	5 (0.6)	1 (0.1)
Perth - 2000 ANEF	850 (98.4)	14 (1.6)	5 (0.6)	2.5 (0.3)	-
Melbourne - 1993 ANEF	2,616 (98.9)	29 (1.1)	6.5 (0.3)	1 (0.05)	-

Current Exposure

- None of the airports sited in Table I also function as military airports, which would have a significant impact on the resulting noise levels.

- Sydney with just over 70,000 people or 2.4% of its population, has the largest number (both in overall magnitude and percentage) exposed to ANEF levels greater than 25, a classification that implies an area not compatible for residential use.

  The Sydney exposures are expected to decrease by a factor of 2 once the new Mascot 3rd runway is in full operation.

- More people in Perth are currently exposed to this same level (ANEF > 25) than in Melbourne, which has three times the population, indicating the benefits of siting a major airport at the fringes of the main population area.

Future Exposure

It is clear that where both present and future ANEF's are available, the noise exposure of the individual population centres is expected to decrease with time. This is a combination of ...

- The continuing quietening of aircraft, and
- The transition in key urban areas (e.g. Sydney) from existing runways which affect large numbers of people (e.g. Mascot's east–west runway) to new runways (e.g. Mascot's 3rd Runway) affecting significantly less people.

EXPOSURE OF THE TOTAL AUSTRALIAN POPULATION

For the total Australian population, only an estimate of the current, i.e. 1990, exposure was computed. The following assumptions were made:

- The exposure of the cities of Sydney, Melbourne, Adelaide and Perth was determined for the baseline cases previously described, referenced nominally to the year 1990.
- Additional data were received from FAC Offices for the cities of Darwin and Coolangatta for their respective airports.

  While a relatively small population is affected by the Coolangatta Airport ANEF's, the Darwin Airport noise exposure is complicated by its use as an RAAF Base as well as a domestic airline civilian airport.
- Although no data was received from Canberra and Hobart, the local FAC Offices confirmed that the lowest ANEF contour (ANEF 20) was either beyond the major population area (e.g. Canberra) and/or mostly out to sea (e.g. Hobart).
- From the above, national exposure figures were determined using the 1986 Census Data to weight the ANEF population ratios. It was assumed that the remainder of the country excluding the above urban centres, was exposed to "nominal" aircraft noise, i.e. approximately half the population exposure ratios which were computed for Melbourne.

This resulted in the following **overall National exposure figures:**

Table II **Noise Exposure of the Australian Population to Aircraft Noise**		
Australian Total Population	**less than 20 ANEF**	**98.0 %**
	greater than 20 ANEF	**2.0 %**
Aircraft Exposure re: 1990	**greater than 25 ANEF**	**0.7 %**
	greater than 30 ANEF	**0.2 %**
	greater than 35 ANEF	**-**

The above indicates that just over 100,000 people throughout Australia are exposed to ANEF levels greater than 25, i.e. living in areas incompatible with residential use. These numbers however are expected to almost halve within the next decade or so as future planned runway modifications are made at primary airports.